PREFACE

The great practical importance of the hydrogen evolution reaction as well as the earlier belief in its probable simplicity have been two of the major reasons for the intensive investigations carried out on the mechanism of cathodic hydrogen evolution since the early history of electrochemical kinetics. Experimental results, however, have shown that the hydrogen evolution reaction is, in reality, quite complex, and to the present day there exists no complete picture of the successive stages involved in this reaction and even some general aspects, as studied in the present work, have by no means been adequately investigated.

Although many of its kinetic characteristics have been firmly established, critical aspects of the temperature dependence of the kinetic behavior of the hydrogen evolution reaction have been neglected. Thus, it was thought desirable to carry out a detailed investigation on this aspect of the hydrogen evolution reaction over a relatively wide range of temperatures, including low ones, and hence establish the appropriate form of the fundamental electrode kinetic parameters, e.g., the Tafel slope, b and the so-called symmetry factor, β (see Chapter III for further details on the aims of the present work). It is this temperature study which provides the basis for most of the work described in this thesis.

In Chapters I and II a number of basic matters involved in the present work have been briefly reviewed in order to provide the necessary background to the problem with respect to the discussion of the results obtained. This review also serves to place the original work in this thesis in perspective and demonstrate its connection with earlier work carried out in this and other laboratories.

In Chapter III are presented the aims of the work and in Chapter IV, the experimental techniques and results. A detailed discussion of the present original results with regard to (a) the temperature dependence of the Tafel slopes, (b) the interpretation and significance of electrochemical activation energies and (c) the difficulties which arise with the supposed involvement of the solvated electron in electrode processes, in general, is given in Chapter V.

Most of the work described in this thesis is in course of publication, as indicated in the following list of papers:

1) Significance of Electrochemical Brønsted Factors: Part I: The Temperature Dependence of Current-Potential Relations, B. E. Conway and D. J. MacKinnon, J. Phys. Chem., submitted for publication.

2) Significance of Electrochemical Brønsted Factors: Part II: Some Theoretical Aspects of the Temperature Dependence of Tafel Slopes, B. E. Conway, B. V. Tilak and D. J. MacKinnon, J. Phys. Chem., submitted for publication.

3) Interpretation and Significance of Heats of Activation for Electrochemical Reactions Exhibiting Anomalous Tafel Slopes, B. E. Conway and D. J. MacKinnon, J. Electrochem. Soc., submitted for publication.

4) Some Problems with the Involvement of Hydrated Electrons in Electrode Processes, B. E. Conway and D. J. MacKinnon, Trans. Faraday Soc., submitted for publication.

ACKNOWLEDGEMENTS

The author wishes to express his thanks for having had the privilege of working under the direction of Professor B. E. Conway. Professor Conway's willingness to discuss each and every problem, his critical approach to these problems and his enthusiasm and originality have been the source and mainstay of this work.

The author also wishes to thank Dr. B. V. Tilak for providing Figures 54-57 inclusive and for many helpful discussions on double layer effects.

Financial assistance from the National Research Council of Canada in the form of a Postgraduate Research Scholarship is gratefully acknowledged.

Thanks are also due to Mrs. W. Storto for typing the thesis.

TABLE OF CONTENTS

Page No.

CHAPTER II

CHAPTER III

CHAPTER IV

LIST OF FIGURES

LIST OF TABLES

ABSTRACT

The fact that for simple discharge processes, the temperature dependence of Tafel's b coefficient (= "RT/βF") is smaller than that indicated by the usual defining relation has been referred to in earlier publications but the significance of this fact has received little attention partly owing to an insufficiency of experimental data. The temperature dependence of Tafel slopes for hydrogen evolution has been examined at several metals including Hg, Ni, Pt, Cd and Pb within the temperature range +65°C to -100°C in methanolic and ethanolic acid solutions. Bromide discharge was also studied in acetonitrile. b usually decreases with T but not with the required slope R/βF or R/αF; in fact, b is better represented by a relation such as $b = (RT/\beta F) + c$ with $\beta > 0.5$. At Ni, two slopes are observed one of which increases with decreasing T, an effect which is probably caused by specific adsorption of anions. In all cases, except that of Hg, b eventually increases with T at low temperature ($< -75°C$) after an initial decrease.

Cases arise where anomalous dependence of Tafel slopes on temperature is observed and cannot be attributed to anion adsorption or proton tunneling effects. Several theoretical approaches are therefore made in order to provide an explanation of such behavior, e.g., in terms of changes of dipole surface potential with temperature, dependence of entropy of activation on potential, surface coverage effects and solvent structure changes with temperature.

Heats of activation for electrochemical reactions studied over a wide range of temperatures are considered in relation to the temperature dependence of the Tafel slope factor b. Experimentally

ABSTRACT

The fact that for simple discharge processes, the temperature dependence of Tafel's b coefficient (= "RT/βF") is smaller than that indicated by the usual defining relation has been referred to in earlier publications but the significance of this fact has received little attention partly owing to an insufficiency of experimental data. The temperature dependence of Tafel slopes for hydrogen evolution has been examined at several metals including Hg, Ni, Pt, Cd and Pb within the temperature range +65°C to -100°C in methanolic and ethanolic acid solutions. Bromide discharge was also studied in acetonitrile. b usually decreases with T but not with the required slope R/βF or R/αF; in fact, b is better represented by a relation such as $b = (RT/\beta F) + c$ with $\beta > 0.5$. At Ni, two slopes are observed one of which increases with decreasing T, an effect which is probably caused by specific adsorption of anions. In all cases, except that of Hg, b eventually increases with T at low temperature (< -75°C) after an initial decrease.

Cases arise where anomalous dependence of Tafel slopes on temperature is observed and cannot be attributed to anion adsorption or proton tunneling effects. Several theoretical approaches are therefore made in order to provide an explanation of such behavior, e.g., in terms of changes of dipole surface potential with temperature, dependence of entropy of activation on potential, surface coverage effects and solvent structure changes with temperature.

Heats of activation for electrochemical reactions studied over a wide range of temperatures are considered in relation to the temperature dependence of the Tafel slope factor b. Experimentally

b is found to have anomalous temperature dependence, i.e., other than the classical form $RT/\alpha F$, for hydrogen evolution at Hg, Cd, Pb, Ni and Pt and the consequences of this behavior in calculation of heats of activation are evaluated. Curvature of the electrochemical Arrhenius plots is shown to arise for certain of the cases treated and is discussed in relation to the problem of detection of proton tunneling at low temperatures. Other difficulties associated with temperature dependence of coverage by atomic H and temperature-dependent structure changes in the solvent are considered.

Recently, pathways in cathodic hydrogen evolution have been proposed which involve the initial production of hydrated electrons. Attention is directed to some kinetic, and under certain conditions, thermodynamic difficulties which arise with this type of mechanism. Problems of microscopic reversibility, electrochemical adsorption of H and the standard potential of the hydrated electron are considered, as well as the chemical basis for distinction between the hydrated electron and atomic H when reduction reactions at electrode surfaces are involved.

CHAPTER I

THEORIES OF PROTON TRANSFER

a) General Introduction

One of the significant problems remaining in the study of the cathodic hydrogen evolution reaction (h. e. r.) is still the interpretation of the detailed mechanism of the electrochemical act of discharge of protons at a metal surface. This reaction, which is a necessary primary step in the h. e. r. (and indeed, is found to be rate-determining at a number of metals, particularly Hg) may be represented as

$$H_3O^+ + M + e_M \rightarrow M\text{-}H + H_2O \qquad [1]$$

Although much work, both theoretical and experimental, has been carried out on this reaction over the past 60 years, questions such as "Where and when does electron transfer occur?", "Does proton tunneling play a significant role?", and "Under what conditions is process [1] rate-controlling?" remain to be answered with a more satisfactory degree of certitude; answers to such questions will depend on the metal surface considered and on other conditions.

In an electrode process, the standard electrochemical free energy of activation $\Delta\bar{G}^{o\ddagger}$ is potential dependent and may be written in terms of "chemical" ($\Delta G^{o\ddagger}$) and electrical component terms where

$$\Delta\bar{G}^{o\ddagger} = \Delta G^{o\ddagger} + \beta\emptyset zF$$

and β is the so-called symmetry factor analogous (see below) to Brønsted's α factor in acid-base reactions, ϕ is the metal-solution potential difference, F the Faraday and z is the number of electronic charges (usually one) transferred in the rate-determining step. The corresponding velocity v of the electrode process expressed in terms of current density i can be written in a generalized way as

$$i = z'Fv = (z'FkT/h)\exp[-\Delta\bar{G}^{o\ddagger}/RT].f(c,\Theta)$$

where $f(c,\Theta)$ represents any concentration and surface coverage terms involved in the kinetics of the reaction and z' is the total number of electrons transferred in a stoichiometric act of the overall process.

Intimately connected with the questions stated above is the molecular significance of the symmetry factor β. It is evident from the relation defining $\Delta\bar{G}^{o\ddagger}$ that

$$\beta = d\Delta\bar{G}^{o\ddagger}/d(zF\phi) \qquad [2]$$

From this expression for β, and differentiating the equation for the rate with respect to potential, it is clear that a quantity characterizing the potential-dependence of the rate may be written as

$$d \ln i/d\phi = -\beta zF/RT = b$$

which is commonly referred to as the Tafel slope of the process and represented by b.

Since the dependence of $\Delta\bar{G}^{o\ddagger}$ on ϕ through β is the main feature distinguishing electrochemical kinetics from chemical kinetics of other homogeneous or heterogeneous processes, it is evident that β is to be regarded as one of the most fundamental factors in the kinetic theory of electrode processes.

The early paper of Gurney (1) published in 1931, together with those of Horiuti and Polanyi (2), Butler (3), Bowden (4), Erdy-Gruz and Volmer (5) and Frumkin (6) laid the foundations for subsequent discussions of charge transfer at electrodes published in more recent years. Thus, a theory of charge transfer in the h. e. r. was published by Bockris and Parsons (7) in 1951 based on Butler's treatment (3), a theory for charge transfer in metal deposition by Conway and Bockris (8) and by Despic and Bockris (9) in 1961 and other theories for charge transfer in redox reactions by Hush (10), Marcus (11, 12, 13, 14, 15), Laidler (73, 74) and Dogonadze and Chizmadzhev (16, 17) have appeared.

While it will be seen in the discussion which follows that the same general principles apply both to bond-breaking and bond-forming charge-transfer processes, and to ionic redox reactions, an important and useful practical distinction can be made on the basis of the type of activation process involved in formation of the transition state; that is, whether bond stretching or solvation shell rearrangement is the activation process. In some cases, both types of process are, in fact, involved.

More recently, Salomon and Conway (18) proposed a theory for proton transfer in the discharge step of the h. e. r. and considered limitingly a fully charged transition state in which the activated complex was regarded as being analogous to that in acid-base proton transfer processes; the electrode was regarded as playing, in a general sense, the role of a base with variable base strength (electron availability).

In 1966, Bockris and Matthews (19) proposed a theory of charge transfer based on Gurney's and Butler's theories in which both the ion and the electron were considered and which was worked out in detail for the discharge step [1]. This theory recognizes the resonance situation in the transition state and claims a better physical understanding of the symmetry factor, β.

Following the early work of Bell (33) on homogeneous proton transfer reactionsand of Bawn and Ogden on the h. e. r. (45), the role of proton tunneling in the h. e. r. has received much attention in more recent years particularly from a theoretical point of view due mainly to the efforts of Christov, Conway, and Bockris and Matthews. In addition, two significant experimental studies on this problem have been recently carried out but, in general, studies of this nature have been few.

Further, several authors have recently proposed that the solvated electron plays an important role in the h. e. r. but a number of arguments against this proposal can be made (see Chapter V).

In the following pages, a discussion of the important early theories of proton transfer in the h. e. r. will be given as well as a review of the more recent treatments. Included in this discussion will be an examination of the role of proton tunneling and the controversial topic of the role of the solvated electron in cathodic processes in aqueous medium.

b) Early Theories of Proton Transfer in the H. E. R.

In 1931, Gurney (1), in an attempt to explain the results obtained by Bowden (4) in his investigation of hydrogen overpotential, published his now classical paper on the theory of charge transfer in the h. e. r. He proposed a theory of electron-transfer by quantum-mechanical tunneling "through" the activation energy barrier, the

effect of the electrode potential being to bring the energy levels on both sides of the barrier to equal values so that "radiationless" tunneling could proceed with a maximum probability. According to this theory, the condition for the neutralization of hydrogen ions near the electrode is approximately given by

$$\phi_e + eV < E_N \qquad [3]$$

where ϕ_e is the thermionic work function of the metal, eV the potential difference between the metal and the ions on the solution side of the double-layer, and E_N the so-called neutralization energy of the hydrogen ions. The latter is defined as

$$E_N = I - L - R \qquad [4]$$

where I is the ionization potential of gaseous atomic hydrogen, L the hydration energy of protons and R the repulsive potential which results from interactions between neutralized atoms and the water molecule after electron transfer. The above theory gave a correct qualitative account of the results of Bowden but it had, however, some drawbacks, mainly because it predicted activation energies that were far too large in comparison with the experimental apparent (see Chapter II) values.

However, Gurney (1) later modified his expression for the activation energy by adding an empirical factor γ which enabled him to obtain more satisfactory agreement with the experimental results of Bowden (4). Also, at about the same time, Erdy-Gruz and Volmer (5) in their theory of the h. e. r. introduced a factor, α, into the rate equation for the neutralization of H^+ ions at an

electrode surface. This quantity*, α, which is approximately equivalent to the reciprocal of Gurney's factor, γ, ($\alpha \equiv 1/\gamma$) was later to become known as the symmetry factor (commonly written as β) and is now recognized as being of fundamental importance in electrode kinetics. This important quantity will be discussed in some detail in the following section of this chapter (see p. 9).

Butler (3) represented Gurney's theory in a graphical form similar to that given by Horiuti and Polanyi (2) who used a potential energy profile as a basis for description of molecular events in the hydrogen ion discharge reaction [1].

The neutralization condition in equation [3] can be written using equation [4] as

$$\phi_e + V + R < I - L \,, \qquad [5]$$

and represented graphically as shown in Figure 1. The curve AA represents I - L plotted as a function of the distance of displacement of the proton from the centre of the water molecule in H_3O^+ (acidic conditions of proton transfer) and the curve BB represents corresponding values of $\phi_e + V + R$. The condition [5] is evidently satisfied for points lying to the left of the point of intersection X of

---

*It is desirable, at this point, to clairify the meaning of the often confused factors α and β. The symbol α was originally used by Erdy-Gruz and Volmer as the Brønsted factor for the discharge reaction. This factor is now, however, usually designated by the symbol β and the symbol α is retained for the overall factor determining the Tafel slope b in the defining relation $b = RT/\alpha F$. For reactions involving more than one step, with a discharge process as the initial stage, α is usually greater than β if the second or subsequent step is rate-controlling. For example, in the atomic H combination step $\alpha = 2$ while in the radical-ion discharge process in the h. e. r. $\alpha = 1 + \beta$. α is only identical with β in the case when an initial simple discharge step is rate-determining. Confusion has for a long time persisted over these quantities and is even maintained in recent publications e. g. (97) but the matter has been discussed well in a recent review (98).

the two curves, and if E' is the energy of the point of intersection, $E'-E_o$ is the activation energy required for the process.

Butler improved the Gurney theory by taking into consideration the energy of adsorption of hydrogen atoms on the metal surface. The variation of the heat of adsorption A of atomic hydrogen on the metal with distance was superimposed on Figure 1 and the result is shown in Figure 2. The energy of adsorption of H at a metal M is assumed to vary with distance in a manner similar to that in a diatomic hydride. The neutralization condition then becomes

$$\Phi_e + V + R - A < I - L \qquad [6]$$

and the inclusion of the A term results in a considerable lowering of the activation energy. In Figure 2 the curves AA and BB have the same significance as in Figure 1 while curve CC represents the values of $\Phi_e + V + R - A$ as a function of the position of the H atom resulting from the discharge event.

Here it is important to point out that the hydrogen atom, formed by the discharge of the H_3O^+ ion, is regarded as remaining in solution near the metal surface in the Gurney theory while it is considered as being adsorbed at the metal surface in the Butler theory. The adsorption of the hydrogen atom results in a lowering of the activation energy to values more in agreement with experiment and allowsfora ready explanation of the dependence of discharge kinetics on the properties of the electrode metal. This was demonstrated by Parsons and Bockris (7) who calculated the activation energy for the discharge reaction at Hg and Ni [cf. Butler (3)]. They considered the activation process for transfer of a proton from its solvation sheath to an adsorption site on the electrode in terms of transition state theory modified for application to charged particles.

Figure 1

Gurney model for proton transfer according to Butler.

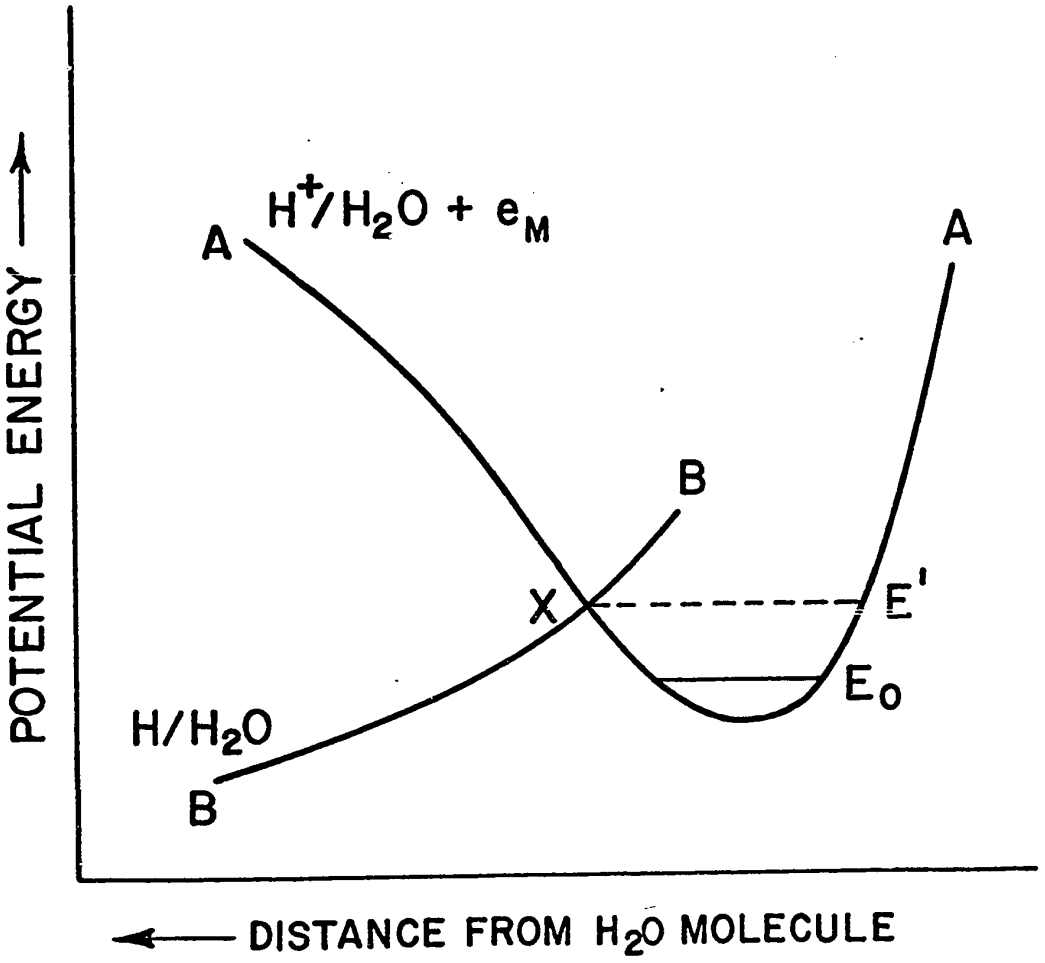
POTENTIAL ENERGY
$H^+/H_2O + e_M$
A
A
B
X
E'
E_0
H/H_2O
B
DISTANCE FROM H_2O MOLECULE

Figure 2

Model for proton transfer according to Butler.

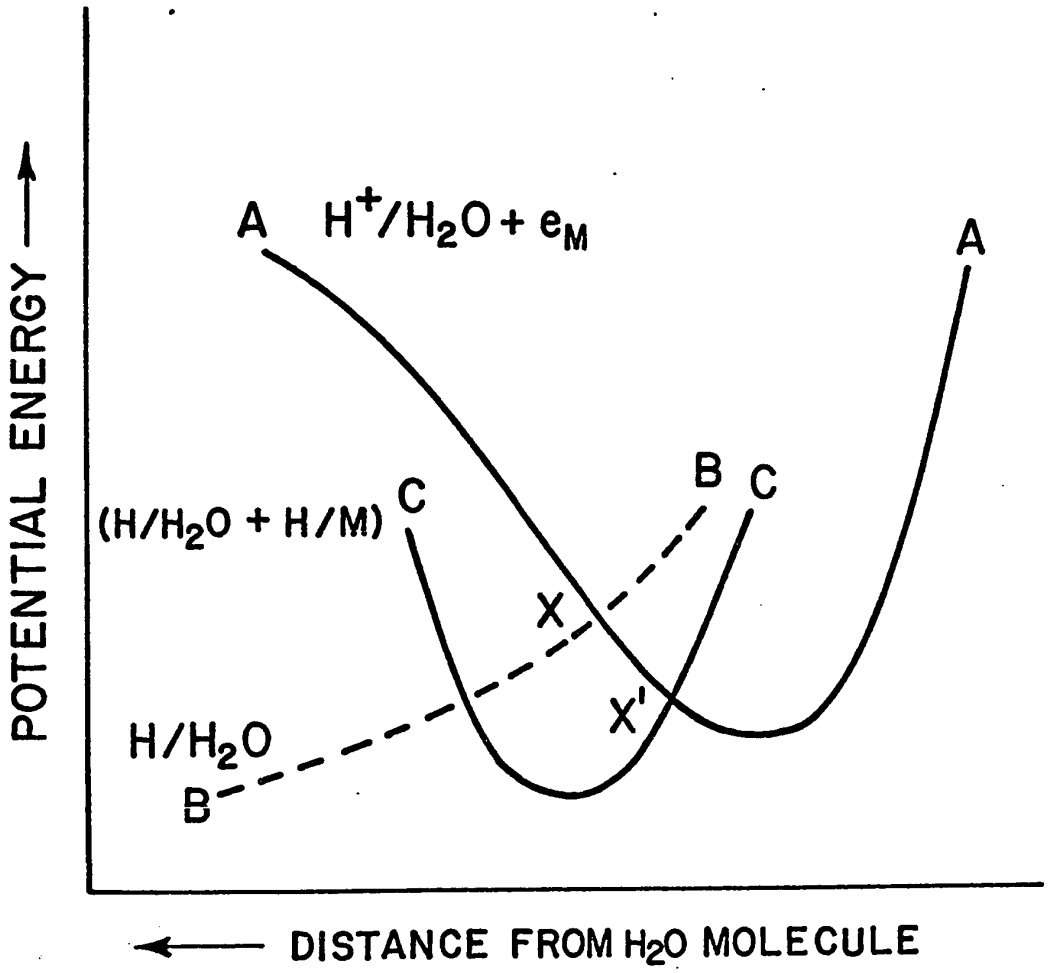
POTENTIAL ENERGY
A
$H^+/H_2O + e_M$
A
B
C
$(H/H_2O + H/M)$
C
X
X'
H/H_2O
B
DISTANCE FROM H_2O MOLECULE

c) The Symmetry Factor, β

The symmetry factor, β, has been defined by equation [2] and in simple terms may be thought of as that fraction of the applied potential which is aiding the discharge of hydrogen ions. In such terms, the quantity β can be represented graphically by means of an energy diagram, after Horiuti and Polanyi (2), as shown in Figure 3. According to these authors, the electrode potential raises the level of the initial state comprising the hydrogen ion plus an electron* in the metal by an energy FV, but not that of the reduced form "MH". The change in activation energy is simply a fraction of the electrical energy FV and depends on the slopes of the curves in the region where they intersect. If, in this region, the slopes are equal, then $\beta = 0.5$. This method was utilized by Parsons and Bockris (7) to show that $\beta \doteqdot 0.5$ for Hg and Ni and was later used to explain the dependence of β on potential for the electrolytic deposition and dissolution of Ag (9).

At this point, it is necessary to distinguish between the terms, "symmetry factor" (β) and "transfer coefficient" (α), two quantities concerning which much confusion has arisen (see footnote p. 5). It is best, perhaps, to reserve β as the factor referring to the potential dependence of the rate of the electron transfer step itself and write α for the corresponding potential dependence of the rate of the overall reaction in cases where the reaction is more complex than the electron-transfer step alone. The two quantities may in simple cases be related (20) by the equation

$$\alpha = \beta\lambda \qquad [7]$$

---

*Thus, it is usually assumed and is implicit in this treatment (2, 3) that the effect of potential is only to modify the availability of electrons by effectively changing the Fermi level. Other effects are not considered but it will be shown in the present work that they may require attention.

Figure 3

Graphical representation for β, according to Horiuti and Polanyi.

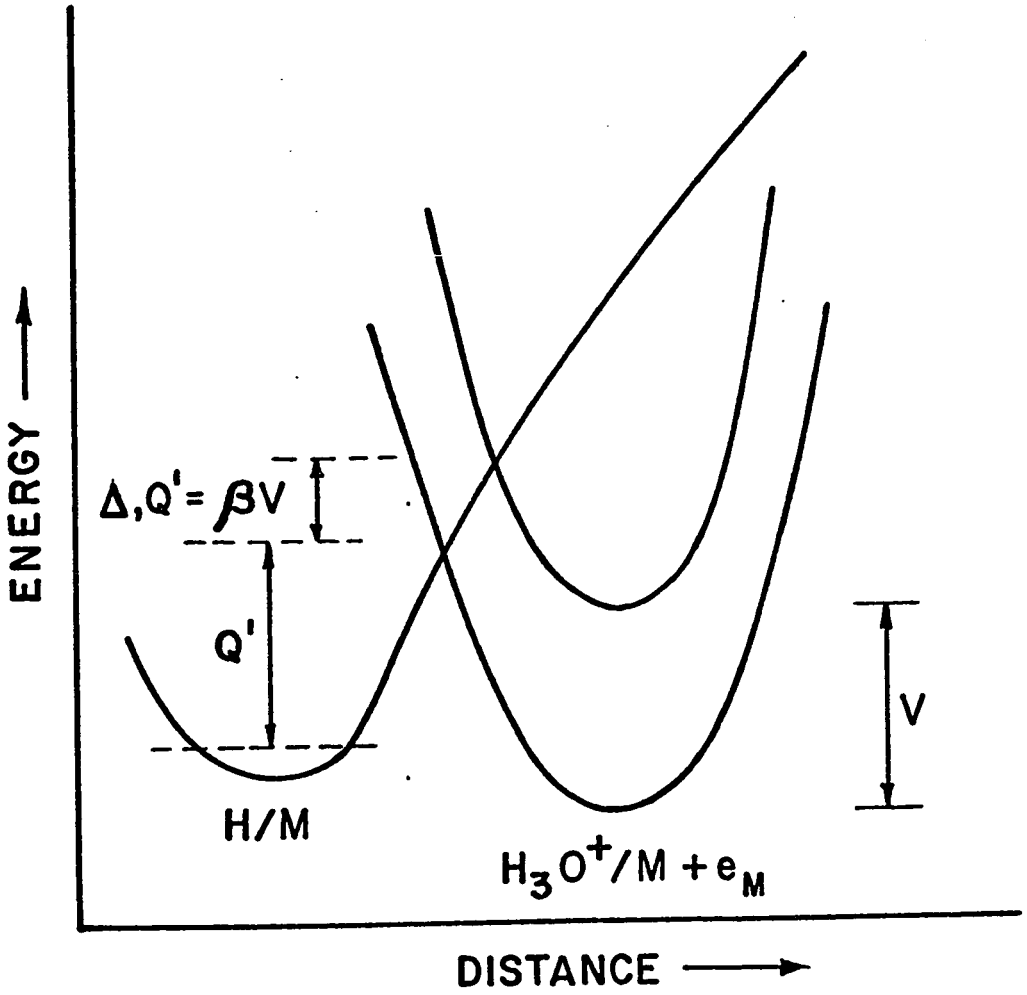
ENERGY
Δ,Q' = βV
Q'
V
H/M
$H_3O^+/M + e_M$
DISTANCE

where λ is the number of electrons necessary for one act of the rate-determining step to occur. Another relation that has been proposed (21) for more complex cases is

$$\alpha = n(\beta + \gamma)/\nu \qquad [8]$$

where ν is the stoichiometric number and γ is a factor referring to that part of the free energy that depends on the potential and not on the composition. In the case of the simple proton discharge step considered here, the values of the symmetry factor and transfer coefficient in fact become identical so that the symbol "β" will hence be used for both.

A different theory of β based on the use of potential energy profiles, but in which the effect of potential was considered in terms of the field across the metal solution-double-layer has been set forth by Mott and Watts-Tobin (22) with further elaboration by Christov (23). This theory has been criticized by Matthews (24) on the basis of an erroneous use of potential energy profiles.

Mott and Watts-Tobin (22) supposed that for an ion to be transferred from the outer Helmholtz plane (95) of the double-layer to the metal, it must surmount an energy barrier of the form shown in Figure 4, where A represents the equilibrium position of the specifically adsorbed ion and C the equilibrium position of the hydrated ion in the outer Helmholtz plane. In the presence of a field introducing a potential ψ between the two equilibrium positions A and C, the chance per unit time that an ion will surmount the barrier was given by

$$\nu \exp[-(U - \beta e \psi)/kT] \qquad [9]$$

where ν is a frequency factor and β is the constant which depends on the shape of the barrier. For a symmetrical barrier, $\beta = 0.5$. The implicit assumption that ψ may be identified with the whole potential

Figure 4

Free energy of an ion near a metal surface according to Mott and Watts-Tobin.

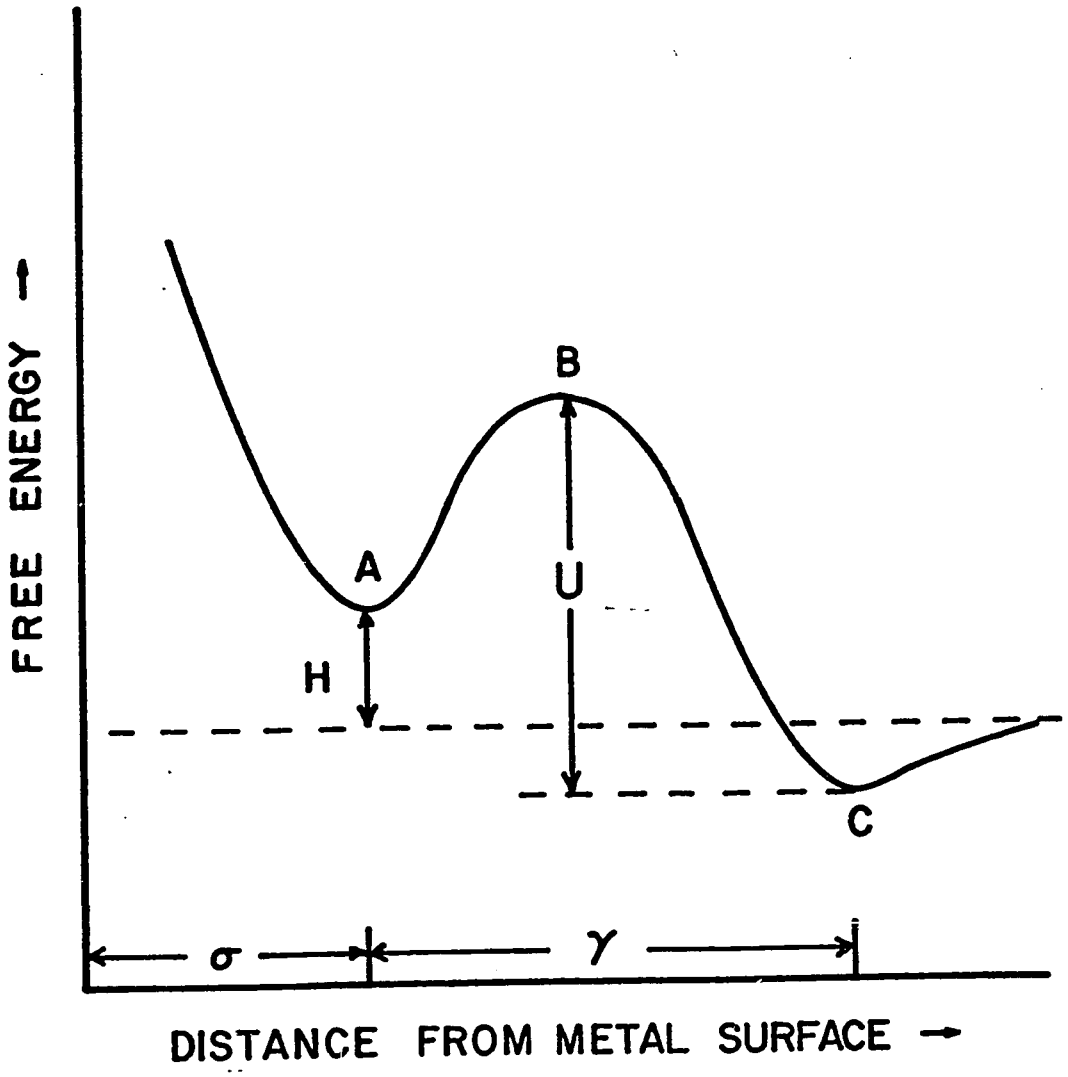
FREE ENERGY →
B
A
U
H
C
σ
γ
DISTANCE FROM METAL SURFACE →

across the double-layer was examined by these authors. For transfer of an ion from the outer Helmholtz plane to an adsorption site they deduced that the work done was $e\lambda\psi$ where

$$\lambda = \gamma/(\sigma + \gamma) \qquad [10]$$

(cf. Figure 4). The chance per unit time that the ion passes from the outer Helmholtz plane (95) to an ad-site was given by,

$$\nu \exp[-(U - \beta\lambda e\psi)/kT] \qquad [11]$$

If the ad-atom carries a positive charge, λ will be less than unity. Inspection of equation [11] gives (cf. Eqn. 7)

$$\alpha \equiv \beta\lambda \qquad [12]$$

Another type of energy curve was given by Christov (25) and is shown in Figure 5. The effect of the applied potential is regarded as leading to a change in energy by an amount that is determined by the potential versus distance function, the latter generally being assumed to be linear or nearly so in the transition state region. In this representation, the symmetry factor is thus related to the position of the activated state in the double-layer and hence the nature of β is connected more explicitly with a physical model than in the treatment of Horiuti and Polanyi (2).

d) Relation to Electron Transfer Theories of Marcus and Hush

The electron transfer theories of Marcus (11, 12, 13, 14, 15) and Hush (10, 26) for homogeneous reactions have been applied to redox reactions at electrodes by these authors. A representation of the course of the electrochemical redox reactions has been given by Randles (75, 76) in terms of potential energy diagrams and an equivalent type of representation was given earlier by Butler (77) in qualitative terms. In these cases no bonds are broken or formed and only a pure electron transfer occurs since the electrode material

Figure 5

Energy curve for reduction according to Christov.

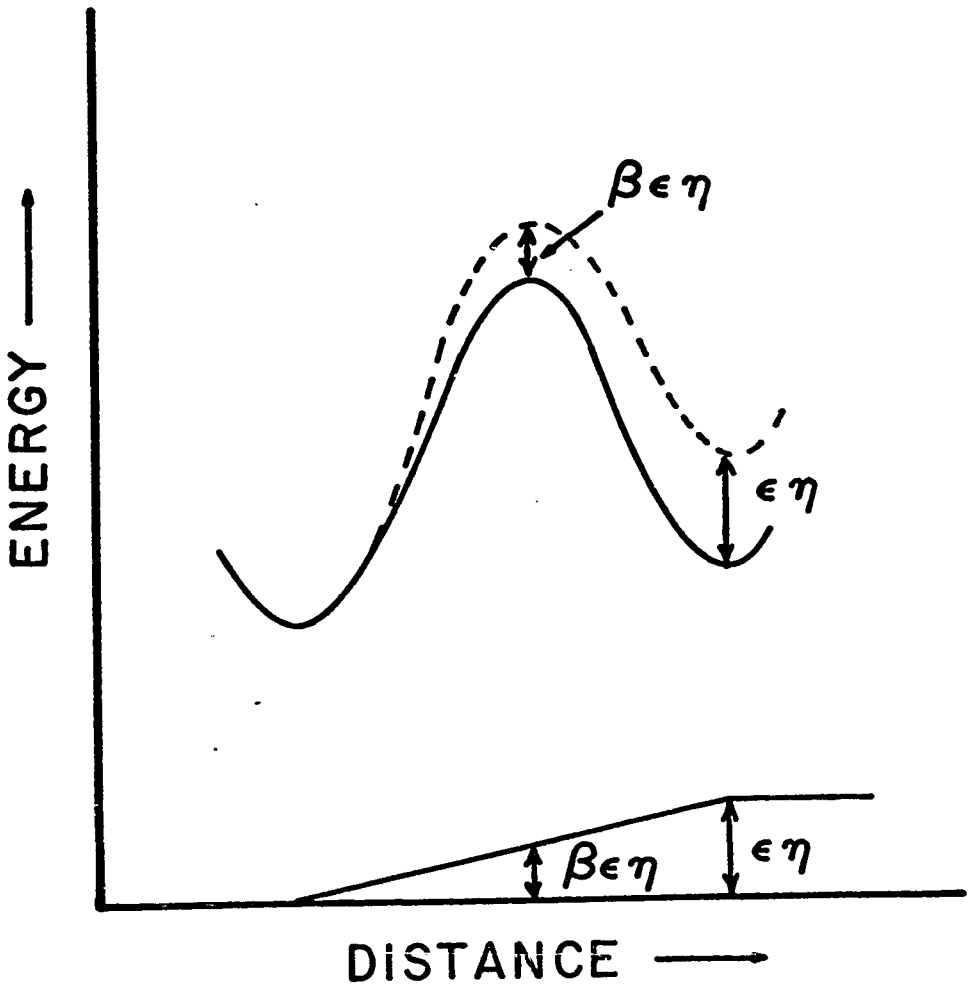
ENERGY
βεη
εη
βεη
εη
DISTANCE

serves ideally only as a "source" or "sink" of electrons. It is for this reason that the discharge of hydrogen ions at electrodes must be distinguished as a more complicated case owing to (a) the bond stretching process and (b) the adsorption of the resulting neutral atom, H. In point of fact, the transition states for the electron transfer from the electrode to an oxidized ion or from a reduced ion back to the electrode will not be identical with the transition state in the corresponding homogeneous redox reaction. This difference will be accentuated if there is specific adsorption of the reactant ions or molecules at the electrode interface and the condition of solvent water adsorbed at the electrode surface will be a critical matter in this regard.

The mechanism for electron transfer according to Marcus (14) can be described in terms of nuclear motion on a potential energy surface as illustrated in Figure 6 for the electrochemical process

$$A_{ox.} + n e^{-} (\text{metal}) \longrightarrow A_{red.} + (\text{metal}).$$

The height of the intersection point relative to any valley is modified by the metal-solution potential difference through the symmetry factor β. In the absence of electronic interaction between the ion and the electrode, a system moving on one surface reaches the intersection region and stays on this surface, i.e., it follows the dashed line with no electron transfer occurring (a non-adiabatic process). Electronic interaction causes degeneracy at the region of intersection to be removed and the reaction can occur solely by passage of the particles over the lower surface with electron transfer (an adiabatic process). The maximum energy on this surface is lower than that at the intersection point by half the resonance energy E_{12} (Figure 6). Since the resonance energy is a measure of the splitting of energy levels characterized by the potential energy surface and brought

Figure 6

Model for electron transfer for redox reactions according to Marcus.

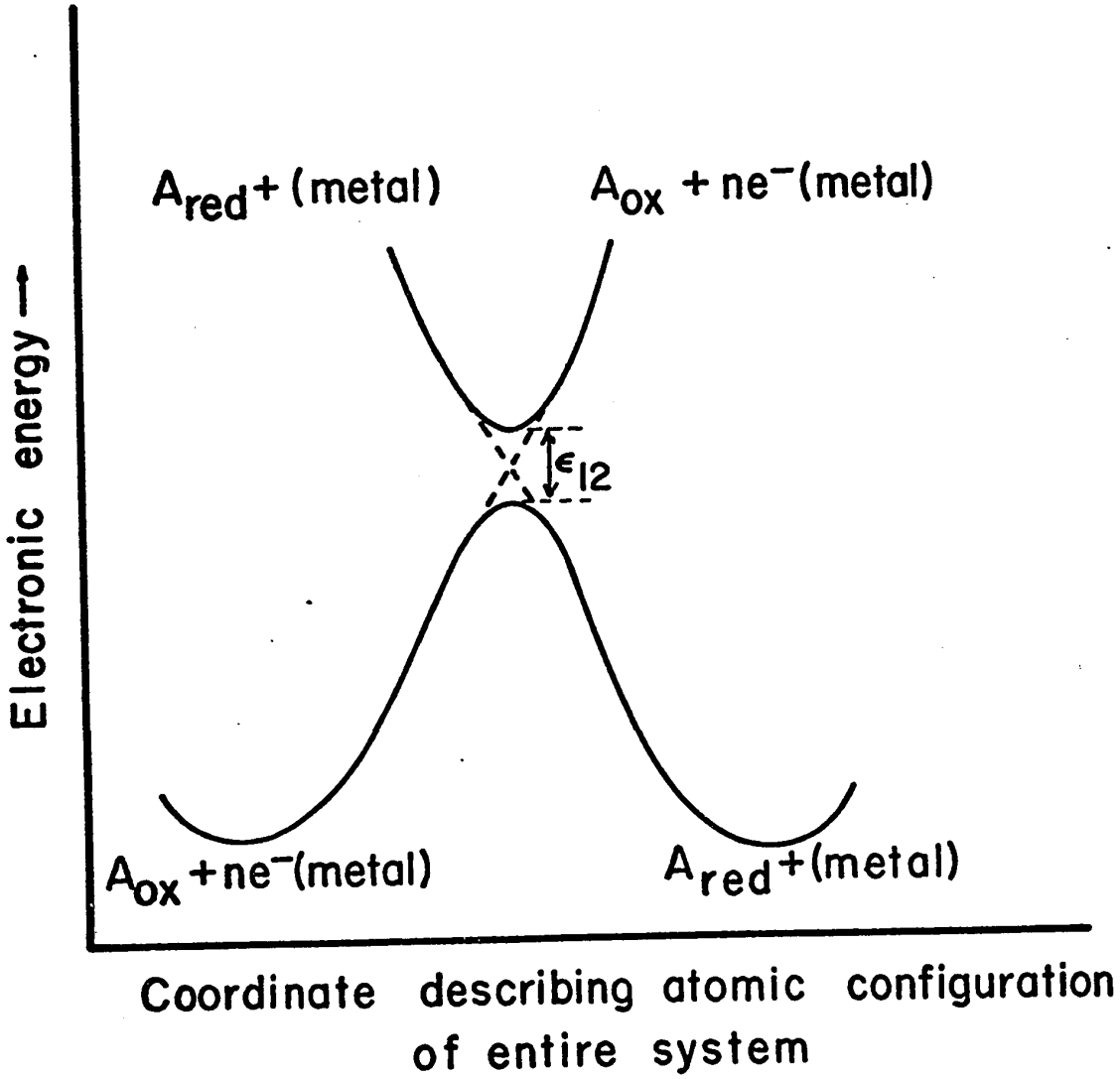
A_{red}+ (metal)
A_{ox} + ne⁻(metal)
ϵ_{12}
Electronic energy →
A_{ox} + ne⁻(metal)
A_{red}+(metal)
Coordinate describing atomic configuration of entire system

about by ion-electrode overlap interaction, it increases with increasing interaction.

In this treatment, β is in general a function of several terms and is not strictly independent of the electrode potential [cf. ref. (9)]; however, it can become approximately independent (a) if the double-layer effects are small and (b) if potentials are not too far removed from the equilibrium potential; moreover, the value of β becomes 0.5 in the limiting case. The treatments by Hush (26) and by Dogonadze and Chizmadzhev (17) lead to qualitatively similar conclusions.

These theories thus provide a rationalization for the frequently observed lack of dependence of β on potential (e.g., in the case of the h.e.r. at mercury in non-specifically adsorbed electrolytes) and for the value of 0.5 commonly found for β. Herein lies their relation to the theories of proton transfer in hydrogen electrode kinetics. Parsons and Passeron (27) have found quantitative agreement with Marcus' theory in the experimentally determined dependence on potential of the symmetry factor for the electrochemical Cr(II)/Cr(III) redox reaction.

e) Relation to Brønsted's Theory of Proton Transfer in Acid-Base Reactions

The existence of a qualitative correlation between the acid strength of a proton-containing species and its ability to act as a homogeneous catalyst in esterification or saponification reactions led Brønsted and Pederson (28) in 1924, as a result of their work on the decomposition of nitramide, to propose a quantitative relation between the "acid-base" strength of a species and its catalytic constant for a given reaction. A generalized acid-base proton transfer reaction may be written in the form

$$AH^+ + B \xrightarrow{k_{AH^+}} A + BH^+ \qquad [13]$$

It will be seen that a Brønsted type relation will be generally expected since the essential step in acid-base catalysis always involves the transfer of a proton between the catalyst and the substrate; similarly, the dissociation equilibrium involved in the characterization of the strength of an acid or base is represented by

$$K_{AH^+} = \frac{[A][BH^+]}{[AH^+][B]} \qquad [14]$$

for reaction [13] above and also involves the transfer of a proton; hence a comparison between the kinetic catalytic constants and the thermodynamic electrolytic dissociation constant constitutes a comparison between two closely related situations. Thus the Brønsted relation for acid catalysis in the above example is

$$k_{AH^+} = G_{AH^+} K^{\alpha}_{AH^+} \qquad [15]$$

where G_{AH^+} and α are constants for a given reaction, solvent, temperature, and series of similar catalysts. Here $0 < \alpha < 1$. The analogous relation for base catalysis is

$$k_B = G_B K_B^{\beta} = G_B \left(\frac{1}{K_{AH^+}} \right)^{\beta} \qquad [16]$$

where G_B and β have the same significance as G_{AH^+} and α.

The Brønsted relation can be interpreted in terms of potential-energy curves for proton transfer and was treated in these terms almost simultaneoulsy for the covalent state (2) and the ionic state (29). The situation may be depicted schematically as shown in Figure 7 typically for the covalent case since the arguments are

Figure 7

The relation between reaction velocity and equilibrium constants according to Bell. (Molecular basis for the Brønsted relation.)

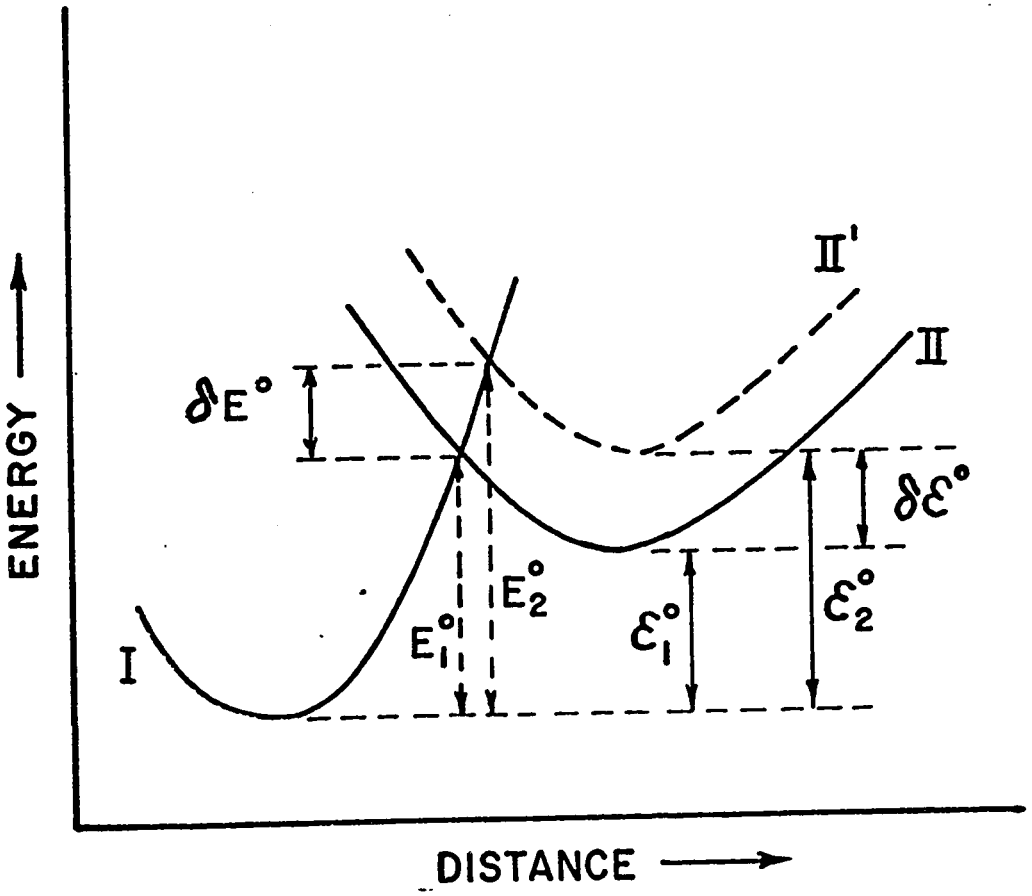
ENERGY
DISTANCE
I
II'
II
δE°
δℰ°
E₁°
E₂°
ℰ₁°
ℰ₂°

almost identical in both cases. The full curves represent the energy changes for a proton-transfer reaction. The proton moves from left to right in the diagram, so that curve I refers to that reacting species which is initially an acid: this may be either the catalyst (in acid catalysis) or the substrate (in base catalysis). The activation energy is then E_1° and the energy change in the reaction (energy absorbed) is ϵ_1°. Now suppose that the base involved is modified slightly in its proton accepting tendency by the introduction of a substituent group thus requiring curve II to be replaced by the slightly different curve II'. The new activation energy and overall free energy change in the reaction are now represented by E_2° and ϵ_2° in the diagram, and the changes produced in these quantities are indicated by δE° and $\delta \epsilon^\circ$. It is assumed that the two curves (II and II') maintain the same shape and relative position (this is not necessarily nor indeed likely to be exactly the case, cf. Badger's rule) and the same position along the reaction coordinate axis, and differ only in their relative vertical positions, or energies, in the diagram. It is thus clear from the geometry of Figure 7 that for small change δE° and $\delta \epsilon^\circ$, a relation of the form

$$\delta E^\circ = \alpha \, \delta \epsilon^\circ \qquad [17]$$

must result where $0 < \alpha < 1$. The numerical value of α depends on the relative slopes of the two curves at the point of intersection and, in particular, $\alpha = 0.5$ if the slopes are equal as in the case of electrochemical proton transfer illustrated in Figure 3.

The changes δE° and $\delta \epsilon^\circ$ can obviously be related, respectively, to the corresponding changes in the reaction velocity constant k (or the rate v) and the equilibrium constant K, and the simplest expressions are

$$\delta \log k = \frac{-\delta E^\circ}{kT} \qquad [18]$$

and

$$\delta \log K = \frac{-\delta \epsilon^{\circ}}{kT} \qquad [19]$$

where k is the gas constant per molecule. Equation [18] corresponds to the Arrhenius equation for the variation of a reaction velocity constant with temperature while equation [19] is related to the van't Hoff isochore for the variation of equilibrium constants with temperature at constant volume. Inserting these results in equation [17] gives

$$\delta \log \underline{k} = \alpha(\delta \log K) \qquad [20]$$

The parallelism between the relations of Figure 3, which provides a graphical basis for the interpretation of the symmetry factor β, and Figure 7 was pointed out by Frumkin (6) in 1933 following an earlier, less explicit analogy mentioned by Brønsted and Ross Kane (78).

In electrode kinetics, the change in potential modifies the activation energy by some fraction β of the change in overall electrochemical free energy in the reaction while a change in base strength in a series of conjugate acid-base pairs modifies the activation energy by some fraction α (the Brønsted exponent) of the overall free energy change in the acid-base reaction in a catalytic or normal proton transfer process. Potential energy diagrams showing this relation between the symmetry factor β in electrochemical kinetics and the α coefficient in Brønsted's relation, in connection with changes in free energy of activation, are presented in Figure 8.

f) Recent Theories of Proton Transfer in the H. E. R.

The above analogy between acid-base proton-transfer reactions and the discharge of hydrogen ions at a metal surface was employed by Salomon and Conway in 1965 (18) in proposing an alternative representation of the discharge step in the h. e. r. Their

Figure 8

Potential energy diagrams showing the relation between the symmetry factor β in electrochemical kinetics and the α coefficient in Brønsted's relation according to Conway.

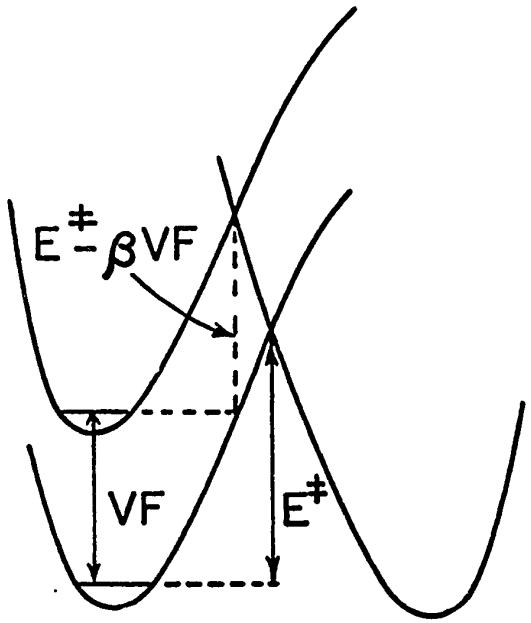

$H_3O^+ + e(M) \longrightarrow MH + H_2O$

(Electrode reaction)

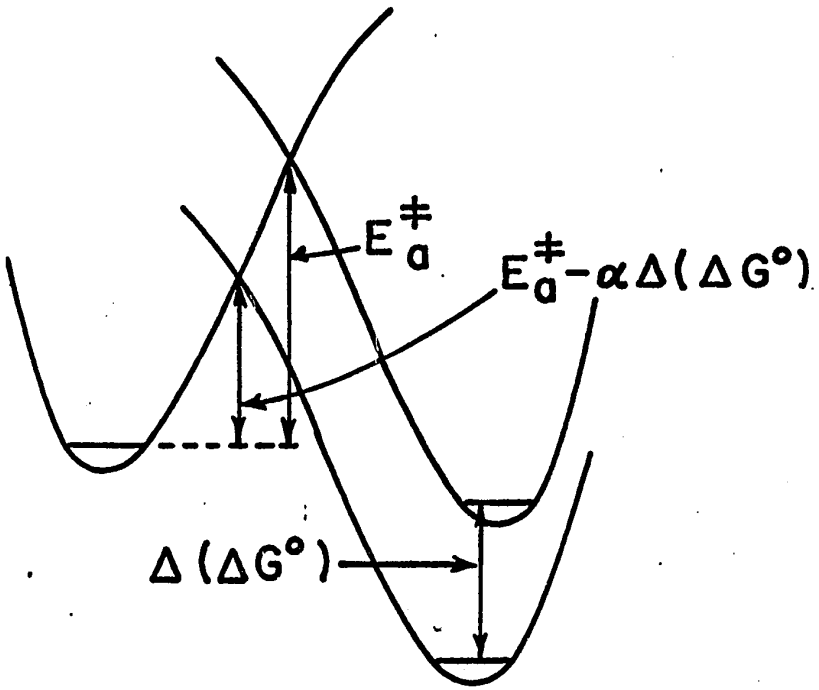

$BH^+ + A^- \longrightarrow B + AH$

(Brønsted acid-base)

treatment was developed on the basis of experimental results obtained at low temperatures as well as on the basis of theoretical considerations, The activated complex was regarded as analogous to that in acid-base proton-transfer processes with the electrode acting as a base of variable base strength, depending on the surface charge. The process of activation involves the motion of a proton over a potential energy surface in which the initial state is Hg (—) + H_3O^+ and the (excited) final state is Hg (—) H^+ + H_2O. At the activated state (i. e., the structure corresponding to the activated complex), a nonadiabatic electron transfer occurs and is associated with a crossing of potential energy surfaces to give the stable final state species, HgH.

More recently, in 1966, Bockris and Matthews (19) worked out in more detail a theory for the discharge step in the h. e. r. in which they considered both the H_3O^+ ion and the electron. This theory, although more elaborate, is in essence similar to that published by Conway and Salomon (18) in (1965).

According to Bockris and Matthews, the potential energy profile for electron transfer, e. g., in the discharge step of the h. e. r., may be represented as shown in Figure 9. The energy of the initial state, $H_3O^+ + Me^-$, with the reactants in their ground states, is represented by E_I. The energy of the neutralized state, M-H + H_2O with the H atom in the position immediately following neutralization (not necessarily the ground state of M-H), is represented by E_{II}.

The probability of electron tunneling from the metal to the H_3O^+ ion for an unactivated electron is zero if there is no acceptor state for the electron at the same energy. Thus, for neutralization of the H_3O^+ ion by transfer of an electron from the Fermi level of the metal, the energy ΔE (Figure 9), equal to $(E_{II} - E_I)$, must be decreased to zero. This is brought about by providing an activation energy corresponding to stretching of the H^+—OH_2 bond and amounting

Figure 9

Potential energy profile for electron transfer according to Bockris and Matthews.

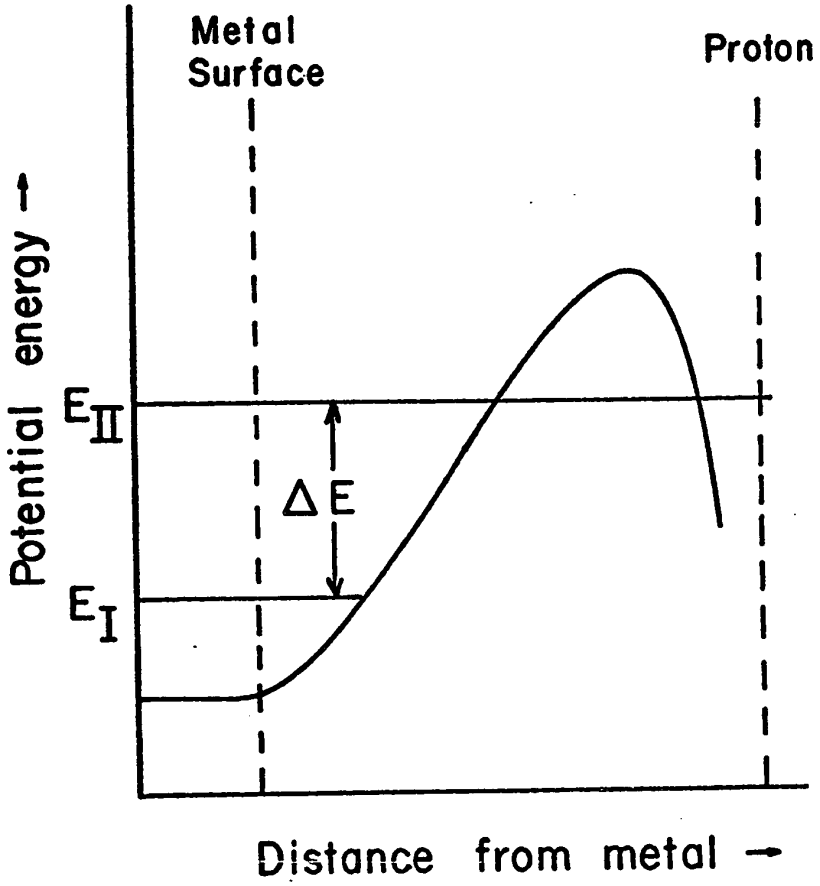
Metal
Surface
Proton
Potential energy →
E_{II}
E_I
ΔE
Distance from metal →

to an energy ΔE. Because stretching of the H^+——OH_2 bond is an activation of the initial state, but allows the resultant neutralized state to be attained, $\Delta \epsilon$ is equal to some fraction β of ΔE, where β can in general itself be a function of E. When the system reaches a condition such that $\Delta E = 0$, radiationless electron tunneling from the Fermi level* of the metal to the solvated proton can occur with a finite probability. The resulting H atom with respect to its interaction with the metal surface may then relax into the ground state of the system MH + H_2O assisted by the H——H_2O repulsion potential, or re-form a proton by electron tunneling to the metal. The discharge step of the h. e. r. may then be written as:

$$H_3O^+ + Me^- \rightleftharpoons [H_2O\text{--}H^+ + Me^-]^{\ddagger} \longleftrightarrow [H_2O + H\text{-}M]^{\ddagger};$$

$$[H_2O + H\text{-}M]^{\ddagger} \longrightarrow H_2O + MH \qquad [21]$$

The activated state is in effect comprised of two resonant states, with the same atomic but different electronic configurations [cf. Marcus 11, 12, 13, 14, 15].

Consideration of the relative electron tunneling probabilities from M to H^+ and H to M, leads to the conclusion that the resonant states are equally probable, and that the effective charge on the H nucleus in the transition state is 1/2 [cf. Hush (26)].

Application of an electrical potential difference $\Delta\phi$ changes the energy gap, ΔE, to $\Delta E_{(\Delta\phi)} = \Delta E + \Delta\phi F$ ($\Delta\phi$ being negative for cathodic potentials in cation discharge). The energy required to provide activation in the H^+——OH_2 bond is then $\beta\Delta E_{(\Delta\phi)}$. Thus, the activation energy at a given $\Delta\phi$ is $\beta\Delta E_{(\Delta\phi)}$ and β is the so-called

---

* A small distribution of electronic states is actually involved so that an integration to obtain the overall probability of electron transfer is required (cf. 1) taking into account also the distribution of energy amongst vibration-rotation states of the H_3O^+ ion.

symmetry factor discussed earlier. Since for the purpose of calculating β, only the energy required to stretch the H^+—OH_2 bond at a given $\Delta\phi$ is of interest, then β may be obtained by the usual method of "vertical shift" (2, 7, 9, 21) of the potential energy curves and the symmetry factor is independent of the charge distribution in the activated state. The symmetry factor at a given $\Delta\phi$ is thus the ratio of the energy involved in activating the H^+—OH_2 bond to that required to close the energy gap $\Delta E_{(\Delta\phi)}$ corresponding to neutralization of an unactivated initial state configuration. It should be noted however, that the representation of β in terms of $\Delta\epsilon/\Delta E$ considered here (see Figure 10 for schematic representation) is not quite identical with the one in terms of slopes discussed earlier (cf. Figure 3). This arises because $\Delta\epsilon/\Delta E$ can obviously have a certain value independent of how the curves actually tend to "cross" in the region of the transition state.

The above model relates the electron movement in charge transfer to that of the ion-solvent and resulting neutral atom-substrate configurations. Means other than the mechanism described above for closing the energy gap $\Delta E_{(\Delta\phi)}$, such as electron activation (cf. Gurney, ref. 1), solvent activation* (19), or activation of modes other than the H^+—OH_2 stretching mode, may lead to higher energies of activation by virtue of the fact that the condition $\Delta\epsilon \approx \Delta E_{(\Delta\phi)}$ would hold for such processes rather than the relation $\Delta\epsilon = \beta\Delta E_{(\Delta\phi)}$.

In summary, the theory discussed above leads to conclusions regarding the charge on the activated state and the significance of the symmetry factor.

---

* It seems, contrary to what these authors (19) have stated, that appropriate solvent activation around H_3O^+ could lead to an equivalent activation with resultant electron transfer at similar activation energies.

Figure 10

Schematic representation of β in terms of the ratio $\Delta \epsilon / \Delta E$.

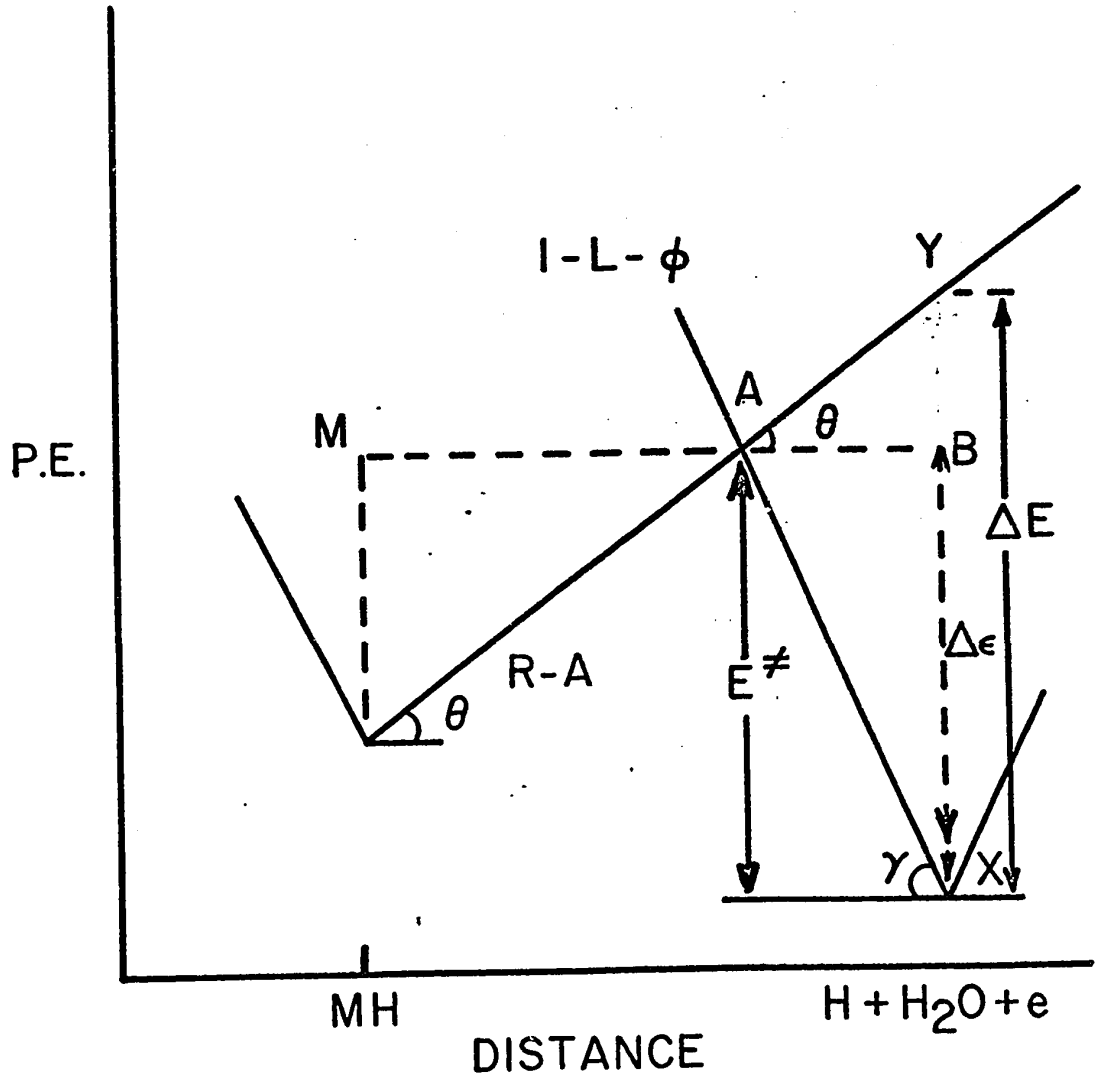

$\beta = \Delta\epsilon / \Delta E$

$\Delta\epsilon = AB \tan \gamma$

$\Delta E = AB \tan \gamma + AB \tan \theta$

Finally, a diagram showing the essential features of the process of proton transfer and neutralization (1, 3, 18, 19) discussed in the preceding pages is given in schematic form in Figure 11. Also it may be noted that while field effects are expected to be significant for transfer of a charged species such as the proton in H^+OH_2, they play a minor role in causing changes of energy of uncharged species such as Hg-H. If the field effect were significant, a linear Tafel relation would not, in fact, be found (96).

g) The Role of Proton Tunneling in the H. E. R.

In any discussion of proton transfer, an examination of the significance of proton tunneling must be included. This requirement arises owing to the small mass of the hydrogen nucleus. Thus, the possibility of quantum mechanical effects arising from tunneling was recognized by Wigner (32) and Bell (33) as a significant factor to be considered in the kinetics of chemical reactions involving H or D.

Bell, using an exact solution for the permeability of the activation energy barrier according to Eckart's (34) function, calculated the effect of tunneling for a hypothetical proton transfer reaction and found that the rate of the process should be increased if participation of tunneling is appreciable, particularly at low temperatures.

The potential energy function used is given by

$$V(x) = \frac{A \exp 2\pi x/L}{1 + \exp 2\pi x/L} + \frac{B \exp 2\pi x/L}{(1 + \exp 2\pi x/L)^2} \qquad [22]$$

where A is the energy change in the reaction, 2L is the barrier width, B is equal to $4E^{\ddagger}$ where $E^{\ddagger}$ is the activation energy.

The permeability function G(w) (or probability of tunneling per approach of the particle to the barrier) was given by Eckart as

Figure 11

Essential features of the process of proton transfer and neutralization.

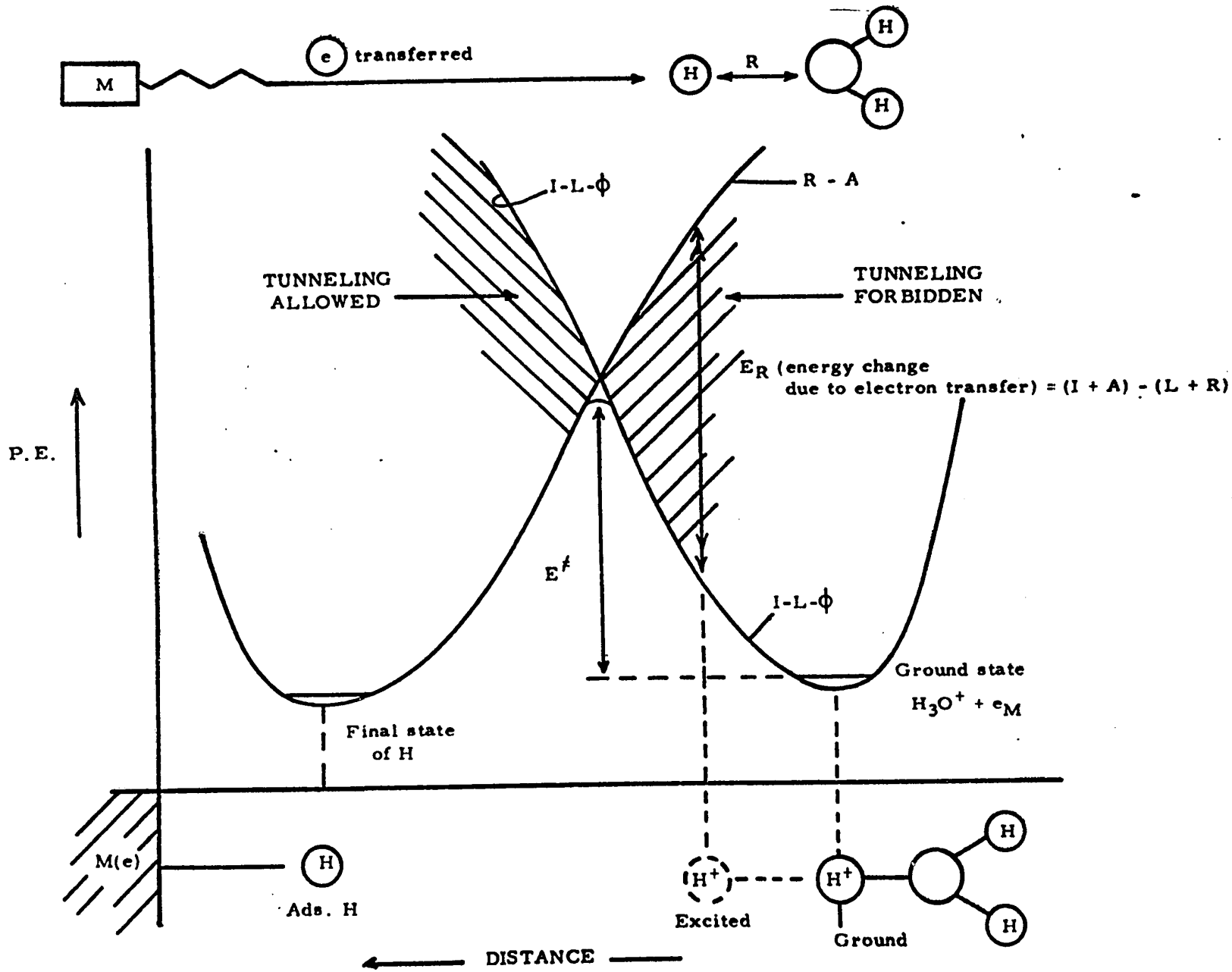
M
e transferred
H
R
H
H
I-L-ϕ
R - A
TUNNELING ALLOWED
TUNNELING FORBIDDEN
E_R (energy change due to electron transfer) = (I + A) - (L + R)
P.E.
E^f
I-L-ϕ
Ground state
$H_3O^+ + e_M$
Final state of H
M(e)
H
Ads. H
H^+
Excited
H^+
Ground
H
H
DISTANCE

$$G(w) = \frac{\cosh 2\pi(\alpha + \beta) - \cos h\, 2\pi(\alpha - \beta)}{\cosh 2\pi(\alpha + \beta) + \cos h\, \pi\left[\frac{B-C}{C}\right]^{1/2}} \qquad [23]$$

where $\alpha = \frac{L}{h}\sqrt{2mW}$, $\beta = \frac{L}{h}\sqrt{2m(W-A)}$, $C = \frac{h^2}{8mL^2}$ and W is the energy of the particle of mass m approaching the barrier.

Bell (35) also treated in terms of an approximation the case of a parabolic energy barrier, the equation for which is given by

$$V(x) = E^{\ddagger}\left(1 - \frac{x^2}{L^2}\right) \qquad [24]$$

and the corresponding permeability function is

$$G(w) = \frac{\exp[-2\pi^2 L(2m)^{1/2}(E^{\ddagger} - w)]}{h(E^{\ddagger})^{1/2}} \qquad [25]$$

These calculations gave, qualitatively, the same results as those for the Eckart barrier although the following approximations were involved:

(a) A parabola is representative of the shape of the real energy barrier only near the saddle point but is inadequate at the bottom of the energy wells corresponding to the initial and final states of the reaction. In this respect, Eckart's barrier function represents the initial state region better.

(b) The possible reflection of particles at the saddle point was not taken into account since it is assumed that all particles having energy W equal to, or greater than, $E^{\ddagger}$ will cross the barrier, i.e., $G(w) = 1$ for $W \geq E^{\ddagger}$. However, calculations show that these approximations are not unsatisfactory since, at the most, there is an error by a factor of two in G(w) values calculated using this approach compared with the values obtained for a corresponding Eckart barrier.

The permeability, G(w), can be related to the rate of reaction using the Boltzmann distribution law. Out of an assembly of N_o particles, the relative number of N/N_o of particles crossing the barrier is given by

$$\frac{N}{N_o} = \frac{1}{kT} \int_{E^{\ddagger}}^{\infty} \exp - W/kT, dW \qquad [26]$$

The tunneling correction for the above equation is

$$\frac{N}{N_o} = \frac{1}{kT} \int_{O}^{\infty} G(w) \cdot \exp - W/kT, dW \qquad [27]$$

Using the permeability function G(w), Bell deduced a rate expression, related to N/N_o given by

$$q = \frac{1}{\beta - \alpha} [\beta e^{-\alpha} - \alpha e^{-\beta}] \qquad [28]$$

where q is the rate constant for the reaction,

$$\beta = 2\pi^2 L(2mE^{\ddagger})^{1/2}/h \quad \text{and} \quad \alpha = E^{\ddagger}/kT \ .$$

The β term here will not easily be confused with the symmetry factor discussed above.

In 1959, Bell (172) obtained an improved solution to the problem by no longer assuming G(w) = 1 for $W \geq E^{\ddagger}$, and by using the function

$$G(w)' = [1 + \exp \frac{2\pi(E^{\ddagger} - W)}{h}]^{-1} \qquad [29]$$

with the curvature at the saddle point expressed in terms of a frequency

$$\nu^{\ddagger} = \frac{(E^{\ddagger})^{1/2}}{\pi L (2m)^{1/2}} \qquad [30]$$

From the above expression he derived the ratio of quantum (i.e., if the process occurred wholly by quantum-mechanical tunneling) to classical rate constants as

$$Q = \frac{k_{quant}}{k_{class}} \cdot \frac{\mu}{2 \sin \mu/2}$$

where $\mu = \frac{2\pi a}{\beta} = \frac{h\nu^{\ddagger}}{kT}$. The above result is a good approximation when $\mu < 2\pi$ and $a > \beta$. Also $E^{*} - E^{\ddagger} = kT[\frac{\mu}{2} \cot \frac{\mu}{2} - 1]$ where E^{*} is the apparent experimental and $E^{\ddagger}$ the true energy of activation.

As a result of these theoretical calculations, Bell proposed that the following experimental results (which will be examined further in Chapter 2) should appear if tunneling is significant.

(i) The apparent energy of activation E^{*} will vary with temperature, and at relatively low temperatures, the reaction velocity will tend to reach an almost constant value. This point will be discussed in more detail in Chapter 2.

(ii) If it is possible to calculate the height of the barrier, $E^{\ddagger}$, from theoretical considerations, the value obtained will be greater than the apparent activation energy $\Delta H^{\ddagger}$ calculated from the temperature coefficient of the rate constant (measured at constant pressure).

(iii) The observed value of q will be equal to neither $e^{-E^{\ddagger}/kT}$ nor $e^{-E^{*}/kT}$; for bimolecular reactions this may lead to discrepancies between the observed reaction rate and the rate calculated by classical formulae from the collision number and $E^{\ddagger}$ or E^{*}.

Several attempts have been made to find experimental indications of significant tunnel effects and some evidence has been

given for quantum-mechanical tunneling of H ions or atoms in the following reactions: (a) the inter-conversion of ortho and para hydrogen (33, 36); (b) the rate-determining proton transfer step in the bromination of 2-carbethoxy-cyclopentanone (37); (c) the proton conductance of water and ice (38, 39, 40); (d) the base-catalyzed elimination reaction involving 1-bromo-2-phenyl propane and its 2-deutero and tritium analogues studied by Shiner and Smith (41) where the isotopic effects (42) confirmed that tunneling occurred; (e) the proton exchange in nitropropane in the presence of pyridine bases where Funderburk and Lewis (43) found large H/D isotope effects, the values increasing with the molecular complexity of the base, thus indicating a relation between steric hindrance and tunneling; and (f) the bromination and detritiation of orthomethyl-acetophenone where Jones and co-workers (44) found an activation energy difference $\Delta H_T^{\ddagger} - \Delta H_H^{\ddagger}$ equal to 3.4 kcal. mole^{-1} and a frequency factor ratio $3A_T/A_H = 16$ (see also ref. 79); also a curved Arrhenius plot for the deprotonation was observed at the lowest temperatures; all these factors indicated appreciable participation of proton tunneling.

Proton tunneling in the ion-discharge step of the h. e. r. was first discussed by Bawn and Ogden (45) and by Appelby and Ogden (46) following the work of Bell (33, 35, 37), but in the early calculations (45), too wide a potential barrier was considered. The high values of the separation factor*, S, obtained by Appelby and Ogden and claimed to support a proton transfer via tunneling have never been confirmed.

---

*The protium-deuterium separation factor is defined by

$$S_{H,D} = (C_H/C_D)_{gas}/(C_H/C_D)_{Soln.}$$

where $(C_H/C_D)_{Soln.}$ and $(C_H/C_D)_{gas}$ are the ratios of the concentrations of protium to deuterium in the solution being electrolyzed and in the gas produced by electrolysis, respectively.

Christov (25, 47, 48, 49) has dealt extensively with the subject of proton tunneling in the h. e. r. using the notation

$$i_q = i' + i'' \qquad [32]$$

where i' is the "penetration current" and i'' the "reflection current" corresponding to passage of particles below and above the barrier maximum, respectively. Based on a calculation of Tafel parameters and their dependence on the barrier parameters, Christov (47) concluded that for the h. e. r. at Hg the penetration current was not negligible. He proposed a characteristic temperature T_k at which $i'/i_q = 0.5$ as a criterion for proton tunneling. In the region of large tunnel effects the Tafel slope was found to be always greater than b_{cl} and to become independent of temperature when passing from the region of moderate to that of high tunnel effects. Similarly, the reaction rate was found to be independent of temperature in this region. The above conclusions were based on a parabolic barrier. For an Eckart barrier the increase of b, compared with b_{cl}, with decrease of temperature was found to be more gradual than for the case of the parabolic barrier and b was found to be temperature dependent in the same region where appreciable degrees of proton tunneling occurred. The effective activation energy decreased slowly as the temperature decreased, so that the rate of the process remained temperature dependent even under conditions where moderate and high tunnel effects were involved.

Christov (48) made calculations for activation energies, pre-exponential factors, and separation factors in terms of barrier height and width and obtained agreement with the experimental results of Post and Hiskey (50) using an Eckart barrier of height 1.6×10^{-12} erg and width $2d = 4.7$ Å. This work has been criticized by Bockris and Matthews in 1966 (51) on the basis that the contributions made by zero-point energy differences in the initial and

activated state, which Conway first took into account in 1959 (40), were neglected and that the distance 2d = 4.7 Å was equated by Christov to the "width" of the double-layer; the proton-transfer distance is not equal to the Eckart barrier width nor is it equal to the effective "width" of the double-layer. Similarly, the parameters taken for the parabolic barrier treatment were: barrier height = 1.6×10^{-12} erg and width 2d = 1.65 Å. Since this value of 1.65 Å was in good agreement with the Helmholtz double-layer width (1.75 Å) accepted at that time, Christov favored the parabolic over the Eckart barrier as a basis for calculating the tunnel effects.

Although Christov was the first to show the tunneling Tafel relation, Conway (40) demonstrated the mass dependence of the slope b and also examined the case where a quantized distribution might be involved in the OH vibrations of the proton donor. The mass dependence of b was also suggested as a critical criterion for the detection of proton tunneling. The slopes calculated by Conway (40) for a particular barrier width are consistent with a general relation obtained by Christov (47).

The mass dependence of the Tafel slope, b, according to Conway (40) who based his calculations on an Eckart barrier width of 0.5 A, is shown in Figure 12, where the logarithm of the integral tunneling probability (to which the electrochemical proton transfer rate is proportional) is plotted as a function of the electrode potential for proton and deuteron transfer at Hg. At intermediate electrode potentials, a linear $\Delta\phi$ - log [rate] relation is predicted, i.e., the Tafel equation holds as in classical proton transfer at an electrode. At very low potentials, Ohm's law is obeyed and hence a linear $\Delta\phi$ - [rate] law is followed, again as in the classical theory. In the potential range where the behavior is approximated by the Tafel equation, the slope b of the $\Delta\phi$ - log [rate] relationship has a value of about 0.25 for proton discharge and 0.17 for deuteron

Figure 12

Tunneling probability and electrode potential according to Conway.

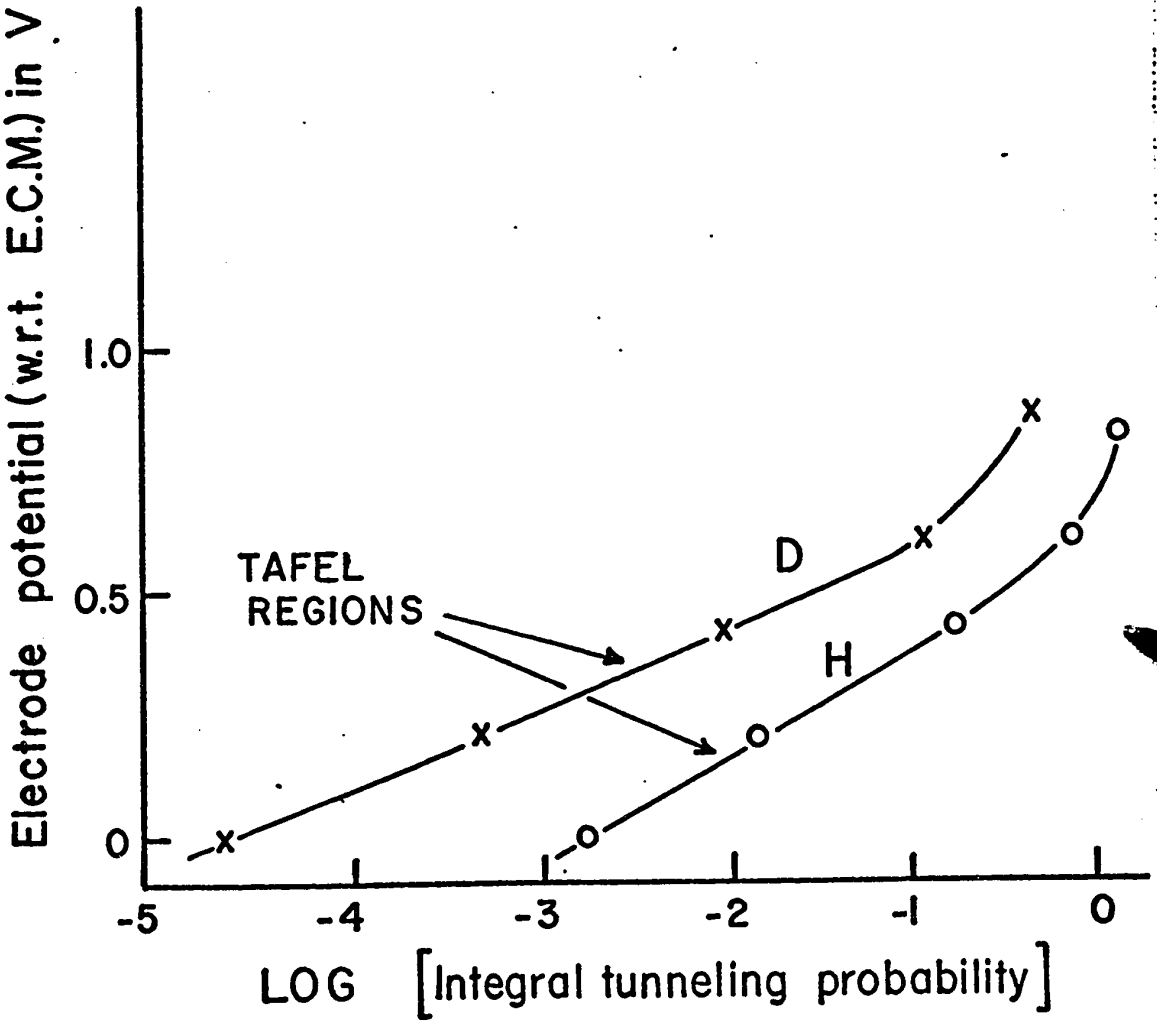
Electrode potential (w.r.t. E.C.M.) in V
1.0
0.5
0
TAFEL
REGIONS
D
H
-5
-4
-3
-2
-1
0
LOG [Integral tunneling probability]

discharge. Thus, the values of these Tafel slopes would be diagnostic for tunneling transfer, since slopes as high as this do not follow from any mechanism yet proposed for the h. e. r., assuming $\beta \neq 0.5$.

In work with Conway, Belanger (52), using the previously discussed model (40), calculated the Tafel parameters with the barrier width taken as the variable parameter. The results are shown in Figure 13. A Tafel relation is observed over part of the curve and again anomalously high values of b arise. The real barrier width was estimated for proton discharge at Hg by the following calculation illustrated by Figure 14. The proton transfer distance is

$$2d = r_{OH} + r_{H} + r_{Hg} - r_{OH} - r_{HgH} \qquad [33]$$

Using the appropriate r values, 2d becomes 0.5 - 0.55 Å. For these values it is found that b is much higher than the values observed experimentally. For b values corresponding to the experimental ones, the Eckart barrier width is about 1.5 Å.

The b values for H and D transfer (Eckart barrier width = 1.5 Å) were also calculated as a function of temperature and were found to decrease with decreasing temperature as shown in Figure 15. However, the rate of decrease is less than that for the classical relation. Thus, it is concluded that the difference in b values for H and D transfer should be large enough to be detected experimentally.

Bockris and Matthews (51) applied the quantum-mechanical theory of tunneling to the proton-discharge step in the h. e. r. using an unsymmetrical Eckart barrier with allowance for zero-point energies (cf. 40). They calculated the quantum-mechanical rate, i_q, for a large number of combinations of barrier width, barrier height, heats of reaction, and temperatures for a large range of potential for protium, deuterium and tritium. From these results, the

Figure 13

Electrode potential $\Delta\phi$ versus Log (Integral Tunneling Probability) plot for various barrier widths at 298°K for hydrogen transfer according to Belanger.

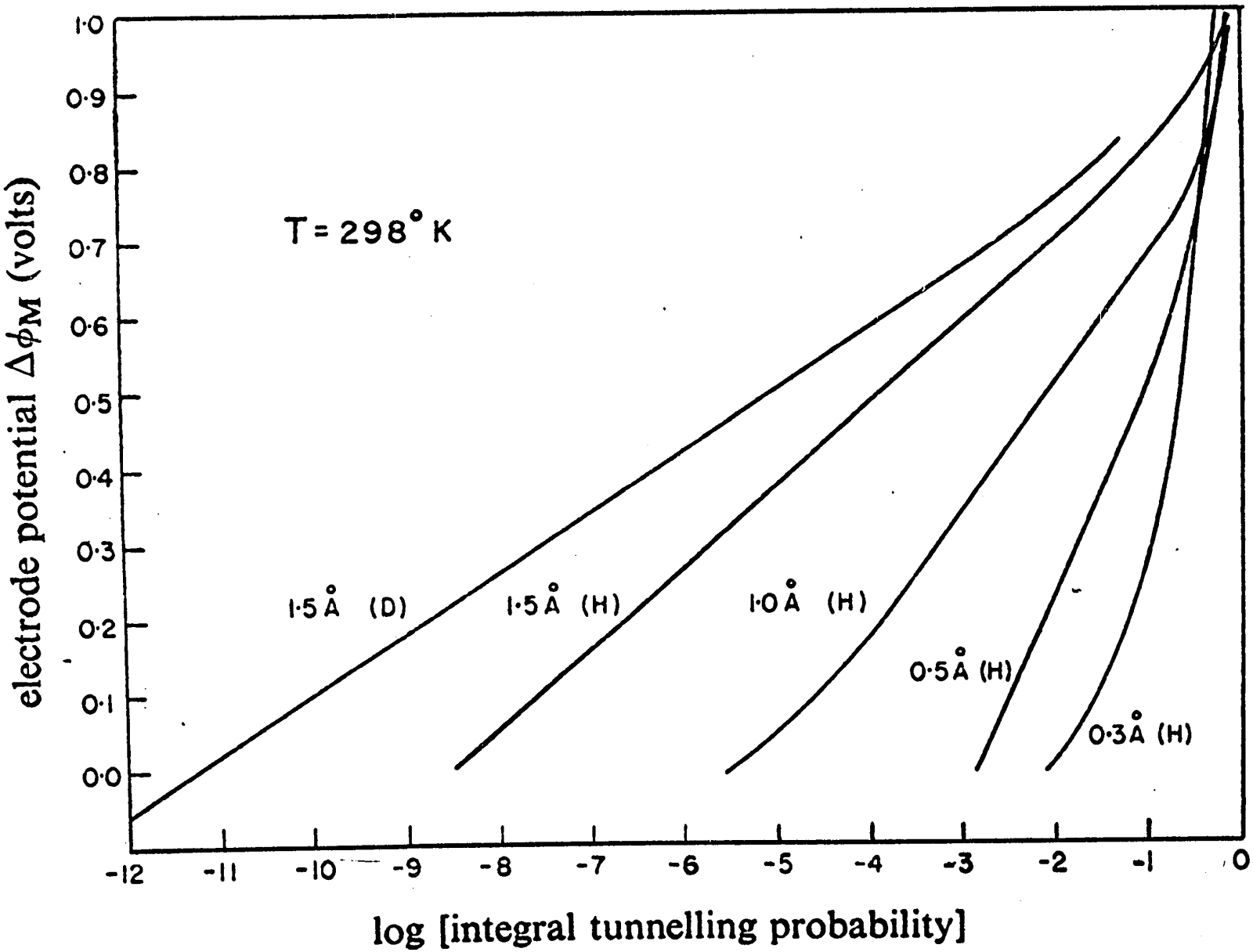
T = 298° K
1·5 Å (D)
1·5 Å (H)
1·0 Å (H)
0·5 Å (H)
0·3 Å (H)
electrode potential $\Delta\phi_M$ (volts)
log [integral tunnelling probability]
1·0
0·9
0·8
0·7
0·6
0·5
0·4
0·3
0·2
0·1
0·0
-12
-11
-10
-9
-8
-7
-6
-5
-4
-3
-2
-1
0

Figure 14

Schematic representation of the distance travelled by H^+ during the charge transfer process according to Conway.

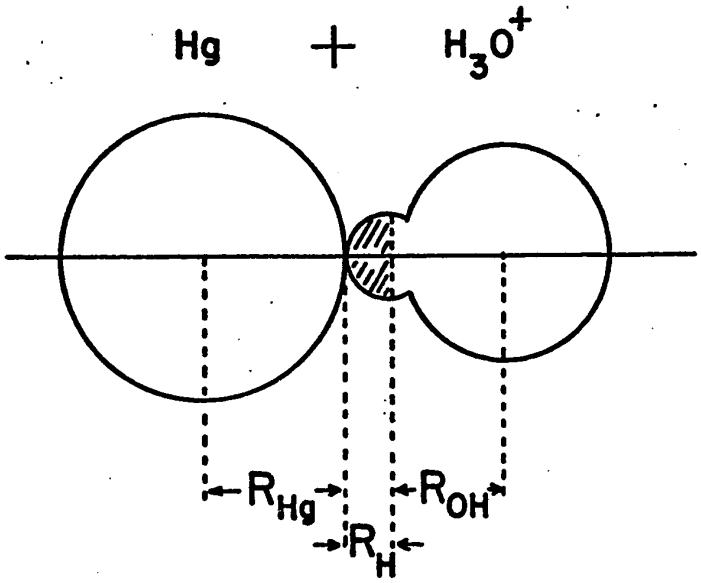
Hg + H_3O^+
R_{Hg}
R_H
R_{OH}

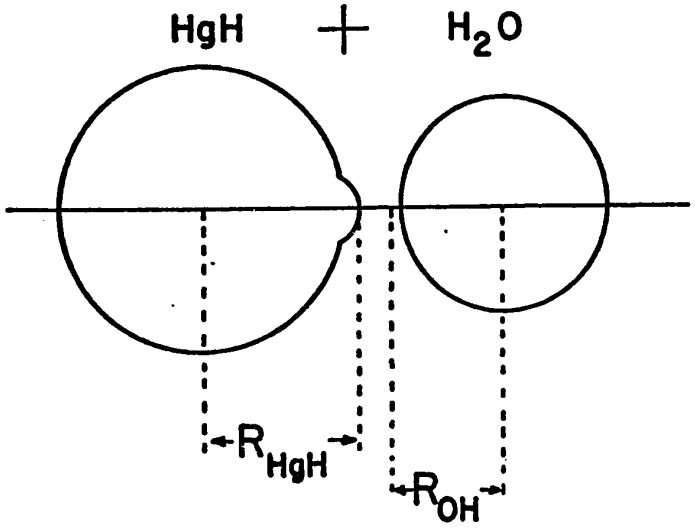
HgH + H_2O
R_{HgH}
R_{OH}

Figure 15

Tafel constant b versus temperature according to Belanger. (Classical values and calculated values with $2L = 1.5$ Å for H and D transfer.)

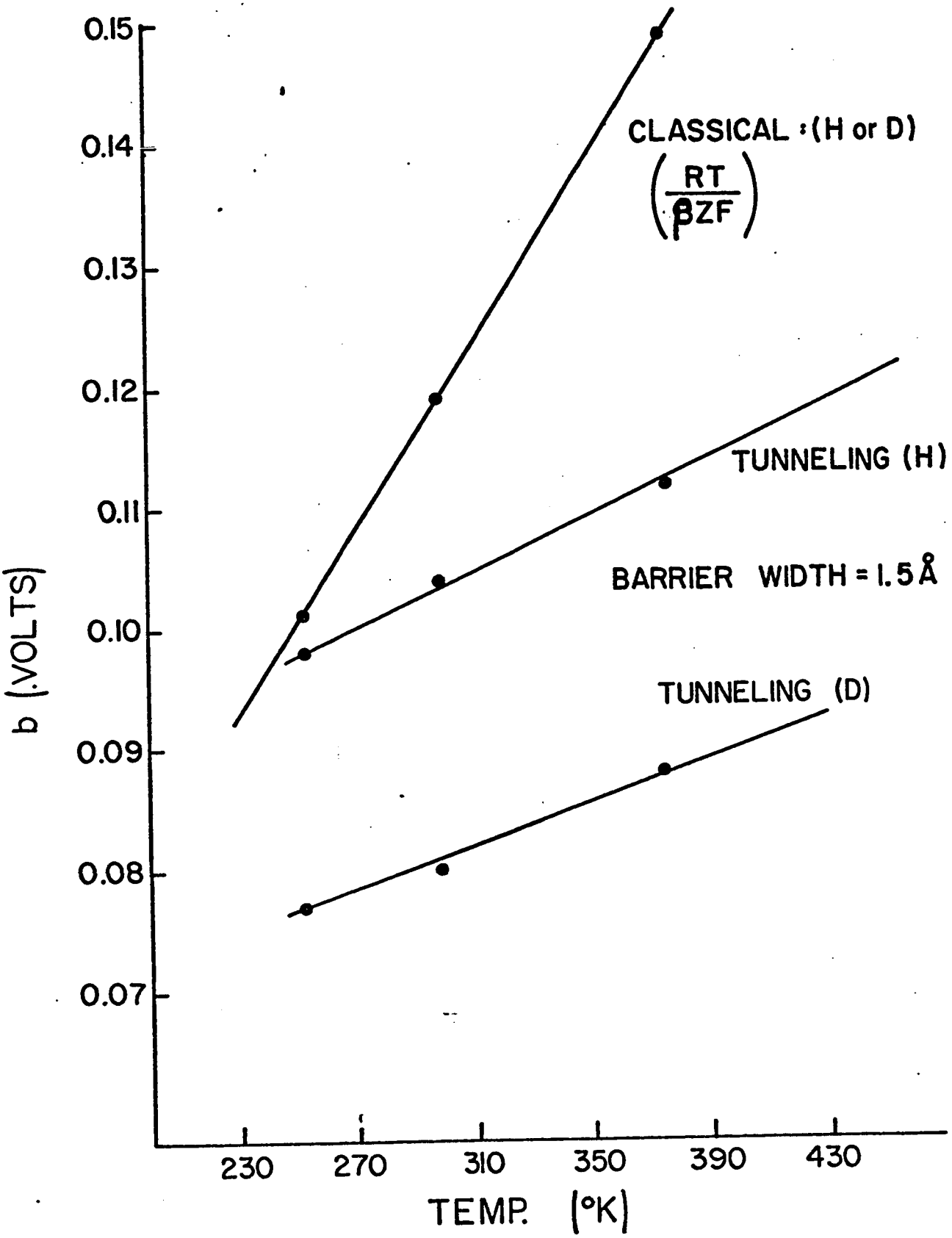
0.15
0.14
0.13
0.12
0.11
0.10
0.09
0.08
0.07
b (VOLTS)
CLASSICAL : (H or D)
$\left(\frac{RT}{\beta ZF}\right)$
TUNNELING (H)
BARRIER WIDTH = 1.5 Å
TUNNELING (D)
230
270
310
350
390
430
TEMP. (°K)

quantum-mechanical transmission coefficient τ ($\tau = i_q/i_{cl}$) and the quantum-mechanical correction Γ ($\Gamma = S/S_{cl}$) to the separation factor, the Tafel slopes and the activation energies were calculated. By an empirical treatment of the observed values of $S_{H,D}$ and $S_{H,T}$ as a function of temperature and potential, the most probable values of the barrier parameters were obtained. These values were tested by comparison of calculated and observed (apparent) activation energies, Tafel slopes, $S_{H,D}$ as a function of potential, and the observed rate of hydrogen evolution at high cathodic overpotentials as a function of temperature. It was concluded that the degree of proton tunneling was 69% at a cathodic overpotential of 1 volt for Hg in acid solution.

Thus, the following criteria for proton tunneling in the discharge step of the h. e. r. may be summarized:

1. As in homogeneous proton-transfer reactions, a non-linear Arrhenius plot should be observed, especially at low temperatures.

2. Anomalously high Tafel slopes should arise at room temperature with $b_H > b_D$ if appreciable participation of the tunneling process is occurring.

3. Anomalous temperature dependence of Tafel slopes should arise with b decreasing with decreasing temperature and the rate of decrease should be much <u>less</u> than that expected from completely classical behavior.

4. There should be an appreciable dependence of $S_{H,D}$ and $S_{H,T}$ on potential, with $S_{H,D}$ and $S_{H,T}$ decreasing with increasing potential, the effect being more pronounced for $S_{H,T}$.

A quantum-mechanical tunnel effect for proton transfer in homogeneous acid-base reactions has been proposed recently by Weiss (53), and as in the theory of electrochemical tunneling of Conway, the case of transfer <u>wholly</u> by tunneling was considered.

The treatment was based on a model in which the proton transfer was envisaged as proceeding along a hydrogen bond between the two reactants with a proton transfer distance of only 0.4 to 0.6 Å. (cf. 40). On the basis of this model, calculations were carried out using a one-dimensional Eckart barrier and the apparent activation energy for the proton transfer was identified with a quantity of energy at least equal to Q, the endothermicity of the reaction:

$$AH + B \longrightarrow A + HB - Q \qquad [34]$$

This model led to an expression for the rate constants that gave a reasonable account of the observed isotope effect. Moreover, a Brønsted-type relation was also obtained from this theory without any further à priori assumptions regarding relations between activation energies and free energy changes in the overall reaction. As a first approximation from the equation for the rate constant for proton tunneling, Weiss obtained theoretically a Brønsted coefficient given by

$$\alpha = 1 - (2\rho\, kT/Q^{1/2}) \qquad [35]$$

where $\rho = (a/h)(2M)^{1/2}$, and 2a denotes the barrier width and M is the mass of the proton (or deuteron). Q is an energy change in the reaction, i.e., the difference between the proton affinities of the donor and acceptor molecules. Thus α depends in fact on the value of the energy difference Q. Approximate constancy of α within a certain series therefore presupposes an approximately constant value of Q, otherwise there should be a variation of α with the value of Q. Eigen (54) has discussed the variation of α with the pK difference of the proton donor and acceptor. His results are fully compatible with the above equation since Q, which reflects the difference in the proton affinities of donor and acceptor, is directly related to the difference of their pK values.

h) The Role of the Solvated Electron in the H. E. R.

Recently, Walker (55), on the basis of kinetic studies, proposed that the hydrated electron (e^-_{aq}) is the reactive intermediate in the following reactions commonly regarded as involving electrolytic evolution of H_2 by the usual proton neutralization mechanism:

(i) reaction between an alkali metal and H_2O (conversion process giving H_2 by the component cathodic reaction $H_2O + e \longrightarrow OH^- + \frac{1}{2}H_2$).

(ii) the cathode reaction itself in the electrolytic decomposition of H_2O with an applied voltage, and

(iii) reduction of H_2O by a cation having an oxidation potential > 0.413 V, e.g., U^{3+}, Cr^{++}. Subsequently, Walker (56) claimed to have corroborated these views by producing what he regarded as spectroscopic evidence for hydrated electrons near silver cathodes in the a.c. electrolysis of water. This led to the proposal that the primary cathode process in the electrolysis of neutral water is

$$e^-_{cathode} \xrightarrow{H_2O} e^-_{aq} \qquad [36]$$

rather than

$$e^-_{cathode} + H^+ \longrightarrow H_{ads.} \ (\longrightarrow \tfrac{1}{2}H_2) \qquad [37]$$

This led to further speculation about the possible general importance of the solvated electron in the h. e. r.

These views are obviously of the greatest importance in regard to the mechanism of the h. e. r. which has been treated in completely different terms over at least the past sixty-four years. It will be desirable to give in a later section of the thesis (Discussion chapter) some further critical examination of the ideas that have been proposed regarding the role of e^-_{aq} in cathodic processes, particularly

as certain of the views that have appeared in the literature (see Chapter V) have been expressed without proper recognition of some of the basic electrochemical principles that may be involved. However, before proceeding further with a critical discussion of this matter in the "Discussion," it is necessary to refer here to several other papers in which the possible role of e^-_{aq} in electrode reactions has been considered.

Hills and Kinnibrugh (57) measured the pressure coefficient of the rate of the hydrogen electrode reaction at Hg and found the (apparent) volume of activation ($\Delta V^{\ddagger}$) to be negative (-3.4 ml. mole^{-1}). They explained this result* by suggesting that the rate-determining step in the h. e. r. at Hg is

$$e^-(\text{metal}) \longrightarrow e^-_{aq} \qquad \text{(cf. [36])}$$

i. e., the emission and hydration of electrons from the metal. However, in the subsequent discussion which followed this paper (presented initially at a Symposium, 57), a number of authors, namely Kristalik, Parsons, Conway and Marcus offered alternative explanations which would resolve the problem of this negative value in a manner not inconsistent with previously proposed mechanisms for the h. e. r. In particular, Conway (100) had previously pointed out the necessity for allowing for the pressure dependence of the reversible potential of the reference electrode.

Pyle and Roberts (58) also proposed that the hydrated electron plays an important role in the h. e. r. and suggested that the production of H_2 molecules is due to the reaction

$$e^-_{aq} + e^-_{aq} \longrightarrow H_2 + 2\,OH^- \qquad [38]$$

---

* That a special explanation is required follows from the fact that the $\Delta V^{\ddagger}$ for ion neutralization reactions is usually positive owing to loss of the electrostriction.

The OH^- ions produced by the above reaction formed, they supposed, a "film" (sic) across the metal surface and it is the dissolution of this film which, they suggested determines the characteristics of the hydrogen evolution process. In support of this claim, they cited the following: (a) calculations on the rates of dissolution of iron in acids made on the basis of this model show good agreement with experimentally observed rates; and (b) the activation energies for the dissolution of the hydroxide film on iron and mercury, estimated from the dissociation constants of the hydroxides, are 11.4 and 19 kcal. $mole^{-1}$, respectively. These values, they claimed, compared favourably with the observed activation energies for the dissolution of iron, viz., 11.5 kcal. $mole^{-1}$, and for hydrogen evolution at a mercury surface, 22 kcal. $mole^{-1}$. It was concluded that this mechanism could play a significant role in the h.e.r. at metal surfaces that do not strongly adsorb hydrogen. However such a mechanism seems more likely for alkali metals undergoing reaction with liquid ammonia or perhaps with aqueous media. Further original discussion of this matter, based on a paper submitted for publication, will follow in Chapter V.

i) Remaining Problems in Electrochemical Proton Transfer

The theory of charge transfer in electrode kinetics, especially for the h.e.r., remains one of the principal difficulties in this subject, although much work has been done during the past decade. Although there has been an appreciable amount of theoretical work devoted to the question of molecular significance of the symmetry factor β, the experimental determination of this quantity and in particular its temperature dependence has been much neglected. In general, the conventional and classical value of $\beta = 0.5$ at all temperatures is really the exception rather than the rule as has been found in the present work; in fact, the validity of using the

expression

$$\beta = 2.3\,RT/bF$$

to evaluate this quantity is open to question as is shown in the present work to be described below.

Also, there exists the theoretical problem of explaining adequately why β should be constant over such wide ranges of potential and why β is apparently (but see Chapters IV and V) approximately equal to 0.5 near room temperature for quite a wide variety of electrode reactions.

Despite the recent theoretical and experimental work on the h. e. r. with regard to proton tunneling, no definite agreement on the significance of this aspect of the problem has yet been reached. In order to confirm significant extents of proton tunneling for the discharge step in the h. e. r., it is necessary to measure Tafel parameters, activation energies and separation factors at low temperatures in the absence of vitiating effects such as specific adsorption which render uncertain the significance of such experiments as those of Bockris and Matthews (83) in strong aq. HCl solution.

The more recent proposal that the hydrated electron plays an important role in the h. e. r. presents new problems, especially since this idea is completely foreign to any electrochemical theory yet proposed for this reaction. In the light of recent experimental work, however, such a possibility must be considered, although as in the case of proton tunneling, more experimental work is required before the significant role of the solvated electron in the h. e. r. can be accepted.

CHAPTER II

ACTIVATION ENERGIES IN ELECTROCHEMICAL REACTIONS

a) Introduction

Determinations of heats of activation ("activation energies") and deductions of frequency factors from the Arrhenius rate equation provide a useful characterization of chemical reactions. The Arrhenius equation is of the form

$$k = A \exp[-\Delta H^{\ddagger}/RT] \qquad [39]$$

where k is the rate constant, A the frequency factor and $\Delta H^{\ddagger}$ is the experimental heat of activation i. e., under constant pressure conditions.

In electrochemical reactions, the measurement of a single activation energy has little significance in regard to the provision of mechanistic information. However, for the same overall reaction proceeding at different metals (e. g., the h. e. r.), the differences of true activation energies and the ratio of true frequency factors can be deduced and are useful in indicating, for a given reaction, if different mechanisms operate at a series of metals (59), or if there is a progressive change of $\Delta H^{\ddagger}$ for a given mechanism with changes from one metal to another. Also, measurements of activation energies and frequency factors for isotopically analogous systems proceeding at the same metal (e. g., the "h. e. r." with H or D species) are useful quantities for testing whether tunneling is significant in H^{+} and D^{+} transfer steps (31).

b) Significance of $\Delta H^{\ddagger}$ in Relation to Temperature Variation of E_H

(i) Temperature dependence of reference electrode potential

Although electrochemical activation energies have often been measured (60), their significance is obscured by the complication that they must be deduced from measurements of current densities at constant electrode potential referred to a reversible reference electrode in the system; alternatively, they can be deduced from temperature coefficient of overpotential at constant current density and the overpotential is of course referred to the potential of the reversible electrode. In both cases, as the temperature of the system is varied, the absolute value of the metal-solution potential difference of this reference electrode will vary in an experimentally undeterminable manner. Although the standard value of the potential of the hydrogen electrode is arbitrarily taken to be zero at all temperatures, the reversible hydrogen electrode, if used, will have a finite absolute temperature coefficient of e.m.f. associated with the entropy change in the half-cell reaction

$$H_3O^+ + e^- \longrightarrow H_2O + \tfrac{1}{2}H_2 . \qquad [40]$$

If the reference electrode is maintained outside that part of the cell where the temperature of the test electrode is varied, an unknown electrolytic thermal junction potential (61) will be included in the measured e.m.f. Thus, a true heat of activation cannot be determined at constant electrode potential, and only an apparent heat of activation at constant overpotential referred to the temperature dependent reversible potential of the reaction being studied may be derived.

The relationship between the true and experimentally accessible apparent heat of activation at constant overpotential (η) was first considered by Temkin (62) and presented more directly in

an alternative form by Conway (63) as follows: the electrochemical rate constant $\bar{k}$ for an ion neutralization process at a given ionic concentration may be written as

$$\bar{k} = \frac{kT}{h} \exp\left[\frac{-\Delta G^{o\ddagger}}{RT}\right] \exp\left[\frac{-\beta \phi zF}{RT}\right] \qquad [41]$$

where $\Delta G^{o\ddagger}$ is the standard chemical free energy of activation, β is the symmetry factor, ϕ the metal-solution potential difference and the remaining terms have their usual significance. Equation [41] can be expressed in terms of $\Delta W^{o\ddagger}$ the true, inaccessible heat of activation at $\phi = 0$, $\Delta S^{o\ddagger}$ and ϕ_R, the reversible potential for the process concerned, by

$$\bar{k} = \frac{kT}{h} \exp\left[\frac{\Delta S^{o\ddagger}}{R}\right] \exp\left[\frac{-\Delta W^{o\ddagger}}{RT}\right] \exp\left[\frac{-\beta(\phi_R + \eta)zF}{RT}\right]. \qquad [42]$$

Noting that ϕ_R may be expressed in terms of the standard potential ϕ^o_R, and hence as $-\Delta G^o/zF$, (where ΔG^o is the standard free energy for the half-cell reaction involved when the process is reversible) $d(\ln \bar{k})/d(1/T)$ taken at $\eta = 0$ $(i = i_o)$ will give a quantity

$$-\frac{\Delta W^{o\ddagger}}{R} - \frac{zF\beta}{RT}\frac{\partial(\phi^o_R)}{\partial(1/T)} - \frac{zF\beta}{R} \cdot \phi^o_R \qquad [43]$$

or

$$-\frac{\Delta W^{o\ddagger}}{R} + \frac{\beta T \Delta S^o}{R} + \frac{\beta \Delta G^o}{R} \qquad [44]$$

neglecting the linear term in T in kT/h and assuming $\Delta S^{o\ddagger}$ is, to a first approximation, independent of T. Then,

$$\left[\frac{\partial(\ln \bar{k})}{\partial(1/T)}\right]_{\eta=0} = -\frac{\Delta W^{o\ddagger}}{R} + \frac{\beta \Delta H^o}{R} = -\frac{1}{R}(\Delta W^{o\ddagger} - \beta \Delta H^o) \qquad [45]$$

if ΔS^o is independent of T. Hence, if double-layer ion distribution and surface coverage effects are regarded as temperature independent, then $\partial(\ln i_o)/\partial(1/T)$, (which corresponds to $[\partial(\ln \bar{k})/\partial(1/T)]_{\eta=0}$)

will give an apparent heat of activation

$$\Delta H_R^{o\ddagger} = \Delta W^{o\ddagger} - \beta \Delta H^o \qquad [46]$$

where $\Delta H_R^{o\ddagger}$ is the apparent experimental heat of activation at the reversible potential ($\eta = 0$). In practice, β may also be a function of temperature as discussed in following sections of this thesis, so that $\Delta H_R^{o\ddagger}$ can also contain a term dependent on $d\beta/d(1/T)$. $\Delta W^{o\ddagger}$ can only be estimated from $\Delta H_R^{o\ddagger}$ by a non-thermodynamic calculation of ΔH^o (β being known from the Tafel slope), e. g., from the cycle:

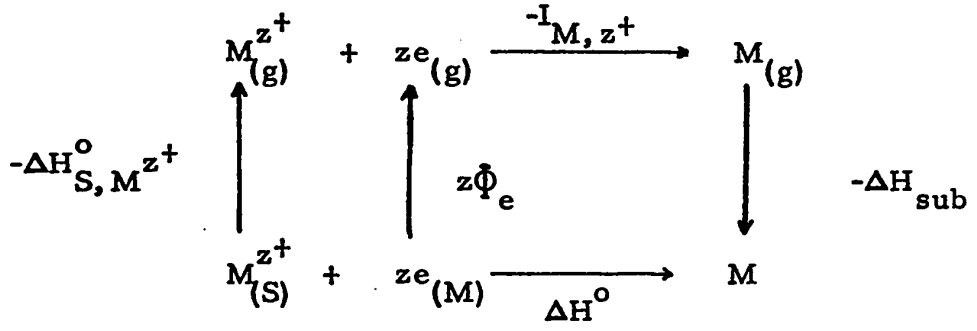

where

$$\Delta H^o = -\Delta H^o_{S,M^{z+}} + z\Phi_e - I_{M,z^+} - \Delta H_{sub} \qquad [47]$$

and $\Delta H^o_{S,M^{z+}}$ is the heat of solvation of M^{z+} ion, I_{M,z^+} the ionization energy of M to M^{z+}, ΔH_{sub} the heat of sublimation of M and Φ_e the electron work function of M. Values of $\Delta H^o_{S,M^{z+}}$ and Φ_e are not known to better than 5-10 kcal. g.mole^{-1} (64), so that $\Delta W^{o\ddagger}$ could not be calculated very precisely from the measured $\Delta H_R^{o\ddagger}$. Since $\Delta W^{o\ddagger}$ is not knowable, the true frequency factor $e(kT/h)\exp[\Delta S^{o\ddagger}/R]$ (65) in equation [42] cannot be obtained from a measured i_o or $\bar{k}$ value together with $\Delta W^{o\ddagger}$, since only $\Delta H_R^{o\ddagger}$ is experimentally accessible. However, measurements of such quantities are useful from a mechanistic viewpoint when determined in the context mentioned earlier.

(ii) Coverage effects in $\Delta H_R^{o\ddagger}$

In addition to the fact that the measured value of $\Delta H_R^{o\ddagger}$ is an apparent value on account of the variation of the reference electrode potential with temperature, a further complication arises with processes involving an adsorbed intermediate. In such cases, the coverage Θ e.g. by H atoms, can vary with temperature and give a contribution to the apparent heat of activation. The consequences of this effect will be treated in Chapter V. The significance of Θ in the kinetic expression for the exchange current was discussed by Devanathan and Selvaratnam (94).

c) Significance of $\Delta H_R^{o\ddagger}$ in Relation to Tunneling

Conway (40) has pointed out that the measurements of electrochemical activation energies in the h. e. r. at low temperatures could be useful in detecting tunneling by protons. At low temperatures the Arrhenius plot should show some curvature if tunneling is occurring, the curvature being most pronounced at the lowest temperature as has been discussed in Chapter I. However, this curvature or deviation from linearity of such a plot is not a sufficient criterion for proton tunneling since small variations of the experimental apparent activation energy, $\Delta H_R^{o\ddagger}$, in the readily accessible temperature range may be due to other phenomena (66, 67) such as a change of mechanism at the lower temperatures or a change in the structure of the solvent; the latter effect will normally give a progressive change of $\Delta H_R^{o\ddagger}$ over a broad temperature range. The lower the temperature achieved experimentally, the more useful does this test for proton tunneling become.

In addition to the test mentioned above, the following experimental consequences (71; cf. Chapter I) of the tunnel effect with regard to the kinetics of proton transfer in general are to be noted:

1. $E^* < E$, that is, the activation energy when tunneling is occurring is less than the classical value. However, since a reliable a priori theoretical calculation of the barrier height is not yet possible even for the simplest reactions, this prediction cannot be tested in practice.

2. A^* should be temperature dependent and less than A. Any exact theory for A demands a detailed knowledge of the properties of the transition state, and again a test is impracticable, except perhaps at very low temperatures, where abnormally low values of A^* are to be expected. The fact that the tunnel effect leads to low rather than high values of A^* is illustrated by Figure 16 where the usual plot of log k vs. 1/T is shown. The value of log A is equal to the extrapolated intercept of the log k plot at $1/T = 0$, and it will be seen that when this extrapolation is made from measurements over a finite temperature range it will lead to $A^* < A$ owing to the curvature of the plot.

The investigation of hydrogen isotope effects in the kinetics offers a better basis for the detection of tunneling owing to the mass dependence of the rate of the process. For the isotopes H and D, the following general theoretical predictions can be made:

1. k_H/k_D should be greater than the value calculated without taking into account the tunnel effect. This, however, is not a sensitive test since the calculated value demands a knowledge of the frequencies of real vibrational modes in the transition state; however, quite large values of k_H/k_D may be observed at low temperatures.

2. $E_D^* - E_H^*$ should be larger than the appropriate differences of zero-point energies. This again demands a knowledge of the properties of the transition (and initial) states but its evaluation may be useful if the effect of tunneling is considerable.

Figure 16

Temperature variation of reaction velocity with and without the tunnel correction according to Bell.

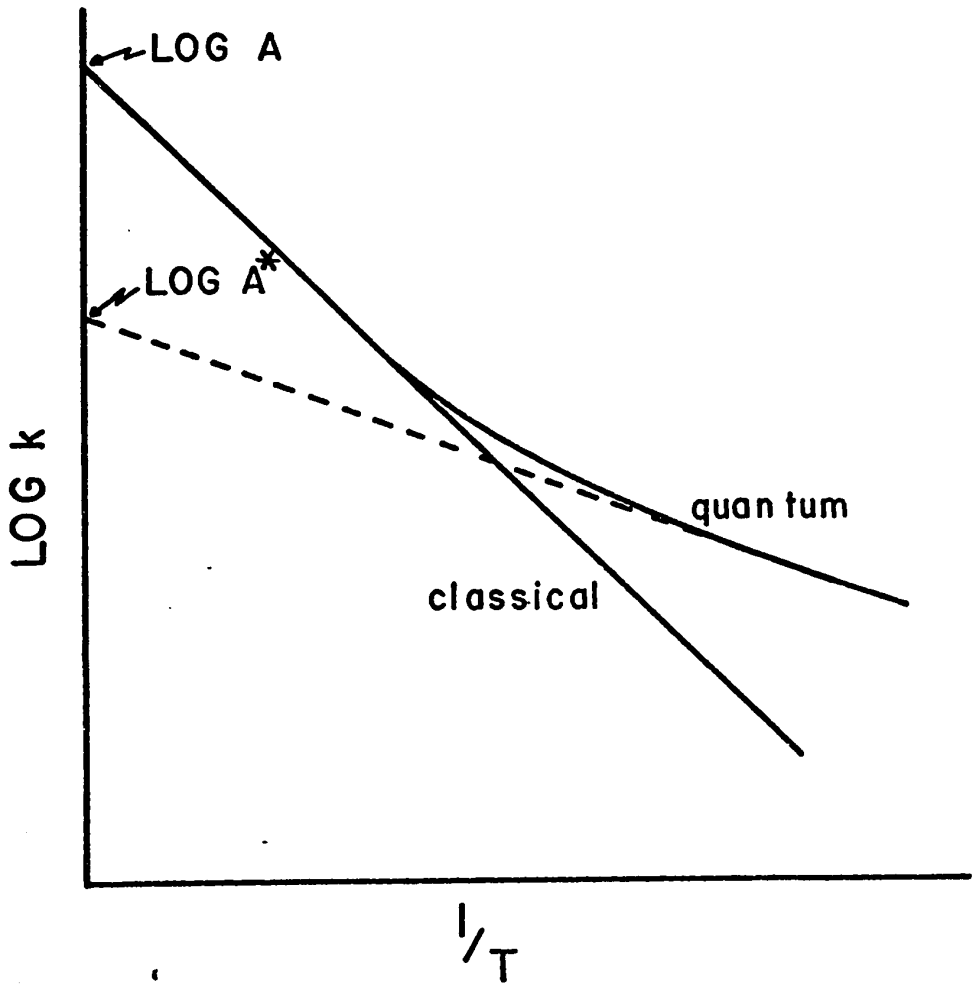
LOG A
LOG A*
LOG k
quan tum
classical
1/T

3. $A_H^* < A_D^*$. This is the most useful method for detection of tunneling since in the absence of the latter process the transition state theory predicts limits of 0.5 up to unity for the ratio A_H^*/A_D^*, with values close to unity being the most probable. Thus, experimental values of A_H^*/A_D^* substantially less than 0.5 can provide evidence for an appreciable degree of proton tunneling.

The above predictions concerning activation energies and frequency factors are quite general and apply to homogeneous proton transfer reactions as well as to analogous electrochemical processes. For the latter case, however, there is the additional criterion involving the temperature dependence of Tafel slopes as discussed in detail in Chapter I, Section (g).

d) Significance of Various Types of Electrochemical "Activation Energy"

The activation energy for electrochemical processes has been expressed in a variety of ways but the kinetically preferable manner is in terms of the variation of the logarithm of the exchange current density (i_o) with the reciprocal of the absolute temperature, i.e.,

$$\left[\frac{d \ln i_o}{d(1/T)}\right]_{\eta = 0} = \frac{-\Delta H_R^{o\ddagger}}{R} \qquad [48]$$

where $\Delta H_R^{o\ddagger}$ is the experimentally determined "apparent" activation energy at the reversible potential.

An alternative way of treating activation energies is in terms of ln i versus 1/T at a given constant overpotential other than zero, but in these cases the value of $\Delta H_\eta^{o\ddagger}$ obtained depends on the particular value of the overpotential chosen. Thus, the Tafel equation may be written in the form

$$i = i_o \exp[\eta/b] \qquad [49]$$

where b is the so-called Tafel slope, and is commonly expressed as $b = RT/\beta F$. In logarithmic form, equation [49] is

$$\ln i = \ln i_o + \frac{\beta \eta F}{RT} \qquad [50]$$

so that differentiating with respect to 1/T at constant η, we have

$$\left[\frac{d \ln i}{d(1/T)}\right]_\eta = \frac{d \ln i_o}{d(1/T)} + \frac{\beta \eta F}{R} \qquad [51]$$

or

$$-\Delta H_\eta^{o\ddagger} = -\frac{1}{R}\left(\Delta H_R^{o\ddagger} - \beta \eta F\right) \qquad [52]$$

It is to be noted that when $\eta = 0$, equation [52] obviously reduces to equation [48]. When β or b is a f(T), more complex expressions result as treated in Chapter V (cf. ref. 72).

Activation energies have also been expressed by Agar (68) in terms of overpotential at constant current density. Thus, if η is measured at any temperature with the reference electrode maintained at the same temperature, then

$$\left[\frac{\partial \ln i}{\partial T}\right]_\eta = \frac{\Delta H^{o\ddagger}}{RT^2} \qquad [53]$$

Since

$$\frac{d \ln i}{dT} = \left[\frac{\partial \ln i}{\partial T}\right]_\eta + \left[\frac{\partial \ln i}{\partial \eta}\right]_T \cdot \frac{d\eta}{dT} \qquad [54]$$

then

$$\frac{d \ln i}{dT} = \frac{\Delta H^{o\ddagger}}{RT^2} + \left[\frac{\partial \ln i}{\partial \eta}\right]_T \cdot \frac{d\eta}{dT} \qquad [55]$$

and the temperature coefficient at constant current density is

$$\left[\frac{\partial \eta}{\partial T}\right]_i = \frac{-\Delta H^{o\ddagger}}{RT^2} \Big/ \left[\frac{\partial \ln i}{\partial \eta}\right]_T \qquad [56]$$

With equation [50], viz.

$$\ln i = \ln i_o + \frac{\beta \eta F}{RT} \qquad [50]$$

$$\left[\frac{\partial \ln i}{\partial \eta}\right]_T = \frac{\beta F}{RT} \qquad [57]$$

and hence from equation [56]

$$\left[\frac{\partial \eta}{\partial T}\right]_i = \frac{-\Delta H_\eta^{o\ddagger}}{\beta F T} = -\frac{1}{\beta F T}\left(\Delta H_R^{o\ddagger} - \beta \eta F\right) \qquad [58]$$

This manner of expressing the activation energy is seen to involve the temperature (contrast equation [48]) in the $\Delta H_\eta^{o\ddagger}$ terms as well as in $(\partial \eta / \partial T)_i$ so that $\Delta H_\eta^{o\ddagger}$ must be obtained from tangents of η - T plots at various values of T.

If the partial derivative of η at constant i is taken with respect to the reciprocal of the absolute temperature, it can be shown that

$$\left[\frac{\partial \eta}{(1/T)}\right]_i = \frac{\Delta H_R^{o\ddagger}}{\beta F} - \eta \qquad [59]$$

arises which, although a somewhat more complicated expression, has the advantage, observed with equation [48], of not involving a T term on the r.h.s.

The use of Agar's expression [58] in earlier work by several authors led to high values for the activation energy. Thus Bockris and Parsons(69) and Minc and Sobkowski (70) found values

of 19 and 18 kcal. mole^{-1} respectively for the h. e. r. on Hg. However, using equation [48] and the data of the above authors, Conway and Salomon (31) showed that $\Delta H_R^{o\ddagger}$ = 8. 8 and 10 kcal. mole^{-1} respectively, values which are in good agreement with their own observed value of 11. 2 kcal. mole^{-1} for the h. e. r. on Hg in alcoholic HCl solutions, calculated by the same procedure.

Thus, in order for a comparison of independently determined values of activation energies for a given reaction to be made, it appears that the experimental activation energy should preferably be calculated by using the method of the variation of the exchange current density with temperature, i. e., equation [48].

CHAPTER III

AIMS OF THE PRESENT WORK

Studies on the cathodic hydrogen evolution reaction (h. e. r.) have, in the past, provided a basis for many of the electrochemical kinetic laws and principles that have emerged over the last sixty years. Whereas systematic studies on the effect of temperature on chemical reactions have been a major and fruitful endeavour in the field of chemical kinetics, and have indeed been carried out with electrochemical reactions, critical aspects of the temperature dependence of the kinetic behavior of electrode processes have, however, been neglected.

Thus, it is the aim of the present work to provide a study on the h. e. r., over a wide temperature range including very low temperatures, at a series of metals exhibiting high, medium and low hydrogen overvoltage. The purpose of this temperature study has been to establish:

(a) the proper form of the kinetic, potential dependence function, i. e., the Tafel slope, b, in relation to temperature. The experimental results of Chapter IV show that the temperature-dependence of b is, in many cases, anomalous and also suggest that inherent errors are involved in the calculation of the symmetry factor, β, from b determined at a single temperature value such as 25°C. Several factors which may give rise to anomalous temperature dependence of b are examined in Chapter V and the necessity for correcting for double-layer effects such as those due to the specific adsorption of anions is clearly demonstrated.

(b) the consequences of the anomalous temperature dependence of b on the interpretation and significance of the apparent electrochemical heat of activation at the reversible potential, $\Delta H_R^{o\ddagger}$. Thus, experimental results over a wide range of temperatures presented in Chapter IV establish $\Delta H_R^{o\ddagger}$ to be a complex quantity from which it is shown (Chapter V) that conclusions regarding barrier height, etc., cannot easily be made.

In addition, similar temperature studies on the analogous deuterium evolution reaction (d. e. r.) and on the anodic Br^- discharge at graphite in acetonitrile have been carried out in order to test whether or not proton tunneling effects are significant in the h. e. r. and to determine if the anomalous temperature dependence of Tafel slopes and $\Delta H_R^{o\ddagger}$ observed for the h. e. r. (see Chapter IV) is associated specifically with proton transfer from a hydrogen-bonded solvent.

Finally, in view of recent general claims that the solvated electron, e_{aq}^-, is the primary source of H_2 in the h. e. r., a critical discussion is presented in Chapter V, in which it is argued on the basis of existing evidence that such a mechanism is not justified except in very special circumstances.

CHAPTER IV

EXPERIMENTAL AND RESULTS

1. EXPERIMENTAL

a) Introduction

Since a principal aim of the present work was the investigation of the dependence of the Tafel parameters b and log i_o on temperature in order to evaluate the significance of activation energies and the electrochemical Brønsted factor β for various processes over a wide range of temperature, steady-state procedures were preferred for most of the experimental work. Conditions were always chosen so that the electrochemical reaction kinetics of the processes studied (hydrogen and deuterium evolution, and Br^- oxidation) were not diffusion controlled; the steady-state procedure was therefore adopted with the rapid point-by-point evaluation of the current-potential relationship, using controlled waiting periods of about 30 sec. at each current density. This method has been shown (81) to be preferable to the "slow" procedure where variations of potential over long times (up to two hours) are followed at each current density. Better reproducibility is always achieved (81) by the "rapid" procedure, partly because long-time electrolytic deposition of residual trace impurities is minimized.

To a limited extent, non-steady-state, potentiodynamic current-potential measurements were made in order to study if significant atomic hydrogen adsorption could be measured in certain cases.

The above procedures will be described in some detail in this chapter, but a general account of essential experimental technique for solution and gas purification, electrode preparation and matters concerning cell design etc., will first be given.

The experimental methods to be described have been applied to (a) the hydrogen evolution reaction at Hg, Pb, Cd, Ni and Pt in anhydrous methanolic and ethanolic HCl solutions; (b) the deuterium evolution reaction at Ni, Cd and Pt in anhydrous 0.5 N DCl-MeOD solutions and (c) the anodic reaction of Br^- at graphite in anhydrous 0.4 M $(C_3H_7)_4NBr$-CH_3CN solutions.

b) The Polarization Cells

The electrolysis cell used for the work on solid electrodes is shown schematically in Figure 17 and in more detail in the photograph, Figure 18. The cell together with its associated electrical apparatus is shown photographically in Figure 19 while Figures 20 and 21 show the cell and the H and D-solution preparation apparatus, respectively.

In this cell, the compartments were separated by tall solution-sealed stopcocks, an arrangement which permitted complete immersion of the cell in a cooling bath without contamination of the solution through the stopcocks which were, of course, ungreased.

The electrolysis cell for liquid Hg is shown in Figure 22. Both the working and reference compartments were provided with glass coils through which thermostated water could be circulated in order to maintain a constant pre-set temperature. The working compartment was also provided with a thermometer which came into contact with the electrolyte so that the temperature could be known accurately.

Figure 17

Schematic diagram of the low temperature cell used for the solid electrodes.

A. Counter electrode compartment

B. Study electrode compartment

C. Reference electrode compartment

W. Study electrode

L. Luggin capillary

S. Side-arm through which the solution is pumped into the cell

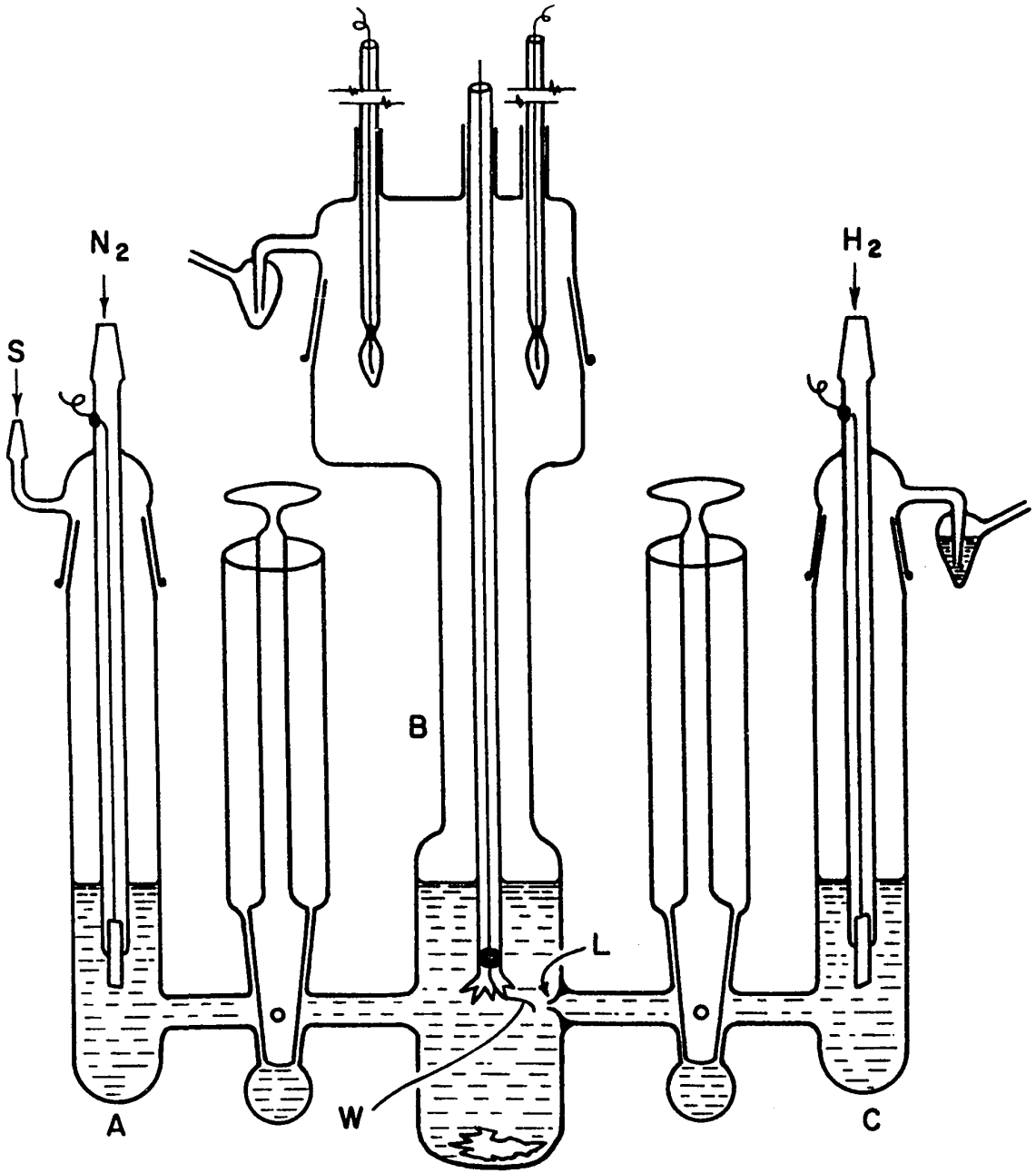
N2
S
H2
B
L
W
A
C

Figure 18

Photograph of the low temperature cell used for the solid electrodes.

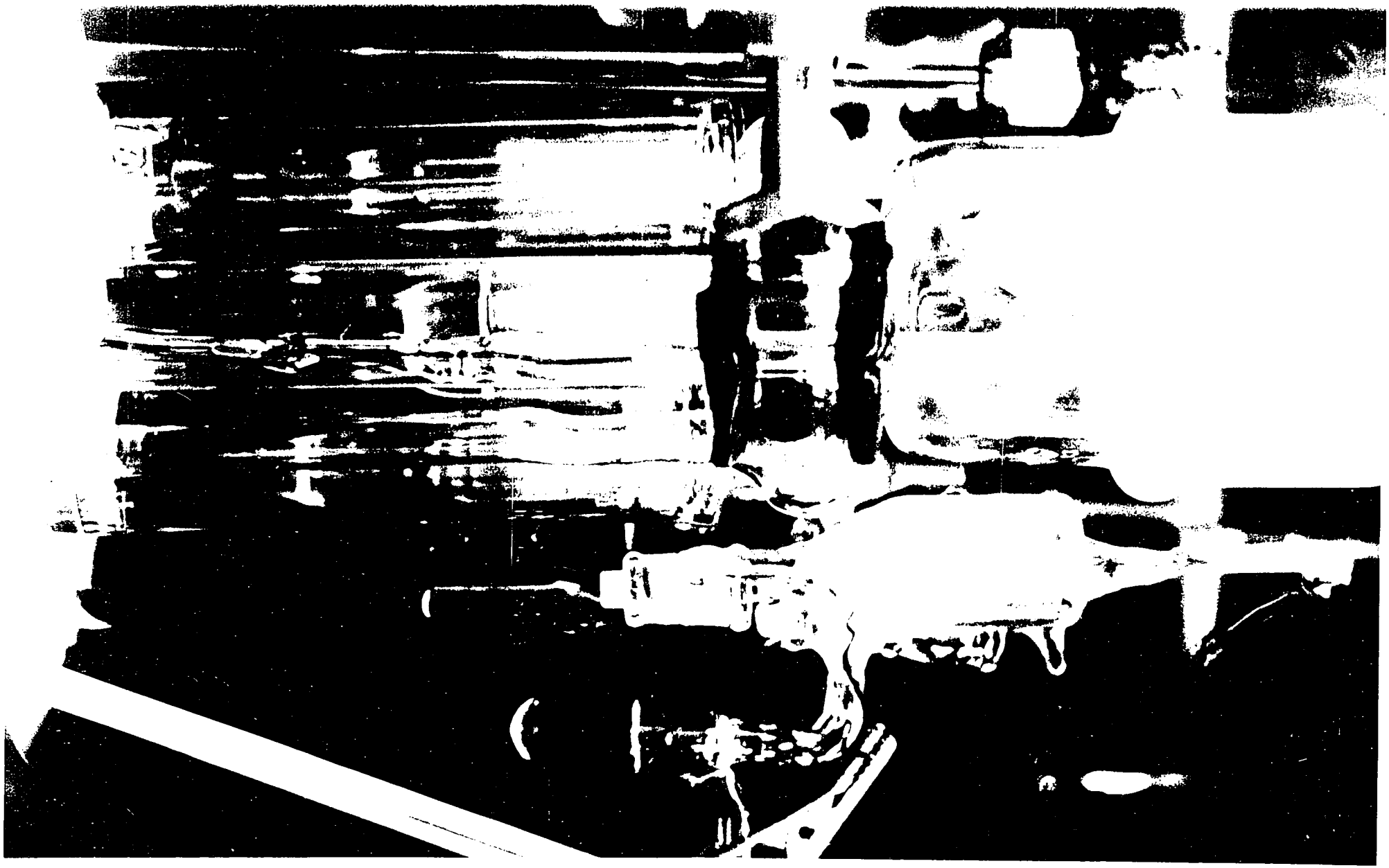

Figure 19

Photograph of the low temperature cell and associated electrical apparatus.

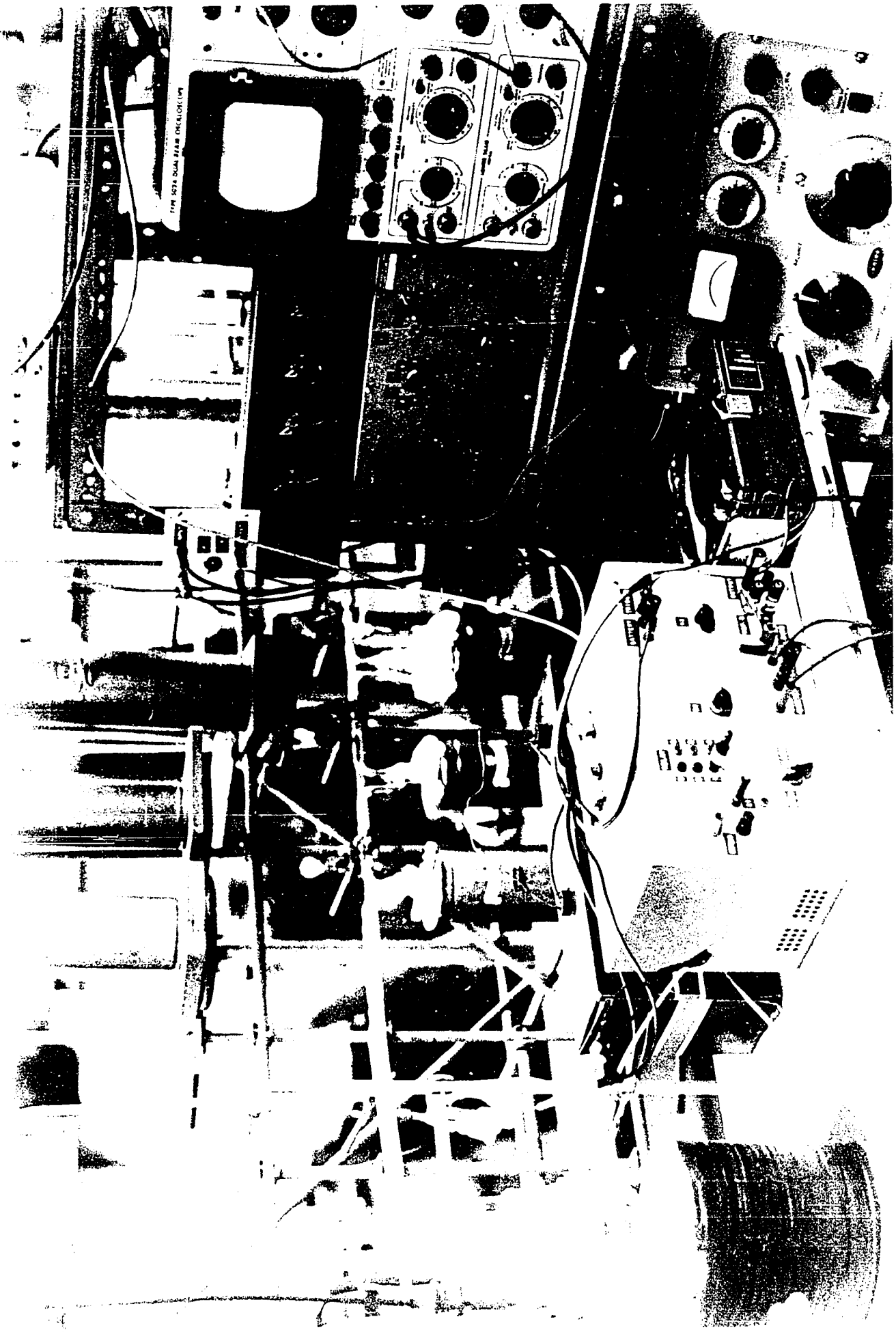

Figure 20

Photograph of the low temperature cell and associated apparatus for H-solution preparation.

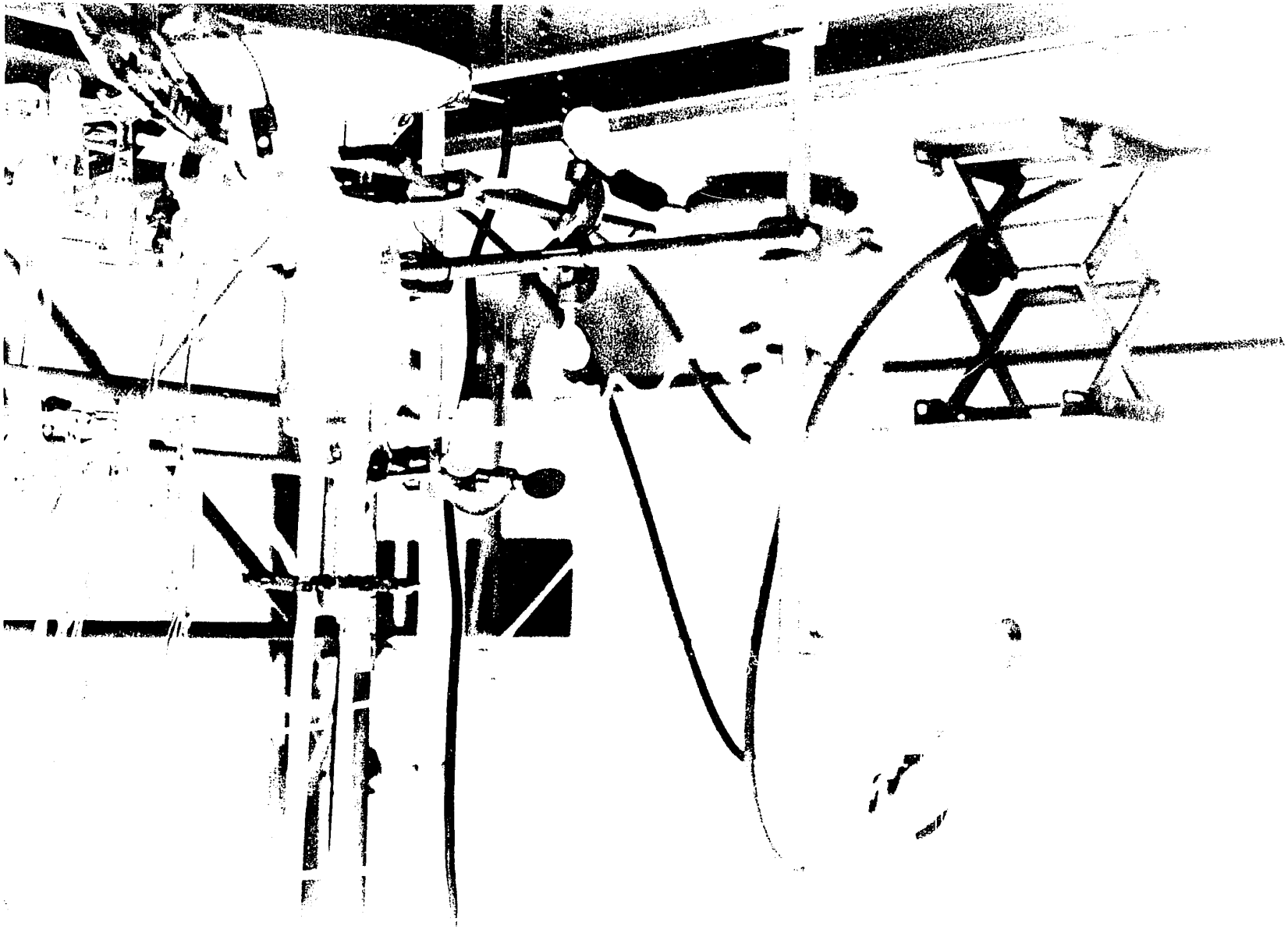

Figure 21

Photograph of the low temperature cell and associated apparatus for D-solution preparation.

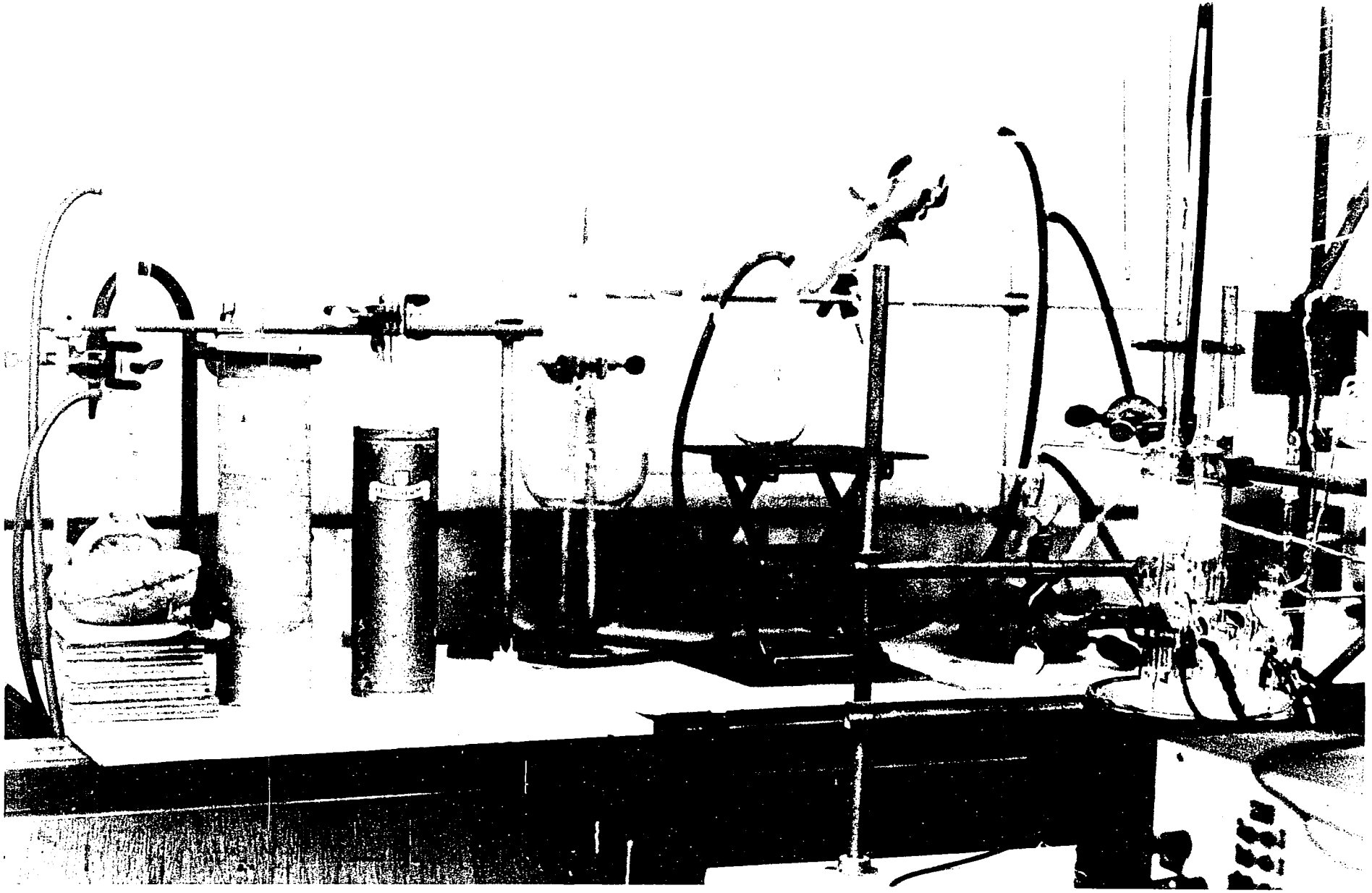

Figure 22

Photograph of the mercury cell.

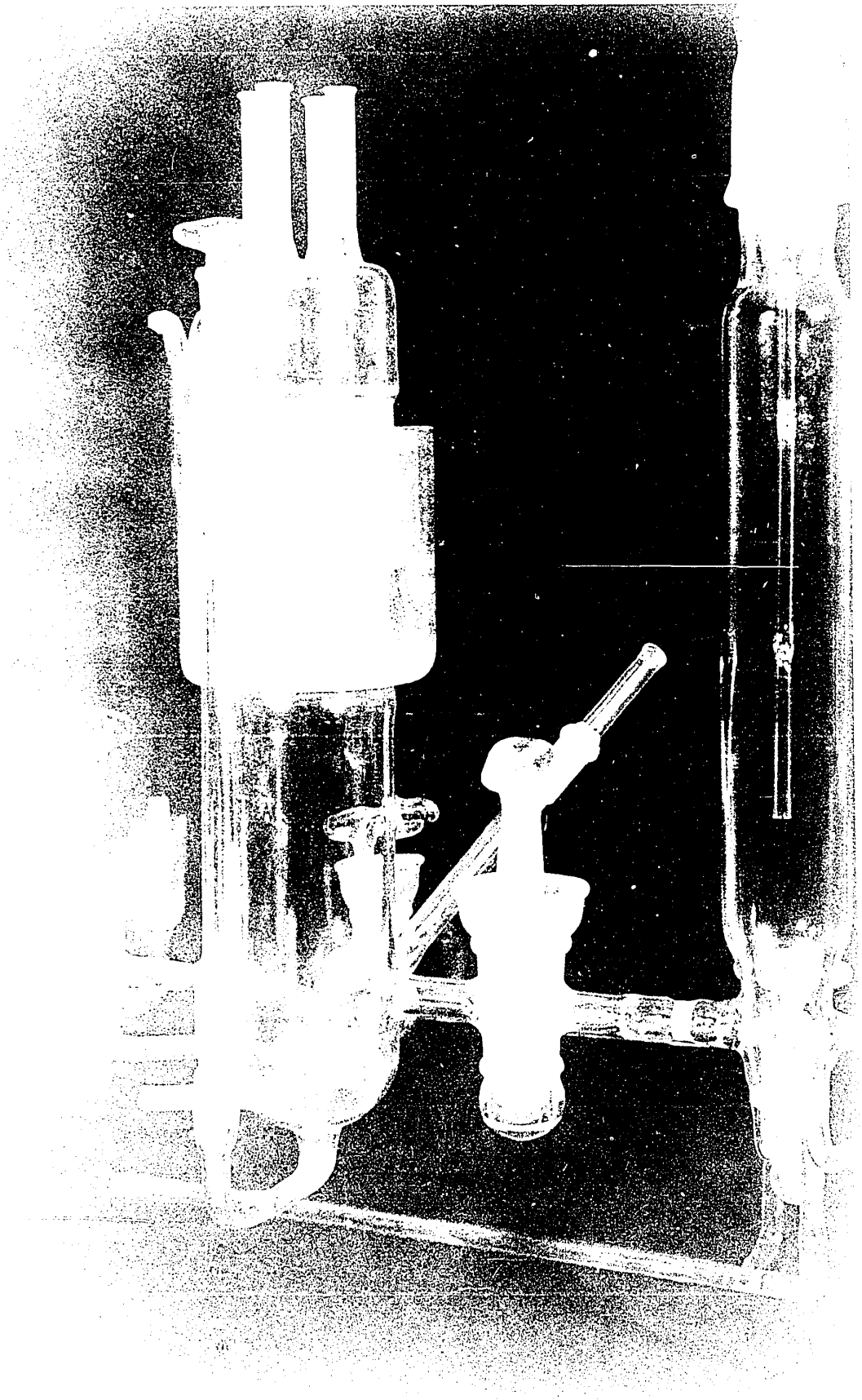

c) Electrical Circuits

Since the present work was carried out in non-aqueous solutions which provide a relatively high resistance to current flow, it was necessary to use the galvanostatic (constant current) d.c. polarization technique in order to obtain a reasonable range of current-densities. The polarization circuit is shown schematically in Figure 23. A Dressen-Barnes regulated power supply, model 22-110A, with output adjustable from 80 to 260 volts d.c. (for these experiments the output was set to 130 volts) provided the source of operating voltage. The current was set at a given value by means of the galvanostat which, as shown in Figure 23, consisted simply of a bank of resistors set up in such a way that the current could be adjusted to various values without the current flow ever being interrupted. The current was measured by means of a Sensitive Research Instrument Corporation ultra-sensitive d.c. milliammeter (Model S, No. 906017) with a range of 0.01 to 1000 mA. The potential between the working and reference electrodes was measured by means of a potentiometer (Radiometer, Model PHM4C, input impedance approximately 10^{13} ohms).

The non-steady state, potentiodynamic current-potential circuit, shown schematically in Figure 24, was used in an attempt to measure coverage by adsorbed H at Pt and Ni in methanolic HCl at low temperatures. As shown in the diagram, the reference input to the potentiostat was biased by feeding into it, at the appropriate sockets, an output from a triangular sweep generator (Servomex Waveform Generator, Type L.F. 141) which was arranged to generate a constant and pre-determined rate of change of potential, dV/dt. The amplitude of the sweep signal was checked by measurements on a potentiometer with the generator in a manual ramp configuration so that the upper and lower limits of potential could be determined. In series in the polarization circuit was also included a resistance box,

Figure 23

Electronic circuit for constant current (galvanostatic) control.

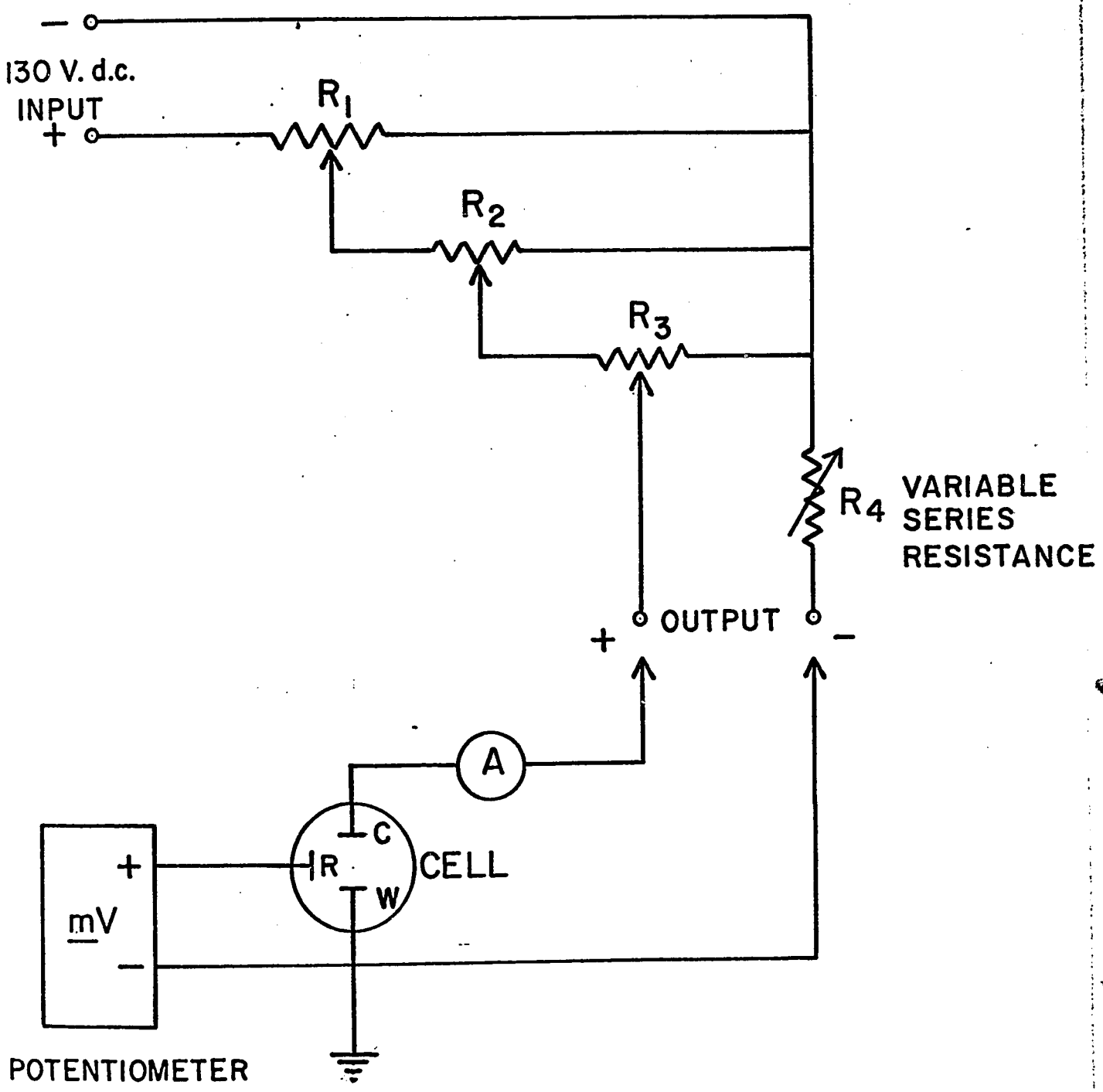
130 V. d.c.
INPUT
+
−
R1
R2
R3
R4
VARIABLE
SERIES
RESISTANCE
+
OUTPUT
−
A
C
R
W
CELL
+
mV
−
POTENTIOMETER

Figure 24

Potentiodynamic voltage sweep circuit.

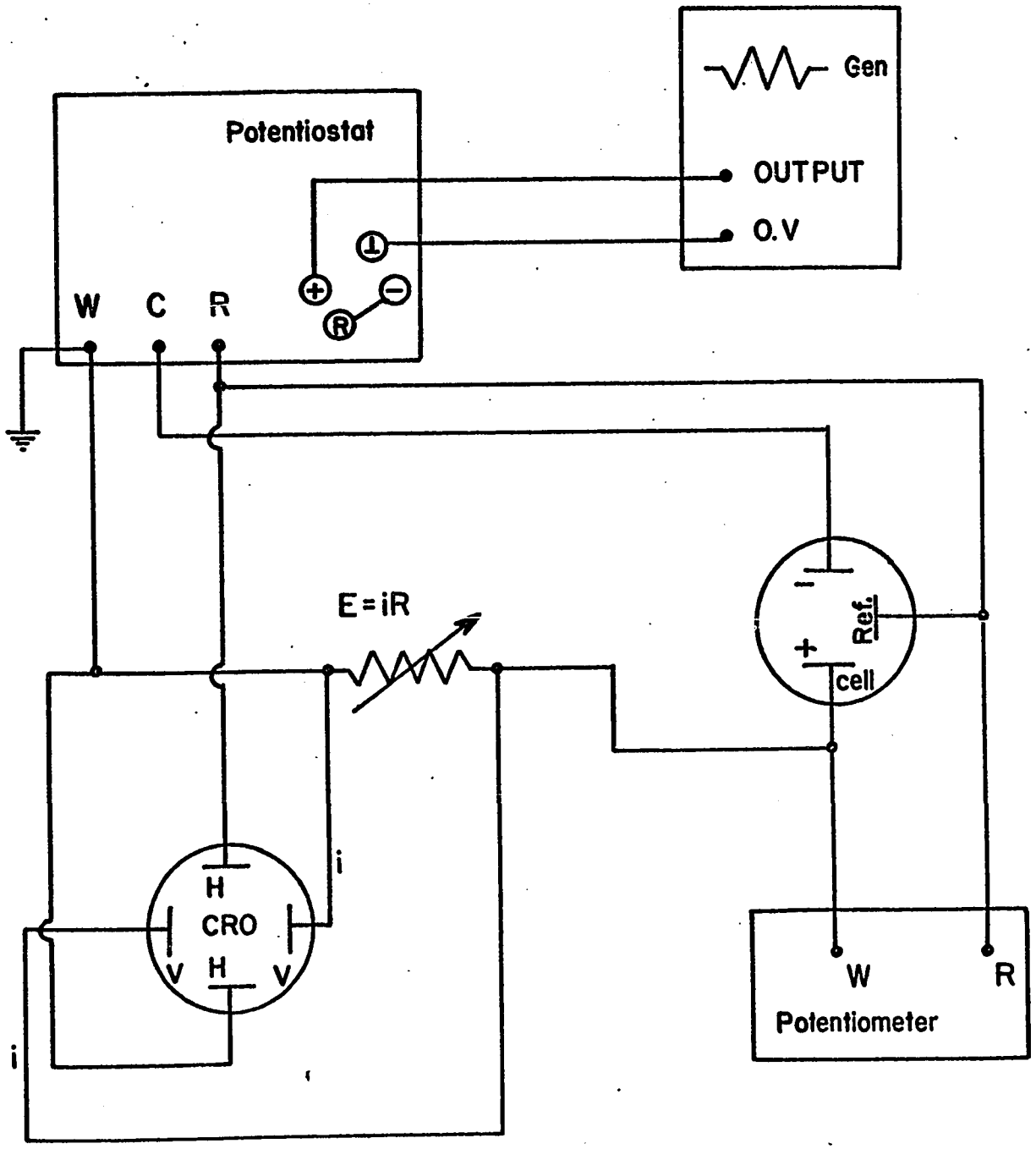
Gen
Potentiostat
OUTPUT
O.V
W
C
R
E=iR
Ref.
cell
H
CRO
V
H
V
i
i
W
R
Potentiometer

the potential across which was used to provide a signal for the measurement of the time-dependent current passing at a given moment in the polarization circuit and through the cell. The voltage drop ΔV across a chosen value R of the resistance gave the current as $\Delta V/R$. This current, measured as ΔV, was fed into the vertical axis of an oscilloscope, the horizontal axis of which (i.e., the time-base) was driven externally by the potentiodynamically controlled, continuously varying potential difference between the working electrode and the reference electrode.

d) Preparation and Purification of Solutions

In order to attain low temperatures it is necessary to use either non-aqueous or concentrated acid solutions. Tafel lines in relatively concentrated aqueous acid solutions exhibit kinks associated with specific adsorption but at the higher concentrations (ca. 7.0 N in HCl for example) linear behavior is exhibited over several decades of current density but the b values are higher than 2RT/F. Although aqueous solutions can be prepared in a state of high purity, it is known that the dependence of Tafel slope on acid concentration and temperature is anomalous (82), probably on account of specific adsorption of anions. In order to avoid this complication, it was therefore decided to use non-aqueous solutions despite the fact that they are more difficult to purify and work in such solvents has, in the past, been characterized by the shortness of the region over which linear-Tafel behavior is observed and by anomalies at medium and low current densities (31, 69). The outstanding advantage of using non-aqueous solutions, e.g. methanol or ethanol, is that the acid concentration can be kept low, e.g. < 0.5 N, so that the anomalous behavior mentioned above, associated with specific adsorption of the anion of the acid, e.g. Cl^- from HCl (83), can be diminished.

Thus, the solutions chosen for the present work were the following:

(i) 0.5 N HCl-methanol-h; 0.5 N HCl-ethanol-h

(ii) 0.5 N DCl-methanol-d

(iii) 0.4 M $(C_3H_7)_4$ N Br-acetonitrile.

The choice of HCl and DCl as electrolytes was an obvious one since both could be easily prepared in the dry, gaseous state. The choice of the system 0.4 M $(C_3H_7)_4$ N Br-acetonitrile was one of necessity, the reasons for which will be given later in the "Results" section. The preparation and purification techniques employed for each of these solutions will now be described in detail.

Methanol-h solutions (CH_3OH) were prepared by first distilling spectroscopic grade methanol in an atomosphere of dry, purified nitrogen from a small quantity of degreased Mg turnings and sodium borohydride to remove traces of water and any possible aldehyde impurities; a second distillation was then made into another flask into which could be bubbled dry, purified HCl gas until the acid concentration was approximately 0.5 N in HCl. The strengths of the various HCl solutions were determined by titration on separate samples. The HCl gas was prepared by the action of concentrated analytical reagent grade sulphuric acid on dry potassium chloride.

Ethanol-h (C_2H_5OH) was prepared from the undenatured material by refluxing over, and then distilling from, dried calcium oxide (CaO). The material thus obtained was then subjected to the treatment described above for the case of methanol solutions.

Methanol-d (CH_3OD) was prepared from magnesium methoxide [$Mg(OCH_3)_2$] and heavy water (99.8% D_2O)(84). Magnesium methoxide was first obtained by the action of spectroscopic grade methanol on degreased (Grignard reagent) Mg turnings

and the product was then dried under vacuum for approximately 20 hours at 60°C. Heavy water (99.8% minimum D_2O content) was then added to the excess dry methoxide and the product, methanol-d (CH_3OD), distilled off under reduced pressure at 60°C into a dry (previously oven baked) flask. The methanol-d thus prepared was again distilled from degreased Mg turnings into another flask into which could be bubbled dry DCl gas, as in the preparation of the alcoholic-HCl solutions, until the concentration of DCl was approximately 0.5 N.

Gaseous deuterium chloride was prepared by the action of D_2O on benzoyl chloride (85). The apparatus is shown schematically in Figure 25. The long capillary tube from the dropping funnel t, which reaches into the reaction flask r through the condenser k, ensured uniform addition of D_2O to the benzoyl chloride in the flask in spite of small fluctuations of pressure during the reaction. In order to trap any benzoyl chloride entrained through the condenser by the DCl gas, trap f was cooled in an ice bath. As an additional precaution, a second trap g which was kept at dry ice-acetone temperatures was included as shown in the diagram.

As an example of the procedure for DCl preparation, 1 ml. of 99.8% D_2O was allowed to react with 2-3 molar excess benzoyl chloride containing some porous boiling chips. The reaction may be represented by the equation

$$2C_6H_5COCl + D_2O = (C_6H_5CO)_2 + 2DCl$$

Benzoyl chloride, before being placed in the reaction flask r, was first distilled and only the fraction boiling at 197°C was used. At first, only a few drops of D_2O were added, while the mixture was carefully heated. This was continued until a moderate rate of gas evolution was developed. This temperature was maintained until all the D_2O had been added. By varying the heat input, DCl gas

Figure 25

Schematic diagram of the apparatus used for the preparation of gaseous DCl.

f. Condensation trap ($0^{\circ}C$)

g. Condensation trap ($-60^{\circ}C$)

k. Reflux condenser

r. Reaction flask

t. Dropping funnel with capillary stem

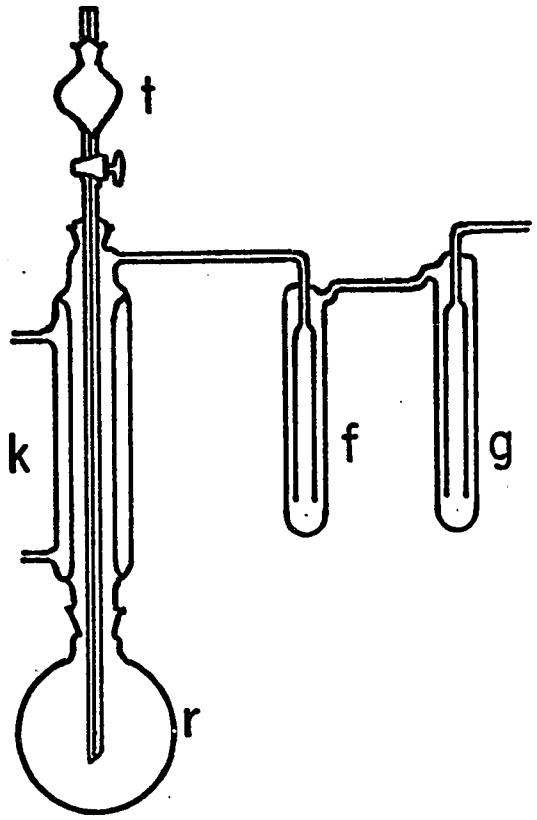
t
k
f
g
r

formation could be easily regulated. As the gas flow decreased, the temperature was gradually raised to the boiling point of benzoyl chloride (197°C) and kept there until no further gas was evolved. The product was analytically pure and the yield was almost quantitative.

For the anodic reaction of Br^- ion at graphite, spectroscopic grade acetonitrile (CH_3CN) was used as the solvent. Recrystallized (99) and dried $(C_3H_7)_4NBr$ was dissolved in the acetonitrile until a maximum concentration of 0.4M was reached.

e) Purification of Gases

Hydrogen gas used for the reference electrode and for bubbling in the cathode compartment during the h.e.r. runs was rigorously purified before use. The purification train was similar to that previously described (86). The train consisted of (a) a dried molecular sieve material (Linde Co., Type 13X), (b) magnesium perchlorate, (c) palladized asbestos at 350°C, (d) a liquid nitrogen trap, (e) two activated charcoal traps maintained at liquid nitrogen temperatures and finally (f) a tube of glass wool to eliminate any transfer of particles of charcoal in the gas stream.

Nitrogen gas was used for bubbling in the anode compartment (and in the cathode compartment for the D-runs) and for provision a moisture-free atmosphere for the solution preparations described previously, the gas was purified by passage through a train identical with that described above for hydrogen except that a tube of copper turnings maintained at 350°C was used instead of palladized asbestos.

f) Preparation of the Electrodes under Study

(i) Platinum and Nickel. These electrodes were prepared from spectroscopically pure wires of platinum and nickel by a standardized method in order to ensure the best reproducibility of the measurements. The wire was first cleaned by washing for twenty-four hours in benzene under reflux. After drying, the wire electrode was then heated for 2-5 minutes in a stream of pure dry hydrogen gas at a temperature just below that for softening of the pyrex glass. The electrode wire was subsequently sealed in a stream of hydrogen in a glass bulb, following the procedure developed by Bockris, Conway and Mehl (87). The electrodes sealed in the bulbs were maintained in the cell until commencement of each run, when the bulbs were successively broken, as required, with an appropriate potential applied before breakage so as to give the desired initial current immediately the metal electrode came in contact with the solution.

(ii) Lead and Cadmium. These electrodes were prepared from spectroscopically pure rods of lead and cadmium in the following manner. A small portion of the metal rod was placed in a porcelain crucible which was set up in such a way as to allow a large flame of purified hydrogen gas to be directed onto the metal in the crucible. The crucible was then heated from the bottom by means of an oxygen torch until the metal became molten. Once it had melted, the metal remained in the crucible with a brilliant clean surface due to the hydrogen flame which also served to exclude oxygen and prevent oxidation of the Pb or Cd. The molten metal was then drawn into a glass capillary tube where it was allowed to solidify. Later, the tube was cut with a diamond wheel to expose the desired metal surface.

(iii) Mercury. Specially distilled mercury (meeting the specifications of A. C. S., A. D. A. and U. S. P.) obtained from Johnson, Matthey and Mallory Ltd., was used directly without further purification.

(iv) Graphite. Pyrolytic (non-porous) ultra-pure graphite rod obtained from the General Electric Co. was used for the studies on the Br^- discharge reaction. Since it was not possible to seal the graphite into glass satisfactorily, a teflon holder was constructed in the following way: One end of a teflon rod (5.0 cm long and 1.10 cm diameter) was drilled so that a length of the graphite rod (1.6 cm long and 0.6 cm diameter) could be tightly fitted. Once drilled, the teflon holder was placed in boiling water for a short time. This caused the opening to expand thus making it easier to insert the graphite. On cooling, the teflon contracted around the graphite, forming a leakproof seal without contamination by any sealing compounds. A similar opening was drilled in the opposite end of the teflon holder so that a "Tru-bore" glass sliding tube could be tightly fitted. The electrical contact was made by means of a drop of mercury.

g) The Counter Electrode

Special consideration had to be given to the counter electrode since the electrolyte used was methanolic or ethanolic HCl (or DCl); thus in the presence of Cl^- ion, oxidation of the alcohol by Cl_2 could arise especially during the pre-electrolysis purification which was carried out for a period of at least ten hours at a current density of the order of 2mA. $cm.^{-2}$. Although a closed stopcock between the anode and cathode compartments decreased the possibility of migration of oxidation products, etc., from the anode to the cathode, it was nevertheless felt that in order to eliminate

entirely the possibility of contamination of the catholyte by anodic products from the counter electrode, it would be best to prevent this type of oxidation of the solvent from occurring.

It was found that a large silver gauze anode met this requirement satisfactorily by reacting with Cl^- ion from the solution forming silver chloride in the anode reaction. A fresh electrode was prepared before each run and a standardized cleaning procedure was followed: the silver gauze was soaked in hot, concentrated ammonium hydroxide followed by thorough rinsing with water and storage in spectroscopic grade methanol until the electrode was required for use as an anode in the cell.

When a bright platinum counter electrode was used, as in some preliminary experiments, it was found that the solution in the anode compartment invariably became yellow in colour, and moreover the platinum would slowly be dissolved due to the action of the Cl^- ion in the non-aqueous medium.

Platinized platinum gauze over which hydrogen gas was bubbled was also tried but was found to lead to unsatisfactory results.

h) Reference Electrodes

(i) Hydrogen Reference Electrodes

1. Preparation

Hydrogen reference electrodes were prepared by cleaning Pt electrodes in hot nitric acid followed by thorough washing in doubly-distilled water. Two such electrodes were then suspended in a platinizing solution containing three grams of platinic chloride in one hundred milliliters of doubly-distilled water and were connected to a d.c. power supply. The current was adjusted to approximately 5 mA. $cm.^{-2}$ so that there was only a moderate evolution of gas

(H_2 and Cl_2); the direction of the current was reversed every minute and the plating was allowed to proceed until a moderately thick coating of platinum was obtained. The coating was greyish-black and velvety in appearance. The electrodes were then washed repeatedly with water and kept in the appropriate non-aqueous solvent (e. g. MeOH, EtOH) until required for use.

2. Reproducibility and Verification of Reversibility

Before commencement of the measurements, the potential of the hydrogen reference electrode used was compared with that of another hydrogen electrode in the same solution; if the potentials were in agreement to within one millivolt, the measurements on the test electrode were carried out. If the comparison was not satisfactory or if the potentials approached the equilibrium value only slowly, the electrodes were replaced by a new set before any measurements were attempted. Electrodes which are not behaving reversibly rarely give identical potentials nor do they give steady, time-independent values of potential. Hydrogen electrodes are known (88) to behave satisfactorily in non-aqueous solvents of the kind used in the present work and they gave no problems in the systems studied.

The reversibility of the hydrogen reference electrode at low temperatures was checked in a series of special experiments as follows:

(a) qualitatively, by bubbling nitrogen rather than hydrogen gas at one of a pair of electrodes. The electrodes recovered their initial relative potential ($\Delta E = 0$) almost immediately if the nitrogen was replaced by hydrogen gas.

(b) quantitatively, by variation of the partial pressure of hydrogen by dilution with nitrogen at one of the electrodes. The apparatus used for this experiment is shown in Figure 26. A plot

Figure 26

Photograph of apparatus for hydrogen reference electrode-partial pressure experiment.

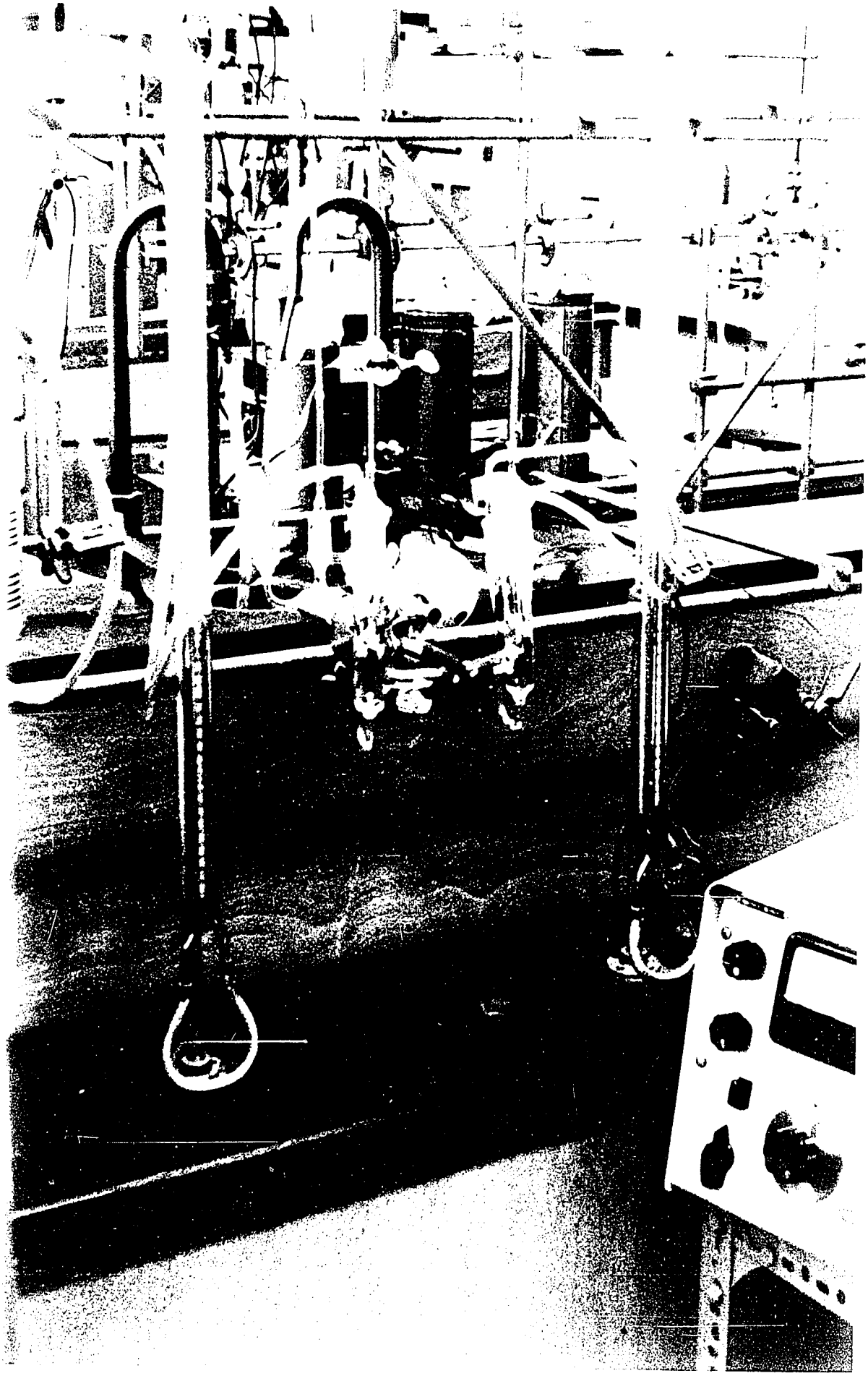

Figure 27

ΔE as a function of P_{H_2} for various temperature values.

0.5 N HCl-MeOH

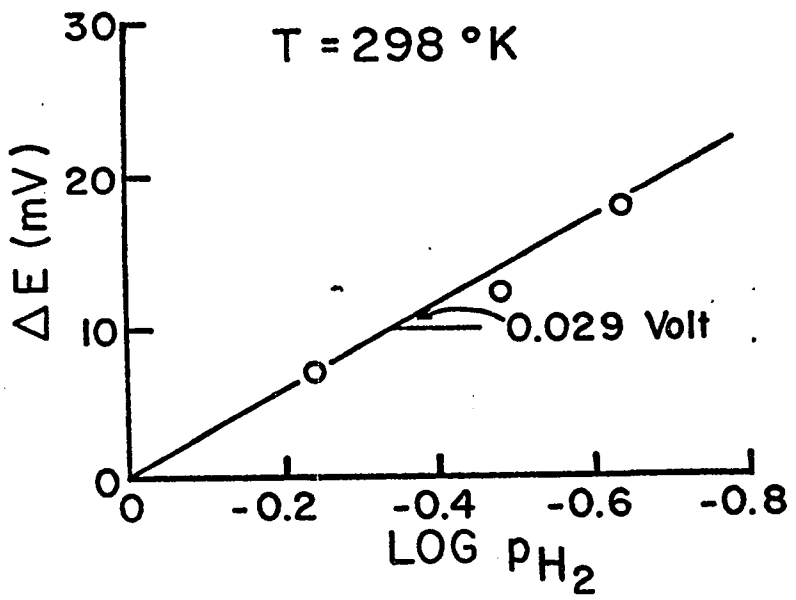
T = 298 °K
ΔE (mV)
30
20
10
0
0
-0.2
-0.4
-0.6
-0.8
LOG p_{H_2}
0.029 Volt

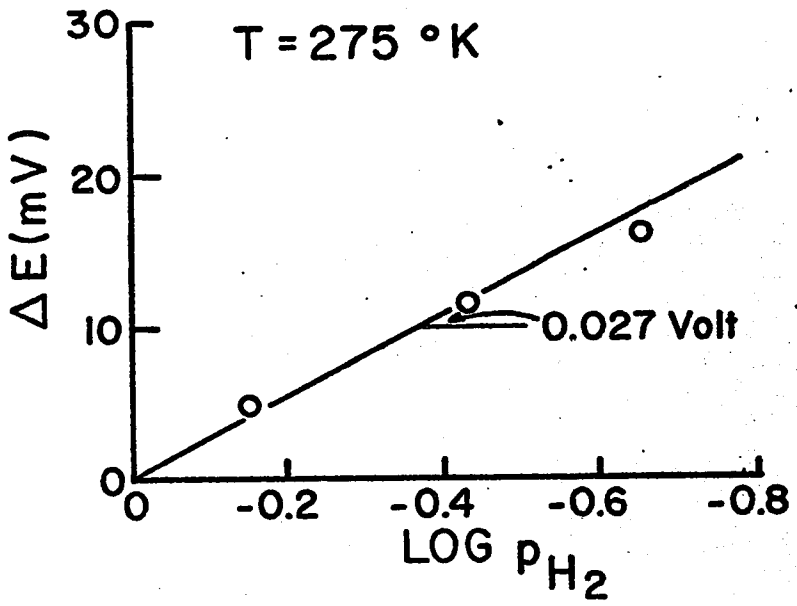
T = 275 °K
ΔE (mV)
30
20
10
0
0
-0.2
-0.4
-0.6
-0.8
LOG p_{H_2}
0.027 Volt

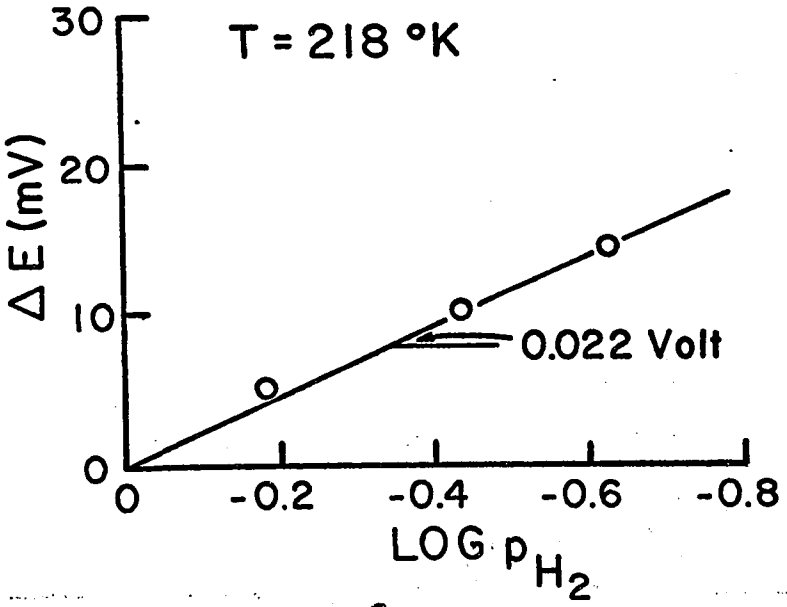
T = 218 °K
ΔE (mV)
30
20
10
0
0
-0.2
-0.4
-0.6
-0.8
LOG p_{H_2}
0.022 Volt

was provided with glass coils through which water was circulated at a pre-set constant temperature. This was achieved by means of a Bronwill Constant Temperature Circulator (type 84-755) operating from a thermostat bath.

j) Experimental Procedure

Prior to each run, the cell and its component parts were immersed in cleaning solution (chromic-sulphuric acid mixture) for several hours. The cell and other parts were then washed many times with doubly-distilled water and then soaked in doubly distilled water for at least twenty-four hours. The cell and all other parts were then finally dried in a special oven at 130°C for twenty-four hours since minimum contamination by H_2O was desired, especially for the runs conducted in the methanol-d solutions.

The electrolyte was prepared in situ as described earlier and transferred to the cell under pressure of nitrogen. The solution was further purified by means of pre-electrolysis at a sacrificial platinum cathode for at least ten hours at a current density of 2 mA. $cm.^{-2}$. The electrode under study to which was already applied an appropriately set voltage, was immersed in the solution; the bulb was then broken and the electrode adjusted carefully against the Luggin capillary. The current-potential behavior was then recorded using the galvanostatic technique, i.e., successive constant values of the current were set (see circuit Figure 23) and the corresponding values of the potential recorded. These polarization curves were obtained first for ascending values of the current and then for descending values at a given temperature. The time required for the measurements taken at each temperature was approximately 15 minutes.

Generally each experiment was started at the highest temperature studied (usually room temperature) and polarization

curves were then determined at various temperature intervals for descending values of the temperature. In selected cases (e.g., Pt and Cd; see "Results" section), the experiments were commenced at the lowest temperature and the polarization curves were obtained at various temperature intervals for ascending values of the temperature. In some cases, the direction of temperature change was found to be important.

Potentiodynamic measurements were also carried out at Ni and Pt at low temperatures in order to examine if quantitative H-adsorption measurements could be made as they can in aqueous solutions at the noble metals. Here the initial setting of the potentiostat and the time-dependent bias potential applied to it from the triangular wave-form generator were so arranged that the potential region under study lay within the two extremes of the time-dependent signal. The value of resistance in the resistance box (joined in series in the polarization circuit) was chosen in the usual way so that a sufficient potential was generated to give a proper display of the charging current peaks (if any) at the appropriate settings of the sensitivity of the y-axis on the oscilloscope. The minimum series resistance was always used with the maximum oscilloscope y-axis sensitivity. The time-dependent current-potential relations thus obtained were recorded photographically on the oscilloscope at several sweep rates. Typical examples are shown in Figure 28 for Pt and Ni in HCl-MeOH solution at -90°C, which are essentially similar to results obtained at 25°C as shown in Figure 29. Since the H-adsorption peaks normally seen in aqueous solution experiments were not detected and because of experimental difficulties arising partly on account of the high solution resistance, these experiments were not developed to any great extent. The absence of significant H adsorption (i.e., $\gtrsim$ 0.05 in coverage Θ by H) is probably due to competitive adsorption of methanol which already

Figure 28

Potentiostatic sweep diagram for detection of H adsorption at Ni and Pt in MeOH at -90°C.

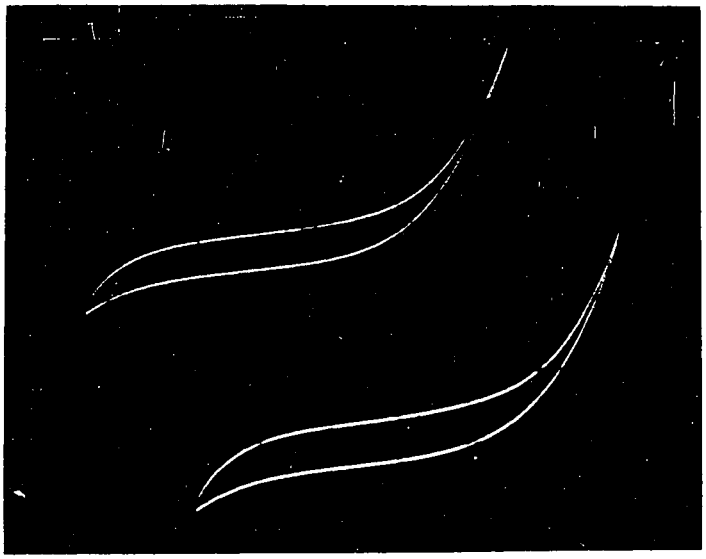

Ni

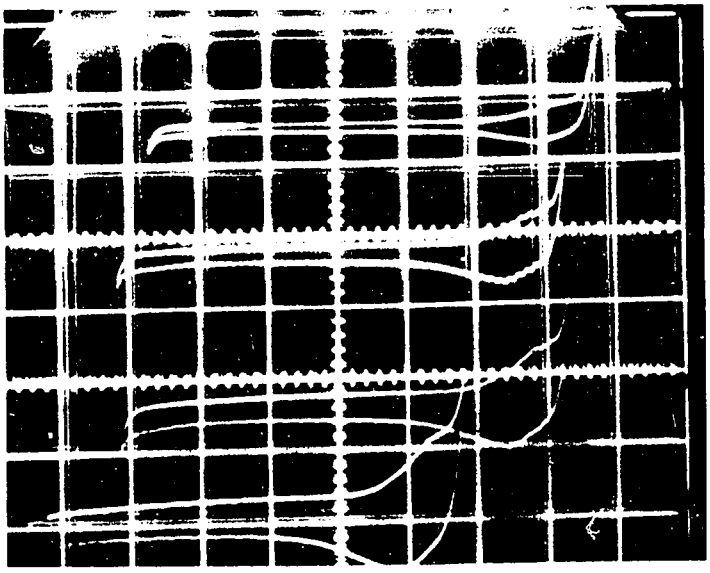

Pt

Figure 29

Potentiodynamic sweep diagram for detection of H adsorption at Ni and Pt in MeOH at +25°C.

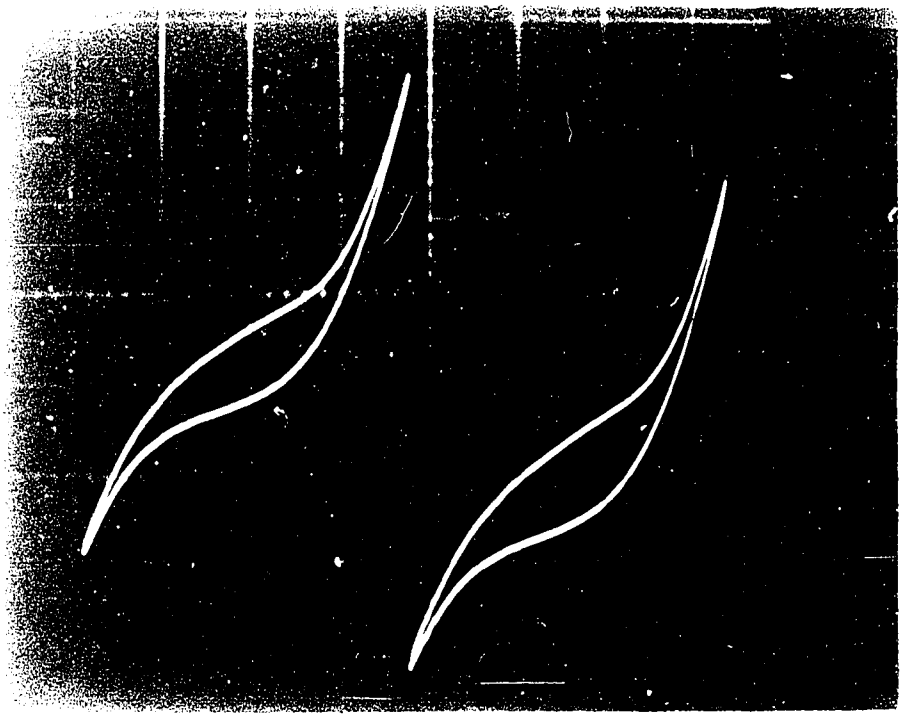

Ni

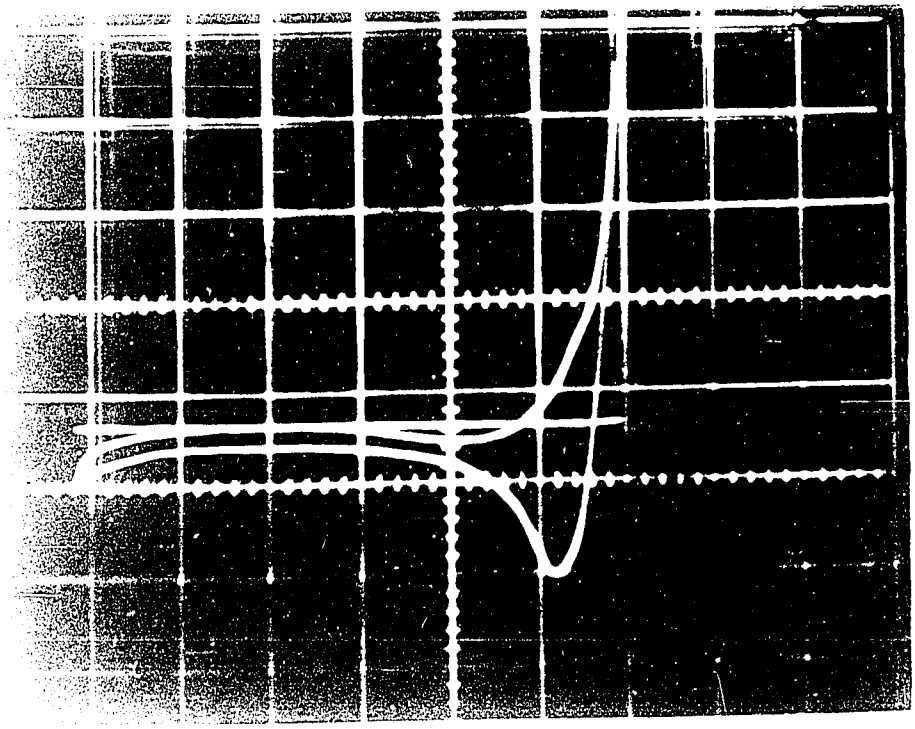

Pt

covers the Pt surface in aqueous solution of methanol (90, 91, 92) except at high anodic potentials where it is known to become oxidatively desorbed (90, 92).

2. RESULTS

a) H.E.R. at Ni, Pt, Cd, and Pb over a Wide Range of Temperatures

(i) Cathodic Polarization Curves

Current-potential relations for a number of metals, Ni, Pt, Cd, and Pb were obtained in ethanol (and methanol) solutions, 0.5 N w.r.t. HCl, at various temperatures ranging from +25 to -125°C. In several cases, the upper limit of the temperature range was extended to +60°C.

1. Nickel. Typical overpotential-log [current density] plots for nickel in 0.5 N HCl-EtOH and 0.5 N HCl-MeOH are shown in Figures 30(a) and 30(b), respectively. It is to be noted that these plots exhibit two distinct and reproducible linear Tafel regions. From about 60°C, through room temperature and down to approximately -40°C, the high current density (c.d.) region is characterized by higher Tafel slopes than those found at lower current densities. This phenomenon is characteristic of a change of mechanism in which reactions in a consecutive or "series" relation to one another are occurring. At approximately -40°C, the Tafel line is linear over the entire c.d. range with a slope of b = 0.120. As the temperature is further decreased below ca. -40°C., the slope in the high c.d. region becomes lower than that in the low c.d. region. This behavior is now characteristic of a mechanistic change in which alternative (or parallel) reactions are occurring, or one in which desorption of anions occurs at a critical potential.

These two cases arise as follows (cf. ref. 59). In the series reaction sequence, the step having the smaller rate constant at any given potential limits the overall rate. Two Tafel lines that

Figure 30

Tafel relations for the h. e. r. as a function of temperature.

(a) Ni cathodes in anhydrous HCl-EtOH.

(b) Ni cathodes in anhydrous HCl-MeOH.

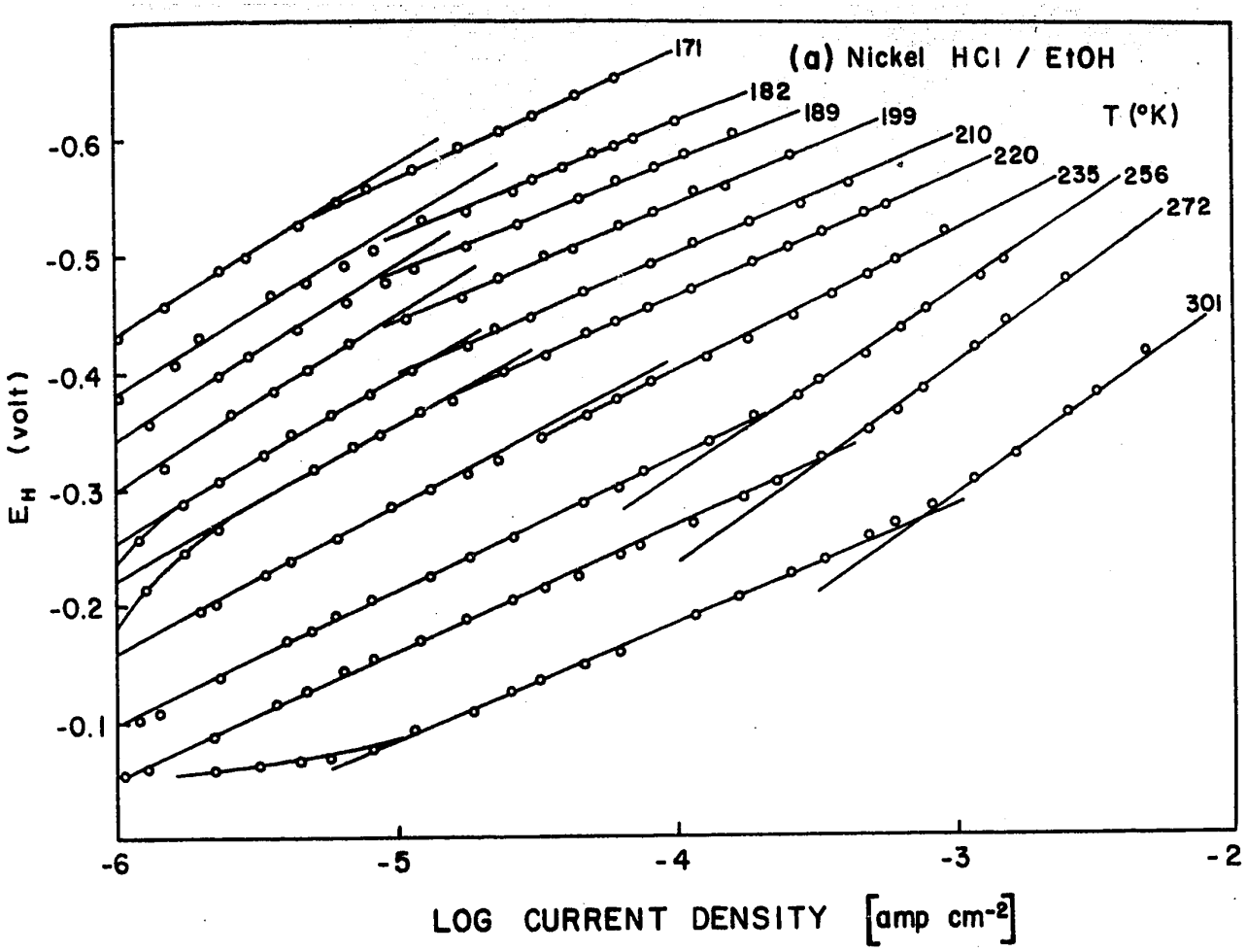
(a) Nickel HCl / EtOH
T (°K)
171
182
189
199
210
220
235
256
272
301
-0.6
-0.5
-0.4
-0.3
-0.2
-0.1
E_H (volt)
-6
-5
-4
-3
-2
LOG CURRENT DENSITY [amp cm⁻²]

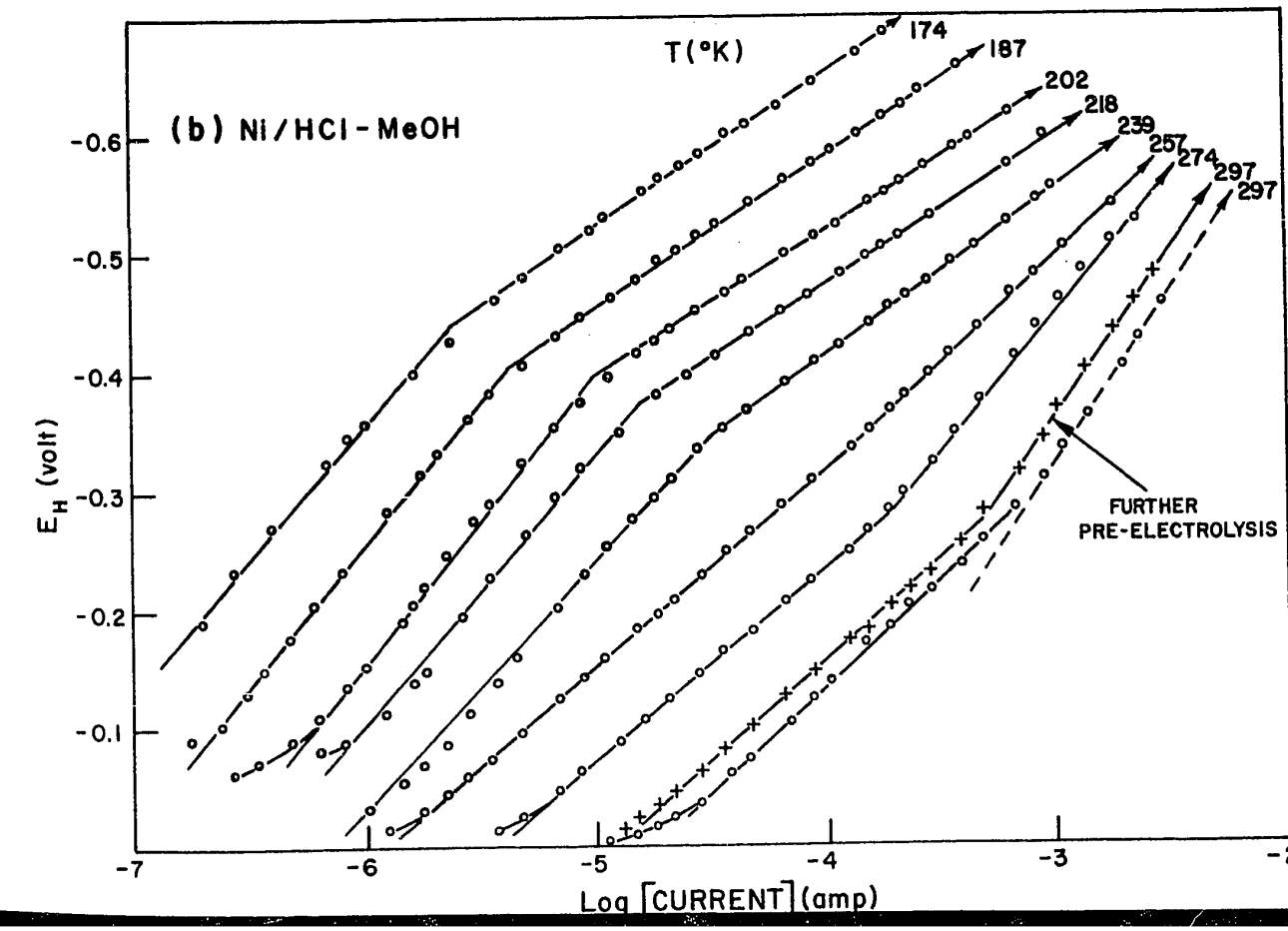
(b) Ni/HCl-MeOH
T(°K)
174
187
202
218
239
257
274
297
297
FURTHER
PRE-ELECTROLYSIS
-0.6
-0.5
-0.4
-0.3
-0.2
-0.1
E_H (volt)
-7
-6
-5
-4
-3
-2
Log [CURRENT] (amp)

proceed one into the other with an increase in slope (relatively higher potentials required for an equivalent increase in rate) thus correspond to a change from one rate-determining step to another in a consecutive sequence of two reactions since in the region of higher slope at higher potentials, the first process of lower slope would have proceeded at a rate i_I at potential η (Figure 31(a)) but the actual rate of the process is limited by a consecutive step so that the overall rate is i_{II} at η .

Correspondingly, in Figure 31(b), the rate of the process occurring at higher potentials in a parallel reaction sequence is determined by the pathway having the greater velocity at a given potential. For two pathways having different Tafel slopes, the one which has a rate constant which increases to the greater extent with potential (slope b lower) will be the dominant pathway in the kinetics of the process. Thus (Figure 31(b)), at potential η , pathway I would have passed a current i_I increasing with potential with a slope b_I but if II is an alternative process, the kinetics will be determined by the faster process passing current i_{II} along the line of slope b_{II}.

In order to test whether the changes of Tafel slope discussed above were due to the effect of specific adsorption of the Cl^- anion, results were also obtained for the h. e. r. at Ni in 0.5 N $HClO_4$-MeOH solutions. These results, which are presented in the Discussion section (see Figures 52 and 53), differ from those obtained in the alcoholic-HCl solutions in that they exhibit a linear Tafel behavior over the entire c. d. range and the Tafel slope corresponds to that obtained for the high c. d. region in the alcoholic-HCl case. The significance of these findings will be discussed in detail in Chapter V.

Figure 31

Changes of mechanism.

(a) Consecutive reactions (series).

(b) Alternative reactions (parallel).

CHANGES OF MECHANISM

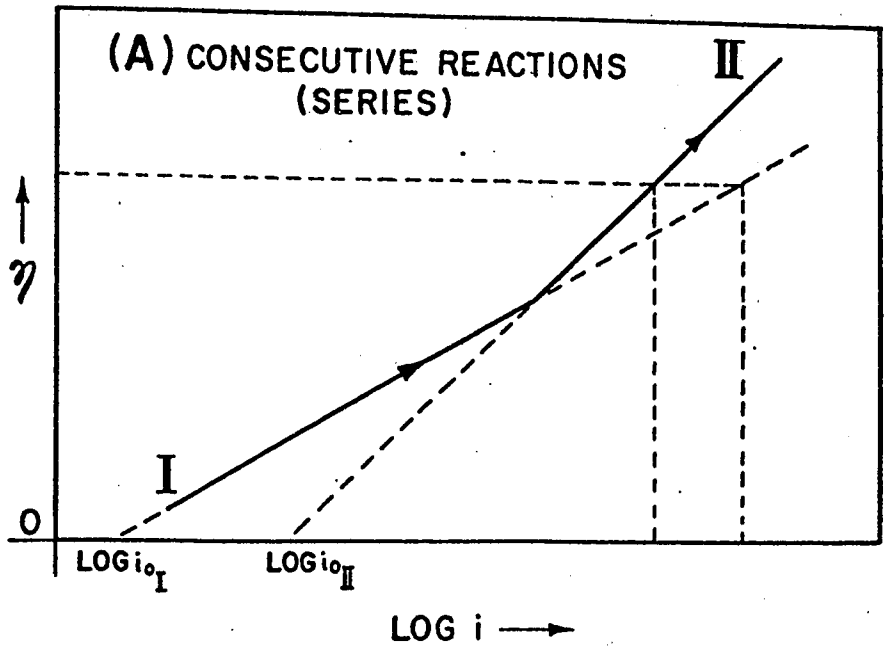

Process I is slower than II but its rate depends more on potential than does that of II.

At high potentials II becomes rate-determining even though $i_{o_{II}} > i_{o_I}$.

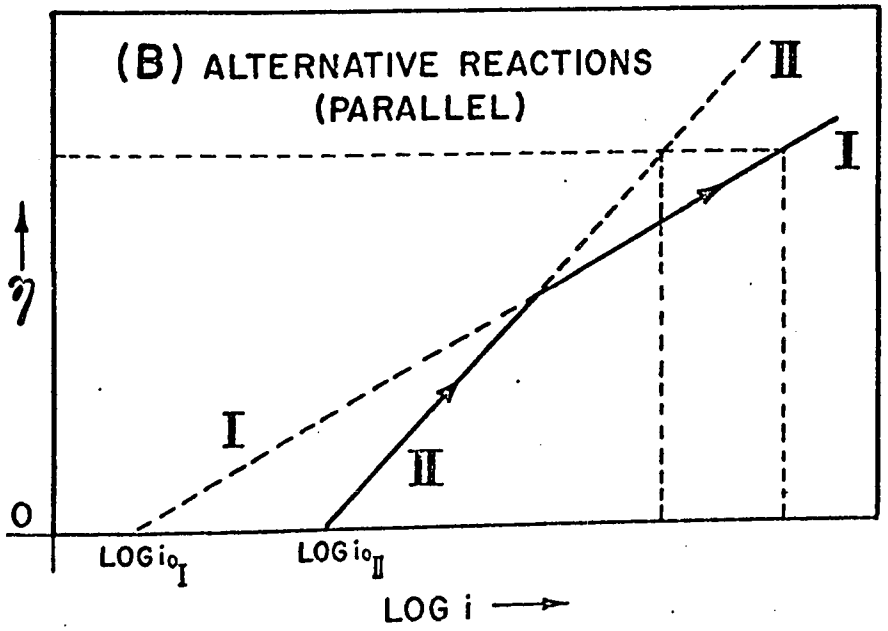

At high potentials, if I and II are alternative, I passes more current than II even though $i_{o_I} < i_{o_{II}}$.

2. Platinum. The current-potential lines are shown in Figure 32(a) and are linear over a c.d. range of up to two decades and are based on 7 to 8 experimental points per decade. Although most measurements were conducted over a series of descending temperatures, Tafel lines for this metal were also obtained by starting from the lowest temperature and gradually increasing the temperature at intervals up to room temperature and the results [which differ markedly from those in Figure 32(a)] are shown in Figure 32(b).

3. Lead. The Tafel lines for this metal are characterized by some shortness of the linear portion of the curve, so that even under optimum conditions, the linear region could be obtained only over 1.5 decades of current density. The Tafel slopes for Pb were extremely high, often reaching values of 300 mV/decade. In order to achieve reasonable values of b for lead, it was necessary to polarize the electrode for several hours at the maximum c.d. The results obtained with electrodes treated in this manner are shown in Figure 33(a). Such high slopes at Pb have been encountered previously (93) and may be associated with residual thin barrier layers which require prolonged cathodic polarization for their reduction.

4. Cadmium. As in the case of lead, the linear region of the Tafel plots for cadmium, shown in Figure 33(b), were limited to a range of current densities of only 1.5 decades. Identical results were, however, obtained at Cd irrespective of whether the measurements were made in an ascending or a descending direction of temperature change.

Figure 32

Tafel relations for the h. e. r. as a function of temperature.

(a) Pt cathodes in anhydrous HCl-EtOH for a descending series of temperatures.

(b) Pt cathodes in anhydrous HCl-EtOH for ascending values of temperatures.

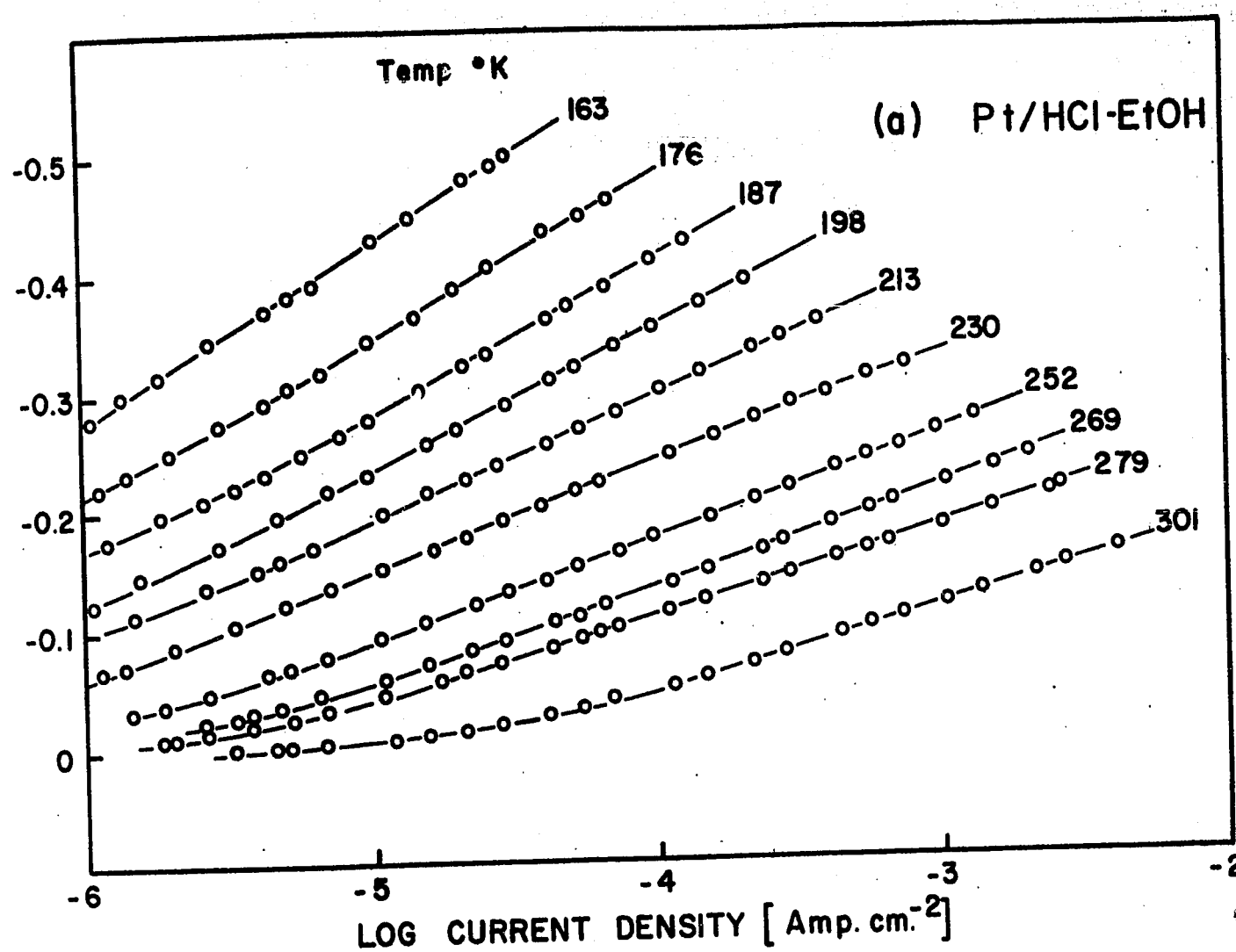
Temp °K
163
176
187
198
213
230
252
269
279
301
(a) Pt/HCl-EtOH
-0.5
-0.4
-0.3
-0.2
-0.1
0
E_H (volts)
-6
-5
-4
-3
-2
LOG CURRENT DENSITY [Amp. cm.$^{-2}$]

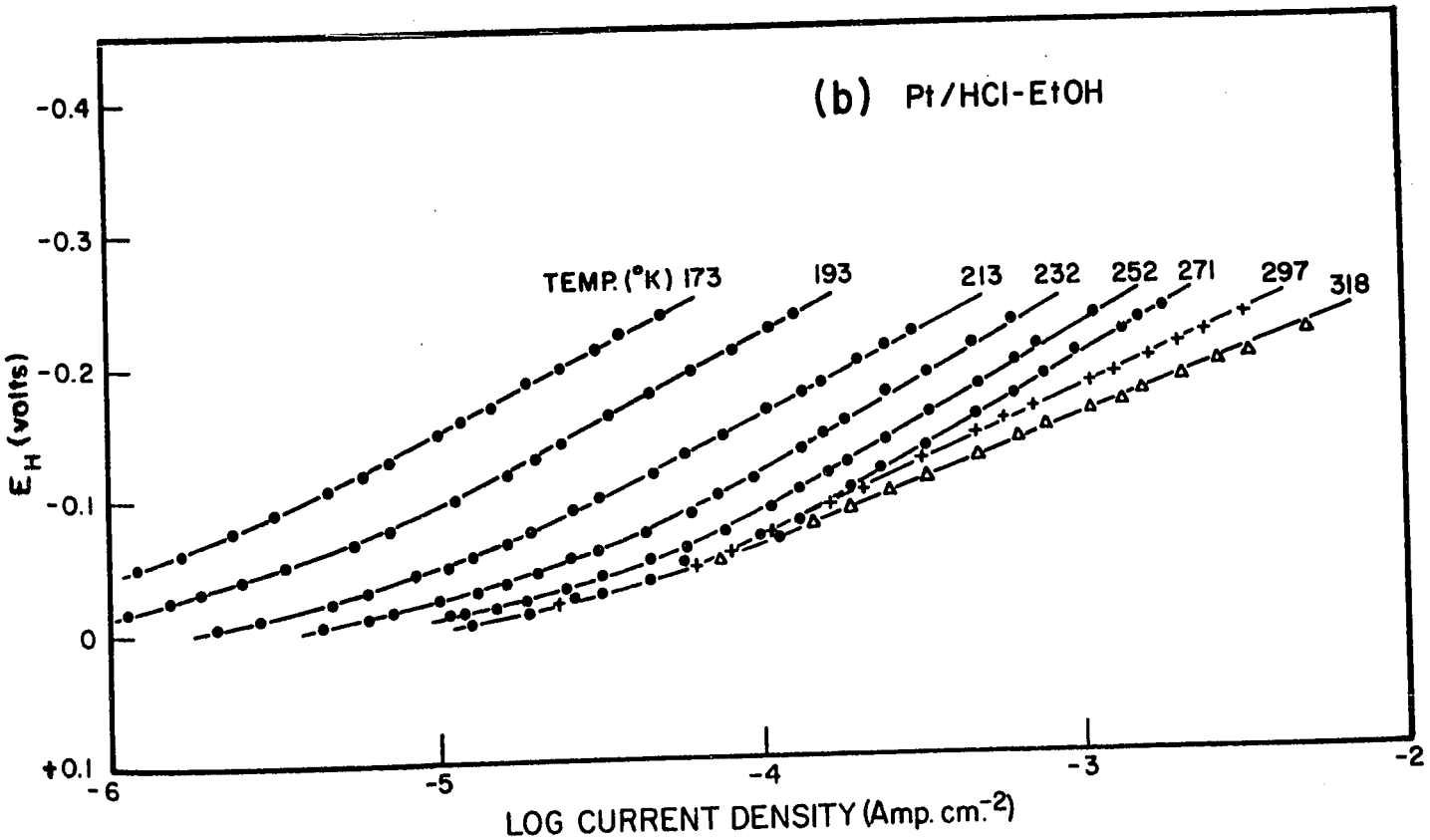
(b) Pt/HCl-EtOH
TEMP.(°K) 173
193
213
232
252
271
297
318
-0.4
-0.3
-0.2
-0.1
0
+0.1
E_H (volts)
-6
-5
-4
-3
-2
LOG CURRENT DENSITY (Amp. cm.$^{-2}$)

Figure 33

Tafel relations for the h. e. r. as a function of temperature.

(a) Pb cathodes in anhydrous HCl-MeOH.

(b) Cd cathodes in anhydrous HCl-EtOH.

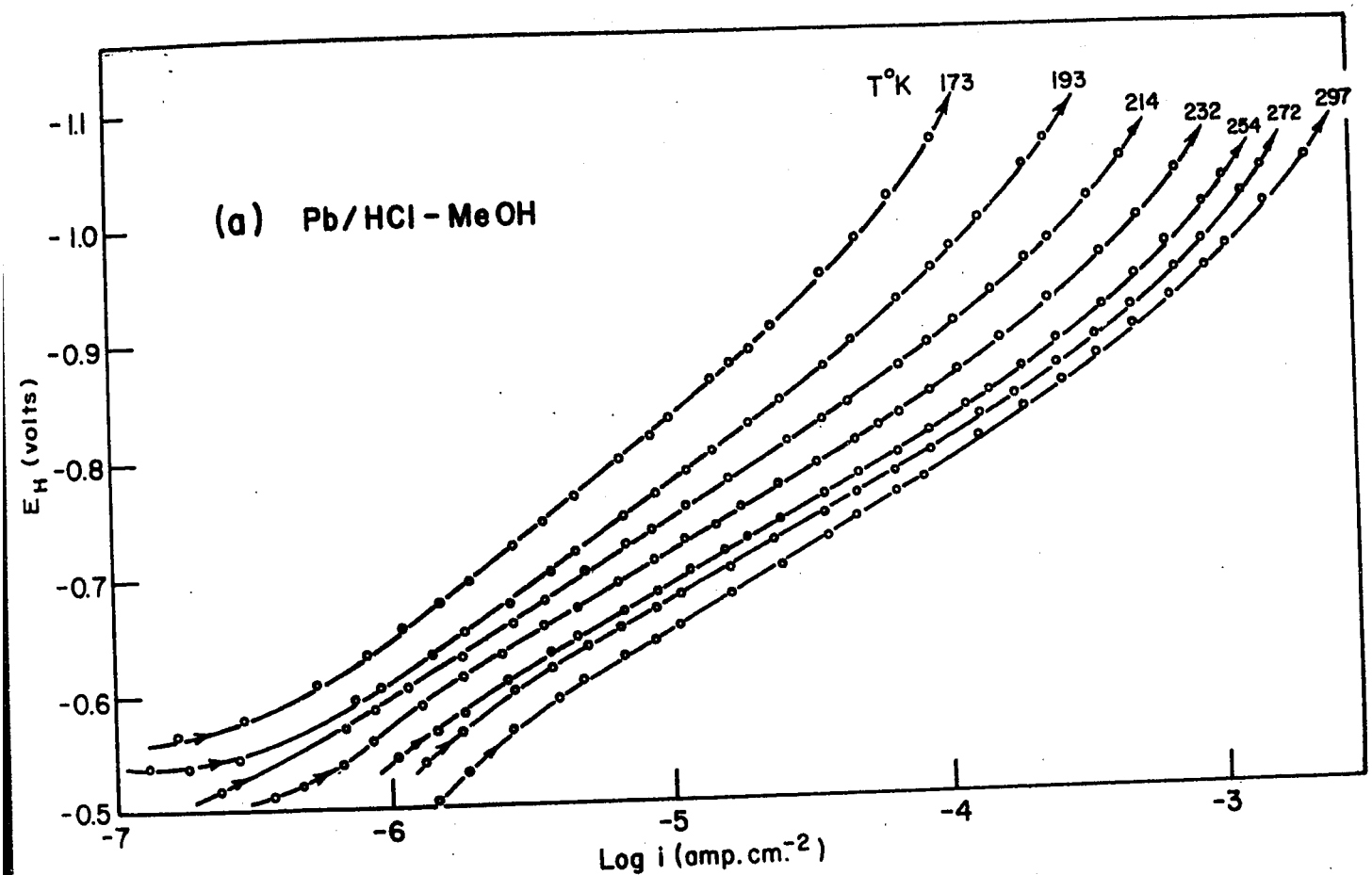
(a) Pb/HCl - MeOH
T°K 173
193
214
232
254
272
297
-1.1
-1.0
-0.9
-0.8
-0.7
-0.6
-0.5
E_H (volts)
-7
-6
-5
-4
-3
Log i (amp. cm.$^{-2}$)

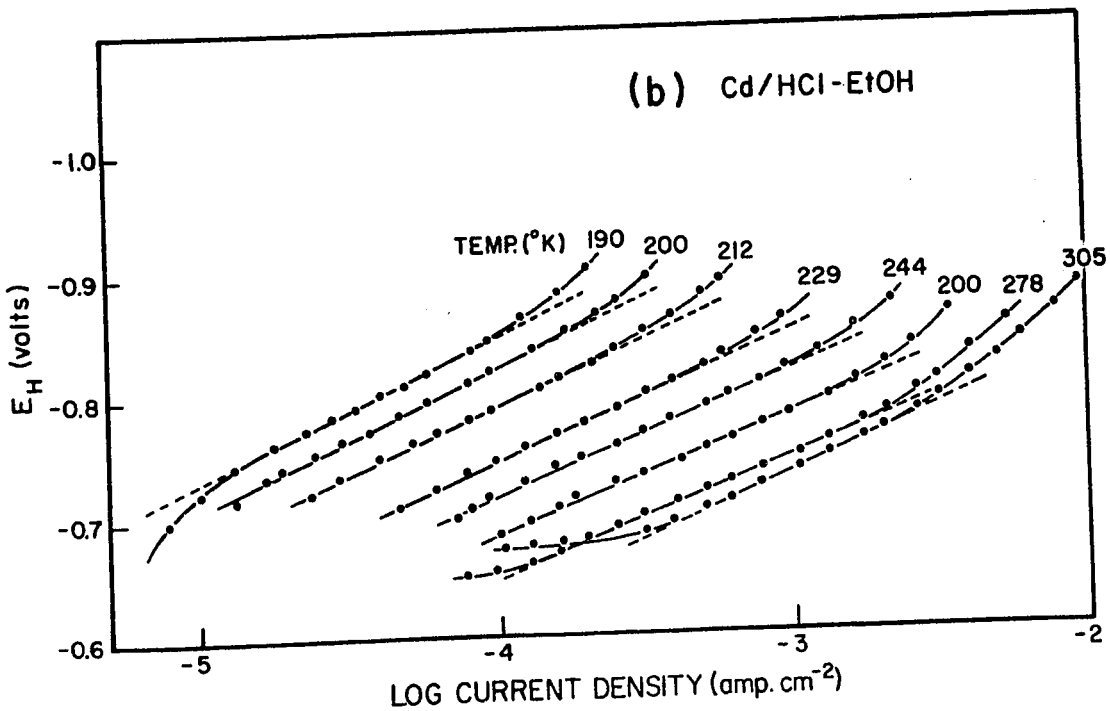
(b) Cd/HCl-EtOH
TEMP.(°K) 190
200
212
229
244
200
278
305
-1.0
-0.9
-0.8
-0.7
-0.6
E_H (volts)
-5
-4
-3
-2
LOG CURRENT DENSITY (amp. cm^{-2})

(ii) Tafel Slope, b, as a Function of Temperature

From the polarization curves described above, values of the Tafel slope, b, were obtained and plotted as a function of the absolute temperature.

1. Nickel. Figures 34(a) and 34(b) show typically the variation of the Tafel slopes (for the two linear η - log i regions) with temperature for this metal. The b values for the high c.d. region decrease linearly with decreasing temperature (T) down to approximately -40°C; but from this point, as the temperature is further decreased, b increases again along a smooth curve. For the low c.d. region, the surprising but qualitatively reproducible result is found that the b values increase linearly as T decreases. Although it was not possible to obtain exactly reproducible b values, the trend was always the same in many independent runs and in Figure 35 a "statistical" b vs. T plot for eight runs is shown.

2. Platinum. The b vs. T plot is shown in Figure 36(a) where the Tafel slope is seen to increase gradually as T decreases and then more rapidly as the temperature is decreased below -50°C. The trend here is somewhat similar to the b vs. T behavior for the low c.d. region at nickel. Figure 36(b) shows the b vs. T plot for Pt under conditions (see Figure 32(b)) where the Tafel lines were obtained by gradually increasing the temperature from an initial low value. Under such conditions, b is found to be practically independent of T until approximately 0°C beyond which there is a sharp decrease in b as T increases.

3. Lead. For this case, the b vs. T curves show an initial decrease as T decreases but begin to increase gradually as T is further decreased. The results are shown in Figure 37(a).

Figure 34

Tafel slope, b, as a function of temperature.

(a) Ni cathodes in anhydrous HCl-MeOH and in anhydrous DCl-MeOD.

(b) Ni cathodes in anhydrous HCl-EtOH.

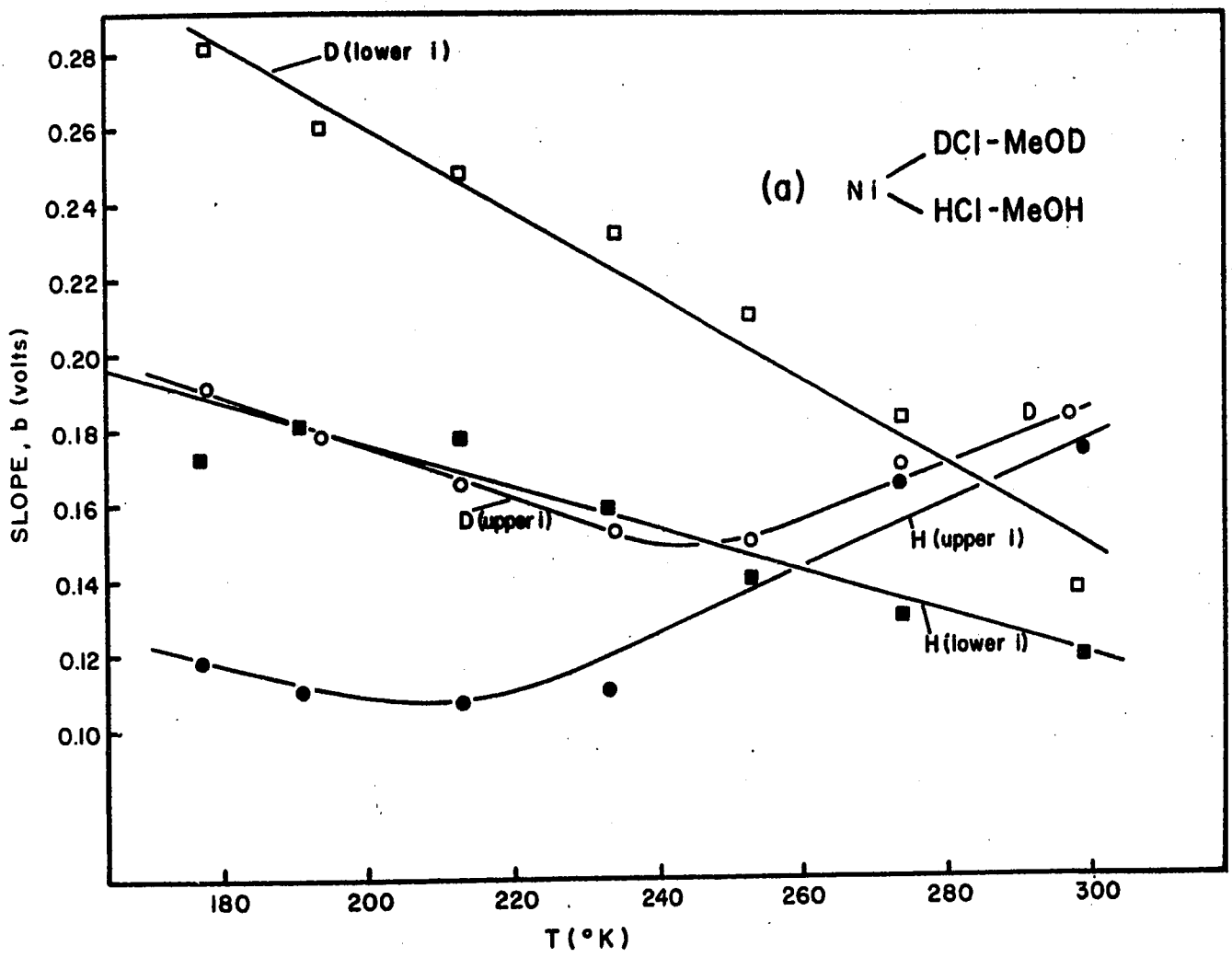
D (lower i)
(a) Ni
DCl-MeOD
HCl-MeOH
D
D (upper i)
H (upper i)
H (lower i)
SLOPE, b (volts)
0.28
0.26
0.24
0.22
0.20
0.18
0.16
0.14
0.12
0.10
180
200
220
240
260
280
300
T (°K)

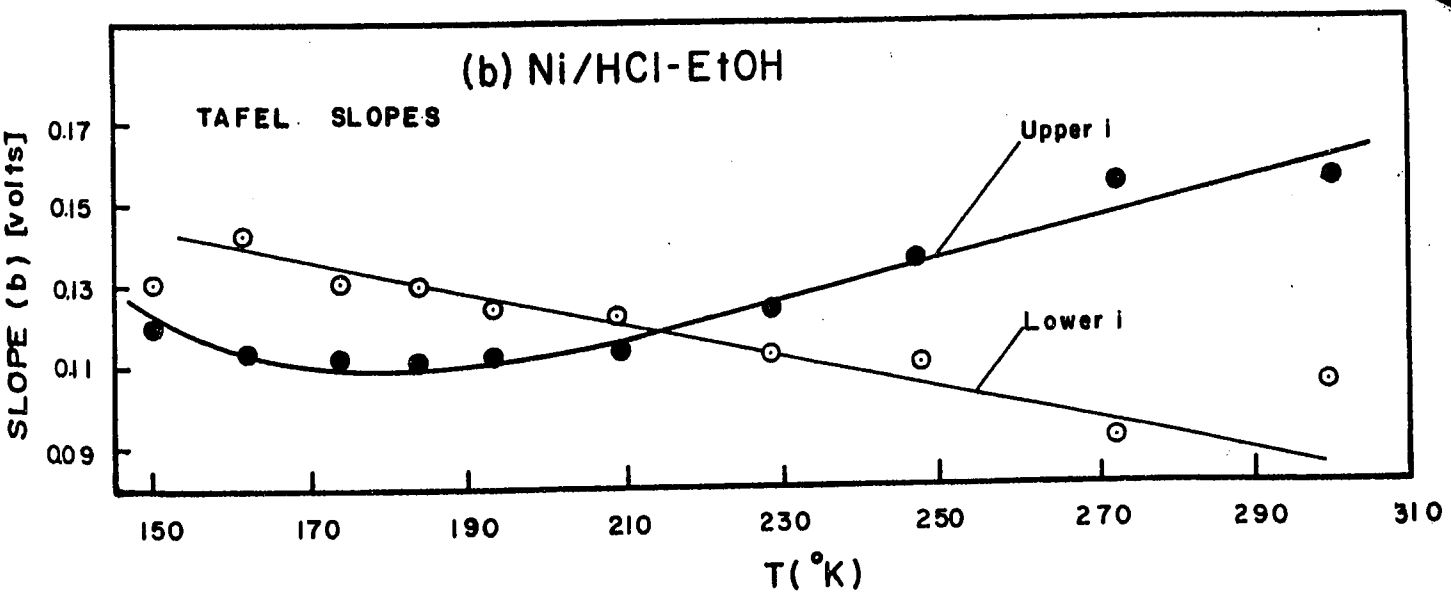
(b) Ni/HCl-EtOH
TAFEL SLOPES
Upper i
Lower i
SLOPE (b) [volts]
0.17
0.15
0.13
0.11
0.09
150
170
190
210
230
250
270
290
310
T(°K)

Figure 35

Statistical plot of Tafel slope, b, as a function of temperature for Ni cathodes in anhydrous HCl-EtOH and in anhydrous DCl-MeOD. (Graphs are based on data for 8 independent runs.).

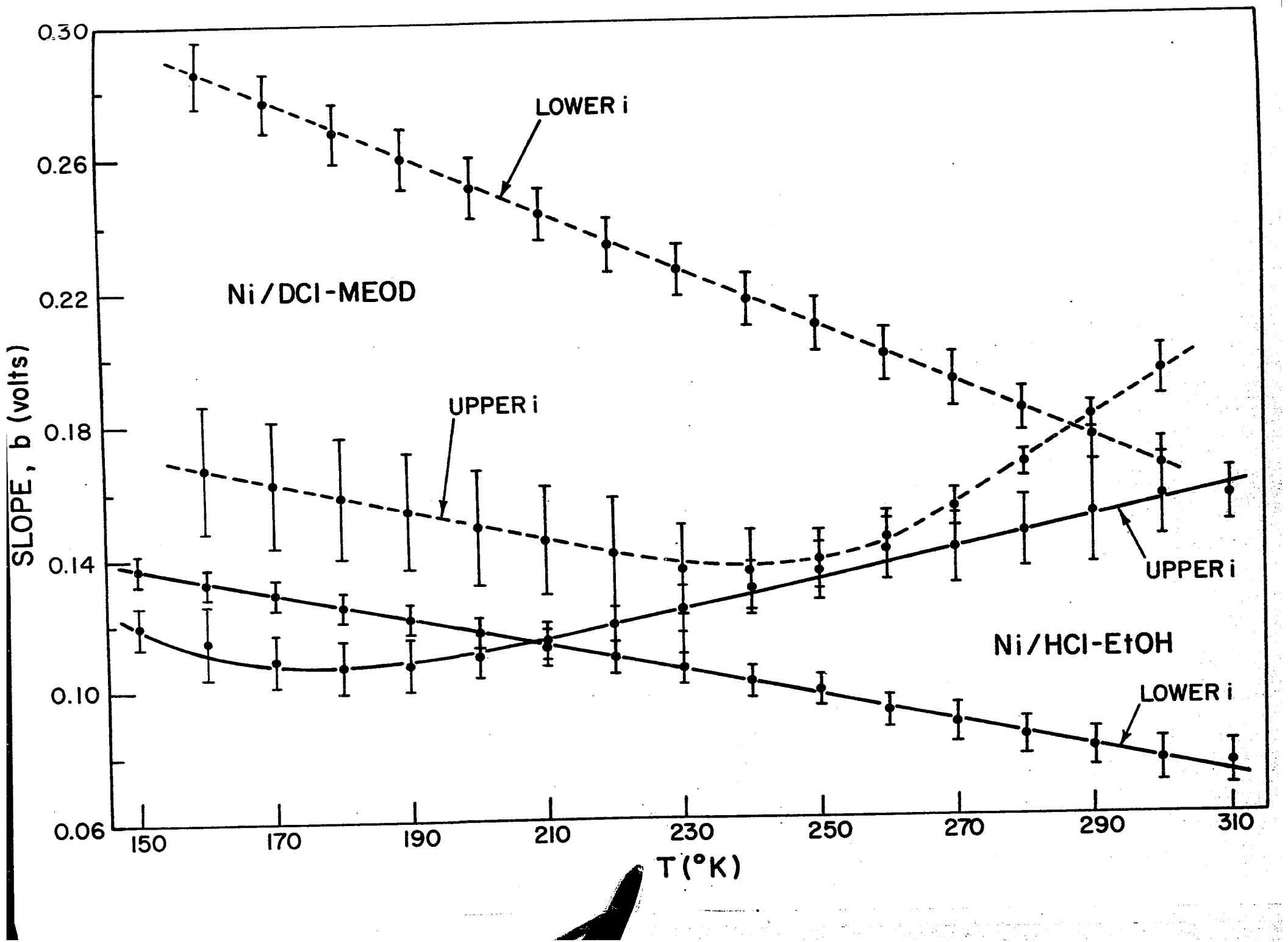
0.30
0.26
0.22
0.18
0.14
0.10
0.06
SLOPE, b (volts)
LOWER i
Ni/DCl-MEOD
UPPER i
UPPER i
Ni/HCl-EtOH
LOWER i
150
170
190
210
230
250
270
290
310
T(°K)

Figure 36

Tafel slope, b, as a function of temperature.

(a) Pt cathodes in anhydrous HCl-MeOH and in anhydrous DCl-MeOD.

(b) Pt cathodes in anhydrous HCl-EtOH for ascending values of temperature.

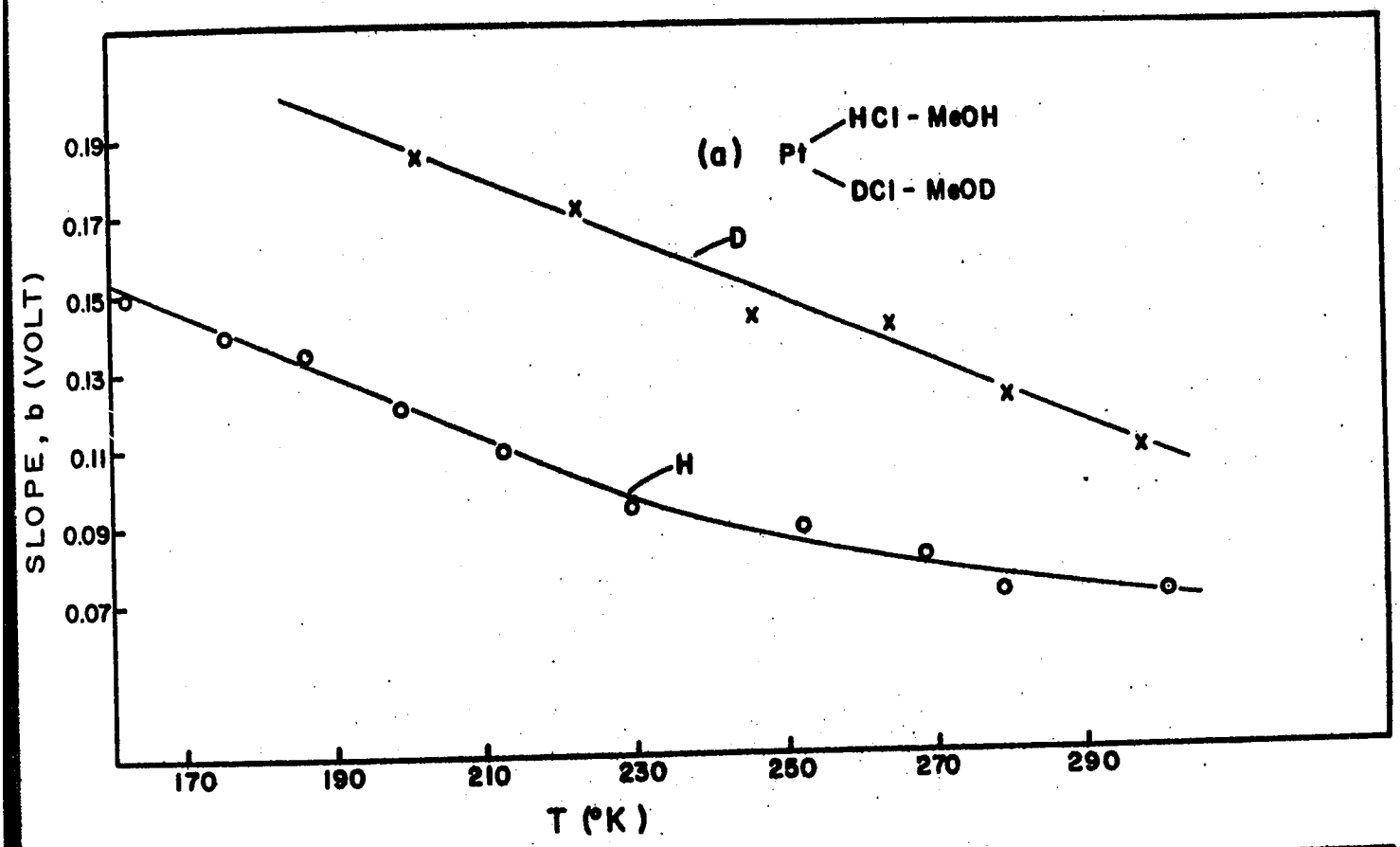
(a) Pt
HCl - MeOH
DCl - MeOD
D
H
SLOPE, b (VOLT)
0.19
0.17
0.15
0.13
0.11
0.09
0.07
170
190
210
230
250
270
290
T (°K)

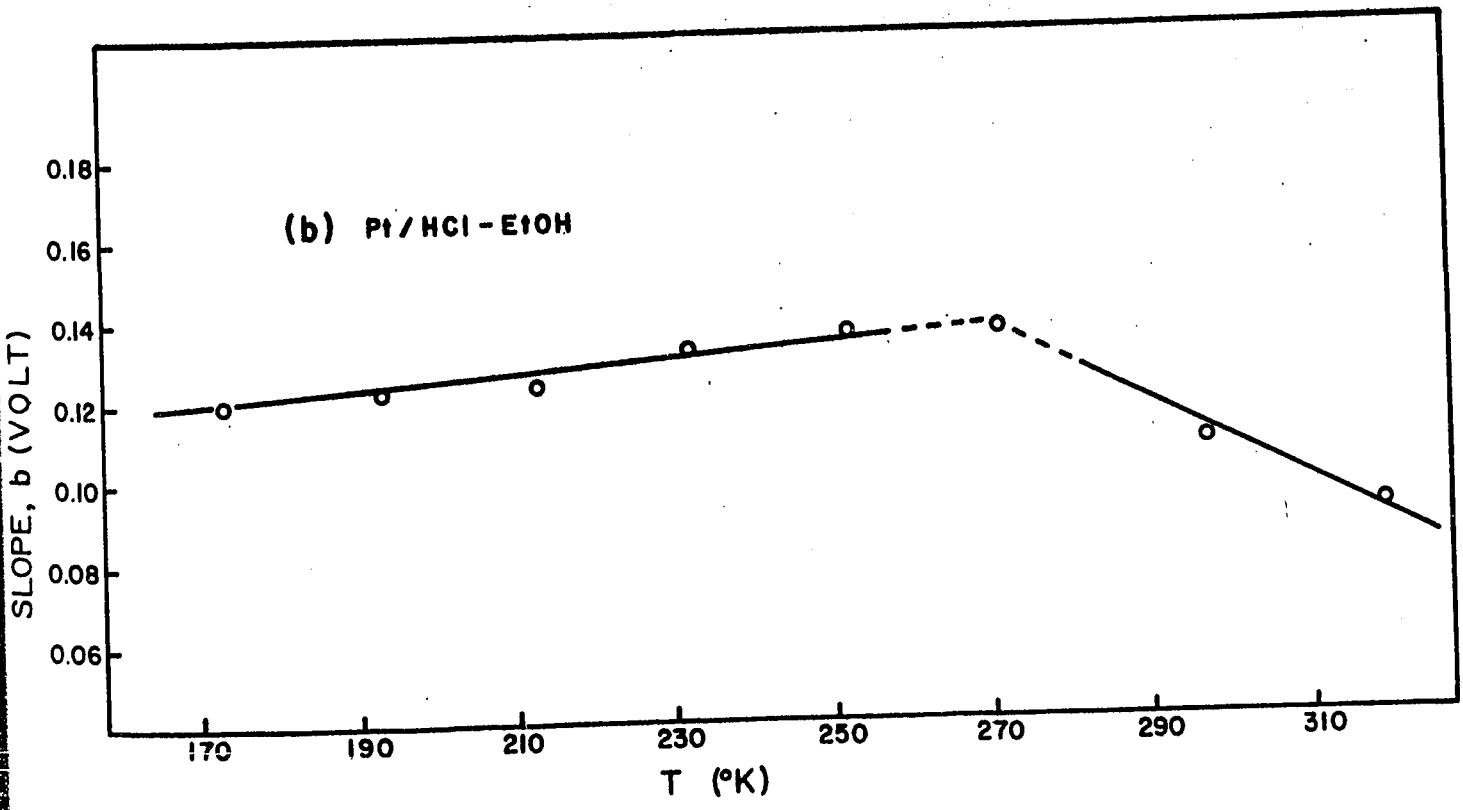
(b) Pt / HCl - EtOH
SLOPE, b (VOLT)
0.18
0.16
0.14
0.12
0.10
0.08
0.06
170
190
210
230
250
270
290
310
T (°K)

4. Cadmium. The plot of b vs. T is shown in Figure 37(b) and the trend in this case is identical with that found at lead although the b values tend to be numerically lower. This trend observed for cadmium is the same irrespective of how the Tafel lines were obtained and is thus to be distinguished from that observed in the case of Pt.

(iii) Exchange c.d. as a Function of Temperature

The logarithm of the exchange c.d. ($\log i_o$), corresponding to the experimental region* of current-potential behavior actually observed, was obtained for each temperature by calculation using the experimental Tafel lines and the equation

$$\eta = a + b \log i \qquad [61]$$

which gives, when $\eta = 0$

$$\log i_o = -a/b \qquad [62]$$

where a is the value (negative for the cathodic process) of η when i is unity; b is also taken as a negative quantity.

1. Nickel. In this case, two lines were obtained for HCl solutions corresponding to the two Tafel regions of Figures 30(a) and 30(b). The plot for the high c.d. region shows a departure from linearity at approximately -40°C and gives an apparent value of $\Delta H_R^{o\ddagger}$ of 10.4 kcal. mole^{-1} as shown in Figure 38. The plot for the low c.d. region exhibits curvature and gives limitingly values of $\Delta H_R^{o\ddagger}$ of 7.1 for the upper region and 3.9 kcal. mole^{-1} for the lower section (see Figure 38).

---

*The value of $\log i_o$ so calculated may not be identical with that actually obtaining at $\eta = 0$ in an inaccessible (e.g. at Pb or Hg) range of current densities i_o to 10 i_o near the reversible potential.

Figure 37

Tafel slope, b, as a function of temperature.

(a) Pb cathodes in anhydrous HCl-EtOH.

(b) Cd cathodes in anhydrous DCl-MeOD and in anhydrous HCl-EtOH for both ascending and descending values of temperature.

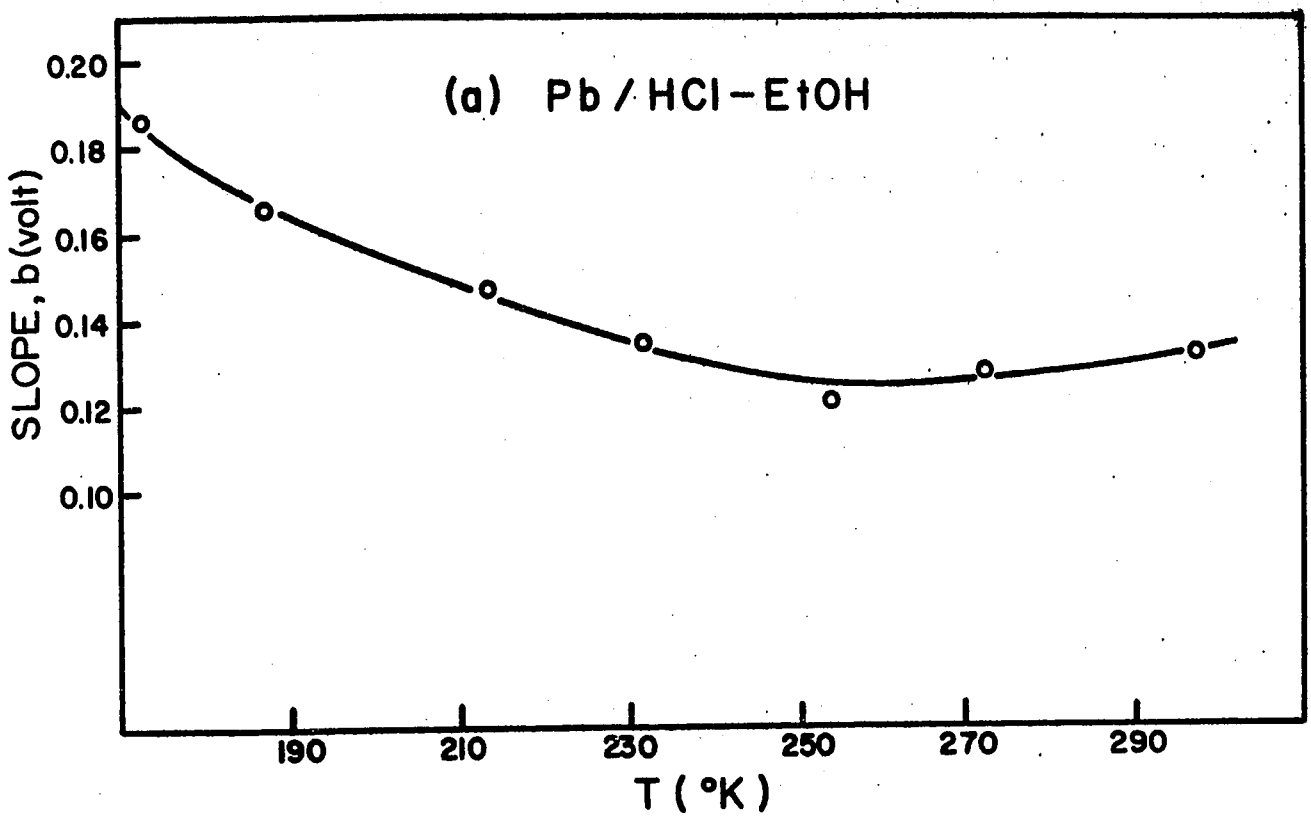
(a) Pb / HCl – EtOH
SLOPE, b (volt)
0.20
0.18
0.16
0.14
0.12
0.10
190
210
230
250
270
290
T (°K)

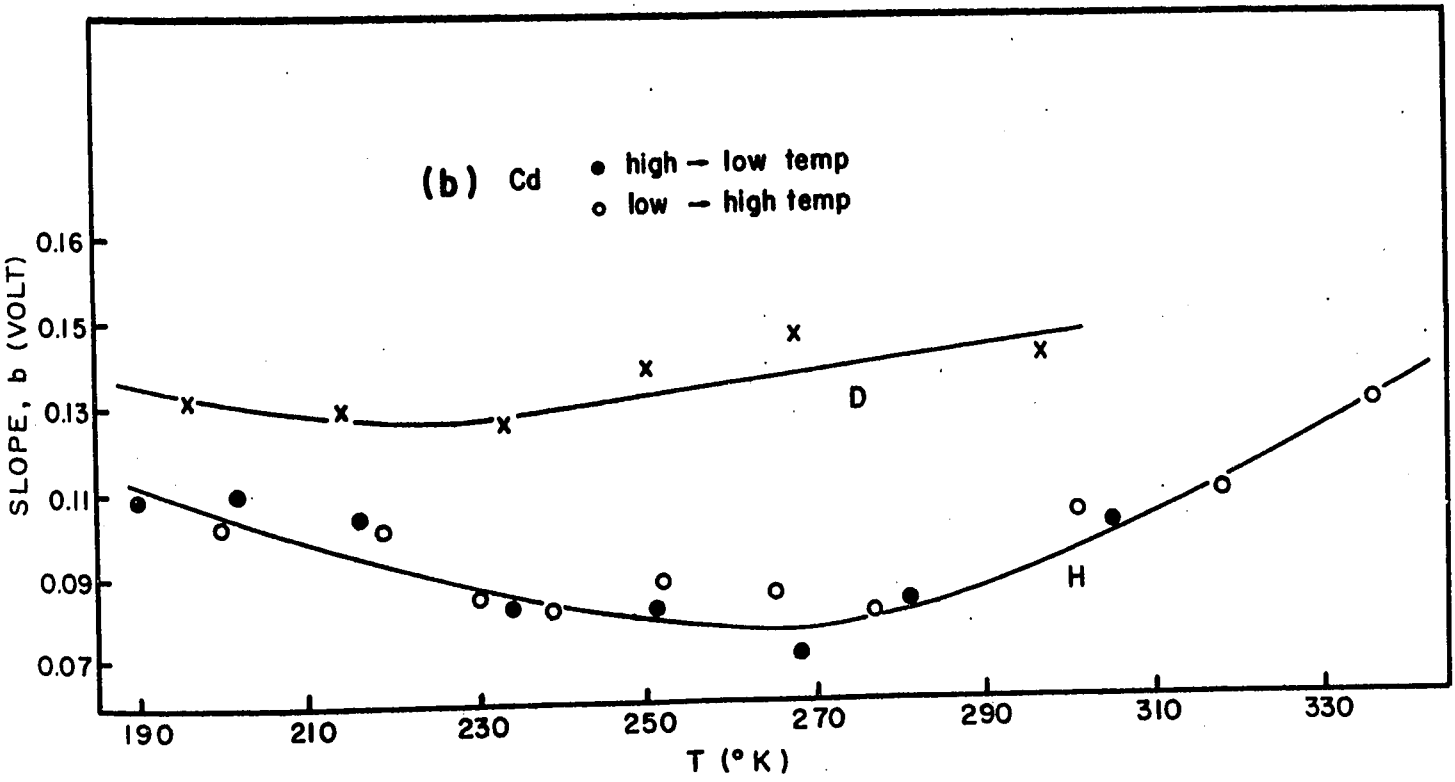
(b) Cd
high – low temp
low – high temp
SLOPE, b (VOLT)
0.16
0.15
0.13
0.11
0.09
0.07
D
H
190
210
230
250
270
290
310
330
T (°K)

Figure 38

Arrhenius type plots for the h. e. r. at Ni cathodes in anhydrous HCl-EtOH.

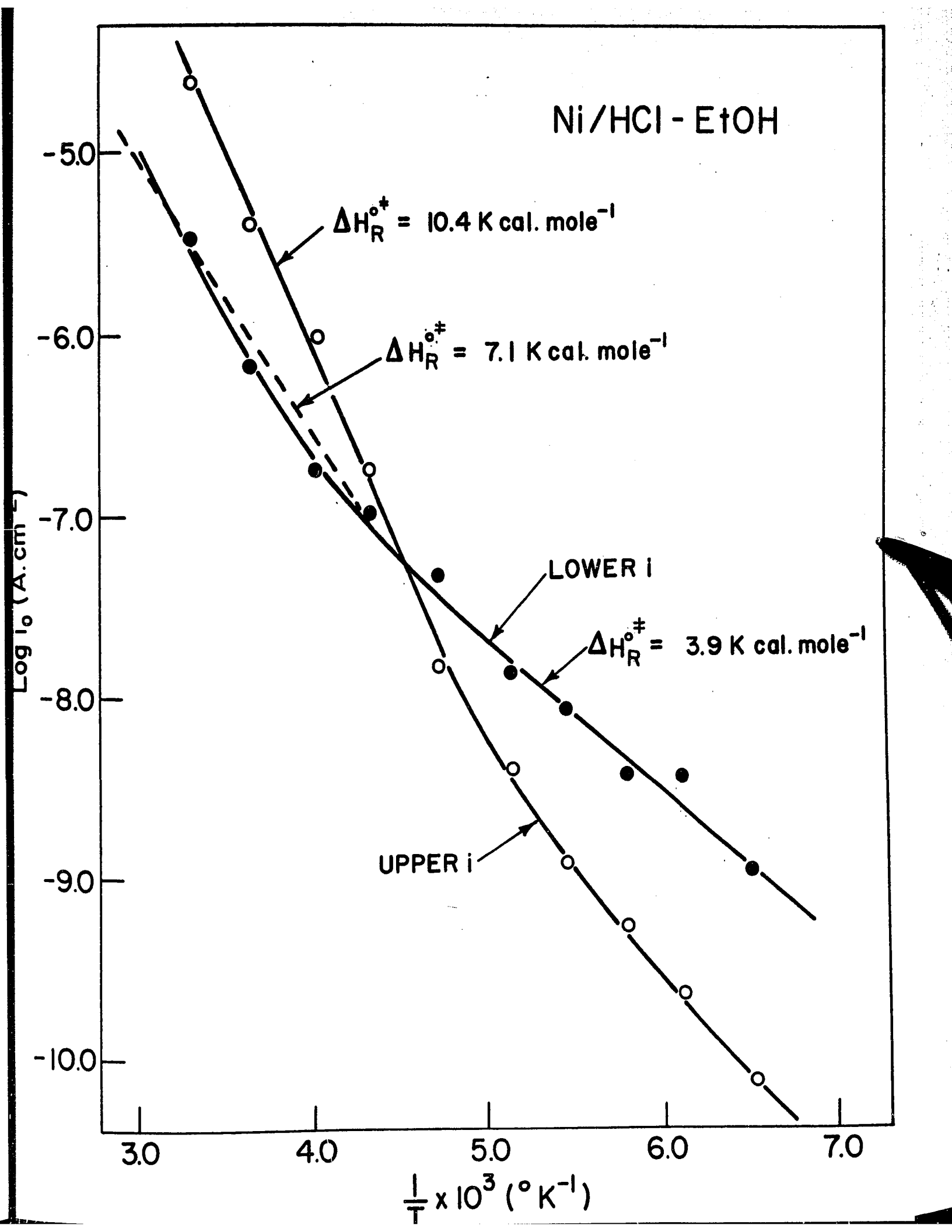
Ni/HCl - EtOH
ΔH_R^{o*} = 10.4 K cal. mole^{-1}
$\Delta H_R^{o\ddagger}$ = 7.1 K cal. mole^{-1}
LOWER i
$\Delta H_R^{o\ddagger}$ = 3.9 K cal. mole^{-1}
UPPER i
Log i_o (A. cm^{-2})
-5.0
-6.0
-7.0
-8.0
-9.0
-10.0
3.0
4.0
5.0
6.0
7.0
$\frac{1}{T} \times 10^3$ (°K^{-1})

2. Platinum. As in the case for the low c.d. region at nickel, the electrochemical Arrhenius plots for platinum exhibit marked curvature especially at higher overpotentials; $\Delta H_R^{o\ddagger}$ varies from ca. 8 kcal. mole^{-1} (+25 to -46°C) to ca. 3.5 kcal. mole^{-1} (-46 to -125°C) as shown in Figure 39(a). The corresponding plot for the experiment conducted over a range of ascending temperatures is shown in Figure 39(b) and exhibits surprisingly an apparent negative activation energy at the high temperature end.

3. Lead. In Figure 40(a) is shown the kinetic behavior which gives an apparent negative energy of activation at values of $1/T > 3.9 \times 10^{-3}$ °K^{-1}. $\Delta H_R^{o\ddagger}$ for $1/T < 3.9 \times 10^{-3}$ °K^{-1} is, however, +6.3 kcal. mole^{-1}.

4. Cadmium. The log i_o vs. (1/T) plot shown in Figure 40(b) shows a break at approximately 4.0×10^{-3} °K^{-1} where log i_o becomes practically independent of temperature. The value of $\Delta H_R^{o\ddagger}$ calculated from the results at the high temperature end (i.e., $1/T < 4.0 \times 10^{-3}$ °K^{-1}) is 7.1 kcal. mole^{-1}.

(iv) Apparent Activation Energies as a Function of η

Values of $(\log i)_\eta$ were plotted as a function of (1/T) for each of the metals under consideration for various values of η. From these plots, values for $\Delta H_\eta^{o\ddagger}$ are obtained (cf. equation in Chapter II) for each η value and can then be plotted as a function of η; according to previous treatments (68), such relations can be represented by the following equation if β is a constant, independent of T:

$$\Delta H_\eta^{o\ddagger} = \Delta H_R^{o\ddagger} - \beta \eta F \qquad [52]$$

in this equation, $\Delta H_R^{o\ddagger}$ is the value of the activation energy at zero

Figure 39

Arrhenius type plots for the h. e. r. and d. e. r.

(a) Pt cathodes in anhydrous HCl-EtOH and in anhydrous DCl-MeOD.

(b) Pt cathodes in anhydrous HCl-EtOH for ascending values of temperature.

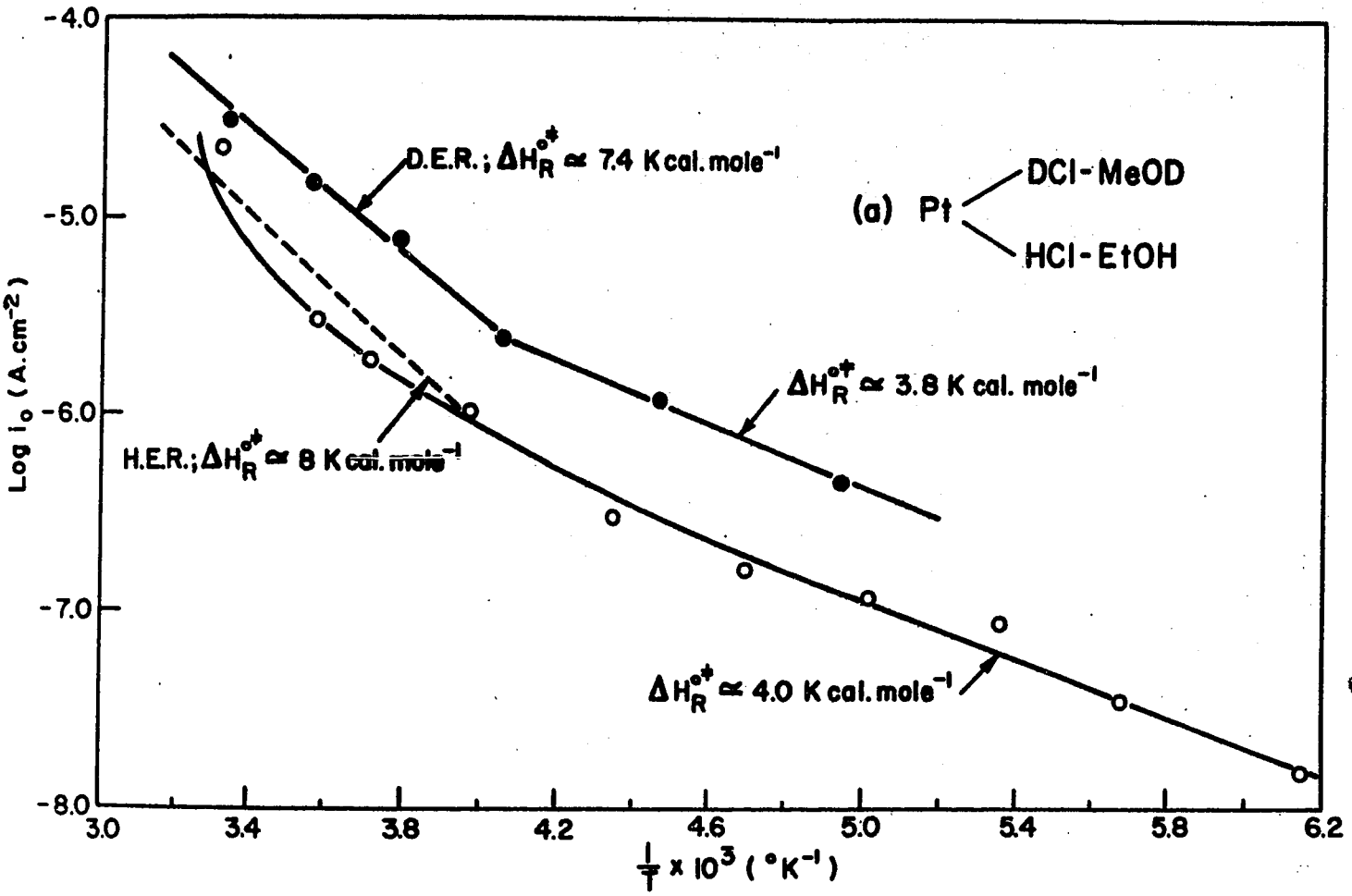
-4.0
-5.0
-6.0
-7.0
-8.0
Log i_o (A.cm^{-2})
D.E.R.; $\Delta H_R^{o\ddagger} \propto$ 7.4 K cal. mole^{-1}
(a) Pt
DCl-MeOD
HCl-EtOH
$\Delta H_R^{o\ddagger} \propto$ 3.8 K cal. mole^{-1}
H.E.R.; $\Delta H_R^{o\ddagger} \propto$ 8 K cal. mole^{-1}
$\Delta H_R^{o\ddagger} \propto$ 4.0 K cal. mole^{-1}
3.0
3.4
3.8
4.2
4.6
5.0
5.4
5.8
6.2
$\frac{1}{T} \times 10^3$ ($^\circ K^{-1}$)

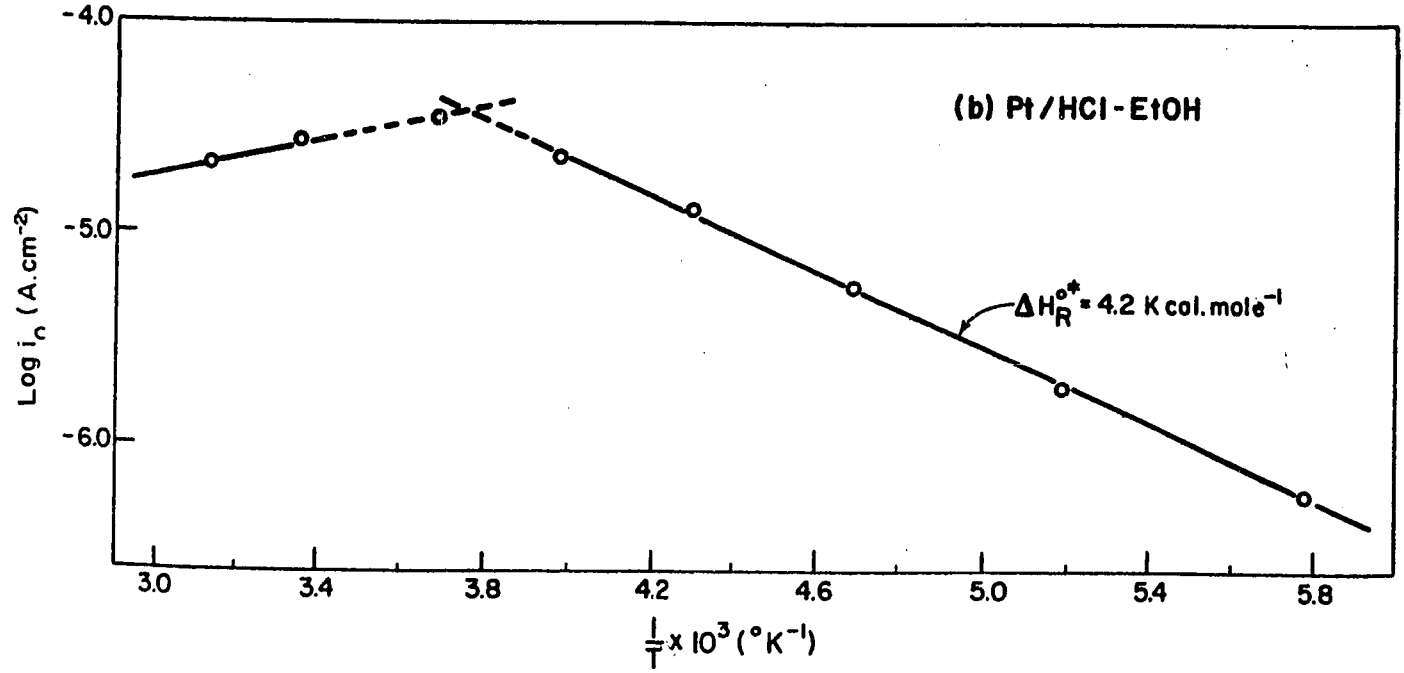
-4.0
-5.0
-6.0
Log i_o (A.cm^{-2})
(b) Pt/HCl-EtOH
$\Delta H_R^{o\ddagger}$ = 4.2 K cal. mole^{-1}
3.0
3.4
3.8
4.2
4.6
5.0
5.4
5.8
$\frac{1}{T} \times 10^3$ ($^\circ K^{-1}$)

Figure 40

Arrhenius type plots for the h. e. r. and d. e. r.

(a) Pb cathodes in anhydrous HCl-MeOH.

(b) Cd cathodes in anhydrous HCl-EtOH and in anhydrous DCl-MeOD.

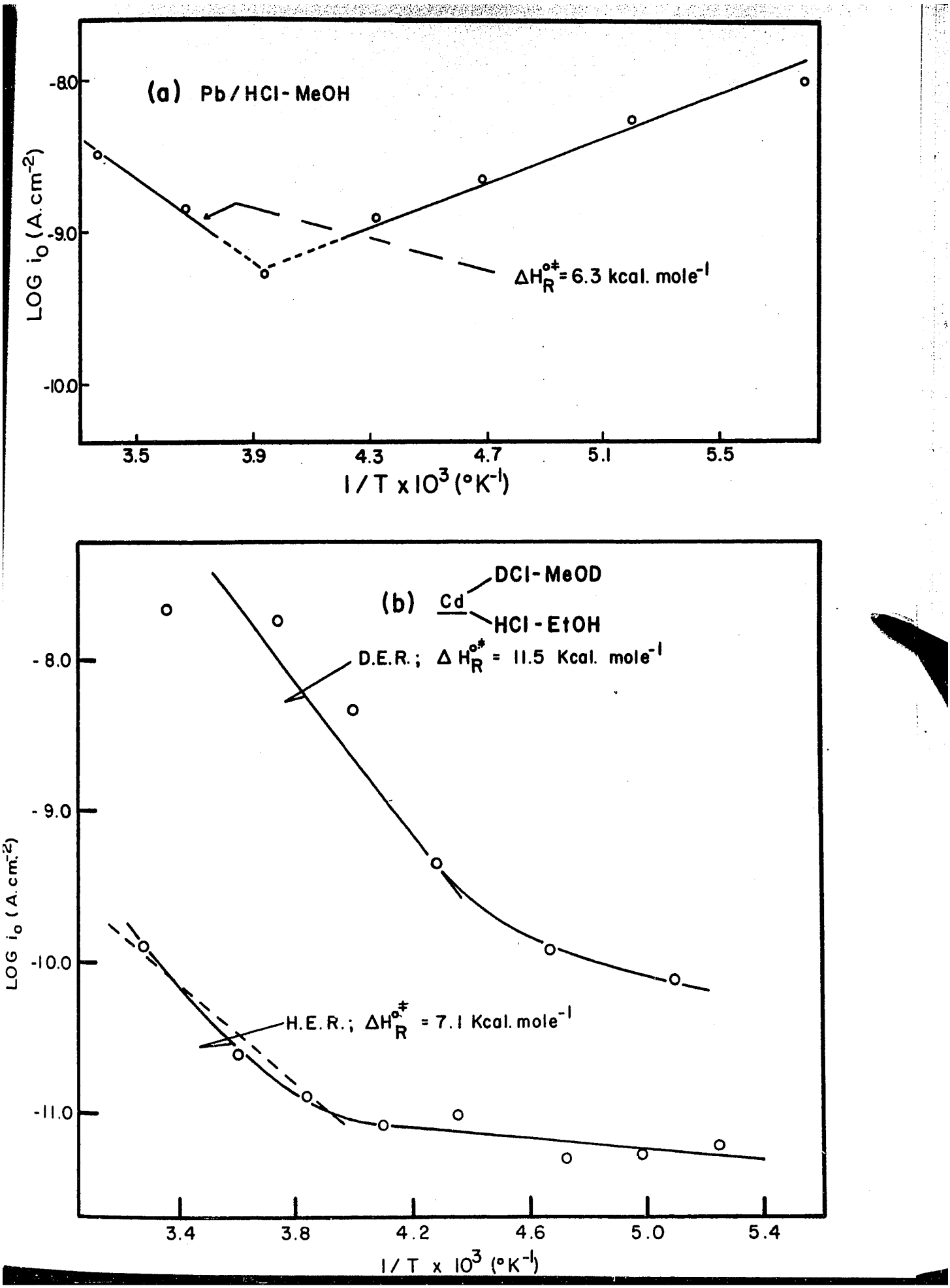
(a) Pb / HCl - MeOH
LOG i_o ($A.cm^{-2}$)
-8.0
-9.0
-10.0
ΔH_R^{o*} = 6.3 kcal. $mole^{-1}$
3.5
3.9
4.3
4.7
5.1
5.5
$1/T \times 10^3$ ($°K^{-1}$)
(b) Cd
DCl - MeOD
HCl - EtOH
D.E.R.; ΔH_R^{o*} = 11.5 Kcal. $mole^{-1}$
H.E.R.; $\Delta H_R^{o\ddagger}$ = 7.1 Kcal. $mole^{-1}$
LOG i_o ($A.cm^{-2}$)
- 8.0
- 9.0
-10.0
-11.0
3.4
3.8
4.2
4.6
5.0
5.4
$1/T \times 10^3$ ($°K^{-1}$)

overpotential, i.e., the value pertaining to the backward and forward directions of the process at the reversible potential. It will be shown in Chapter V, however, that the relation between $\Delta H_\eta^{o\ddagger}$ and $\Delta H_R^{o\ddagger}$ is more complex when β is f(T) or if b is not simply $RT/\beta F$.

1. Nickel; High c.d. region: In Figure 41(a) is shown a plot of $(\log i)_\eta$ vs. (1/T) for η values ranging from 0 to -0.6 V. $\Delta H_\eta^{o\ddagger}$ decreases as η increases as required by the above equation, and the non-linearity of the $\log i_o$ vs. (1/T) plot gradually disappears as η increases, the relation becoming more or less linear over the entire temperature range at the higher η values. A plot of $\Delta H_\eta^{o\ddagger}$ vs. η is shown in Figure 41(b).

Lower c.d. region: The results are shown in Figure 42 but, contrary to the above equation, $\Delta H_\eta^{o\ddagger}$ increases as η increases and there is curvature in the plot which becomes more pronounced as η becomes more negative.

2. Platinum. The plot of $(\log i)_\eta$ vs. (1/T) is shown in Figure 43(a); it is evident that there is some resemblance to the results for the low c.d. region at nickel as shown in Figure 42. Figure 43(b) shows a plot of $\Delta H_\eta^{o\ddagger}$ vs. η and indicates again an apparent negative value of β, the symmetry factor in equation [52].

3. Lead. In Figure 44(a) is shown the plot of $(\log i)_\eta$ vs. (1/T) and it can be seen that as η increases the apparent negative activation energy at the lower temperature disappears and the relations become linear at approximately η = -0.9 volt.

4. Cadmium. The results for this case are quite similar to those for lead and are shown in Figure 44(b).

Figure 41

The h. e. r. at Ni cathodes in anhydrous HCl-EtOH; upper c. d. region.

(a) Arrhenius type plots as a function of over-potential.

(b) Apparent heat of activation as a function of overpotential.

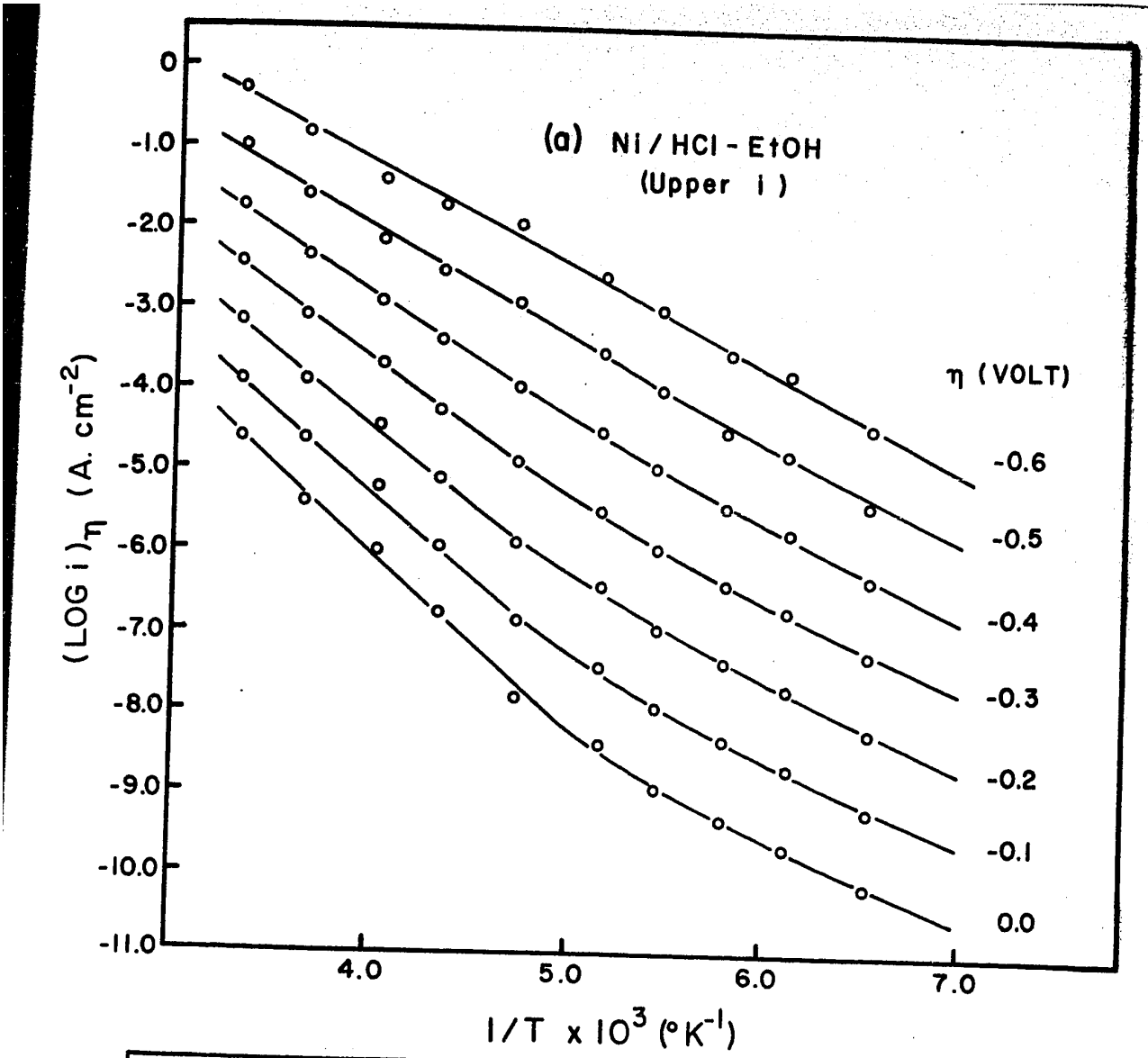
(a) Ni / HCl - EtOH
(Upper i)
η (VOLT)
-0.6
-0.5
-0.4
-0.3
-0.2
-0.1
0.0
(LOG i)η (A. cm-2)
0
-1.0
-2.0
-3.0
-4.0
-5.0
-6.0
-7.0
-8.0
-9.0
-10.0
-11.0
4.0
5.0
6.0
7.0
1/T x 10^3 (°K^-1)

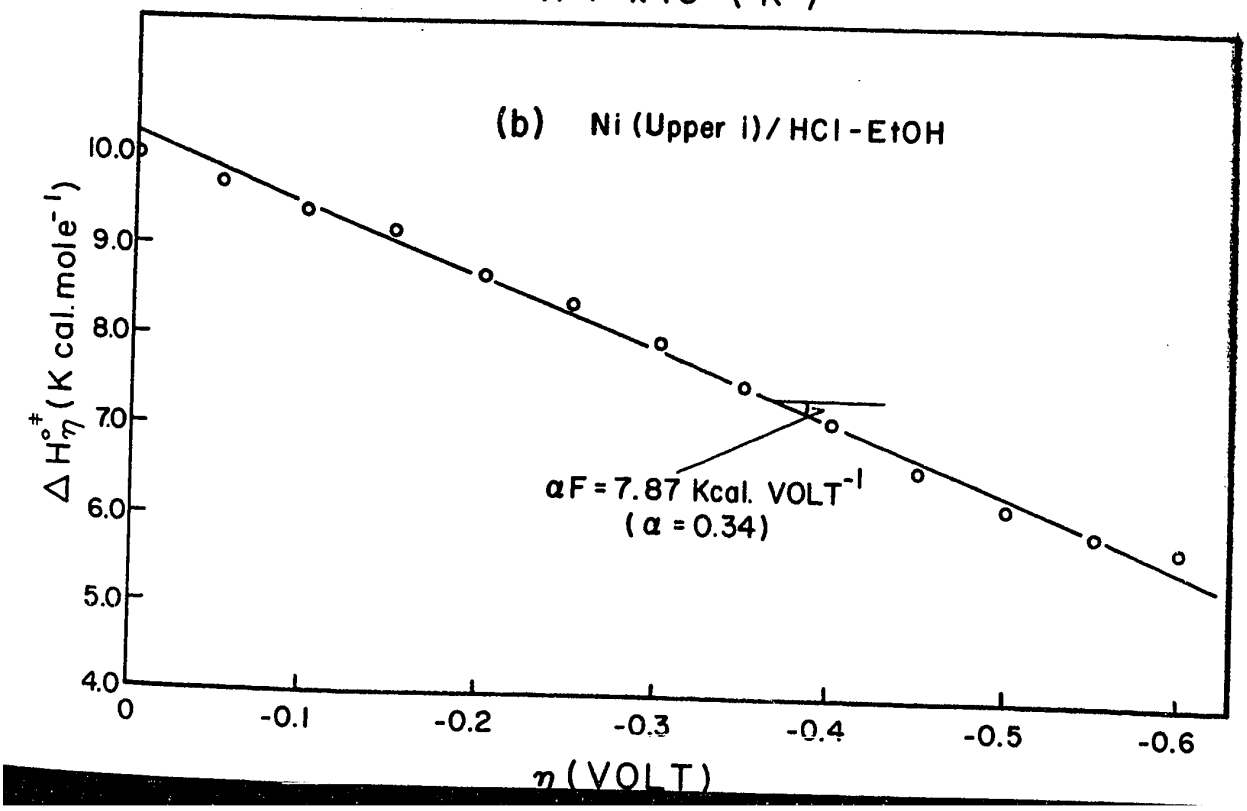
(b) Ni (Upper i) / HCl - EtOH
ΔH°η# (K cal. mole-1)
10.0
9.0
8.0
7.0
6.0
5.0
4.0
αF = 7.87 Kcal. VOLT-1
(α = 0.34)
0
-0.1
-0.2
-0.3
-0.4
-0.5
-0.6
η (VOLT)

Figure 42

Arrhenius type plots as a function of overpotential for the h. e. r. at Ni cathodes in anhydrous HCl-EtOH; lower c. d. region.

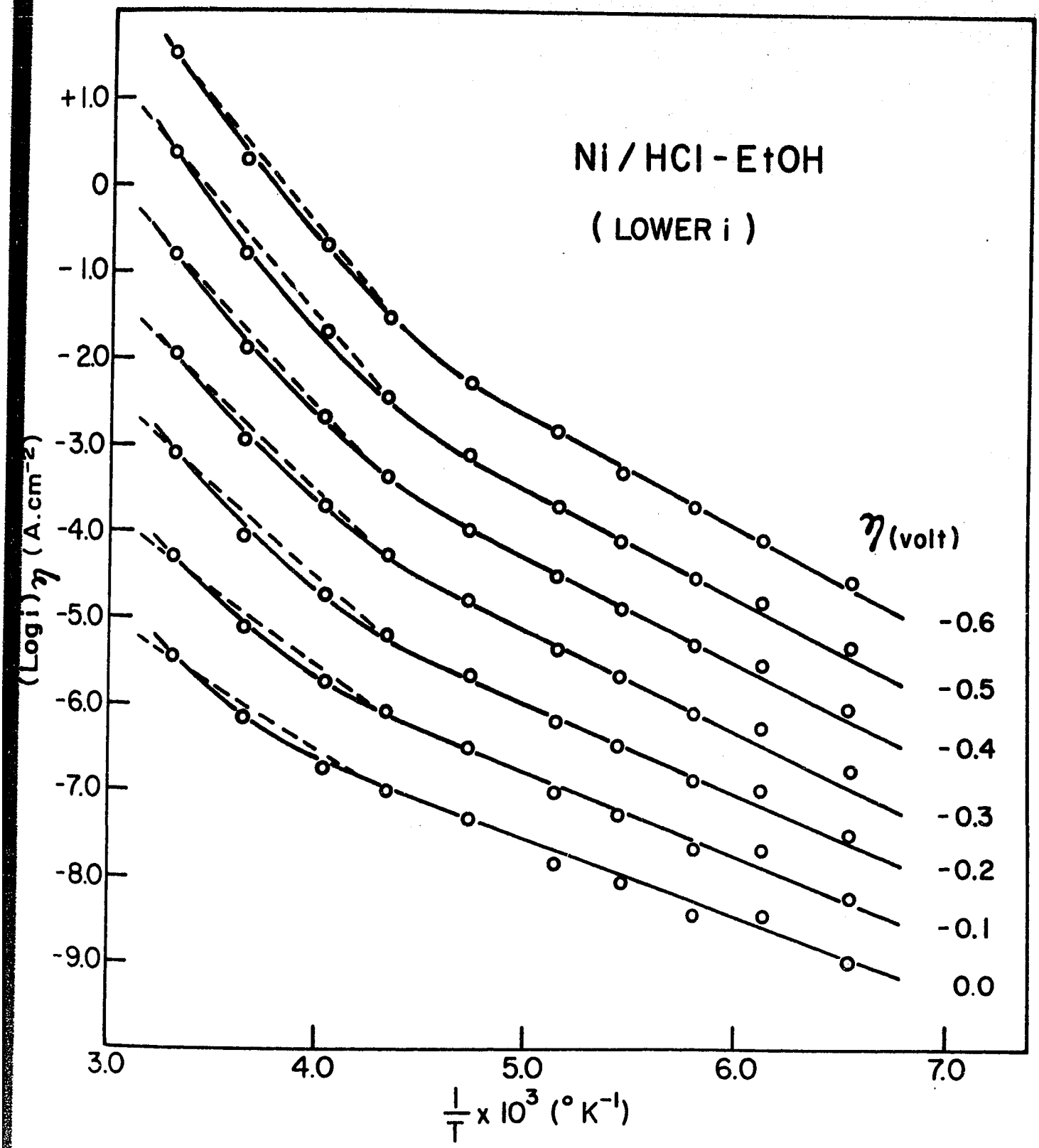
Ni / HCl - EtOH
(LOWER i)
+1.0
0
-1.0
-2.0
-3.0
-4.0
-5.0
-6.0
-7.0
-8.0
-9.0
(Log i) η (A.cm⁻²)
η (volt)
-0.6
-0.5
-0.4
-0.3
-0.2
-0.1
0.0
3.0
4.0
5.0
6.0
7.0
1/T x 10³ (°K⁻¹)

Figure 43

The h. e. r. at Pt cathodes in anhydrous HCl-EtOH.

(a) Arrhenius type plots as a function of over-potential.

(b) Apparent heat of activation as a function of overpotential.

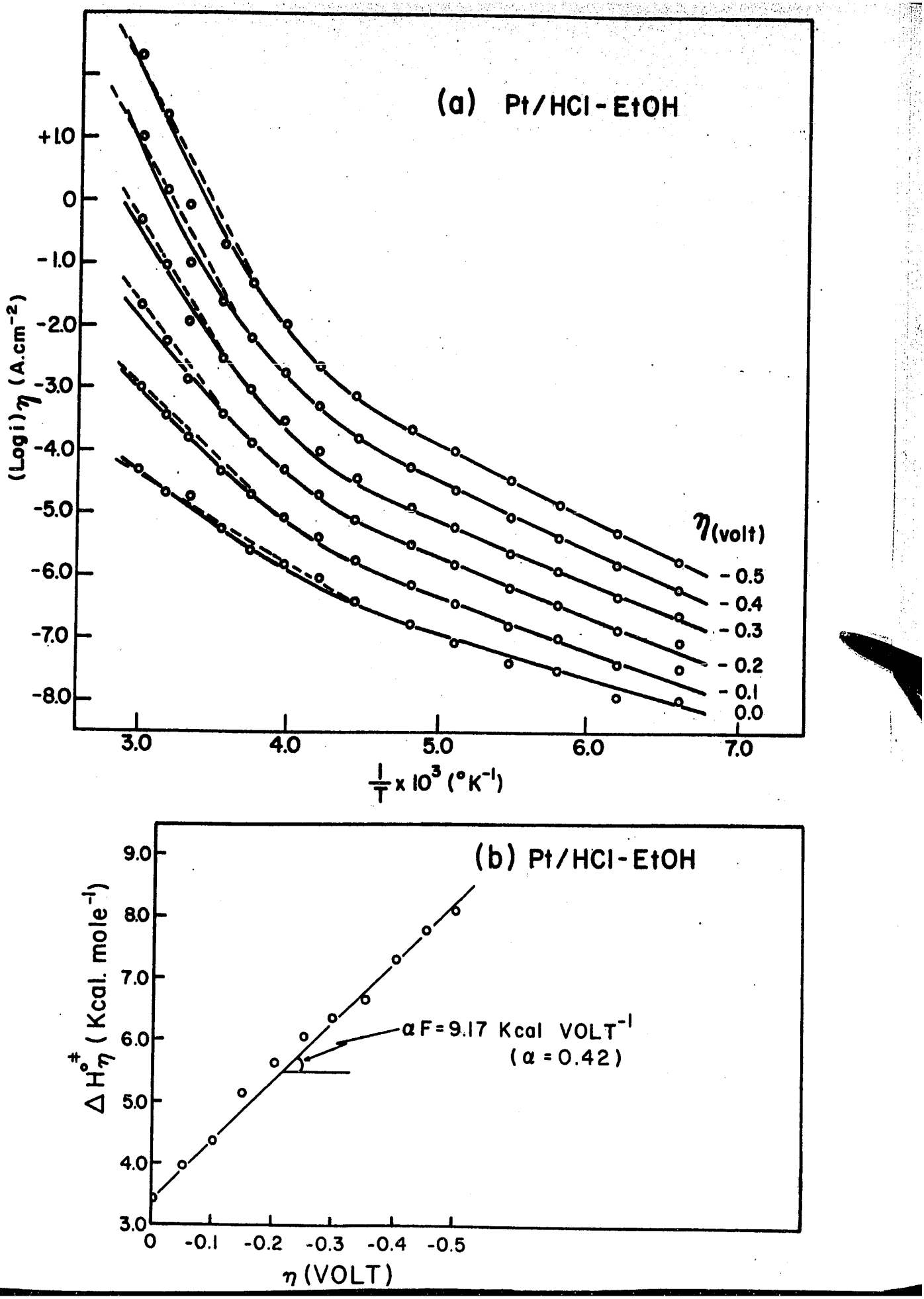
(a) Pt/HCl-EtOH
+1.0
0
-1.0
-2.0
-3.0
-4.0
-5.0
-6.0
-7.0
-8.0
(Logi)η (A.cm⁻²)
η(volt)
-0.5
-0.4
-0.3
-0.2
-0.1
0.0
3.0
4.0
5.0
6.0
7.0
1/T x 10³ (°K⁻¹)
(b) Pt/HCl-EtOH
9.0
8.0
7.0
6.0
5.0
4.0
3.0
ΔH°η* (Kcal. mole⁻¹)
αF = 9.17 Kcal VOLT⁻¹
(α = 0.42)
0
-0.1
-0.2
-0.3
-0.4
-0.5
η (VOLT)

Figure 44

Arrhenius type plots as a function of overpotential for the h. e. r.

(a) Pb cathodes in anhydrous HCl-EtOH.

(b) Cd cathodes in anhydrous HCl-EtOH.

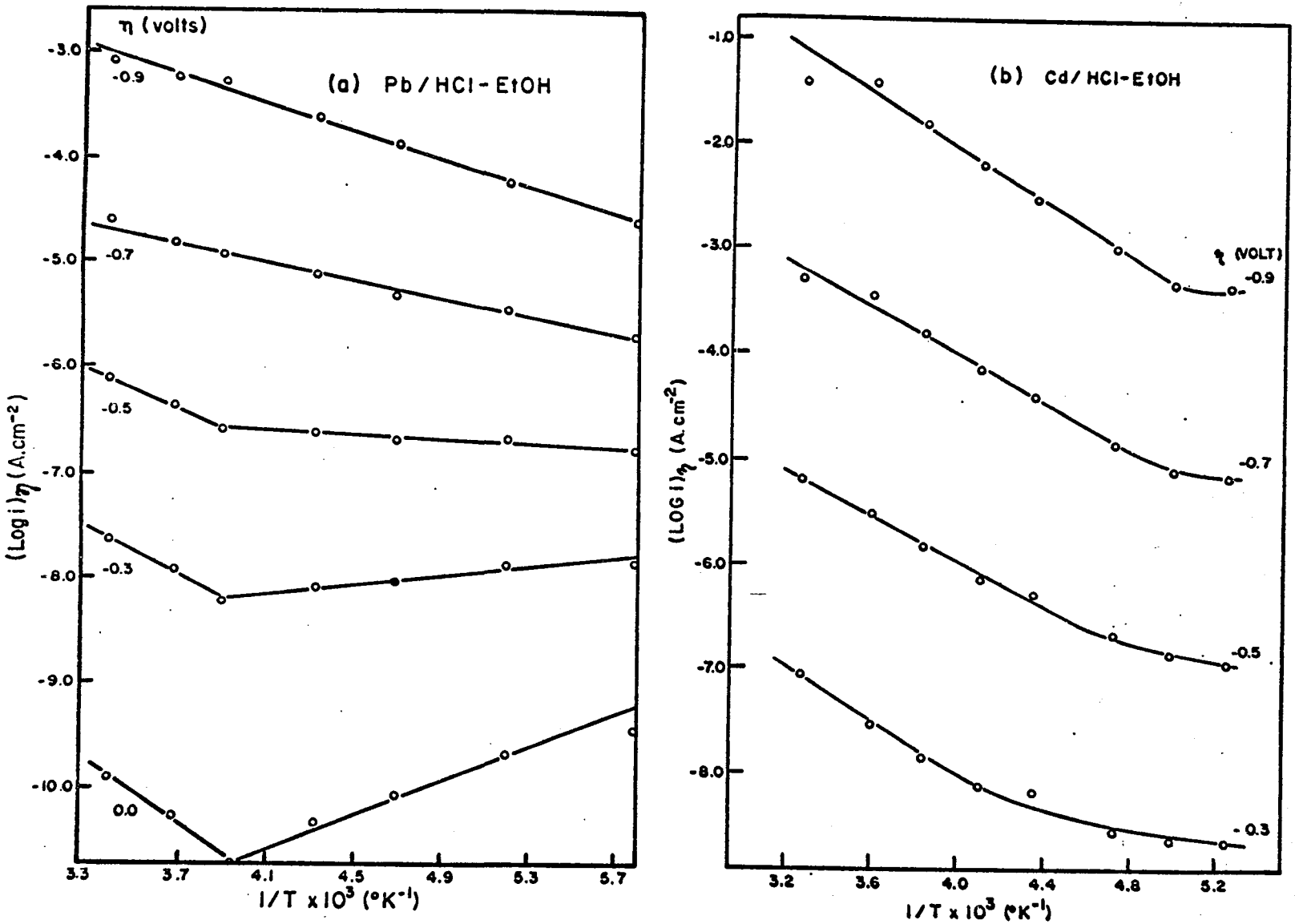
η (volts)
(a) Pb / HCl - EtOH
-0.9
-0.7
-0.5
-0.3
0.0
(Log i)η (A.cm⁻²)
-3.0
-4.0
-5.0
-6.0
-7.0
-8.0
-9.0
-10.0
3.3
3.7
4.1
4.5
4.9
5.3
5.7
1/T x 10³ (°K⁻¹)
(b) Cd / HCl-EtOH
η (VOLT)
-0.9
-0.7
-0.5
-0.3
(LOG i)η (A.cm⁻²)
-1.0
-2.0
-3.0
-4.0
-5.0
-6.0
-7.0
-8.0
3.2
3.6
4.0
4.4
4.8
5.2
1/T x 10³ (°K⁻¹)

b) Deuterium Evolution Reaction (D. E. R.) at Ni, Cd, and Pt over a Wide Range of Temperatures

(i) Cathodic Polarization Curves

Tafel relations for the deuterium evolution reaction at nickel, cadmium and platinum were obtained over a wide range of temperatures for comparison with the results presented above for the analogous h. e. r. studied under similar conditions. Usually, however, the reproducibility of the results was not as good as that in the protic solutions.

1. Nickel. A typical set of polarization curves is shown in Figure 45(a) and, as in the case of the h. e. r., two easily distinguishable linear Tafel regions arise. However, in this case, the change over from the "consecutive" to the "alternative" relation between the lines occurs at a higher temperature (cf. Figures 30(a) and 30(b)).

2. Platinum. Again, the general trend shown in Figure 45(b) is similar to that in the case of the h. e. r. but the Tafel slopes are higher and the polarization curves are not so satisfactory or reproducible as they are in ordinary alcohol solutions.

3. Cadmium. The trend here, as shown in Figure 45(c) is similar to the h. e. r. case although the b values are somewhat higher (cf. Figure 33(b)).

(ii) Tafel Slopes as a Function of Temperature for the D. E. R.

Values of the Tafel slope b were obtained from the polarization curves described above and were plotted as a function of the absolute temperature.

1. Nickel. The trend in the b vs. T plots as shown in Figure 34(a) is the same as for the h. e. r. at nickel except that the bend in the curve for the high c. d. region occurs at a higher

Figure 45

Tafel relations for the d. e. r. as a function of temperature.

(a) Ni cathodes in anhydrous DCl-MeOD.

(b) Pt cathodes in anhydrous DCl-MeOD.

(c) Cd cathodes in anhydrous DCl-MeOD.

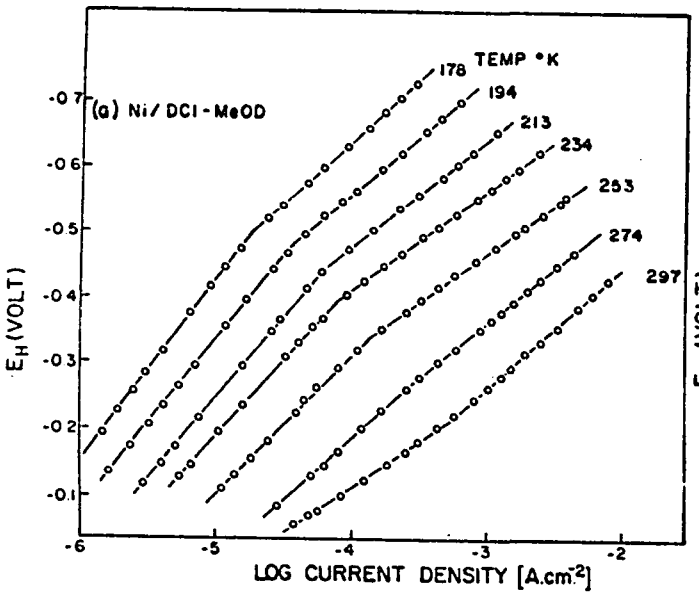
(a) Ni / DCl - MeOD
TEMP °K
178
194
213
234
253
274
297
E_H (VOLT)
LOG CURRENT DENSITY [A.cm⁻²]

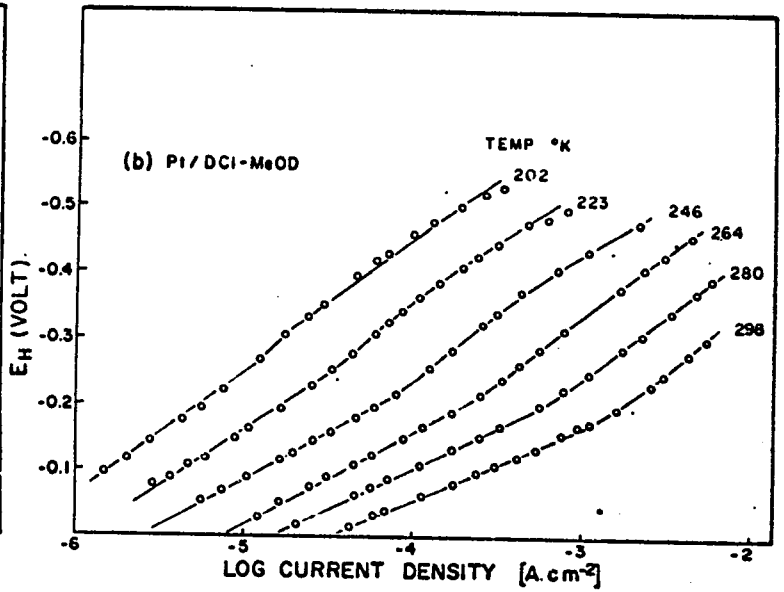
(b) Pt / DCl - MeOD
TEMP °K
202
223
246
264
280
298
E_H (VOLT)
LOG CURRENT DENSITY [A.cm⁻²]

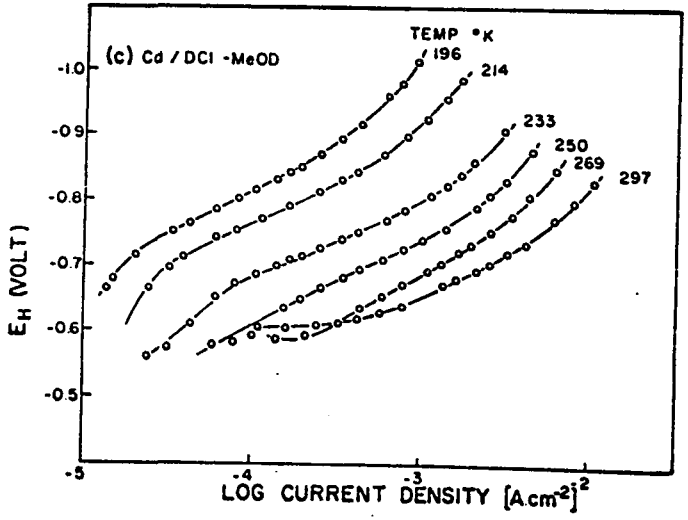
(c) Cd / DCl - MeOD
TEMP °K
196
214
233
250
269
297
E_H (VOLT)
LOG CURRENT DENSITY [A.cm⁻²]²

temperature. In Figure 34(a) are given the results for two typical runs of H_2 and D_2 evolution at Ni while "statistical" b values for the d. e. r. and h. e. r. are shown comparatively in Figure 35.

2. Platinum. Figure 36(a) shows the plot of b vs. T for the d. e. r. at platinum and, although the trend is similar to that for the h. e. r., the b values are generally higher than those found in ordinary alcohol solutions.

3. Cadmium. The trend here is similar to that for the h. e. r. and the results are shown in Figure 37(b).

(iii) Exchange Current Density for the D. E. R. as a Function of Temperature

As in the case of the h. e. r., log i_o values were derived from the Tafel parameters and plotted against the reciprocal of the absolute temperature (1/T).

1. Nickel. A plot of log i_o vs. (1/T) is given in Figure 46. The plots for low c. d.'s exhibit two linear regions with $\Delta H_R^{o\ddagger}$ = 5.2 and 1.4 kcal. mole^{-1} respectively, while those for high c. d.'s exhibit a marked curvature which occurs, however, at a temperature higher than that in the corresponding H case with $\Delta H_R^{o\ddagger}$ = 14 kcal. mole^{-1}; a comparison of the results for the H and D cases is also shown in Figure 46.

2. Cadmium. The curvature in the log i_o vs. (1/T) plot shown in Figure 40(b) occurs at a lower temperature than that for the corresponding plot in the H.case. In the high temperature region $\Delta H_{R,D}^{o\ddagger}$ = 11.5 and $\Delta H_{R,H}^{o\ddagger}$ = 7.1 kcal. mole^{-1}, but the derived apparent $i_{o,D}$ values are greater than the $i_{o,H}$ values, an unusual

Figure 46

Comparative Arrhenius type plots for the h. e. r. and d. e. r. at Ni cathodes in anhydrous HCl-MeOH and in anhydrous DCl-MeOD.

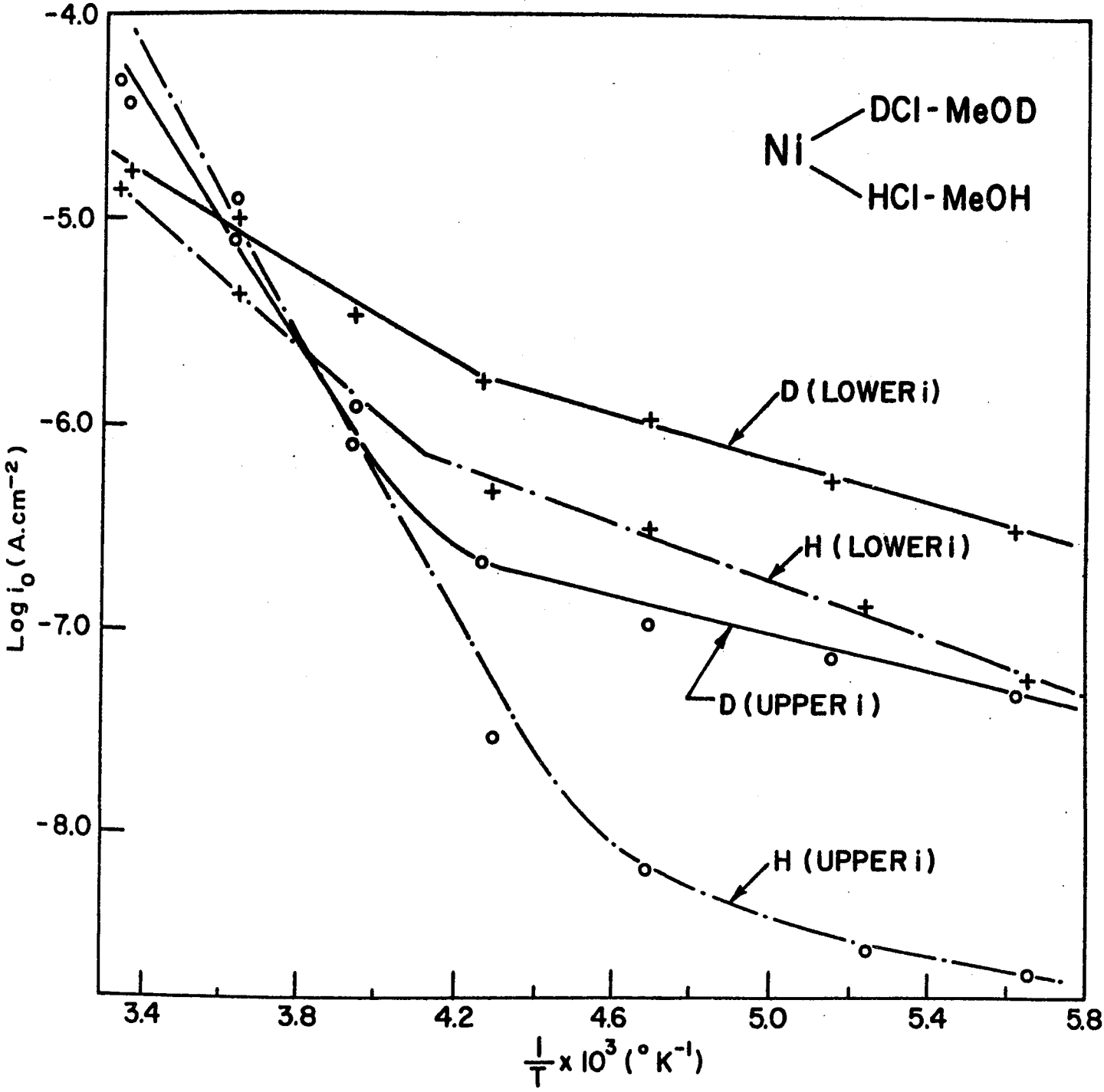
-4.0
-5.0
-6.0
-7.0
-8.0
Log i_o (A.cm^{-2})
Ni
DCl - MeOD
HCl - MeOH
D (LOWER i)
H (LOWER i)
D (UPPER i)
H (UPPER i)
3.4
3.8
4.2
4.6
5.0
5.4
5.8
$\frac{1}{T} \times 10^3$ (°K^{-1})

result* which arises, however, because of the fact that $b_D > b_H$. Figure 40(b) also shows a comparison between the results for the H and D behavior of this metal.

3. Platinum. Figure 39(a) shows a plot of log i_o vs. (1/T) for the d. e. r. at Pt and, as in the h. e. r. case, two linear regions are observed. Again the apparent $i_{o,D} > i_{o,H}$, Figure 39(a) also shows a comparison between the results for the H and D cases.

(iv) Apparent Activation Energies as a Function of η

As in the case of the h. e. r., values of $(\log i)_\eta$ were calculated and plotted against (1/T).

1. Nickel. Figures 47(a) and 47(b) show plots of $(\log i)_\eta$ vs. (1/T) for the lower and upper c. d. regions, respectively. It is to be noted that the behavior is similar to that for the h. e. r. at this metal.

2. Cadmium. Figure 48(a) shows the trend of the results for the d. e. r. at cadmium which are again similar to those for the h. e. r. at this metal.

3. Platinum. Figure 48(b) gives the trend at Pt; again the similarity to the behavior in the h. e. r. case is to be noted.

c) H. E. R. at Mercury in Methanol for Temperatures above 20°C

Cathodic polarization curves were obtained at mercury for the temperatures +24, +41, +52 and +58°C. The purpose of these experiments was to provide carefully obtained results for

---

*See footnote on p.99 which applies again here; the order of the extrapolated values for H and D doesnot necessarily mean that at the respective reversible potentials there would actually be an inverse isotope effect. The apparent i_o values simply characterize the parts of the Tafel lines for which the experimental results were obtained, i. e., above the reversible potentials.

Figure 47

Arrhenius type plots as a function of overpotential for the d. e. r.

(a) Ni cathodes in anhydrous DCl-MeOD; lower c. d. region.

(b) Ni cathodes in anhydrous DCl-MeOD; upper c. d. region.

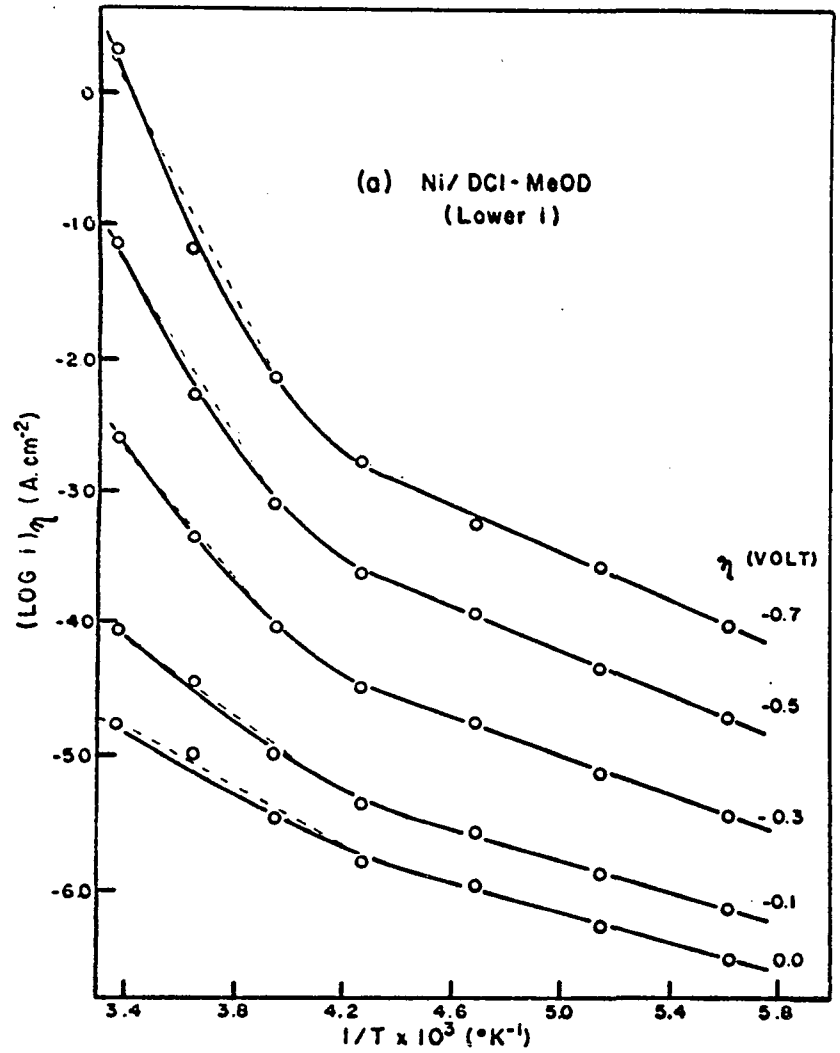
(a) Ni/ DCl - MeOD
(Lower I)
(LOG I)η (A.cm⁻²)
η (VOLT)
-0.7
-0.5
-0.3
-0.1
0.0
0
-10
-20
-30
-40
-50
-60
3.4
3.8
4.2
4.6
5.0
5.4
5.8
1/T x 10³ (°K⁻¹)

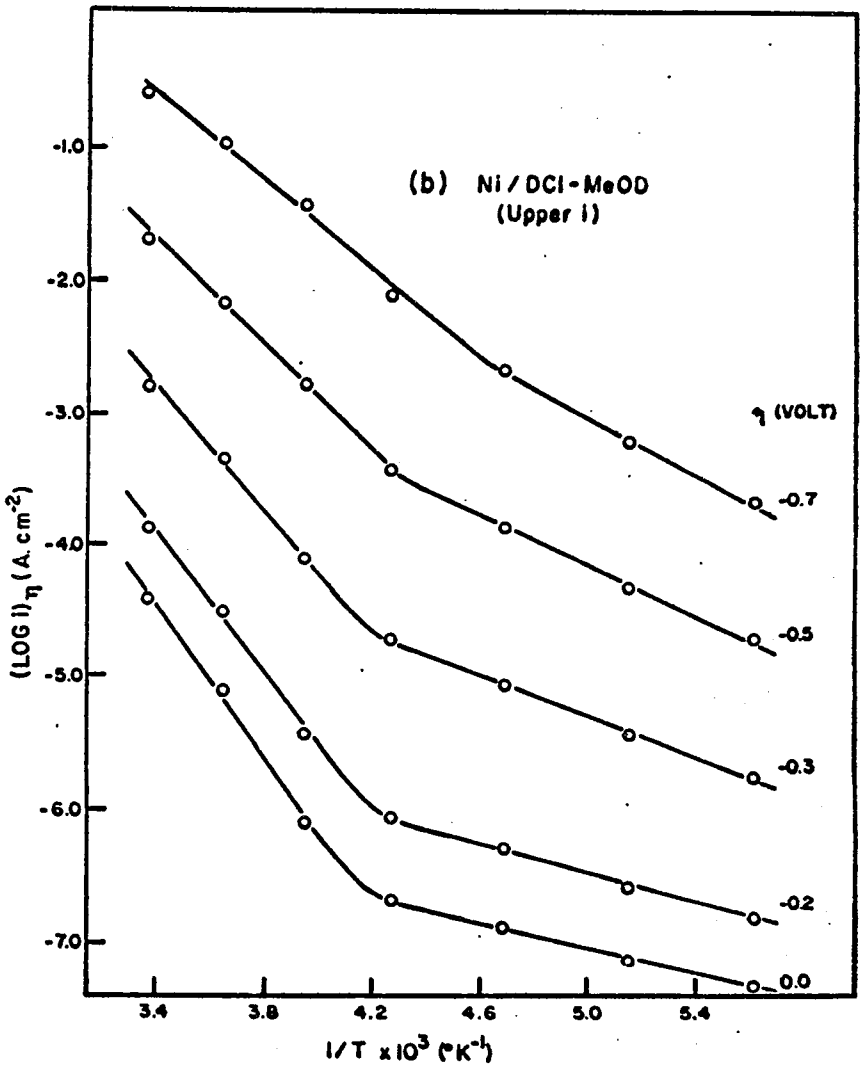
(b) Ni / DCl - MeOD
(Upper I)
(LOG I)η (A.cm⁻²)
η (VOLT)
-0.7
-0.5
-0.3
-0.2
0.0
-1.0
-2.0
-3.0
-4.0
-5.0
-6.0
-7.0
3.4
3.8
4.2
4.6
5.0
5.4
1/T x10³ (°K⁻¹)

Figure 48

Arrhenius type plots as a function of overpotential for the d. e. r.

(a) Cd cathodes in anhydrous DCl-MeOD.

(b) Pt cathodes in anhydrous DCl-MeOD.

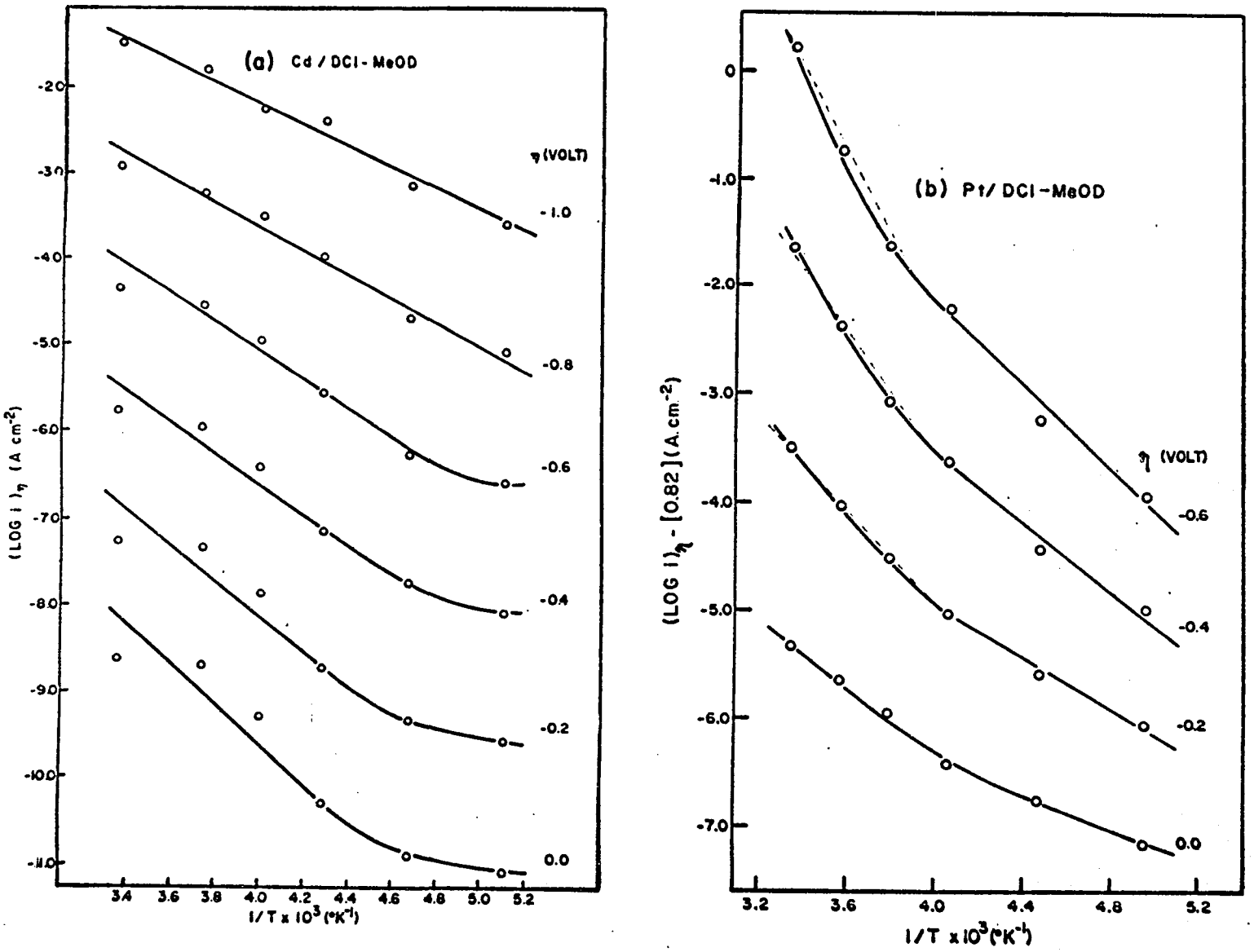
(a) Cd / DCl - MeOD
η (VOLT)
-1.0
-0.8
-0.6
-0.4
-0.2
0.0
(LOG I)η (A cm-2)
1/T x 10³ (°K⁻¹)
(b) Pt/ DCl - MeOD
η (VOLT)
-0.6
-0.4
-0.2
0.0
(LOG I)η - [0.82] (A.cm-2)
1/T x 10³ (°K⁻¹)

comparison with those found in earlier work by Salomon (86) in this laboratory but carried out at temperatures between -110°C and +25°C in alcoholic solutions.

From the polarization curves, values of the Tafel slope b were obtained and plotted against the absolute temperature together with Salomon's results; the data are shown in Figure 49. It is gratifying that all the points fall on the same line. Also, in Figure 49 are shown the results of Post and Hiskey (50) for aqueous solution and it is seen that they are in excellent agreement with the data obtained in the present work in a different solvent. This section of the work provided some of the most satisfactory data for b as f(T) which will be discussed below.

The activation energy for the range of temperatures used in this work has the value $\Delta H_R^{o\ddagger} = 8.1$ kcal. mole^{-1} which is in moderate agreement with that of 11.2 kcal mole^{-1} found by Salomon (86).

d) The Anodic Reaction of Br^- at Graphite

The purpose of this part of the work was to provide for comparative purposes some low temperature results for a one-electron oxidation process not involving H or D transfer. The most suitable solution for this study was found to be 0.4 M$(C_3H_7)_4NBr$ in spectroscopically pure acetonitrile (CH_3CN).

Early trials to find a suitable system for this study included the following:

(1) The anodic Cl_2 evolution reaction at graphite from constant boiling (7.5N) HCl solutions. This system was not satisfactory as anomalous Tafel slopes were observed at low temperatures and the reproducibility of the results was not satisfactory.

Figure 49

Tafel slope, b, as a function of temperature for the h. e. r. at Hg cathodes; results of various workers.

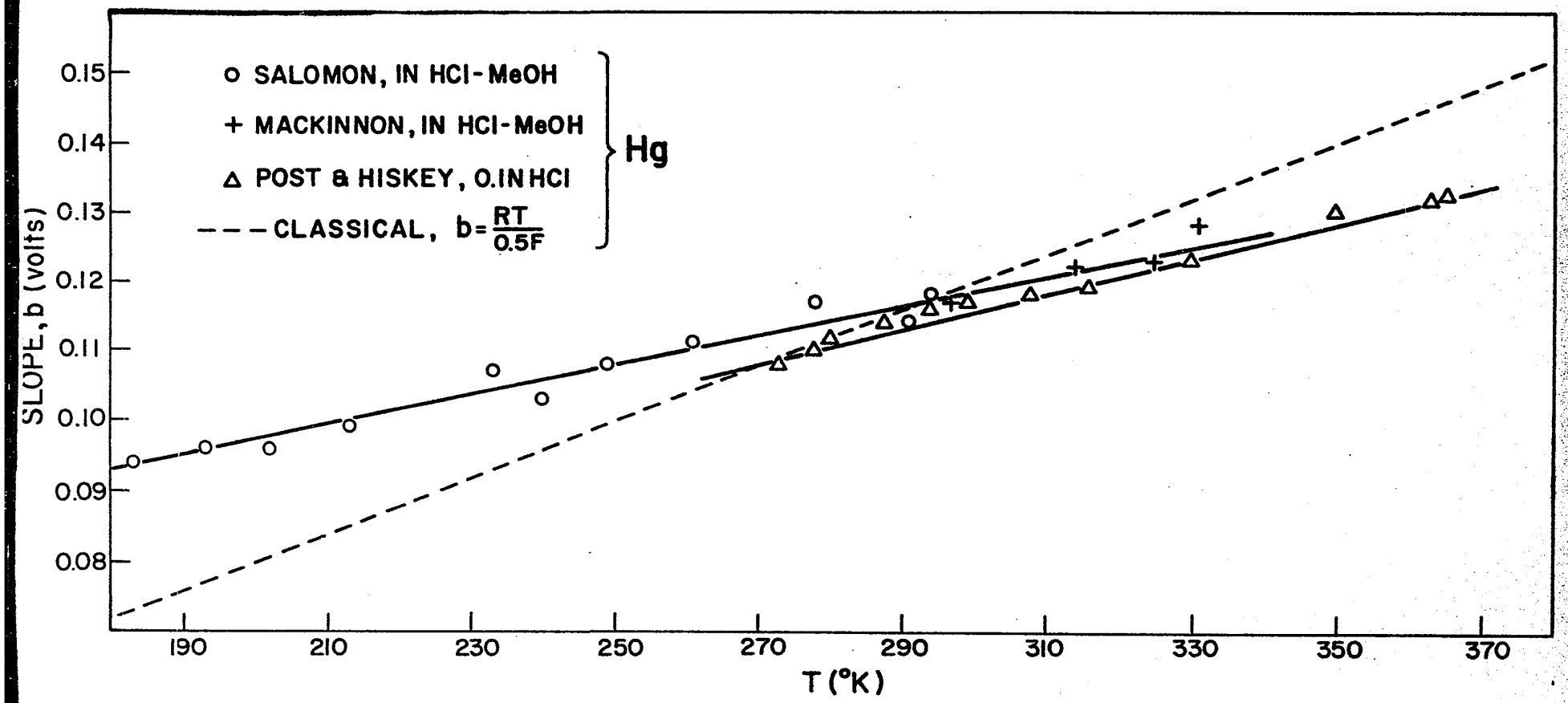
o SALOMON, IN HCl-MeOH
+ MACKINNON, IN HCl-MeOH
Δ POST & HISKEY, 0.1N HCl
--- CLASSICAL, b = RT/0.5F
Hg
SLOPE, b (volts)
0.15
0.14
0.13
0.12
0.11
0.10
0.09
0.08
190
210
230
250
270
290
310
330
350
370
T (°K)

(2) An attempt to use the system graphite/HCl-trifluoroacetic anhydride was unsuccessful as no significant current could be passed, possibly because the HCl gas was not readily soluble in the anhydride, or dissociated.

(3) The following inorganic chlorides were tested for their solubility in acetonitrile: LiCl, AgCl, CuCl, Hg_2Cl_2, $NiCl_2$, $CdCl_2$, $MnCl_2$, $BaCl_2$ and $SnCl_2$. It was found that these salts were not sufficiently soluble to provide a reasonable current density range over which satisfactory polarization curves could be obtained.

(4) Organic chloride salts such as $(CH_3)_4NCl$ were also not soluble to any great extent in acetonitrile. However, the tetraalkyl ammonium bromides were more soluble than their chloride analogues and it was subsequently found, as mentioned above, that the system graphite/$(C_3H_7)_4NBr$-CH_3CN was satisfactory.

Although the inorganic bromides were more soluble than their chloride analogues, they were, however, not soluble enough to be used for this study.

Typical anodic polarization curves for the Br^- discharge reaction at pyrolytic graphite (see Experimental Section, p. 77) are shown in Figure 50(a) for measurements carried out over the temperature range of +26 to -45°C. A decrease in temperature below -45°C caused the electrolyte to solidify.

In Figure 50(b), b values and apparent α values are plotted together as a function of temperature for three independent runs and it is seen that for all practical purposes b is independent of T and α is linear in T.

Figure 50

Bromine evolution reaction (b. e. r.) at graphite in 0.4M $(C_3H_7)_4NBr$-CH_3CN.

(a) Tafel relations for the b. e. r. as a function of temperature.

(b) Tafel slope, b, and apparent α values as a function of temperature for the b. e. r.

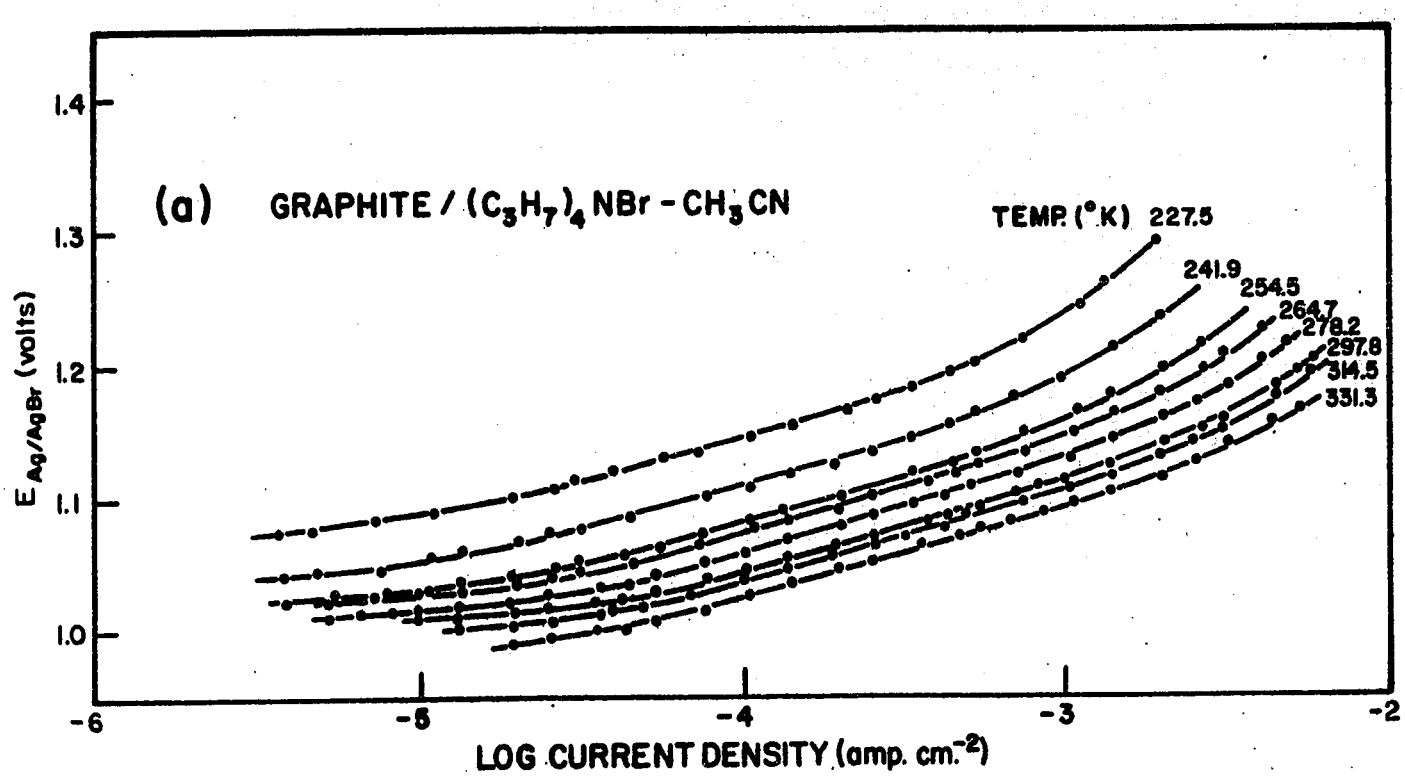
(a) GRAPHITE / $(C_3H_7)_4NBr - CH_3CN$
TEMP. (°K) 227.5
241.9
254.5
264.7
278.2
297.8
314.5
331.3
$E_{Ag/AgBr}$ (volts)
1.4
1.3
1.2
1.1
1.0
-6
-5
-4
-3
-2
LOG CURRENT DENSITY (amp. cm^{-2})

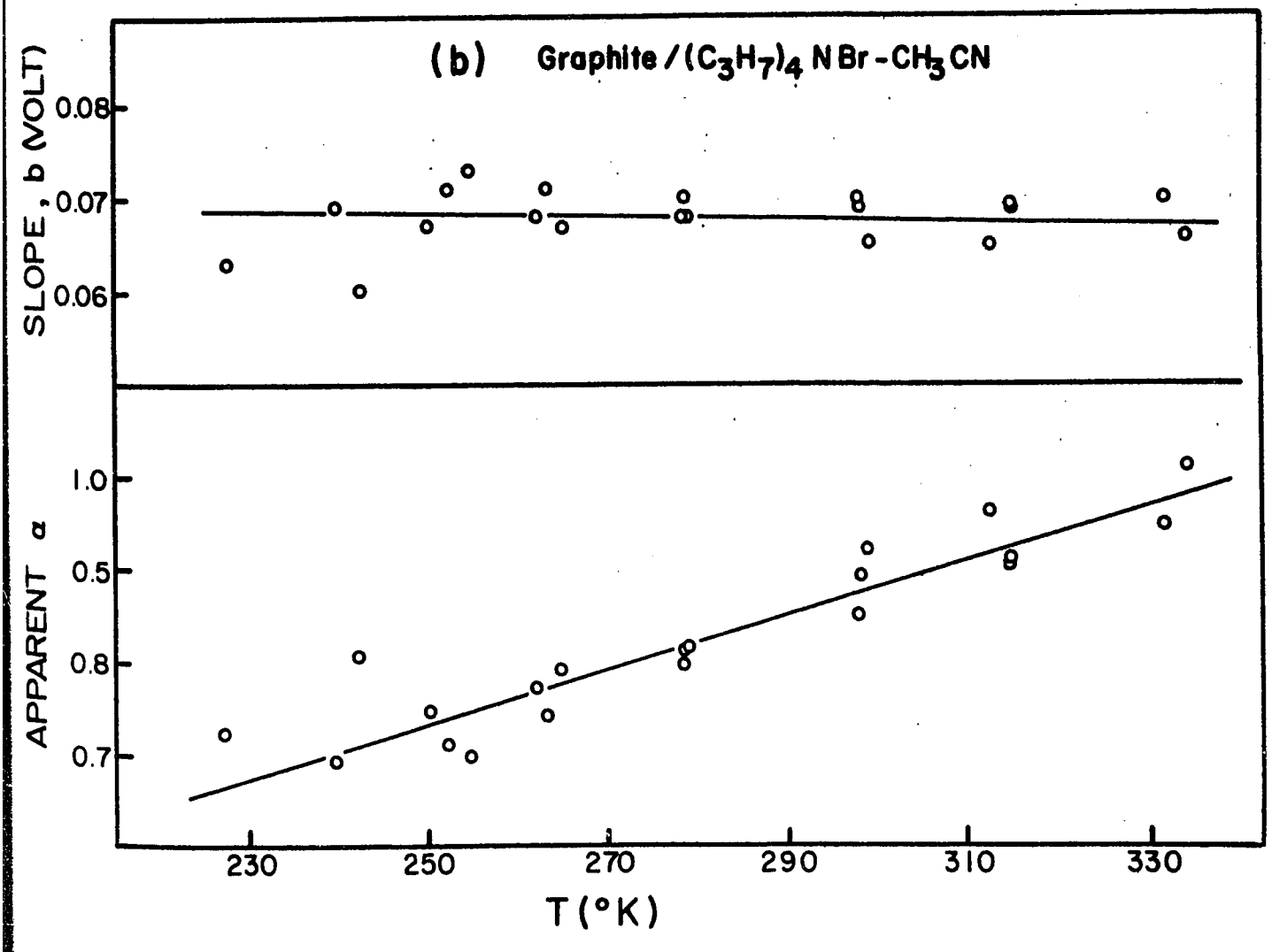
(b) Graphite / $(C_3H_7)_4$ N Br - CH_3CN
SLOPE, b (VOLT)
0.08
0.07
0.06
APPARENT α
1.0
0.5
0.8
0.7
230
250
270
290
310
330
T (°K)

e) Accuracy of the log i_o and b Values

Slopes of the lines drawn through the linear regions of log[current density]-potential data can be estimated to ± 2 mV. In the cases of mercury, lead, cadmium and the high c.d. region for nickel, extrapolation of the linear portion of these lines to obtain log i_o can lead to appreciable error since the extrapolation is made over 5-6 decades of current density. Therefore, the method employed to obtain the log i_o values was to draw the best lines through the experimental η -log i points and calculate log i_o by the method described on page 99. This procedure, also used to obtain the log i_o values for Pt and for the low c.d. region at Ni where such long extrapolations are not involved, is rather more precise than the direct graphical method especially when a long extrapolation is required.

CHAPTER V

DISCUSSION

a) General Introduction

A complete and rigorously quantitative interpretation of the experimental results presented in Chapter IV of this thesis is rendered difficult on account of the complicated nature of the experimentally observed behavior. However, it is the aim of this Chapter to present a qualitative (and where possible, a quantitative) interpretation of the results and to comment on their general significance with regard to the h. e. r. in particular and electrode kinetics in general.

The role of the structure of the double-layer* is of fundamental importance in electrochemical kinetics (95, 96, 101) and double-layer effects, such as the specific adsorption of anions, provide a basis for some of the qualitative interpretations presented in this Chapter (see Section c) of the experimental results.

Electrochemical proton transfer reactions are by their nature heterogeneous. Hence, the rates of proton transfer will depend upon such factors as the adsorptive properties of the metal cathode, the presence of adsorbed intermediates (e. g. atomic H in the case of the h. e. r.), reaction products or anions adsorbed on the cathode, and the metal-solution potential difference. The influence of these and other factors on the kinetics of the h. e. r. in relation to the interpretation of the experimental results obtained in the present work is discussed in detail below.

---

*Previous work on the structure of the double-layer has been reviewed in detail elsewhere (95, 96, 101, 102) and in a previous thesis from this Department and hence will not be dealt with in the present discussion.

b) Behavior of the Tafel Slopes as a Function of Temperature

(i) General

A summary of those earlier studies on the h. e. r. at various temperatures, which may be considered adequately reliable, is presented in this section in order to provide a basis for comparison with the temperature dependence of the Tafel slopes, b, found in the present work. Also, a brief discussion of the form of the relation for b for the h. e. r. at Hg and Ni is presented.

(ii) Tafel Slope for the h. e. r. at Hg in acid solutions

Although the h. e. r. has been studied more thoroughly at Hg than at any other metal, a relatively small amount of work has been done on the temperature dependence of the kinetics of this reaction, particularly with regard to the variation of the Tafel slope, b with temperature. Since it has generally been assumed that b varies with temperature according to the usual relation $b = RT/\beta F$ where $\beta \neq f(T)$, previous temperature studies on the h. e. r. at Hg (4, 50, 69, 82, 103) (with a few notable exceptions (31, 83)), were concerned mainly with obtaining electrochemical activation energies and consequently a relatively small range of temperatures (usually for T values near and including +25°C) was investigated.

However, with the current interest in the possibility that proton tunneling plays a significant role in the mechanism of the h. e. r., two recent studies (31, 83) have been reported in which Tafel slopes were obtained over a very wide temperature range, including experiments carried out in this laboratory down to a temperature as low as -100°C (31).

The b vs. T behavior observed in some of the earlier (4, 50, 69), as well as the more recent work (31, 83) on the h. e. r. at Hg, is shown comparatively in Figure 51. Several interesting features of these plots should be noted:

Figure 51

Tafel slope, b, as a function of temperature for the h. e. r. at Hg in acid solution; results of various workers.

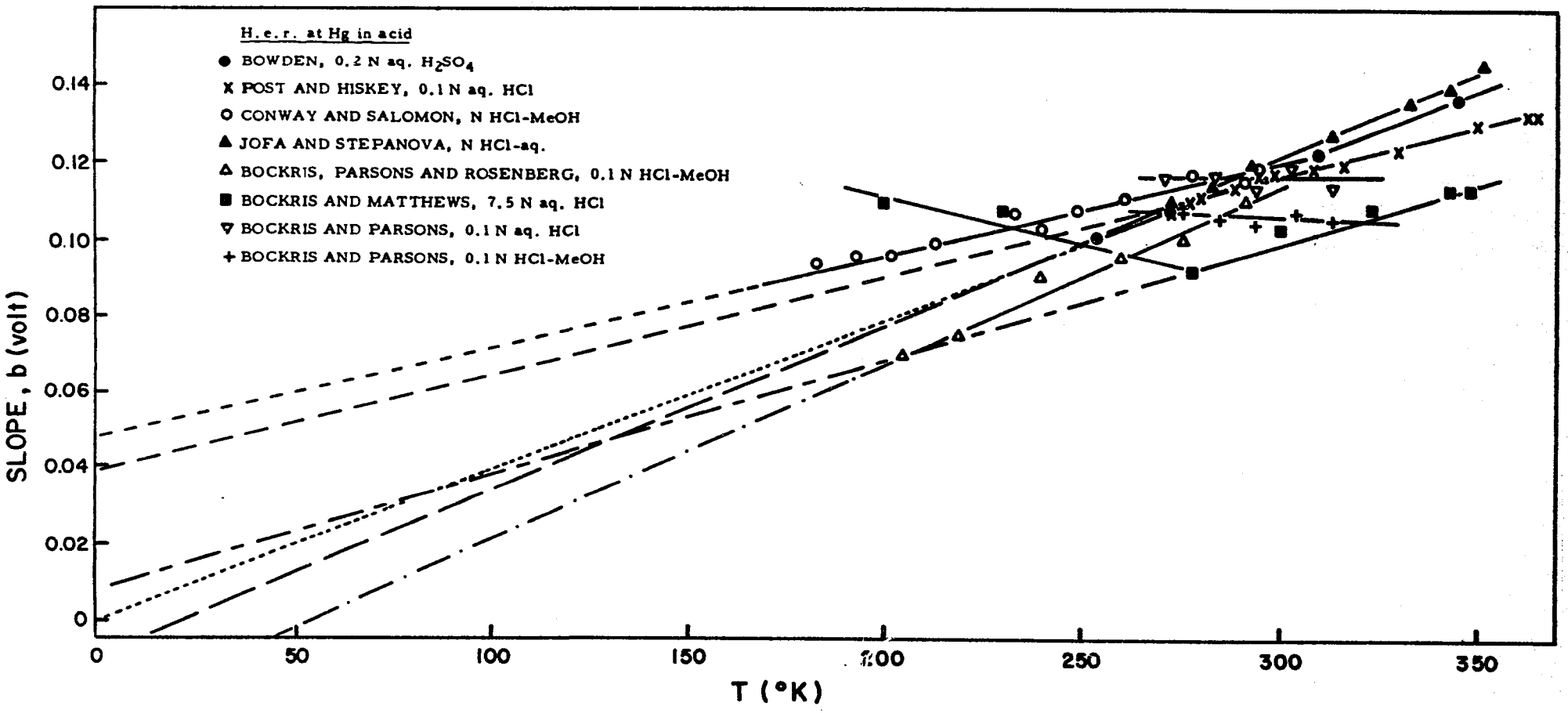
H.e.r. at Hg in acid
BOWDEN, 0.2 N aq. H_2SO_4
POST AND HISKEY, 0.1 N aq. HCl
CONWAY AND SALOMON, N HCl-MeOH
JOFA AND STEPANOVA, N HCl-aq.
BOCKRIS, PARSONS AND ROSENBERG, 0.1 N HCl-MeOH
BOCKRIS AND MATTHEWS, 7.5 N aq. HCl
BOCKRIS AND PARSONS, 0.1 N aq. HCl
BOCKRIS AND PARSONS, 0.1 N HCl-MeOH
SLOPE, b (volt)
0.14
0.12
0.10
0.08
0.06
0.04
0.02
0
0
50
100
150
200
250
300
350
T (°K)

(a) Although b = 0.116 at room temperature for the majority of the results (Figure 51), thus apparently indicating that b is $RT/\beta F$ with an apparent value of $\beta = 0.5$, this appears to be coincidental, since over a sufficiently wide range of temperatures, b is not represented adequately by the relation $b = RT/\beta F$.

(b) A notable exception is the work of Bowden (4) in 0.2N H_2SO_4 at 0, 36 and 72°C where b is found to vary with temperature in the manner required by the relation $b = RT/\beta F$ with $\beta = 0.5 \pm 0.01$; this may be regarded as the "classical" case.

(c) The results of Bockris and Matthews (83) show that the Tafel slope is less than 0.116 at room temperature. This exceptional result seems to be due to effects associated with specific adsorption of the Cl^- anion* (83) since the measurements had to be carried out in 7.5N aqueous HCl solution.

(d) The results of Conway and Salomon (31) for b as f(T) in 1N HCl methanol solution over the temperature range of +25 to -100°C are in excellent agreement with the results of Post and Hiskey (50) in 0.1N aqueous HCl solutions over the temperature range 0 to +90°C (cf. Figure 49). Both these sets of results may be represented by the relation $b = (RT/\beta F) + c$, where c is a constant, rather than by $b = RT/\beta F$. The extrapolation of these results to T = 0°K gives almost identical values for the constant c (Figure 51).

The b vs. T data (4, 31, 50, 69, 82, 83) plotted in Figure 51 are listed in Table I.

---

*A discussion of the effects of specific adsorption of anions on the kinetics of the cathodic hydrogen evolution reaction is presented in a following section of this Chapter.

Table I

Temperature Behavior of Tafel Slopes for the H. E. R. at Hg.

TABLE I

Temperature Behavior of Tafel Slopes for the H. E. R. at Hg

Post and Hiskey(50) 0.1N aq. HCl		Conway and Salomon(31) 1N HCl-MeOH		Bockris and Matthews(83) 7.5N aq. HCl	
T(°K)	b(volt)	T(°K)	b(volt)	T(°K)	b(volt)
273	0.108	183	0.094	200	0.111
278	0.110	193	0.096	230	0.108
280	0.111	202	0.096	253	0.101
288	0.114	213	0.099	278	0.092
294	0.116	233	0.107	300	0.103
299	0.117	240	0.103	323	0.108
308	0.118	249	0.108	343	0.113
316	0.119	261	0.111	348	0.113
330	0.123	278	0.117		
350	0.130	291	0.114		
363	0.132	294	0.118		
365	0.132				

Jofa and Stepanova(82) 1N aq. HCl		Bockris, Parsons and Rosenberg(103) 1N HCl-MeOH		Bowden(4) 0.2N aq. H_2SO_4	
T(°K)	b(volt)	T(°K)	b(volt)	T(°K)	b(volt)
273	0.110	205	0.070	273	0.108
283	0.114	219	0.075	309	0.122
293	0.119	240	0.090	345	0.136
313	0.127	260	0.095		
333	0.135	276	0.100		
343	0.139	292	0.110		
351	0.145				

The work of Bockris and Parsons (69) on the activation energy of the h. e. r. at Hg carried out in solutions of aq. 0.1N HCl, 0.1N HCl-MeOH and 0.1N HCl-H_2O-MeOH mixtures over the narrow temperature range 0 to +40°C enables b values to be derived that are, however, independent of temperature (see Figure 51). Temperature independent Tafel slopes have also been observed for (a) the h. e. r. at Ni in aqueous HCl (104); (b) the h. e. r. at solid In in 0.1M aqueous $HClO_4$ (105); (c) the electrodeposition of the azide ion (106) and (d) the anodic reaction of Br^- at graphite in the present work (see Figures 50(a) and 50(b)). The results giving temperature-independent Tafel slopes for the h. e. r. (69, 104, 105, 106) are summarized in Table II.

(iii) Form of the relation for b

The experimental observations indicate empirically that for Hg and for Ni at higher current densities

$$b = \frac{RT}{\beta F} + c \qquad [63]$$

or

$$b = c' - \frac{RT}{\beta F} \qquad [64]$$

the latter relation applying to cases where b increases with decreasing temperature (Figures 34, 36). When b varies with T according to equation [63], yet equals approximately 0.12 V at 25°C (e. g. as for the h. e. r. at Hg), β must be greater than 0.5 and $c > 0$. This suggests that β should not be estimated from the value of b at a single temperature such as 25°C assuming that $b = RT/\beta F$ as is usually done, but rather must be obtained from equation [63] by the operation

$$db/dT = R/\beta F \qquad [65]$$

Table II

Temperature-Independent Tafel Slopes for the H. E. R.

TABLE II

Temperature-Independent Tafel Slopes for the H. E. R.

Bockris and Parsons(69) h. e. r. at Hg in 0.1N HCl			Bockris and Potter(104) h. e. r. at Ni in aq. HCl			Butler(105) h. e. r. at solid In 0.1M aq. $HClO_4$	
x_{MeOH}	T(°K)	b(volt)	a_{HCl}	T(°K)	b(volt)	T(°K)	b(volt)
0	273	0.116	0.001N	273	0.099	294	0.118
	284	0.117		283	0.104	298	0.120
	294	0.113		293	0.093	303	0.114
	303	0.119		303	0.099	314	0.116
	313	0.114		313	0.104	324	0.116
						333	0.118
0.36	275	0.105	0.01N	273	0.090		
	286	0.102		283	0.090		
	295	0.100		293	0.091		
	303	0.100		303	0.090		
	314	0.101		313	0.094		
1.00	275	0.108	0.1N	273	0.101		
	285	0.106		283	0.103		
	294	0.104		293	0.104		
	303	0.107		303	0.102		
	313	0.106		313	0.106		

a = activity
x = mole fraction

assuming both β and c are independent of T. The fact that the usually assumed relation $b = RT/\beta F$ with $\beta = 0.5$ gives the correct result for the Tafel slope at Hg at or near room temperature seems simply fortuitous but it is clear that the relation is incorrect in form over any appreciable range of temperatures. Indeed the form represented by the conventional relation $b = RT/\beta F$ seems to be the exception rather than the "rule".

Alternatively, it may be assumed that a relation of the form $b = RT/\beta' F$ is correct but β', an apparent symmetry factor, is f(T). Since the empirical relation which represents the experimental results is, however, equation [63] with β taken as a constant, the temperature dependence of β' must be obtained from the identity

$$b = \frac{RT}{\beta F} + c \equiv \frac{RT}{\beta' F} \quad , \qquad [66]$$

i. e. the required temperature dependent apparent symmetry factor $\beta'(T)$ which would equally well account for the results at Hg is given by:

$$\beta'_{(T)} = \beta RT/(RT + \beta Fc) \qquad [67]$$

where β is now a true constant symmetry factor. This is an unwieldy type of expression so that it may be suspected that the observed "non-conventional" variation of b with T might be better accounted for by an equation of the type [63] involving a temperature-independent component in b rather than by the more complex expression [67]. The exponential term in the kinetic expressions for current in the h. e. r. would then be

$$\exp[-\eta/b] = \exp[-\beta \eta F/(RT + \beta Fc)] \qquad [68]$$

for b given by equation [63] or

$$\exp[-\eta/b] = \exp[-\beta'_{(T)}\eta F/RT] \qquad [69]$$

for b given by equation [66], and these expressions are, of course, equivalent when $\beta'_{(T)}$ is given by equation [67] with β still a temperature independent true symmetry factor.

In limiting cases where b is observed to be almost independent of temperature (see Figures 50(b) and 51), the problem of representing b in terms of equation [63] is more difficult. For such cases, $b = c$, so that β would apparently have to be $\gg 1$, a situation which is, by definition, impossible since $1 > \beta > 0$. For such cases, we are forced to suppose that the apparent independence of b with T arises mainly on account of β really being linearly temperature dependent, i.e. $\beta = \gamma T$, so that with the definition $b = RT/\beta F$, $b = R/\gamma F$ where γ is another temperature-independent constant. In the general case, β may be of the form

$$\beta = \gamma T + \delta \qquad [70]$$

giving b the form

$$b = RT/(\gamma T + \delta)F \qquad [71]$$

However, a relation of this type does not represent very well the observed behavior over the wide range of temperatures experimentally investigated in the present work: thus, according to equation [71] b would not be linear with T nor would it have a finite value as $T \rightarrow 0$ since then $\gamma T + \delta \rightarrow \delta$ and $b \rightarrow RT/\delta F \rightarrow 0$ as $T \rightarrow 0$. The empirical relations [66] and [67] are therefore to be preferred with $\beta = \gamma T$ in the limiting case when b is independent of T.

c) Qualitative Interpretation of the Temperature Dependence of the Tafel Slopes

(i) General

A qualitative interpretation of the behavior of the Tafel slopes with temperature, described previously (Chapter IV and Chapter V, Section b), is given in this section in terms of the effects associated with the specific adsorption of anions*. The empirical forms for b (cf. equations [63] and [64]) for the h. e. r. at Hg and Ni are also discussed in terms of these effects.

The specific adsorption of anions has the following principal effects in relation to the kinetics of the hydrogen evolution reaction (h. e. r.): (i) changes of the ψ_1 potential (usage as in the Russian work) in the outer Helmholtz plane (o. h. p.) are brought about and influence the local concentration of H_3O^+ ions in that plane; (ii) variation of the standard free energy of hydrogen adsorption arises; (iii) the available area for hydrogen adsorption is decreased. The kinetics are influenced by each of these effects but the relative importance of the various effects varies from one metal to another and, for a given metal, can be dependent on the current-density.

A substantial body of information has been gathered on this matter, mostly by the Russian workers, and two excellent reviews by Frumkin (96, 107) and one by Parsons (102), have been published. These review articles refer mainly to specific adsorption from aqueous solutions at room temperature but stronger adsorption effects can arise in non-aqueous solvents (e. g. methanol (18, 31) and at low temperatures, where anion adsorption can be stronger. For example, it is known (108) that specific adsorption of anions occurs at Hg to a greater extent in methanolic than in aqueous HCl solutions

---

*cf. footnote on p.122.

for a given charge on the metal and for similar acid concentrations. Since specific adsorption of anions increases with decreasing temperature, results may be more anomalous at low temperatures than at high.

(ii) Effect of Specific Adsorption of Anions

1. Mercury

In aqueous medium at the high η values involved in most steady-state studies at Hg, specific adsorption of Cl^- ion in dilute HCl is not indicated by electrocapillary and capacitance (95, 96, 109) studies and does not seem to be involved in the reliable work of Post and Hiskey (50). Similarly, in the alcoholic solutions of HCl, specific adsorption of Cl^- ion does not appear to be significant at the potentials used in this and the previous work carried out in this laboratory (18, 31), although nearer the electrocapillary maximum (e.c.m.) potential, specific adsorption of Cl^- is greater (108) than it is in aqueous HCl at the same concentrations. Hence the reproducible dependence of b on T shown in Figure 49 for Hg and represented by equation [63] with $\beta = 0.71$ and $c = 0.04$ is unlikely to be the result of specific adsorption of Cl^- and an explanation of the forms of [63] or [66] must be sought in other terms.

At high acid concentrations, however, the kinetic results are undoubtedly complicated by anion adsorption (96, 109) particularly in the case of halides; interpretation of the kinetics (b and $\log i_o$) in terms of proton tunneling (cf. 83) or other factors is then difficult and special models must be introduced. For example, Parsons (110) has suggested that anion adsorption causes the H^+ ion to be pulled in nearer to the electrode interface and various authors (e.g. see ref. 96) of the Russian school have considered the double-layer effects associated with anion adsorption in so far as they may effect the kinetics of the h.e.r. Very recently, Parsons (111) proposed a

simple model to account for the effect of specifically adsorbed ions on the rate of the h. e. r. The treatment introduces an electrostatic interaction between the activated complex of the electrode reaction and the adsorbed ions in the form of an activity coefficient which can be calculated from the adsorption isotherm. This approach is claimed to give a reasonable account of the experimental data already published and to provide a framework for future experimental and theoretical work.

From this recent treatment of Parsons (111), it is possible to show rather approximately how a temperature-dependent apparent contribution to β can arise in the case of specific adsorption. If adsorbed anions affect the activity coefficient of the activated complex (109), then the relative change of rate constant k/k_o with coverage by anions is given by

$$\ln \; k/k_o = -2B\Theta$$

where k_o is the rate constant in the absence of adsorption of anions and resulting interaction effects involving the activated complex, Θ is the coverage or surface excess and B the second virial coefficient in the equation of state for the ad-species. If the coverage by the adsorbed ions is approximately linear in potential ϕ (constant inner layer capacity contribution C) then

$$\ln \; k/k_o = -2BC\phi$$

The overall rate expression will then involve an exponential factor in ϕ of the form $\exp[-\beta\phi F/RT] \exp[-2BC\phi]$, i.e., $\exp \frac{-\phi F}{RT}[\beta + 2BCTR/F] \equiv \exp -\beta' F\phi/RT$. The apparent symmetry factor β' is hence composed of the normal β plus a temperature-

dependent term involving the interaction parameter B and a capacity term C characterizing the potential dependence of coverage of the adsorbed anion species. This is of the correct form required to explain cases where b varies anomalously with T in the case of anion adsorption.

2. Nickel and Platinum

The results shown in Figure 34 for Ni in alcoholic HCl are to be considered together with those of Bockris and Potter (104) obtained in dilute aqueous acid and alkaline solutions. The Tafel lines for Ni in alcoholic HCl solutions consistently showed two linear regions both for the protium and the deuterium solvents (CH_3OD/DCl). Changes of slope were not, however, observed in a similar study carried out in methanolic-$HClO_4$ solutions (see Figure 52). Reasonably linear Tafel relations were observed at all temperatures (down to low T) and the b values corresponded closely to those obtained for the high c.d. region at Ni in the alcoholic-HCl solutions. The b vs. T plot (Figure 53) shows that b decreases linearly with T down to the lowest temperature attained (i.e., -89°C). This behavior is to be contrasted with the b vs. T behavior at Ni for the alcoholic-HCl solution (cf. Figure 34). This additional experimental evidence lends support to the qualitative interpretation in terms of anion (Cl^-) specific adsorption effects given above for the b vs. T behavior at Ni in alcoholic-HCl solutions.

On the basis of these results it may be argued that the lower Tafel lines at Ni represent the kinetics of the h.e.r. at a Ni surface in the presence of specifically adsorbed Cl^- ions (cf. 108) while the upper lines (which have b values similar to those for the

Figure 52

Tafel relation for the h. e. r. at Ni in 0. 5M $HClO_4$-MeOH at 296°K.

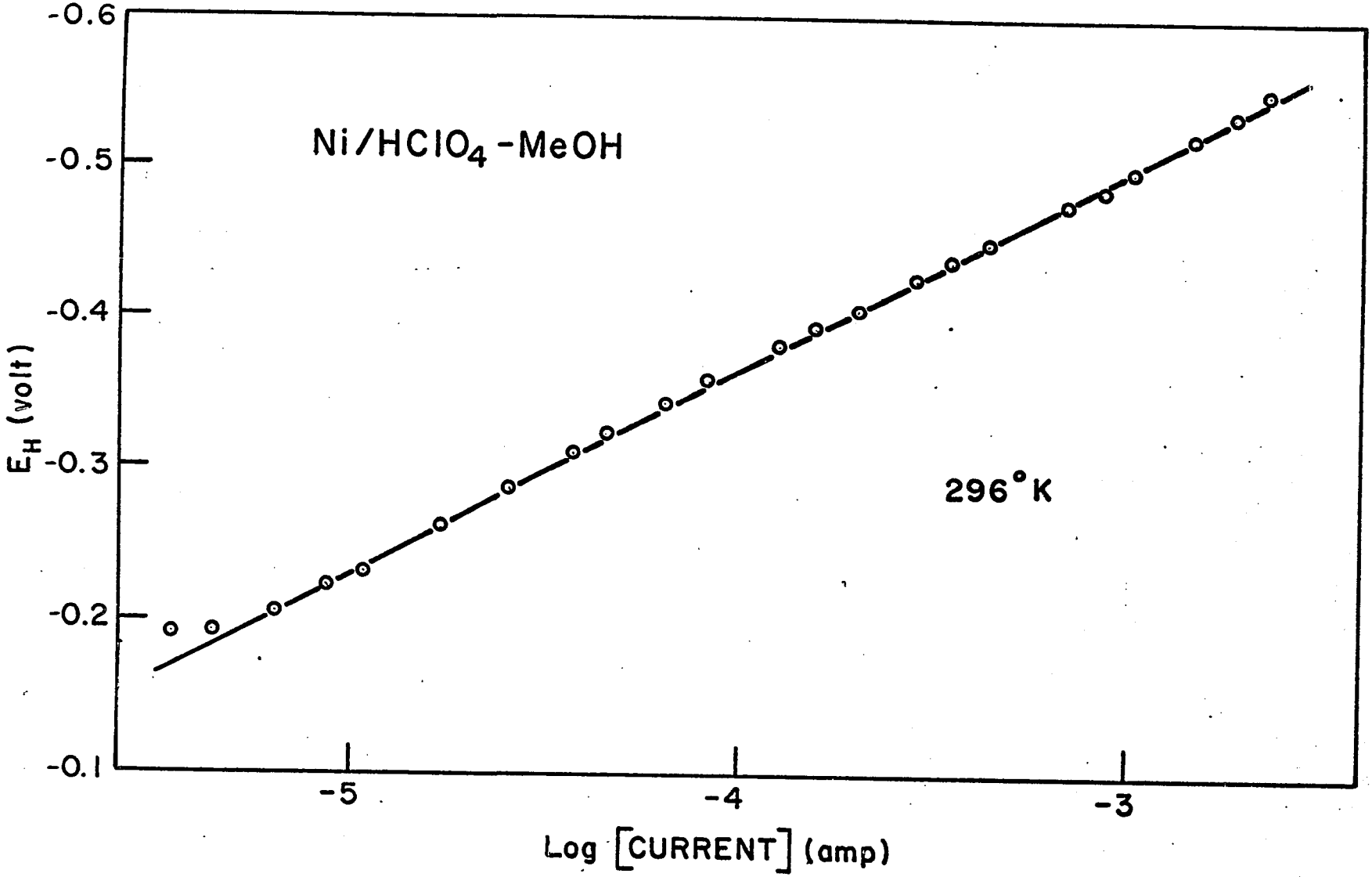
Ni/HClO4 -MeOH
296°K
-0.6
-0.5
-0.4
-0.3
-0.2
-0.1
E_H (volt)
-5
-4
-3
Log [CURRENT] (amp)

Figure 53

Tafel slope, b, as a function of temperature for the h. e. r. at Ni in 0. 5M $HClO_4$-MeOH.

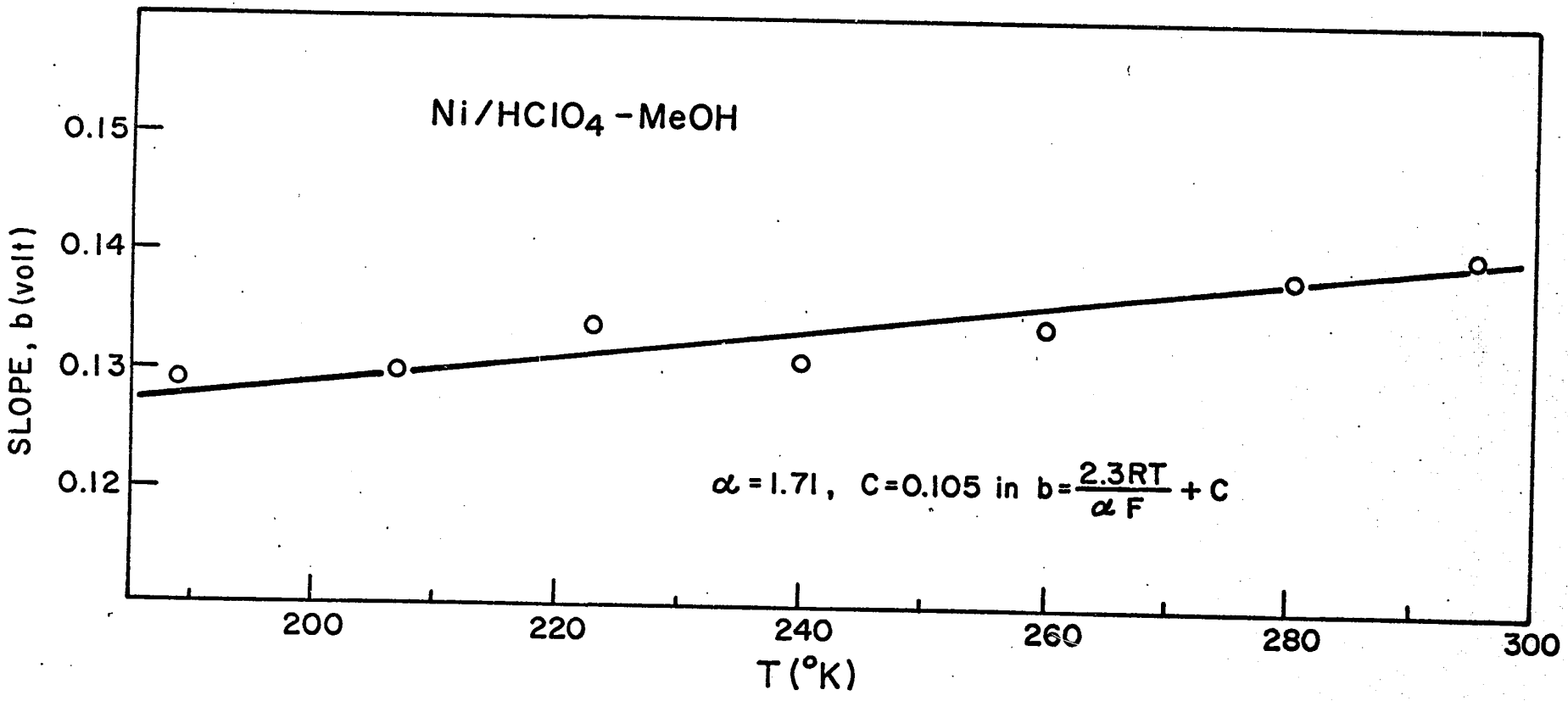
Ni/HClO4 - MeOH
SLOPE, b (volt)
0.15
0.14
0.13
0.12
200
220
240
260
280
300
T (°K)
α = 1.71, C = 0.105 in b = 2.3RT/αF + C

$HClO_4$ solutions at Ni) represents the kinetics in the absence of specific adsorption. That the Cl^- ion may have more of a kinetic effect at Ni than it does at Hg probably arises since (a) overpotentials at Ni are nearer the potential of zero charge (p. z. c.) than they are at Hg for current densities $\geq 10^{-6}$ A. cm.$^{-2}$; and (b) atomic H is appreciably adsorbed at the Ni electrode surface (cf. 94) and its coverage and binding energy (112) may hence be sensitive to co-adsorption of Cl^- [cf. the results of Breiter (113) at Pt]. Similar conclusions apply to the results for Pt. The results of Bockris and Potter (104) over a small temperature range in aqueous HCl indicate that b is almost independent of T. Since this result was observed in 0.001 and 0.01N HCl, and in dilute NaOH, it seems justified to regard it as also applying to the h. e. r. in the absence of specific adsorption of anions.

The lower Tafel region at Ni and the whole behavior at Pt seem consistent with anion adsorption effects since (a) the Tafel slope (at Ni) becomes changed at higher potentials and then varies more normally with T; and (b) for ascending changes of T at Pt (Figure 36(b)), b remains almost constant with T and suddenly changes at ca. 270°K whereas for descending changes of T (Figure 36(a)), b, both for the h. e. r. and d. e. r., continuously increases with decreasing T. Similarly, in the bromide ion discharge reaction (Figure 50(b)), b is independent of T and since this is an anodic reaction, Br^- adsorption may be anticipated.

3. Lead and Cadmium

More complex relationships between hydrogen overpotential and anion specific adsorption are observed for these metals (107). A considerable lowering of η is observed in HCl and HBr solutions as the concentration is increased.

In contrast to the behavior observed with Hg, the

establishment of the adsorption equilibrium proceeds slowly, a situation which results in the appearance of a hysteresis loop on the η vs. ln i curve (112). The differences in the behavior of Hg and of Pb and Cd may be associated with the presence of active centers at the surface of the solid metals at which stronger bonds between the anion and the metal can be established.

In the present work (Figures 37(a) and 37(b)), the b vs. T behavior of the h. e. r. at Pb and Cd was found to be similar except that the b values for Pb were higher than those for Cd. However, it was found that prolonged cathodization at the highest c. d. reduced the Tafel slopes on Pb to more acceptable values, i. e., ca. 130 mV/ decade at 25°C. Similar effects of polarization were observed by Ives and Smith (114) and high values of b at Pb were already observed in early work by Hickling (115). Although the polarization treatment reduced the Tafel slopes for Pb, they still remained higher than those for Cd.

The observed behavior for these metals over a range of temperature may be due to the effects associated with specific adsorption of Cl^- ions, mentioned above, and to the possible formation of "hydrides". On Pb, and to a lesser extent on Cd, it is possible that hydrogen evolution occurs on a "hydride" surface film rather than on the bare metal surface. This possibility is suggested by the fact that the Pb surface at the end of the measurements is black, in sharp contrast to the "mirror-like" surface at the beginning of the measurements. Cd does not, however, turn black, but becomes light grey in color, a fact which suggests that a thicker film is formed on Pb. Cathodic disintegration of Pb at high current densities is thought to occur (114, 116) and the formation of what is stated to be PbH_2 as a result of this process has been suggested (116).

(iii) Behavior of b at the lowest temperature

Both for the upper Tafel lines at Ni (Figure 34) and for Cd (Figure 37(b)) (and to some extent for Pb), b initially decreases with T in a qualitatively normal way but increases again with further decrease in T. In the d. e. r. at Ni, the effect already occurs at 240°K. While qualitatively such effects could be ascribed to increasing participation of proton tunneling as T is lowered, the fact that the trend toward higher slopes arises in the d. e. r. already at 240°K (while for the h. e. r. it arises only at 190-200°K) renders this an unlikely possibility. Since related changes of slope of the Arrhenius plots, corresponding to lower values of heat of activation also arise both for the h. e. r. and the d. e. r. (see Figure 46) at the lowest temperatures, it seems necessary to ascribe this behavior to effects of solvent structure changes on the entropy of activation (66). rather than to tunneling (the effects are in the opposite direction to those that might arise from increasing heat of activation due to increased H-bonding in the solvent at the lower temperatures; cf. Section e). Such effects would be consistent with the H/D isotope effect observed in the present work which cannot be clearly attributed to differences of tunneling rates.

(iv) Isotope Effects and Specific Anion Adsorption

The differences observed (see Chapter IV) for the h. e. r. and d. e. r. could also be interpreted in terms of specific adsorption of Cl^- anions. If specifically adsorbed anions, situated in the inner Helmholtz plane (i. h. p.), interact with the initial or transition states as discussed by Parsons (111) then the H/D isotope effect which normally arises may be dependent on the anion concentration and hence on the electrode potential. Moreover, the solvation properties of simple ions such as Na^+, Cl^-, have recently been shown in this laboratory to be appreciably different in H_2O and D_2O and the

electrostriction, for example, of Na^+Cl^- is appreciably greater in D_2O than in H_2O (117). In the interphase region near the electrode surface where water dipoles are adsorbed and oriented by the field, the effects of anions may be significantly different in H_2O and D_2O and thus affect the transition state for H^+ or D^+ neutralization. (Electrocapillary experiments are in progress to investigate this matter further.)

d) Some Theoretical Aspects of the Temperature Dependence of Tafel Slopes

(i) General

Following the general discussion of experimental results given in the previous Section, several possible reasons why the temperature dependence of Tafel slopes, b, differs from that hitherto considered in conventional representations of charge-transfer kinetics are examined; in particular, factors which can lead to a temperature dependence of the "Brønsted factor" (157) β are investigated. In the previous Section, it was shown that under certain conditions, e.g. at Hg and Ni, Tafel relations arose which gave b of the forms

$$b = \frac{RT}{\beta F} + c \qquad \text{or} \qquad b = \frac{RT}{\beta_T F} \qquad \text{(cf. equation [63]}$$

and [66]) where β_T is an approximately linear function of T. Alternatively, it was shown that equation [66] could be written in terms of a temperature dependent β factor, denoted by β'_T, given by

$$\beta'_T = \beta RT/(RT + \beta Fc) \qquad [67]$$

giving consistency with equation [63]. These relations were shown to apply under conditions for which it could be assumed that anion

specific adsorption effects were absent. Hence other factors have to be considered such as (a) temperature-dependent orientation of solvent dipoles at the interface in relation to the dipole surface potential χ ; (b) related changes of solvent structure with temperature; (c) effects of potential on the entropy of activation in relation to solvent orientation characterized by χ , and (d) temperature dependence of H coverage.

(ii) Significance of the Constant c in the Results for Hg

On the basis of equation [63] for the results at Hg, it is clear that $b \rightarrow c$ as $T \rightarrow 0$, i.e. the results of Figure 49 are characterized by an apparent residual current contribution logarithmically proportional to $\emptyset$ but independent of T at the absolute zero. This suggests a contribution from the proton tunneling mechanism considered experimentally and theoretically in previous papers (18, 31, 47, 48, 83, 119). Such a view receives some support from the shapes of the b vs. T plots, e.g. for the upper Tafel region for Ni, and for Cd, where b after initially decreasing with decreasing temperature, rises again as the temperature is taken to the lowest values. This behavior, being characteristic of the upper Tafel region at Ni, is probably not associated with anion adsorption since it has been argued (Section c) that such an effect is only significant for the lower lines where b continuously increases as T decreases from 298°K. However, while the above suggestion is an attractive one in providing an interpretation of c, difficulties concerned with such an explanation in terms of an appreciable extent of proton tunneling have been referred to in Section c. In particular, the b values for the h.e.r. and d.e.r. do not differ in the expected way, and curvature both in the Arrhenius and in the b vs. T plots arises for both reactions. In these circumstances, it seems that an explanation for the "anomalous" behavior of b as f(T) must be sought in other directions.

(iii) Role of Dipole Surface Potential, χ

The local solvent dipole potential-difference in the ad-layer adjacent to the electrode has hitherto received little attention in relation to electrode kinetics but its role in determining double-layer capacitance has been treated (118). If it is of importance in the latter connection, it seems necessary to consider it further in relation to Tafel slopes although these are usually to a large extent independent of potential.

The initial state of the proton prior to the act of discharge has been considered variously (3, 7) as being in the inner layer* adjacent to the electrode or some 2.5 water molecule diameters away from the surface (119). In the latter situation, direct tunneling to the surface has been postulated (119) but this view seems difficult to envisage (120, 121) since the proton may reach the inner water layer by successive proton jumps and charge delocalizations similar to those in the homogeneous conductance mechanism (38). In absolute rate calculations the proton has been considered as located in this inner solvent region (7). Thus Conway (120) has pointed out that in the discharge step, the rapid proton jump mechanism must play a role and this viewpoint has been further taken up by Nürnberg (121). In the outer Helmholtz plane (o.h.p.) the hydrated (or solvated) proton $H_9O_4^+$ or $H_9O_4^+H_2O$ will be present and the three or four H_2O molecules around H_3O^+ will be optimally oriented both for hydration of the proton and with respect to solvent orientation in the double-layer. Under these conditions, very rapid proton transfer amongst the 4 oxygen-centres

---

*In the equilibrium situation of the proton, which determines the double-layer capacitance behavior, e.g. of dilute mineral acid solutions, the cations are probably situated at the outer Helmholtz plane (120) (o.h.p.) since the capacitance behavior of HCl does not materially differ from that of KCl.

in $H_9O_4^+$ will arise according to the model of Eigen, Wicke and Ackermann (127) probably by the tunneling mechanism (38) (no reorientation of dipoles being required in this situation (120, 121)). Hence, kinetically the proton may be able to be discharged from the inner layer in a coupled proton activation-electron transfer step while the thermodynamic properties of the double-layer and the resulting potential profile could still be determined by the time-average concentration of protons existing as "H_3O^+" ions at the o. h. p.

Some difficulties arise with the long-distance tunneling mechanism when this process is compared with the discharge step in alkaline solution where proton transfer occurs from a water molecule ($H_2O + M + e \rightarrow MH_{ads} + OH^-$); in the latter case, it seems difficult to envisage water molecules other than those close to the electrode in the inner layer as constituting the kinetically significant initial state of the reaction. If it is accepted that the kinetically significant situation of the proton in the act of discharge is in or near the inner solvent layer, then the local orientation of neighbouring water molecules may be expected to influence the discharge kinetics. A statistical expression of this orientation is given by the dipole surface potential contribution χ which will be dependent on the electrode potential (or charge and hence field). The potential χ can constitute an appreciable fraction of the metal-solution p. d. ϕ which influences the kinetics through the β term. It has been claimed (118) that χ remains small ($\pm$ 120 mV.) as the surface charge q_M on the metal varies from q = 20 to q = -20μC.cm^{-2}. It would hence not appreciably influence kinetics of electrode processes. This calculated variation of χ seems, however, too small since it may be shown by substitution of the previously assumed (118) values for the dipole moment of water and the surface dielectric

constant ϵ_s (= 6) that χ varies* from ca. +1.2 V to -1.2 V rather than over only ±0.12 V in the above range of q. The value of χ as a function of field E is*

$$\chi = \frac{4\pi \mu N_T}{\epsilon_s} \tanh \left[-f_i \left(\frac{N\uparrow - N\downarrow}{N_T}\right) + \mu E/kT \right] \qquad [72]$$

and the orientation distribution function for $N\uparrow$, $N\downarrow$, the number of solvent dipoles oriented each way normal to the surface, is

$$\frac{N\uparrow - N\downarrow}{N_T} = \tanh\left[-f_i\left(\frac{N\uparrow - N\downarrow}{N_T}\right) + \mu E/kT\right] \qquad [73]$$

where f_i is an interaction parameter dependent on dipole-dipole interaction, surface coordination number and temperature, μ is the solvent dipole moment and N_T is the total number of dipoles per cm^2. The limiting values for complete orientation are independent of the form of the distribution function and are determined simply by the term

$$2\pi N\mu/\epsilon_s \quad \text{(ref. 118)} \qquad \text{or} \qquad 4\pi N\mu/\epsilon_s$$

where N is taken as 10^{15} molecules cm^{-2} for water or the end of the $-CH_2OH$ group.

Values of χ as a function of charge or field E are shown in Figure 54 for various values of the interaction parameter f_i and as a function of temperature in Figure 55. While χ of course increases to the saturation value of ca. 1.2 V with increasing field

*The term 4π rather than 2π used (118) in the Helmholtz expression for χ seems the preferred quantity (122), but this is not the source of the whole of the difference referred to above. Normally over the experimentally accessible range of q_M, χ_d will, of course, be appreciably less than 1.2 V since the interaction parameter for -OH dipoles will be of the order 3-4 kcal. $mole^{-1}$.

Figure 54

Calculated values of the surface dipole potential χ_d from the B. D. M. model for various temperatures and values of the dipole interaction parameter f_i, as a function of electrode surface charge.

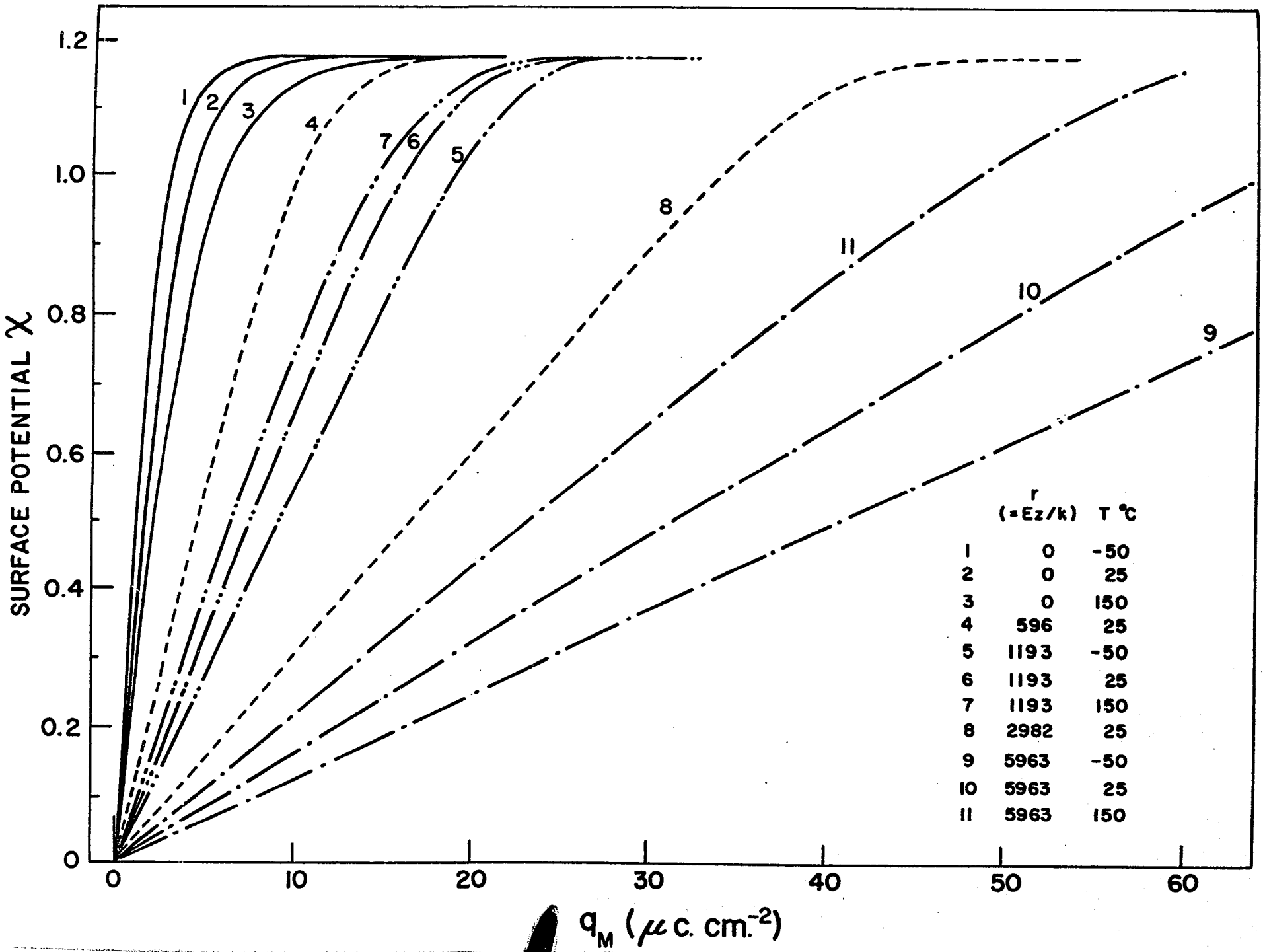
SURFACE POTENTIAL χ
1.2
1.0
0.8
0.6
0.4
0.2
0
0
10
20
30
40
50
60
q_M (μc. cm.$^{-2}$)
1
2
3
4
5
6
7
8
9
10
11
r (=Ez/k) T °C
1 0 -50
2 0 25
3 0 150
4 596 25
5 1193 -50
6 1193 25
7 1193 150
8 2982 25
9 5963 -50
10 5963 25
11 5963 150

Figure 55

Temperature dependence of χ_d for various values of f_i.

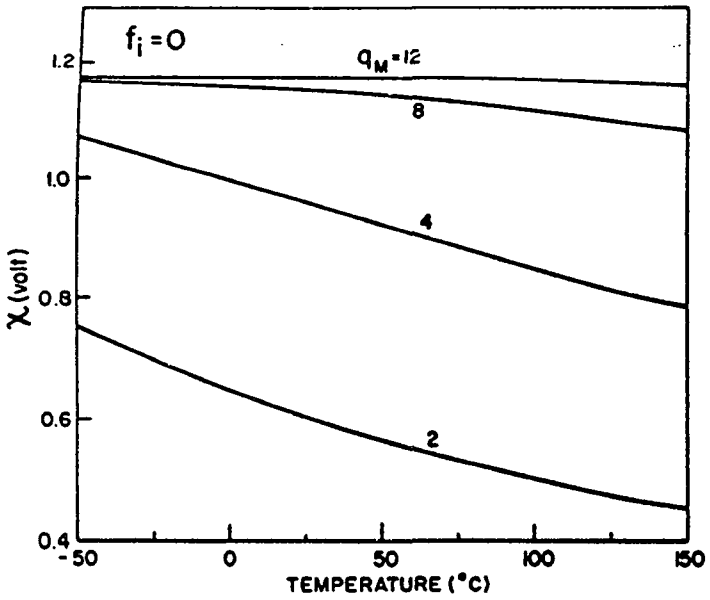
$f_i = 0$
$q_M = 12$
8
4
2
χ (volt)
1.2
1.0
0.8
0.6
0.4
-50
0
50
100
150
TEMPERATURE (°C)

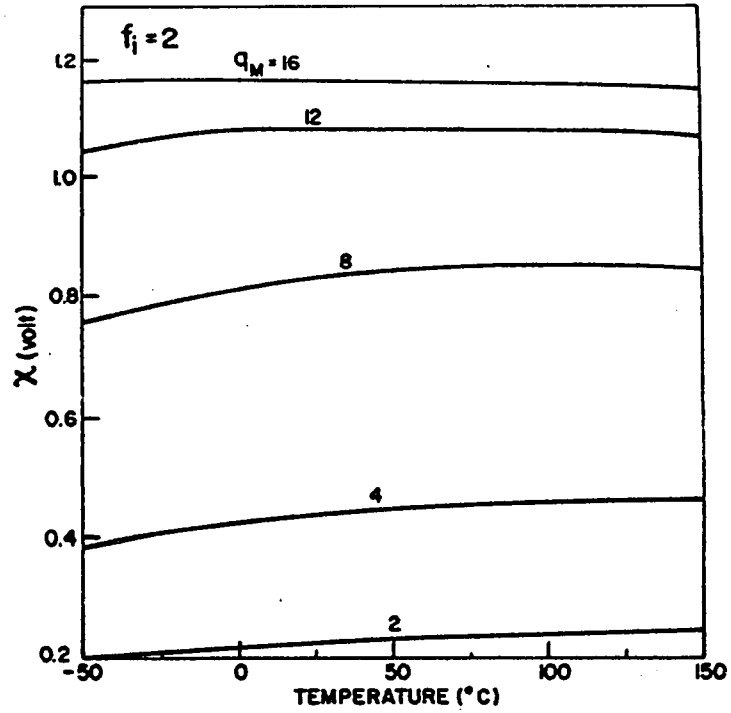
$f_i = 2$
$q_M = 16$
12
8
4
2
χ (volt)
1.2
1.0
0.8
0.6
0.4
0.2
-50
0
50
100
150
TEMPERATURE (°C)

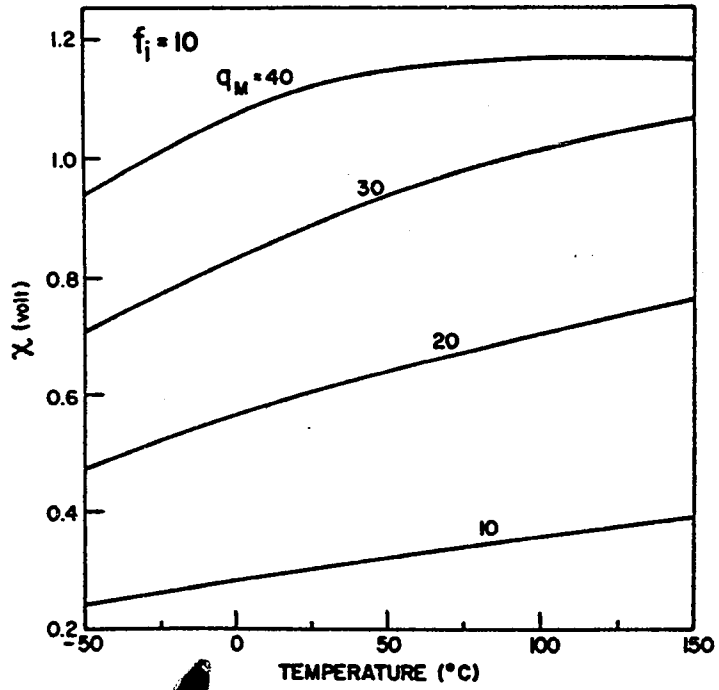
$f_i = 10$
$q_M = 40$
30
20
10
χ (volt)
1.2
1.0
0.8
0.6
0.4
0.2
-50
0
50
100
150
TEMPERATURE (°C)

or surface charge, the range of values of the field over which it does so is greater the larger is the value of f_i. Of great interest, is the temperature dependence of χ which decreases (for a given value of field) with increasing temperature when $f_i = 0$ or small, as expected, but <u>increases</u> with increasing temperature when f_i is larger. This is a result of the opposing influences of the orienting field and the dipole repulsion.

The next problem is how the overall metal-solution p. d. ϕ depends on the contribution χ (123). Certainly at the potential of zero-charge (p. z. c.) the total surface potential is equal to ϕ.

The total intrinsic surface potential χ_o at the p. z. c. arises from asymmetry at the surface of the metal and anisotropy of structure at the solvent interface, and may depend on temperature. At other potentials, the metal-solution p. d. can be regarded as made up of the contribution χ_o modified by the outer potential generated by excess charge q on the interface where $-\psi = \frac{1}{\Delta} \cdot \frac{4\pi q}{\epsilon_s}$ and Δ is the thickness of the region over which a mean field ψ/Δ is set up and within which an effective, field-dependent dielectric constant ϵ_s applies. When excess charge is on the interface, it seems difficult (cf. 123) to regard χ_d (arising from field orientation of solvent dipoles according to equation [73] and ψ as separate or additive terms since χ_d determines the ϵ_s to be used in Gauss's equation commonly employed (cf. 101) to express ψ/Δ. Hence ϕ is either to be expressed in an approximately additive way as $\chi_o + \chi_d$ where χ_d is a f(q) (equation [72]) or $\phi = \chi_o + \frac{4\pi q \Delta}{\epsilon_s}$ and ϵ_s is determined by the orientation distribution function $(N\uparrow - N\downarrow)/N_T$ (equation [73]). It is evident that $|\chi|$ will generally increase with increasing positive or negative field due to further electrostatic orientation (118) beyond that associated with χ_o. Attention is restricted to a consideration

of the latter effect in relation to the potential and temperature dependence of reaction velocity of an electrochemical discharge step, such as that occuring in the h. e. r. at Hg, where complications due to coverage of the surface by atomic H are not significant.

With regard to effects of temperature, it seems reasonable to state that the change of χ_d due to a change of surface charge from the zero charge condition to a finite value of q_M will be larger the lower the temperature if $f_i = 0$ or small (Figure 55). Correspondingly, for a given change of p. d., $\Delta\phi$, a relatively greater contribution from the change of charge of Δq_M will arise at higher temperatures than lower, so that a relatively greater driving force for proton discharge may arise if the increased negative charge density on the electrode is regarded (cf. 157) as leading to the enhancement of the rate of proton transfer (Brønsted effect). Thus, a given p. d. ϕ could have a relatively greater effect in modifying the rate constant at high than at low temperatures, i. e. β should be an increasing function of temperature. Such an effect of χ may evidently, however, increase or decrease with T depending on the coordination or structure in the dipole ad-layer at the interface, since f_i determines how χ will vary with temperature and field. In fact, f_i itself will probably depend on the extent of field induced orientation and on local solvent structure effects particularly in H-bonded, associated solvents such as were used in the present work. Qualitatively, then, changes of χ and dipole orientation could lead to temperature dependence of β.

In the absence of interaction effects, field E and temperature are, of course, conjugate variables in the ratio $\mu E/kT$ which determines the orientation distribution function (equation [73]), so that decrease of T is equivalent to an increase of E at a given temperature. Hence any changes of β with T which might arise on the above basis would also be expected to be manifested at

increasing fields. There is no evidence for the latter effect since β or α are quite constant for the h. e. r., at a number of metals, particularly at Hg, over a rather wide range of potentials (121). However, when f_i is appreciable, the orientation (and hence χ) is no longer a simple function of $\mu E/kT$ so that χ may decrease with decreasing temperature but still increase with increasing E (Figure 55). The difficulty here is that any orientation effect which may influence the local profile of p. d. in the interphase with changing T and hence provide a possible basis for an explanation of the variation of β with T would seemingly require an equivalent variation of β with E.

From thermodynamic considerations of a charge-transfer process at equilibrium, it is clear, however, that β must operate on the total metal-solution p. d. set up; similarly it must apply to the whole value of any other potential applied under non-reversible conditions. However, the local environment of ions awaiting discharge will depend on the orientation of solvent dipoles in the double-layer determined by χ_o and χ_d, the latter depending on q (equation [72]). Such an effect of local solvent dipole environment may be of particular importance with respect to proton discharge since the proton can penetrate by the anomalous conductivity mechanism into the inner layer where solvent dipole orientation will be most important. Any effect of temperature on β in the absence of anion adsorption, should therefore preferably be considered as an indirect structural effect arising from (a) temperature dependence of χ_o and χ_d; (b) the resulting local influence of solvent orientation on the free energy profile (see below) for thermal activation of the $O\text{-}H^+$ bond in H_3O^+ or $CH_3OH_2^+$ and (c) the associated rearrangement (125) of the three or four other solvating molecules about the ion necessary for the act of electron transfer.

(iv) Solvent Structure Effects

Solvent structure effects in the interphase are obviously closely connected with the question of dipole orientation but little attention has been paid to the role of changes of solvent structure with temperature in determining β as a function of temperature, although thermodynamic studies indicate (124,126) important effects of this kind in adsorption at Hg and in ionic solvation. It has been argued above that the kinetically significant location of the proton in the discharge step may be in the oriented solvent layer. The temperature dependent structure of the interphase in which the protons find themselves may therefore be an important factor in determining, for example, (a) the time-average location of the initial state, (b) the entropy of activation $\Delta S^{o\ddagger}$ and (c) the effect of local field or electrode potential on $\Delta S^{o\ddagger}$ (to be considered below).

(v) Effects of Potential on the Entropy of Activation $\Delta S^{o\ddagger}$

Normally it is assumed that change of electrode potential shifts the Fermi level so that the initial state potential energy curve for the profile representing the course of the rate-controlling step is simply moved up or down relative to the final state curve. This implies that the local metal-solution field or excess electron charge on the metal has no direct effect on the state of the reactant H_3O^+ ion or on its environment, so that only the enthalpy or internal energy component of the standard free energy of activation is modified by potential. At the large and charge-dependent fields that exist at electrode interfaces it seems unlikely that $\Delta S^{o\ddagger}$ would remain unaffected if only for the reason that the local environment of solvent dipoles in the interphase can change with q_M (see Figure 54) as discussed above. The usual rate equation for current density i is

$$i = zF\frac{kT}{h}.\ \exp[-\frac{\Delta G^{o\ddagger}}{RT}]\ \exp[-\beta\phi F/RT].\ f(c,\Theta) \qquad [74]$$

where $f(c,\Theta)$ formally allows for any dependence of i on the reactant concentration, double-layer effects, or surface coverage by H, none of which we shall be concerned with here. Normally equation [74] expresses the assumption that ϕ simply modifies the enthalpy or energy term in $\Delta G^{o\ddagger}$. Strictly, however, $d \ln i/d\phi$ is determined by $-d[\Delta\bar{G}^{o\ddagger}/RT]/d\phi$ where $\Delta\bar{G}^{o\ddagger}$ is the standard <u>electrochemical</u> free energy of activation, i.e. for the Tafel slope b

$$1/b = d \ln i/d\phi = \frac{-d}{d\phi}(\Delta H^{o\ddagger} - T\Delta S^{o\ddagger} + \beta\phi F)/RT. \qquad [75]$$

Noting that ϕ is negative and assuming for the purpose of the argument here that $f(c,\Theta)$ is independent of ϕ, then

$$1/b = d \ln i/d\phi = \frac{d(\Delta S^{o\ddagger}/R)}{d\phi} - \frac{\beta F}{RT} \qquad [76]$$

if it is assumed that $\beta\phi F$ already takes into account the potential dependence of the enthalpy or energy term in $\Delta\bar{G}^{o\ddagger}$. Limitingly, Agar has shown (68) that this type of relation can give β <u>proportional</u> to T if $\Delta S^{o\ddagger}$ only, rather than $\Delta H^{o\ddagger}$, is the quantity affected by potential. In fact, both quantities may be functions of potential leading to the result given in equation [76]. If $T\Delta S^{o\ddagger}$ were affected by potential, or the corresponding field, through a term $\beta'\phi F$, then equation [76] could be written

$$1/b = \frac{-d}{d\phi}(\Delta H^{o\ddagger} - [T(\Delta S_o^{o\ddagger} \pm \beta'\phi F)] + \beta\phi F)/RT = \frac{-\beta F}{RT} \pm \frac{\beta' F}{R} = \frac{-F}{RT}(\beta \pm \beta' T) \qquad [77]$$

so that the apparent value of β calculated from b would be temperature dependent. The result in equation [77] is not, however, quite

identical in form with equation [63] which empirically expresses the results for Hg, although for appropriate values of β and β' a relation similar to that observed experimentally can be shown to arise over a limited range of temperatures. It can account for other cases, however, where the apparent β decreases or increases linearly with temperature. Strictly the results (Figure 49) for Hg indicate β is independent of temperature but with a value different from 0.5, b being determined also by a temperature independent constant c (equation [63]). However, equation [67] allows the possibility of dependence on T.

It is of interest to speculate on a physical explanation of a potential dependence of $\Delta S^{o\ddagger}$. The true (cf. 100,136) volume of activation in proton discharge at Hg is positive so it may be assumed by analogy with homogeneous ion neutralization processes (171) and the behavior of water in the double-layer (126) that $\Delta S^{o\ddagger}$ is also positive.* Increasing field, and the resulting orientation of the solvent dipoles at the electrode interface (Figure 54), will tend to allow less relaxation of molecules in the solvation shell of the H_3O^+ ion when the latter is discharged, than would be the case for lower fields in the double-layer. On this basis $\Delta S^{o\ddagger}$ would tend to be less positive or more negative at higher overpotentials; β' would hence be positive, i.e. the positive sign is taken in the term $T(\Delta S_o^{o\ddagger} \pm \beta' \phi F)$ of equation [77] since ϕ is taken negative for a cathodic process. This would cause the numerical value of the apparent β in the defining relation "$b = RT/\beta F$" relatively to decrease with decreasing temperature which is the direction required to account for the experimental results for the h.e.r. at Hg (Figure 49).

---

*Experimental evaluation of $\Delta S^{o\ddagger}$ is rendered difficult (cf. 7, 18, 31) on account of the impossibility of directly determining an absolute heat of activation for an electrode process.

Elsewhere (124,165), it has been shown that the decrease of librational entropy of oriented solvent dipoles in the double-layer with increasing field can be appreciable and this effect can be relatively greater at lower temperatures. On the other hand, field effects on bond energies, e.g. of $O\text{-}H^+$ in H_3O^+ are negligible (31). Hence, a reasonable explanation for the observed temperature dependence of b can be given at least qualitatively in terms of field effects on the entropy of activation through solvent orientation effects.

When f_i is appreciable, χ_d varies linearly with q_M and hence (approximately) with electrode potential. χ_d also varies approximately linearly with the change of librational entropy (124) of oriented solvent molecules. Hence the orientation and entropy effects will not cause a change of shape of the Tafel line at any given temperature but only contribute to a temperature dependence of β. This is as required by the experimental current-potential behavior where β is usually constant with changing ϕ except when changes of mechanism or anion adsorption are involved.

(vi) Double-layer Thickness Effects

The proportionality of β or a to T has been attributed by Parsons and Bockris (7) to changing double-layer thickness δ with temperature. Their calculations for Hg and Ni were based on changing relative positions of potential energy curves along the reaction coordinate and predicted β would vary inversely with δ. However, changes of relative position on the energy axis produce changes in β similar to those arising from changes of position on the reaction coordinate axis, as indeed is found (7) when other energy parameters are varied in the calculations. However, for the h.e.r. at Hg, β is almost exactly constant (121) over 1.2 V or 10 decades of change of rate. Hence it is difficult to adopt the above explanation as a basis for the temperature dependence of β.

(vii) Bromide Discharge Reaction in Acetonitrile at Graphite

Here the dependence of b on temperature was sought for (a) a case in which proton transfer was not involved and (b) a solvent which was not hydrogen-bonded and hence would show less of a temperature-dependent structural contribution to the heat of activation and transfer coefficient of an electrode process. b is found to be independent of temperature over 104°C so that α is linear with temperature (Figure 50(b)). The anomalous temperature dependence of β in cases where b is independent of T, e.g. for the h.e.r. discussed above, is hence not specifically associated with proton discharge. In the anodic Br^- discharge case, the effects of specific adsorption should be simpler than in the case of the cathodic h.e.r. since the ions discharged in the reaction originate from the inner Helmholtz plane (i.h.p.) and their local concentration is directly determined by the total adsorption potential and the resulting electric potential at that plane. Since in the b.e.r., b is completely independent of temperature, the limiting case of equation [63] apparently applies where only c determines b. However, it is difficult to see how β could be ∞, so that temperature-dependent anion adsorption effects must be invoked leading to a linear temperature dependence of β , in order to explain the constancy of b over a range of 104°C.

(viii) Temperature Dependence of b for a Process Involving H Desorption

Normally for the atom-ion desorption mechanism (128) $MH_{ads} + H^+ + e \rightarrow H_2$ which may be rate-controlling at Ni, two limiting cases arise giving $b = 2RT/(1 + \beta)F$ or $2RT/\beta F$ for low, potential-dependent coverage Θ_H by H, or for $\Theta_H = 1$, respectively. Both of these terms imply a normal temperature dependence for b. Under conditions where the H is adsorbed at a "Langmuir" surface,

the transition between the two Tafel regions is relatively sharp. Values of b, including those for the h. e. r. at Ni studied here and at Ag do not, however, always fall into the two limiting cases (nor do they have the values of RT/2F or RT/F for recombination processes) so it is of interest to examine the form of b with potential or coverage, and its temperature dependence, when appreciable heterogeneity and/or interaction effects arise (cf. 129,130). For a heterogeneous surface or for one with significant interactions (e. g. the induced heterogeneity case), the transition can occur over a wider range of potential and the resulting Tafel slope and its temperature dependence is then more complex. In the general case, it must be recognized (131) that there may be incomplete equilibrium in the prior discharge step so that the relative values of rate constants in the prior discharge step and in the rate-controlling step must also be considered. Under such circumstances, $d \ln i/d\eta$ is not simply determined by the terms $\exp[\eta F/RT]$ (for the variation of Θ_H with η and T) and $\exp[\beta \eta F/RT]$ for the effect of potential on the rate-controlling charge transfer desorption step.

For interaction or heterogeneity effects, the coverage Θ by H is given (cf. 128,129) by

$$\frac{\Theta}{1 - \Theta} \exp r\Theta = KC_{H^+} \exp \phi F/RT \qquad [78]$$

where r is a measure of the change of adsorption energy of H from $\Theta_H = 0$ to 1. As in the case of calculations previously published (132, 133) where it was shown how reaction order, Tafel slope and coverage by intermediates are related through the electrochemical isotherm, $d\phi/d \ln i$ can be obtained from $(d\phi/d \ln \Theta)\ (d \ln \Theta/d \ln i)$. Thus

$$d\phi/d \ln \Theta = \frac{RT}{F} \cdot \frac{1 + r\Theta(1 - \Theta)}{1 - \Theta} \qquad [79]$$

so that the Tafel slope for the atom-ion desorption process is

$$d\phi/d \ln i = \frac{RT}{F} \Big/ \left[\beta + \frac{1 - \Theta}{1 + r\Theta(1 - \Theta)} \right] \qquad [80]$$

and Θ can be evaluated numerically as $f(\phi)$ from [78]. In the more general steady-state case (131), the previously published kinetic equations for this mechanism may be used which yield, with $\beta = 0.5$,

$$d \ln i/d\phi = \frac{d\Theta}{d\phi} \left(\frac{1}{\Theta} + \frac{r}{2RT}\right) - \frac{F}{2RT}$$

and

$$\frac{d\Theta}{d\phi} = -\frac{F}{RT}(K_E)^{1/2}\Theta^2 BA^2 \left[\frac{1 - \Theta}{A^2\Theta} - K_{NE} \right]^{1/2} (1 + f\Theta(1 - \Theta))^{-1} \qquad [81]$$

where $$B = K_E^{-1/2} \left[\frac{1 - \Theta}{A^2 O} - K_{NE} \right]^{1/2}$$

and $A = K_E = k_{-1}/k_1$ (the reciprocal of the quasi-equilibrium constant (131) for the H-producing discharge step) and $K_{NE} = k_2/k_1$ the ratio of the rate constants for the rate-controlling and the prior discharge steps.

Numerical evaluations of these functions for various values of K_{NE} and $\frac{r}{RT}$ are shown in Figures 56 and 57 for b as $f(\eta)$ at various K_{NE} values and for b as f(T) at various η values. The changes of b with η may be compared with the potential dependence of the coverage by H calculated previously (131). The results of the calculations show that if f(=r/RT) is large enough, e.g. 20, b can have a relatively constant value (but not either of the limiting values mentioned above) over an appreciable range of potentials with changes to the limiting value of 2RT/F depending on the magnitudes of f and K_{NE}. The temperature dependence, e.g. for $K_{NE} = 0$, $f = 20$, is correspondingly less than that expected for the limiting cases (b = 2RT/3F or 2RT/F) (Figure 56) but, in conclusion,

Figure 56

Calculated curves for the Tafel slope b of the step $H^+ + MH + e \rightarrow H_2$ as a function of η for various values of K_{NE} and the heterogeneity parameter f:

(1) $K_{NE} = 0$, $f = 0$;

(2) $K_{NE} = 1$, $f = 0$;

(3) $K_{NE} = 0$, $f = 20$;

(4) $K_{NE} = 10^{-5}$, $f = 20$;

(5) $K_{NE} = 10^{-3}$, $f = 20$;

(6) $K_{NE} = 10^{-1}$, $f = 20$;

(7) $K_{NE} = 1$, $f = 20$;

(8) $K_{NE} = 0$, $f = 10$.

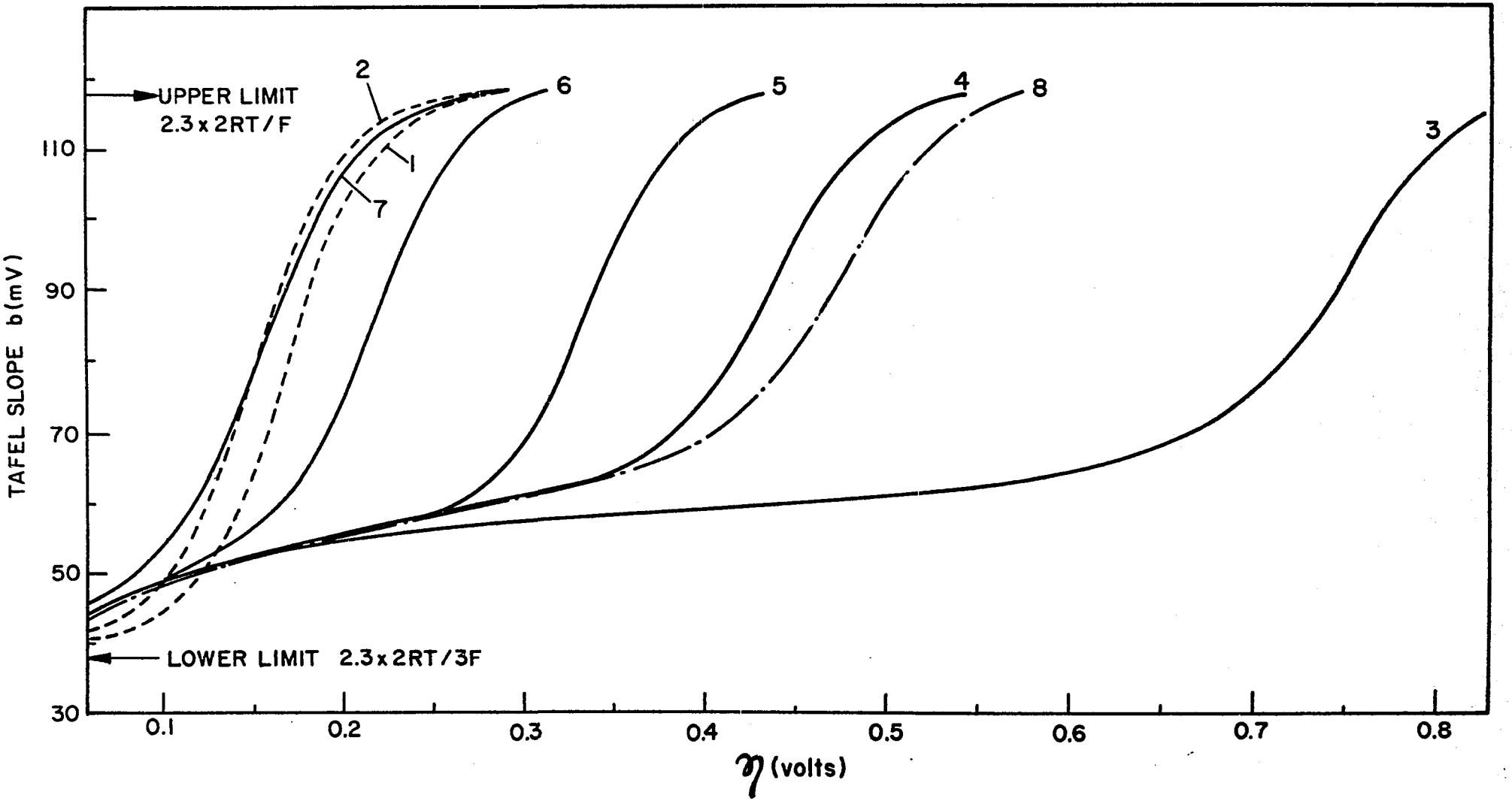
UPPER LIMIT
2.3 x 2RT / F
LOWER LIMIT 2.3 x 2RT / 3F
TAFEL SLOPE b(mV)
110
90
70
50
30
0.1
0.2
0.3
0.4
0.5
0.6
0.7
0.8
η (volts)
1
2
3
4
5
6
7
8

Figure 57

Values of b as in Figure 56 but as a function of temperature for various values of η . (Heavy lines in diagram for $K_{NE} = 0$ and $f = 20$ refer to the normal Langmuir limiting case for b, viz., $b = RT/\beta F$ or $RT/(1 + \beta)F$ with $\beta = 0.5$).

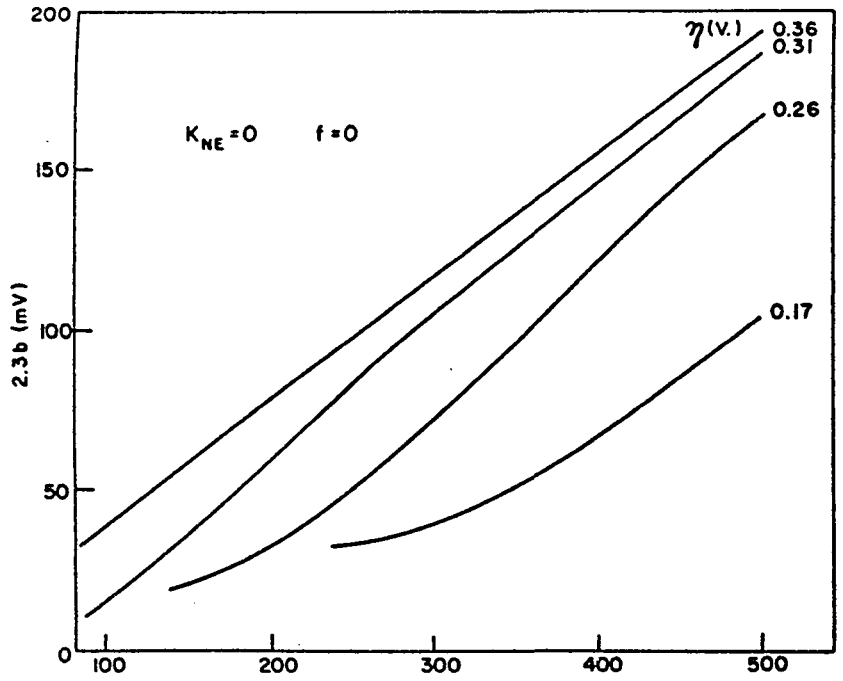
200
150
100
50
0
2.3b (mV)
η(V.)
0.36
0.31
0.26
0.17
K_NE = 0
f = 0
100
200
300
400
500

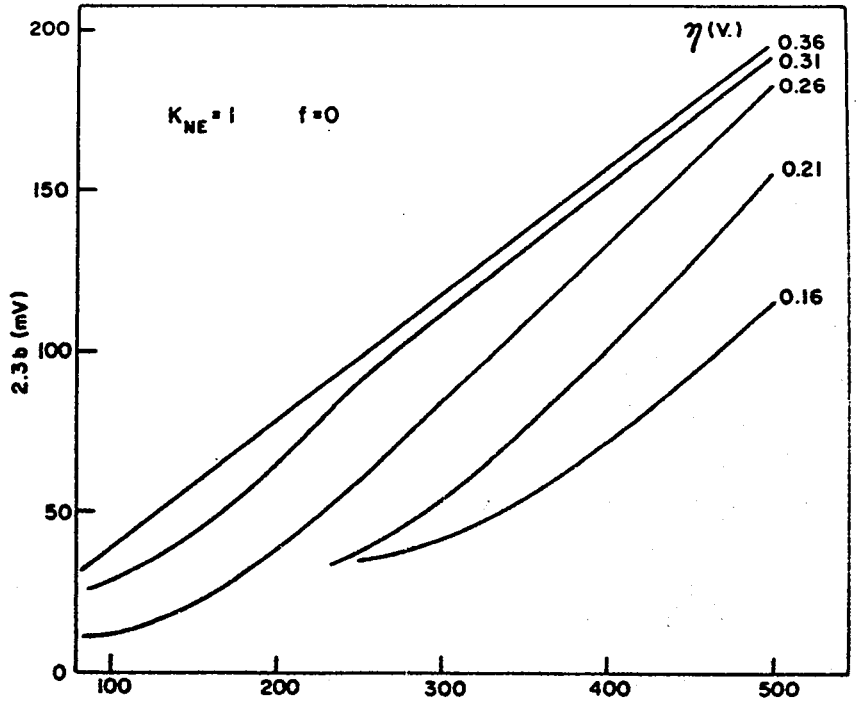
200
150
100
50
0
2.3b (mV)
η(V.)
0.36
0.31
0.26
0.21
0.16
K_NE = 1
f = 0
100
200
300
400
500

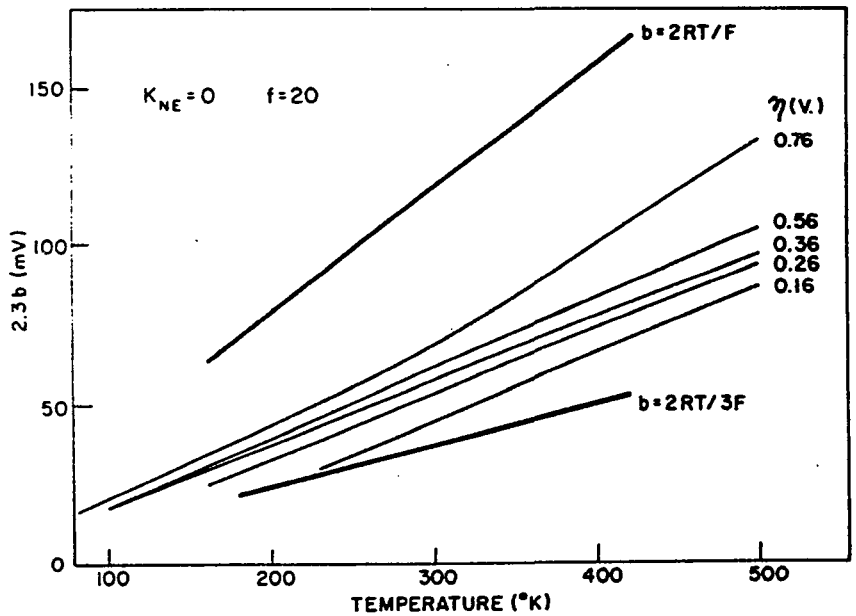
150
100
50
0
2.3b (mV)
b = 2RT/F
K_NE = 0
f = 20
η(V.)
0.76
0.56
0.36
0.26
0.16
b = 2RT/3F
100
200
300
400
500
TEMPERATURE (°K)

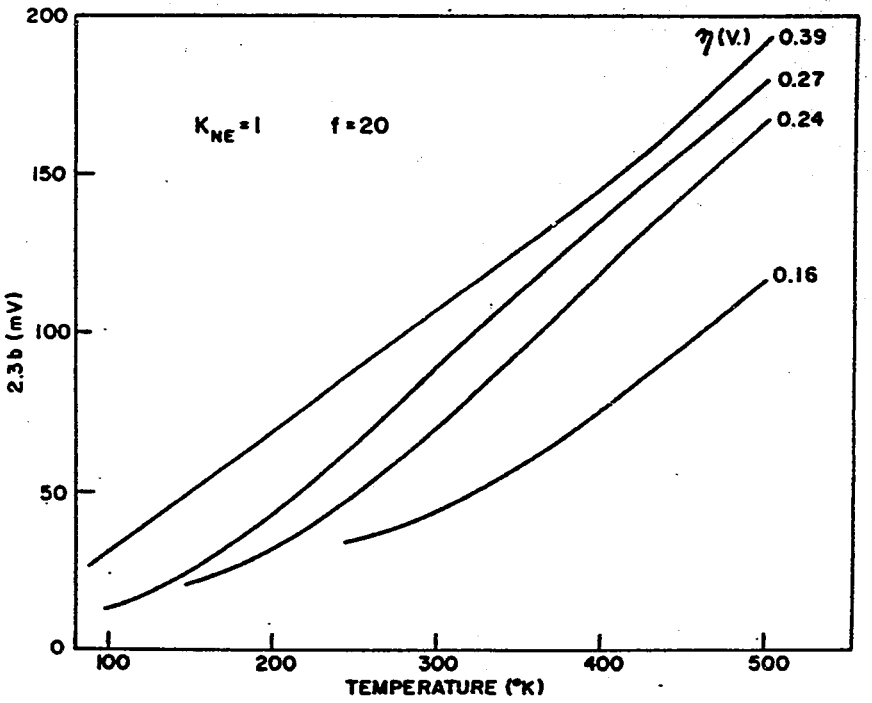
200
150
100
50
0
2.3b (mV)
η(V.)
0.39
0.27
0.24
0.16
K_NE = 1
f = 20
100
200
300
400
500
TEMPERATURE (°K)

it is important to note that no inverse temperature dependence of b evidently arises from these coverage effects.

e) Interpretation and Significance of Heats of Activation for Electrochemical Reactions Exhibiting Anomalous Tafel Slopes

(i) General

The results for the temperature dependence of the Tafel slope, b, for the hydrogen (h. e. r.) and bromine evolution reactions over a wide range of temperatures (including low temperatures down to -125°C), presented in Chapter IV and discussed in the previous section of this Chapter, show that b is rarely given by the "defining" relation $b = RT/\beta F$ where $\beta \neq f(T)$. In fact, b is usually less temperature dependent than is implied by the above relation and reference has been made to the fact that under some conditions b can be almost independent of temperature (104, 105, 106) while for other conditions b may even increase with decreasing temperature.

The consequences of this situation with regard to the evaluation and significance of $\Delta H_R^{o\ddagger}$ (the experimental, apparent heat of activation at the reversible potential, i. e., at $\eta = 0$) will be discussed in this section in relation to the experimental results presented in Chapter IV of this thesis. The interpretation of temperature variations of $\Delta H_R^{o\ddagger}$ is of interest in regard to (a) the role of proton tunneling (33, 37, 134) in the h. e. r.; (b) the effects of solvent structure changes on $\Delta H_R^{o\ddagger}$ in hydrogen-bonded media as the temperature changes and (c) the role of temperature-dependent solvent orientation (118, 124) at the electrode interface in the kinetics of the h. e. r.

(ii) Illustrative Numerical Calculations of $\Delta H_R^{o\ddagger}$

Thus, with regard to the above statements, it was thought desirable first to make exploratory evaluations of $\Delta H_R^{o\ddagger}$ for various situations in which complications may arise, e.g. if β is f(T) or if b is not simply equal to $RT/\beta F$. Results are therefore presented here of illustrative numerical calculations of activation energies in which various means of expressing $\Delta H_R^{o\ddagger}$ have been used. The following approach was employed: the usual relation

$$i_o = k \exp -\Delta H_R^{o\ddagger}/RT \qquad [82]$$

is used and a value of 10.0 kcal. mole^{-1} was arbitrarily chosen for $\Delta H_R^{o\ddagger}$ and i_o values were calculated for a series of T values. These values were then put into the equation

$$\log i = \log i_o + \eta /2.3\, b \qquad [83]$$

where b was assumed to take one of the four possible forms listed below:

1. $b = RT/\beta F$; where $\beta = 0.5 = \text{const.}$; this is the form usually assumed for b, so that $\Delta H_R^{o\ddagger}$ should be recovered without complications; this is simply a "reference" case.

2. $b = (RT/\beta F) + c$ where c was taken as a constant equal to 0.04 volt. and $\beta = 0.71$ (to give $b = 0.116$ at $T = 298^oK$; cf. the actual results obtained at Hg in methanolic HCl).

3. b = constant value of 0.120 volt. at all temperatures (cf. the observed experimental behavior at certain metals described above), that is β is linear in T.

4. $b = c' - 2.3RT/\beta F$; i.e., b increases as T decreases, as found for example for Pt and in the low c.d. region at Ni when anion adsorption is significant.

For each of the cases listed above, $\Delta H_R^{o\ddagger}$ and $\Delta H_\eta^{o\ddagger}$ were recovered by each of the following methods and the results were compared (Figure 58):

(A). $d \log i_o/d(1/T) = -\Delta H_R^{o\ddagger}/2.3R$ - This is the kinetically most convenient way of obtaining the heat of activation.

(B). $d(\log i)_\eta /d(1/T) = -(\Delta H_R^{o\ddagger} - \beta \eta F)/2.3R$ for various η values.

(C). $(d\eta/dT)_i = -\Delta H_\eta^{o\ddagger}/\beta FT$.

(D). $(d\eta/d \log T)_i = -2.3\Delta H_\eta^{o\ddagger}/\beta F$.

Case 1. $b = RT/\beta F$; $\beta = 0.5$ and constant (Figures 58 and 59).

This case is trivial in that a value of $\Delta H_R^{o\ddagger} = 10.0$ kcal. mole^{-1} was chosen to calculate the i_o values from which $\Delta H_R^{o\ddagger}$ will obviously be recovered with the required value of 10.0 kcal. mole^{-1}. However, this shows that the method is consistent and also serves as a basis for comparisons amongst the remaining three cases. For this case, the values of $\Delta H_\eta^{o\ddagger}$ calculated by method B are in good agreement (as they must be) with values of $\Delta H_\eta^{o\ddagger}$ calculated from methods C and D.

Case 2. $b = (RT/\beta F) + c$ which the form of the b vs. T plot experimentally observed at Hg where $\beta = 0.71$ and $c = 0.04$ volts. A plot of $(\log i)_\eta$ vs. $(1/T)$ is shown in Figure 58. Unlike their counterparts in Case 1, the plots exhibit curvature which is more pronounced at the higher η values. Thus $\Delta H_\eta^{o\ddagger}$ must be determined for particular values of $(1/T)$ and is hence temperature-dependent. The plots of η vs. T and η vs. log T for this Case 2 are shown in Figure 60 and values of $\Delta H_\eta^{o\ddagger}$ calculated by method B are found not to be in agreement with values of $\Delta H_\eta^{o\ddagger}$ computed by methods C and D; however, the results of C and D are in agreement with each other.

Figure 58

Plot of $(\log i)_\eta$ vs. 1/T for the four test cases examined by numerical computation.

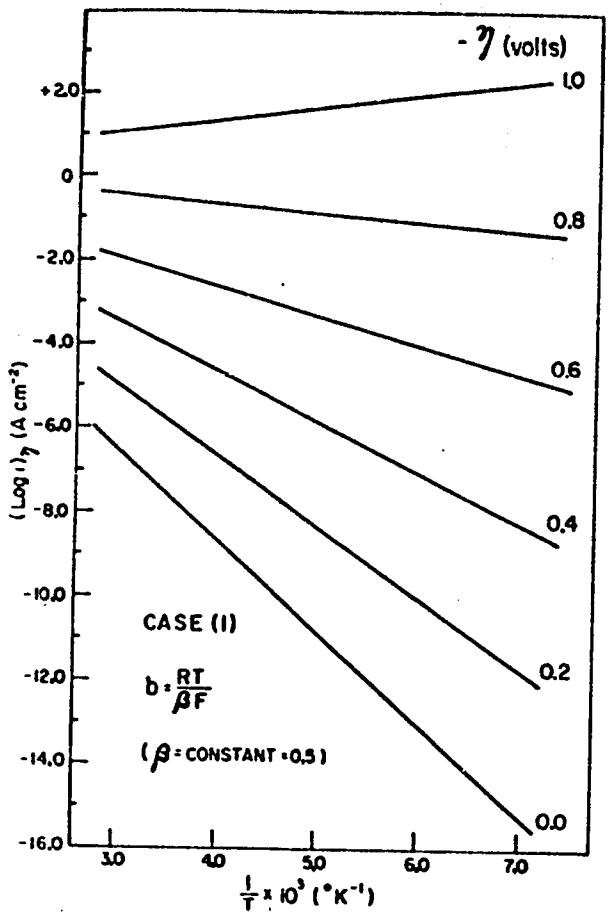
- η (volts)
1.0
0.8
0.6
0.4
0.2
0.0
CASE (1)
b = RT/βF
(β = CONSTANT = 0.5)
(Log i)η (A cm⁻²)
1/T x 10³ (°K⁻¹)

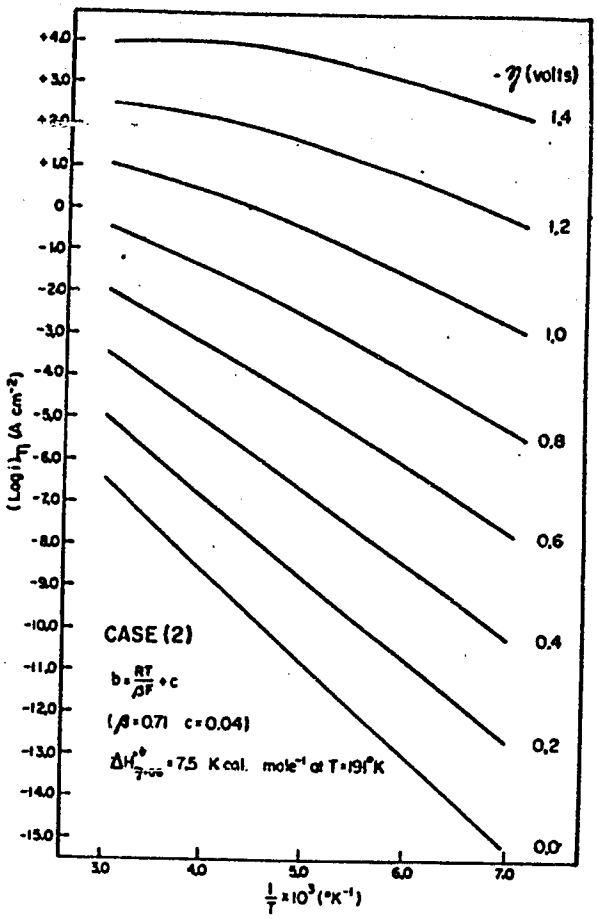
- η (volts)
1.4
1.2
1.0
0.8
0.6
0.4
0.2
0.0
CASE (2)
b = RT/βF + c
(β = 0.71 c = 0.04)
ΔH°η→0 = 7.5 K cal. mole⁻¹ at T = 191°K
(Log i)η (A cm⁻²)
1/T x 10³ (°K⁻¹)

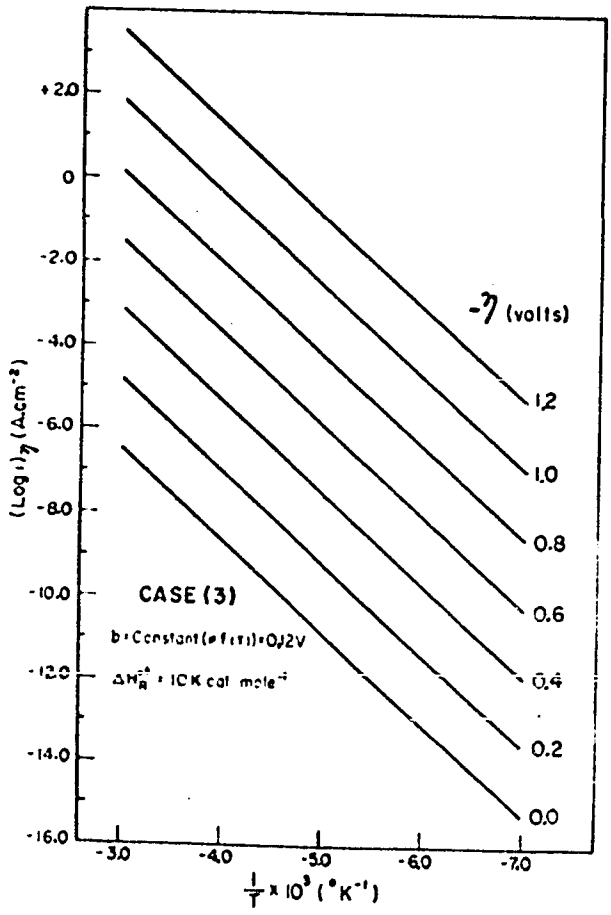
- η (volts)
1.2
1.0
0.8
0.6
0.4
0.2
0.0
CASE (3)
b = Constant (≠ f(T)) = 0.12V
ΔH°R = 10 K cal mole⁻¹
(Log i)η (A cm⁻²)
1/T x 10³ (°K⁻¹)

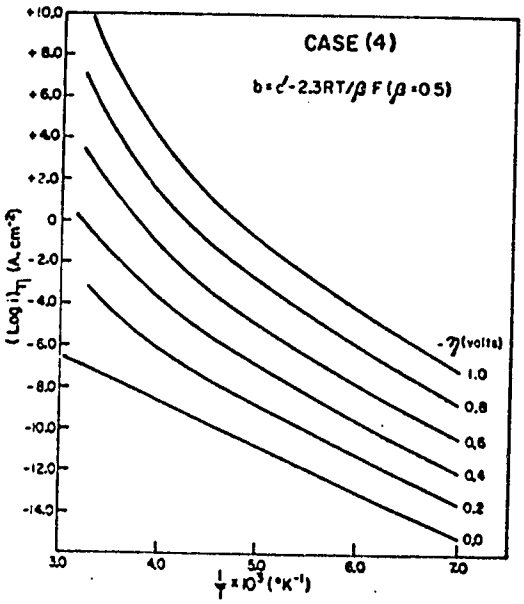
CASE (4)
b = 2.3RT/β F (β = 0.5)
- η (volts)
1.0
0.8
0.6
0.4
0.2
0.0
(Log i)η (A cm⁻²)
1/T x 10³ (°K⁻¹)

Figure 59

Plots of $(\eta)_i$ vs. T and log T for case (1).

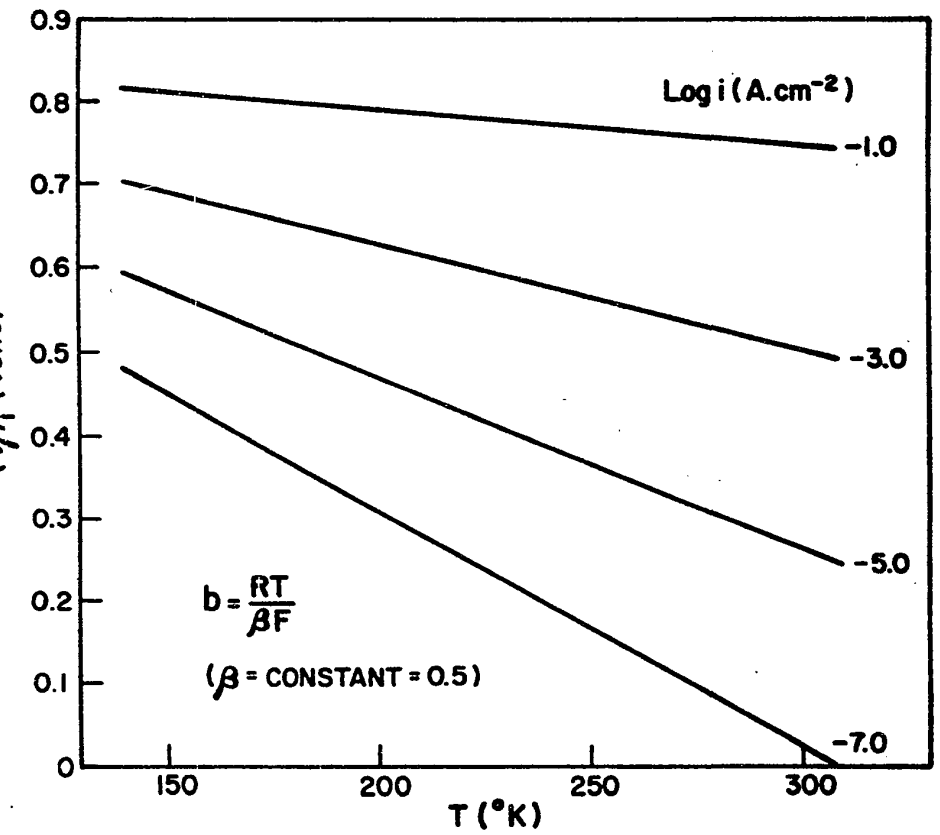
Log i (A.cm⁻²)
-1.0
-3.0
-5.0
-7.0
b = RT/βF
(β = CONSTANT = 0.5)
0.9
0.8
0.7
0.6
0.5
0.4
0.3
0.2
0.1
0
150
200
250
300
T (°K)

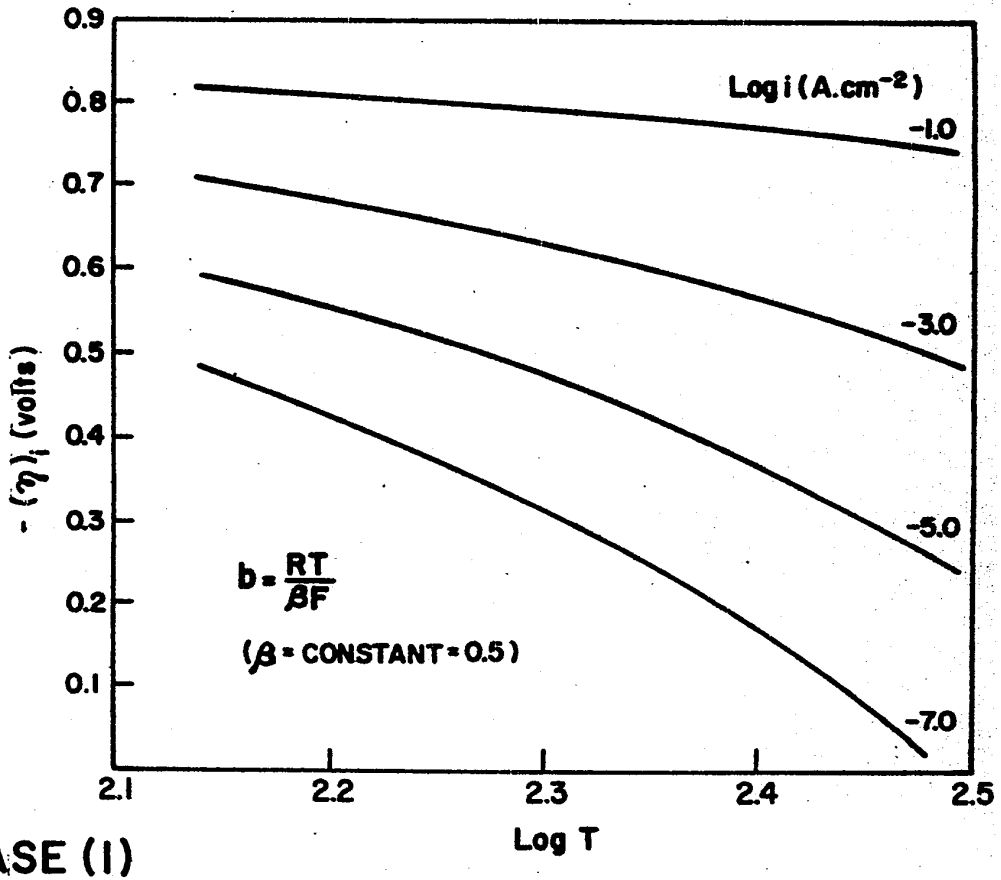
Log i (A.cm⁻²)
-1.0
-3.0
-5.0
-7.0
b = RT/βF
(β = CONSTANT = 0.5)
- (η)i (volts)
0.9
0.8
0.7
0.6
0.5
0.4
0.3
0.2
0.1
2.1
2.2
2.3
2.4
2.5
Log T

CASE (I)

Figure 60

Plots of $(\eta)_i$ vs. T and log T for case (2).

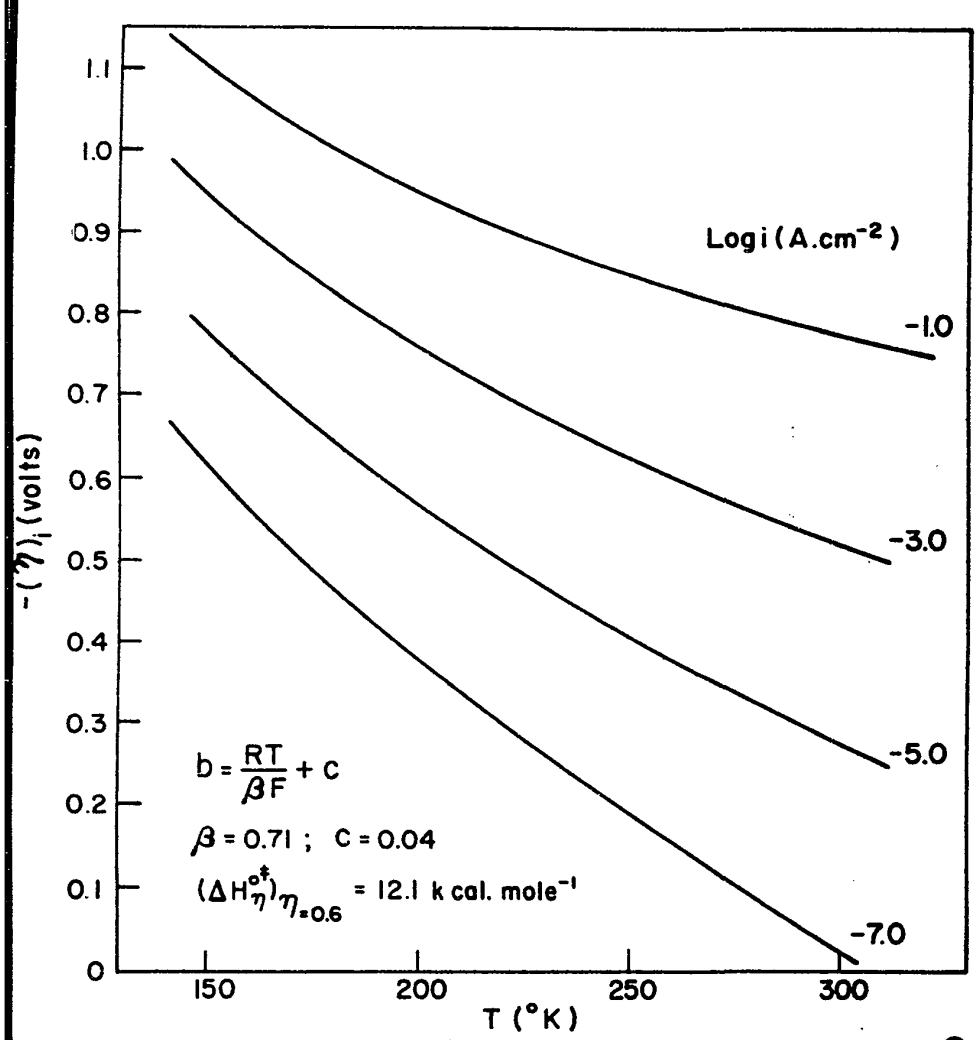
Log i (A.cm^{-2})
-1.0
-3.0
-5.0
-7.0
$b = \frac{RT}{\beta F} + c$
$\beta = 0.71$; $c = 0.04$
$(\Delta H^{o\ddagger}_{\eta})_{\eta=0.6}$ = 12.1 k cal. mole^{-1}
$-(\eta)_i$ (volts)
T (°K)
0
0.1
0.2
0.3
0.4
0.5
0.6
0.7
0.8
0.9
1.0
1.1
150
200
250
300

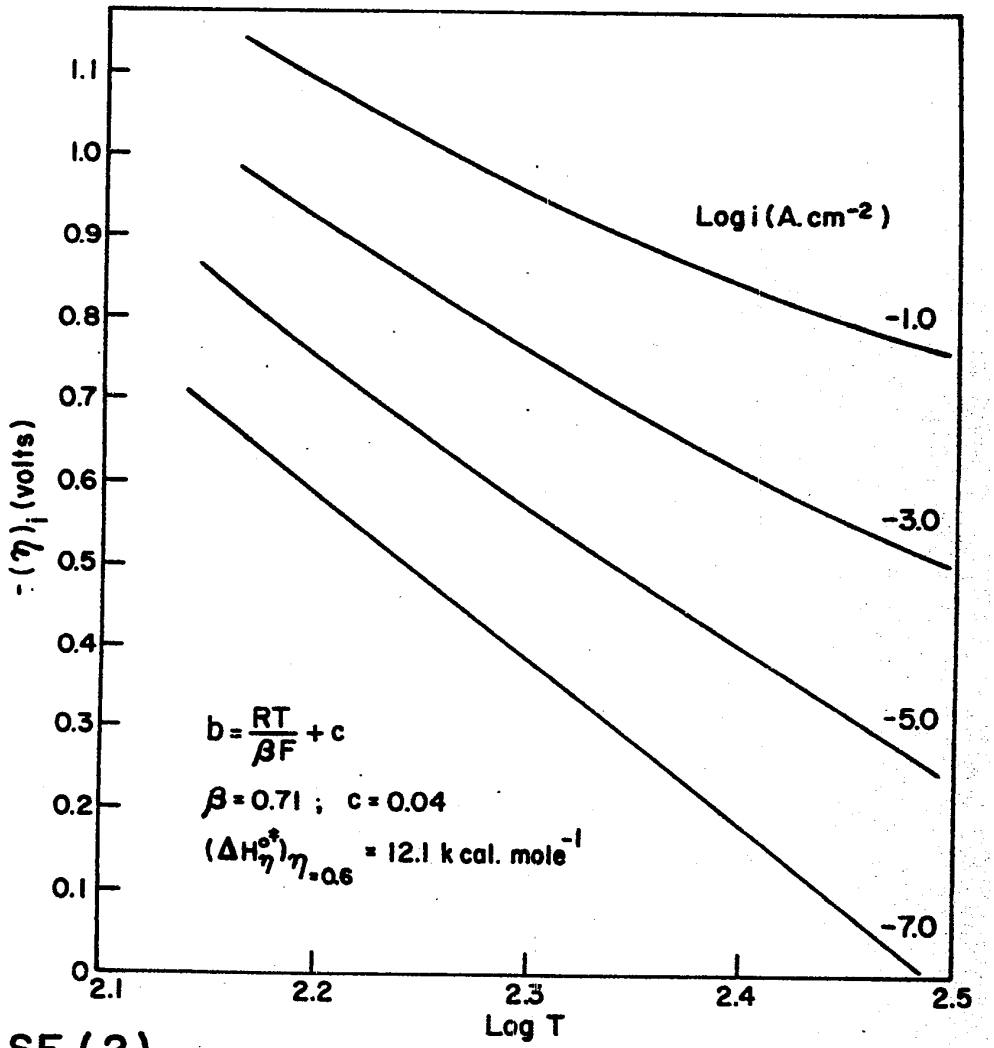
Log i (A.cm^{-2})
-1.0
-3.0
-5.0
-7.0
$b = \frac{RT}{\beta F} + c$
$\beta = 0.71$; $c = 0.04$
$(\Delta H^{o\ddagger}_{\eta})_{\eta=0.6}$ = 12.1 k cal. mole^{-1}
$-(\eta)_i$ (volts)
Log T
0
0.1
0.2
0.3
0.4
0.5
0.6
0.7
0.8
0.9
1.0
1.1
2.1
2.2
2.3
2.4
2.5

CASE (2)

The results derived from plots of log i_o vs. 1/T agree, of course, for all cases since here $\eta = 0$ (log i = log i_o at $\eta = 0$) and thus the form of b does not enter into the calculations (see lowest lines for $\eta = 0$ in Figure 58).

Case 3. b = const. = 0.120 volts.

Here β is changing with temperature so that $b \neq f(T)$. Thus $b = RT/\beta F$ with $\beta = kT$.

The $(\log i)_\eta$ vs. 1/T plot shown in Figure 58 will obviously give the assumed reference value of 10.0 kcal. mole^{-1} at all η values and hence $\Delta H_\eta^{o\ddagger}$ is independent of η. When values of $\Delta H_\eta^{o\ddagger}$ are, however, evaluated from the plots $(\eta)_i$ vs. T or log T (Figure 61), they are found to be a function of temperature (or c.d.) as follows by taking tangents to the curves in Figure 61. Values of $\Delta H_{\eta=0.8}^{o\ddagger}$, calculated for various c.d. values, are found to vary by about 1 kcal. mole^{-1} when derived by methods C and D. Thus, from Figure 61, $\Delta H_{\eta=0.8}^{o\ddagger}$ = 9.6-10.6 kcal. mole^{-1} over 7 decades of i.

Case 4. b increases with decreasing T according to a relation of the form $b = c' - 2.3RT/\beta F$ where $\beta = 0.5$ and constant. It is shown in the present work that this case is encountered experimentally. The plots of $(\log i)_\eta$ vs. 1/T for Case 4 are shown in Figure 58 and, except for $\eta = 0$, the Arrhenius plots are curved in a manner not unlike that observed experimentally at Pt and the low c.d. region at Ni. The curvature increases with increasing η. From Figure 62, it can be shown that $\Delta H_\eta^{o\ddagger}$ increases linearly with η for a given value of T, the rate of increase becoming greater at higher temperatures. This is to be contrasted with the results for the conventional Case 1, also shown in Figure 62.

In Figure 63, b is shown comparatively as a function T for Cases 1 to 4, reflecting the various cases encountered experimentally (Chapter IV) for the variation of b with T.

Figure 61

Plots of $(\eta)_i$ vs. T and log T for case (3).

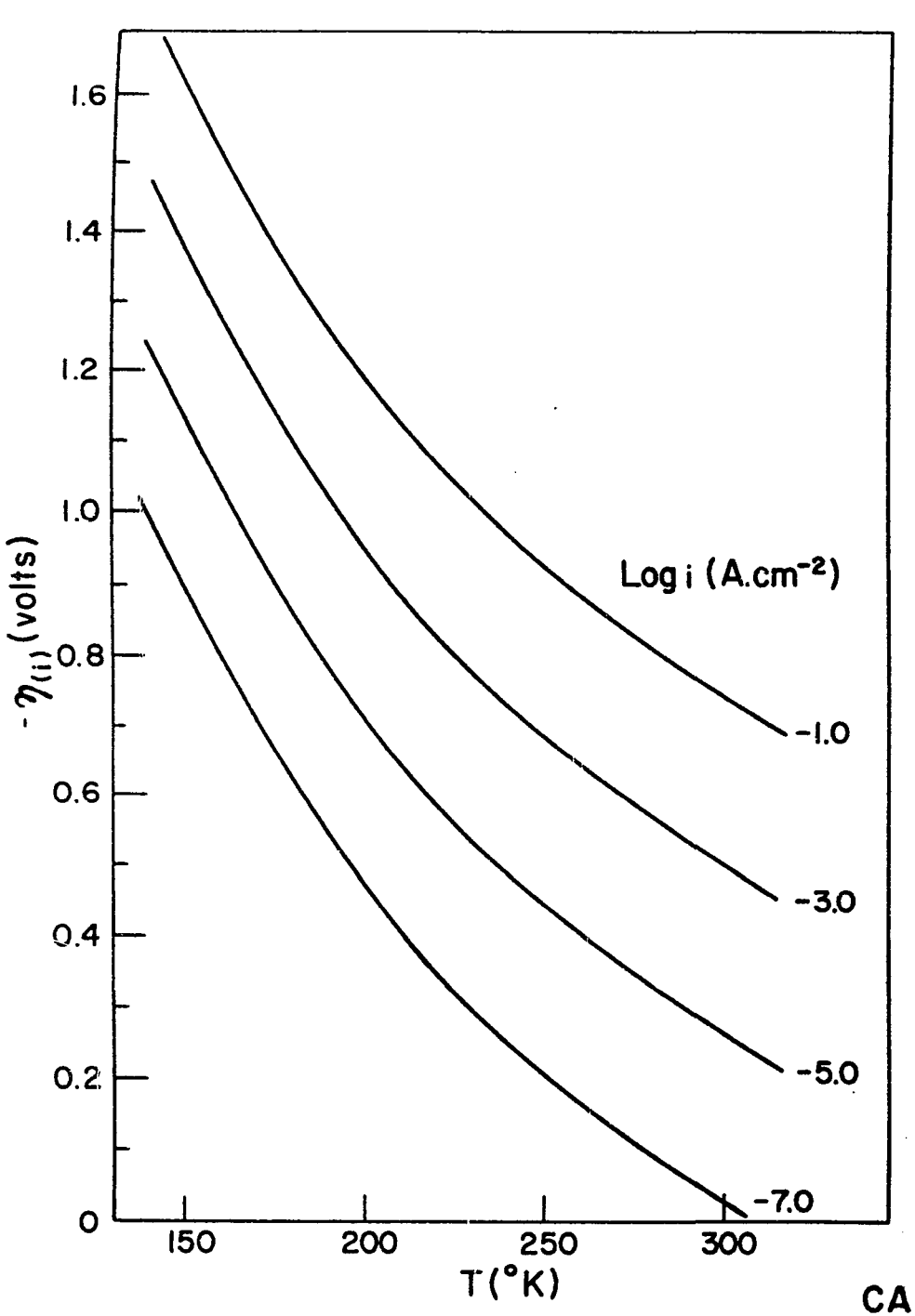
1.6
1.4
1.2
1.0
0.8
0.6
0.4
0.2
0
$-\eta_{(i)}$ (volts)
Log i (A.cm^{-2})
-1.0
-3.0
-5.0
-7.0
150
200
250
300
T(°K)

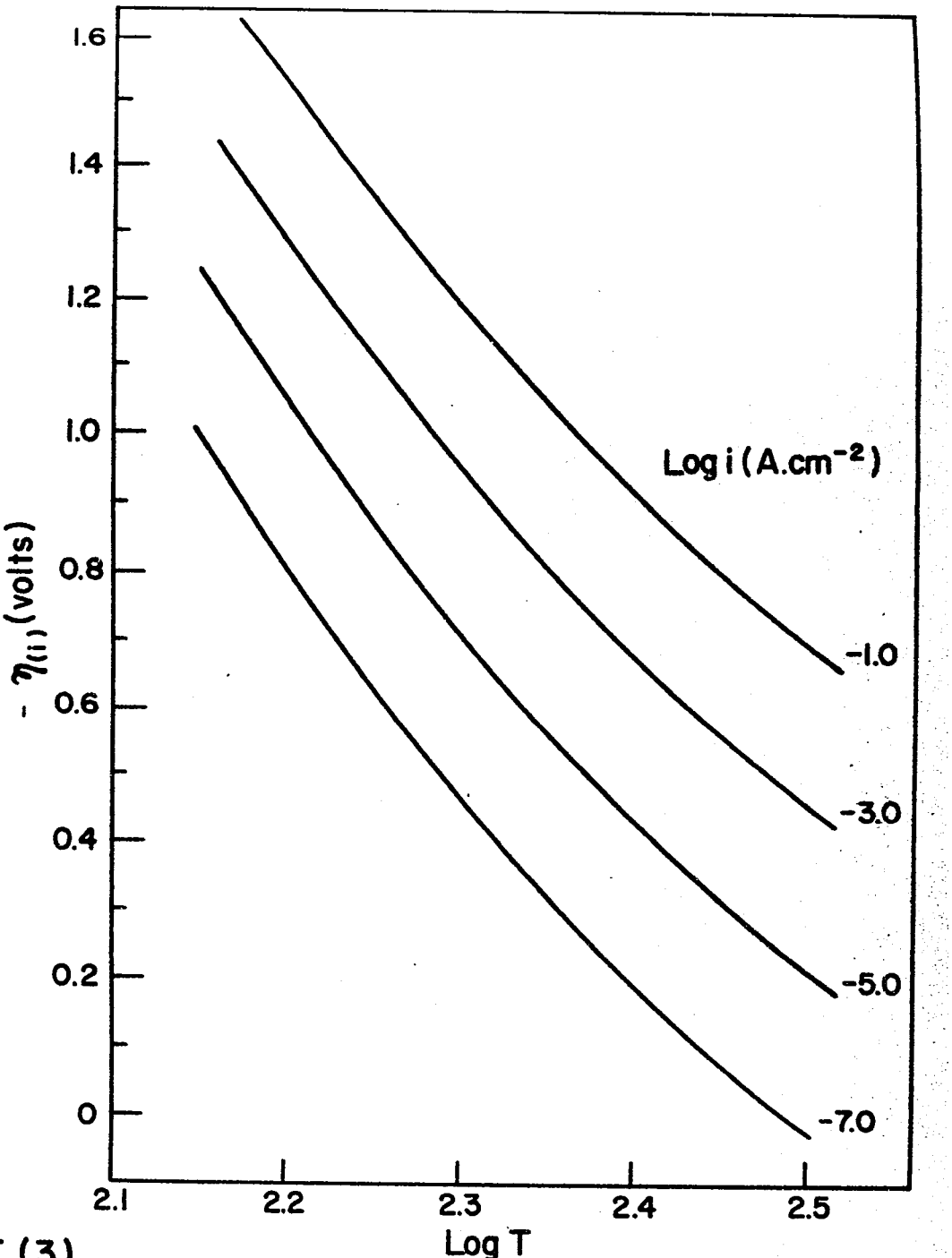
1.6
1.4
1.2
1.0
0.8
0.6
0.4
0.2
0
$-\eta_{(i)}$ (volts)
Log i (A.cm^{-2})
-1.0
-3.0
-5.0
-7.0
2.1
2.2
2.3
2.4
2.5
Log T

CASE (3)

Figure 62

Dependence of $\Delta H_{\eta}^{o\ddagger}$ upon η for cases (1) and (4).

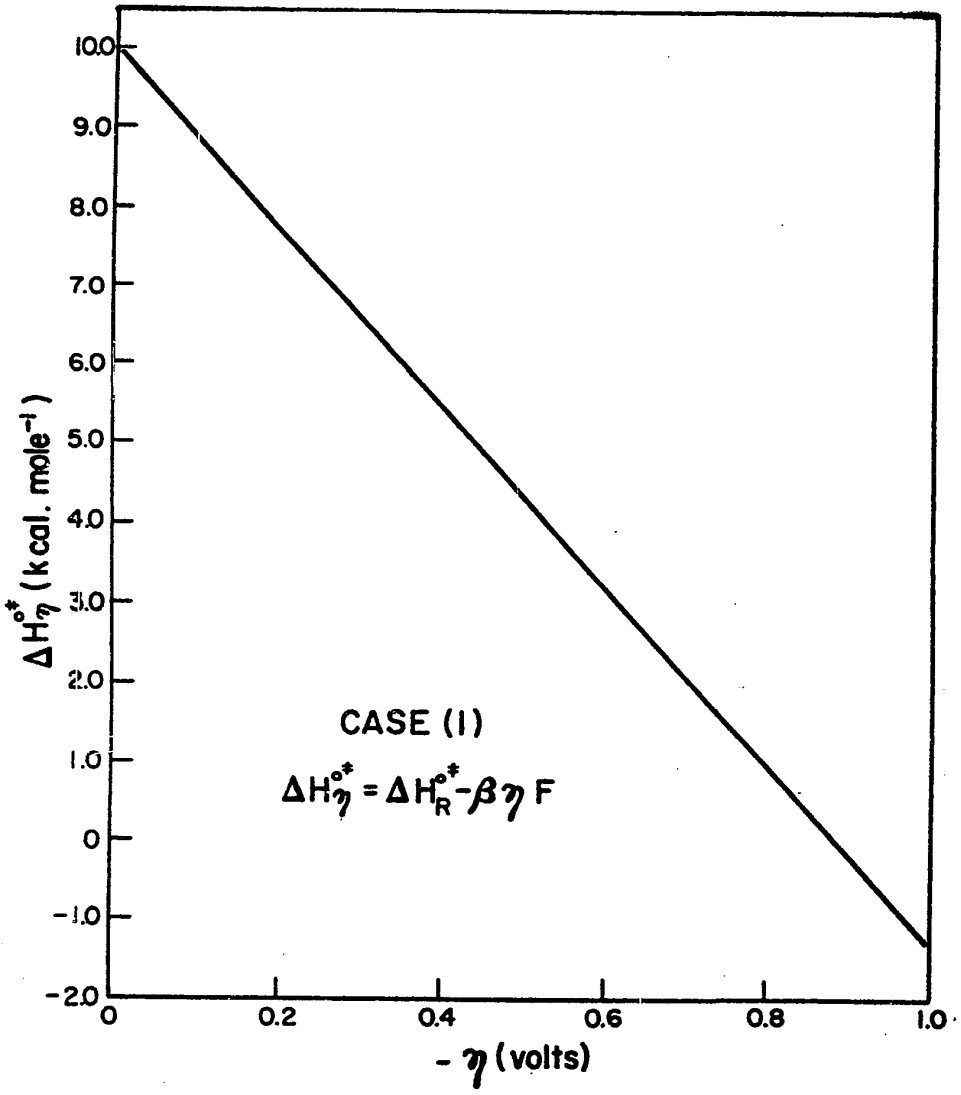
10.0
9.0
8.0
7.0
6.0
5.0
4.0
3.0
2.0
1.0
0
-1.0
-2.0
ΔH_η^{o*} (k cal. mole^{-1})
CASE (1)
$\Delta H_\eta^{o*} = \Delta H_R^{o*} - \beta \eta F$
0
0.2
0.4
0.6
0.8
1.0
$-\eta$ (volts)

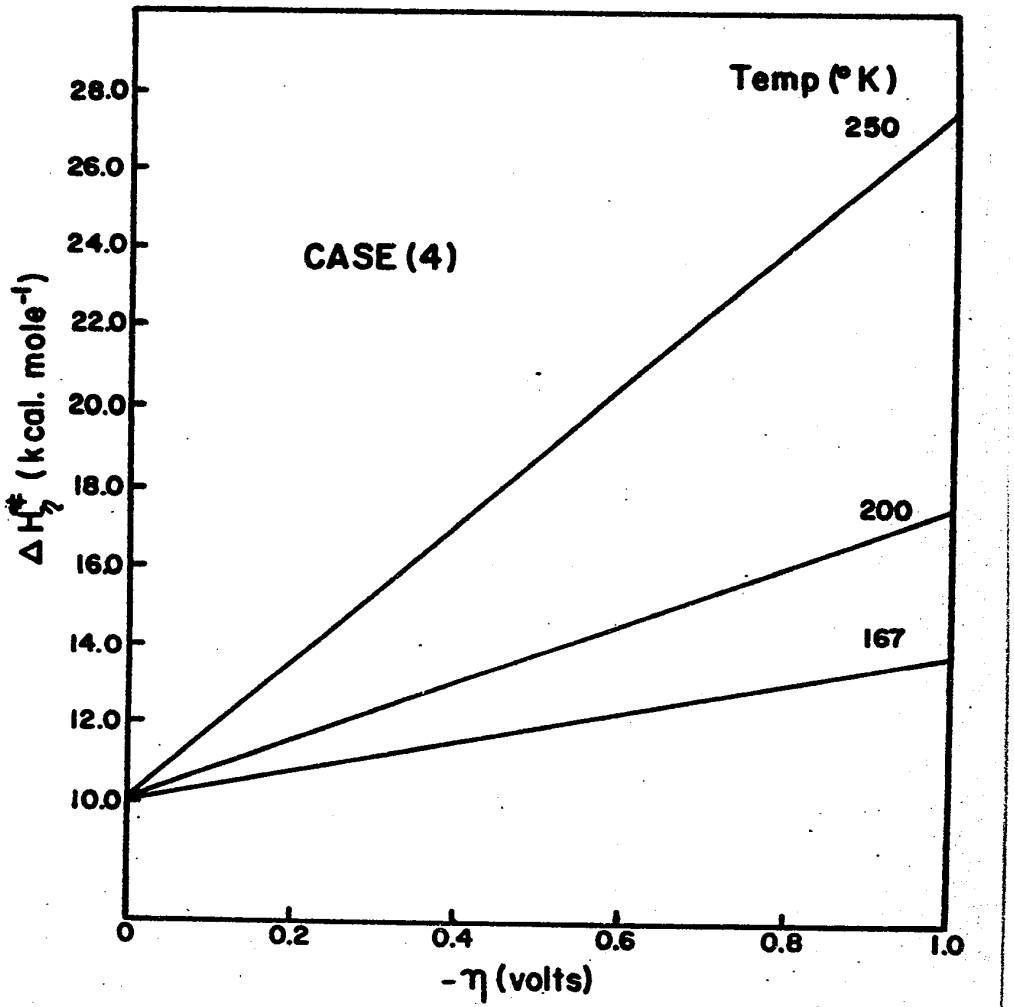
28.0
26.0
24.0
22.0
20.0
18.0
16.0
14.0
12.0
10.0
ΔH_η^{*} (k cal. mole^{-1})
Temp (°K)
250
CASE (4)
200
167
0
0.2
0.4
0.6
0.8
1.0
$-\eta$ (volts)

Figure 63

Comparative plots for b as a function of temperature for the various cases considered and encountered experimentally.

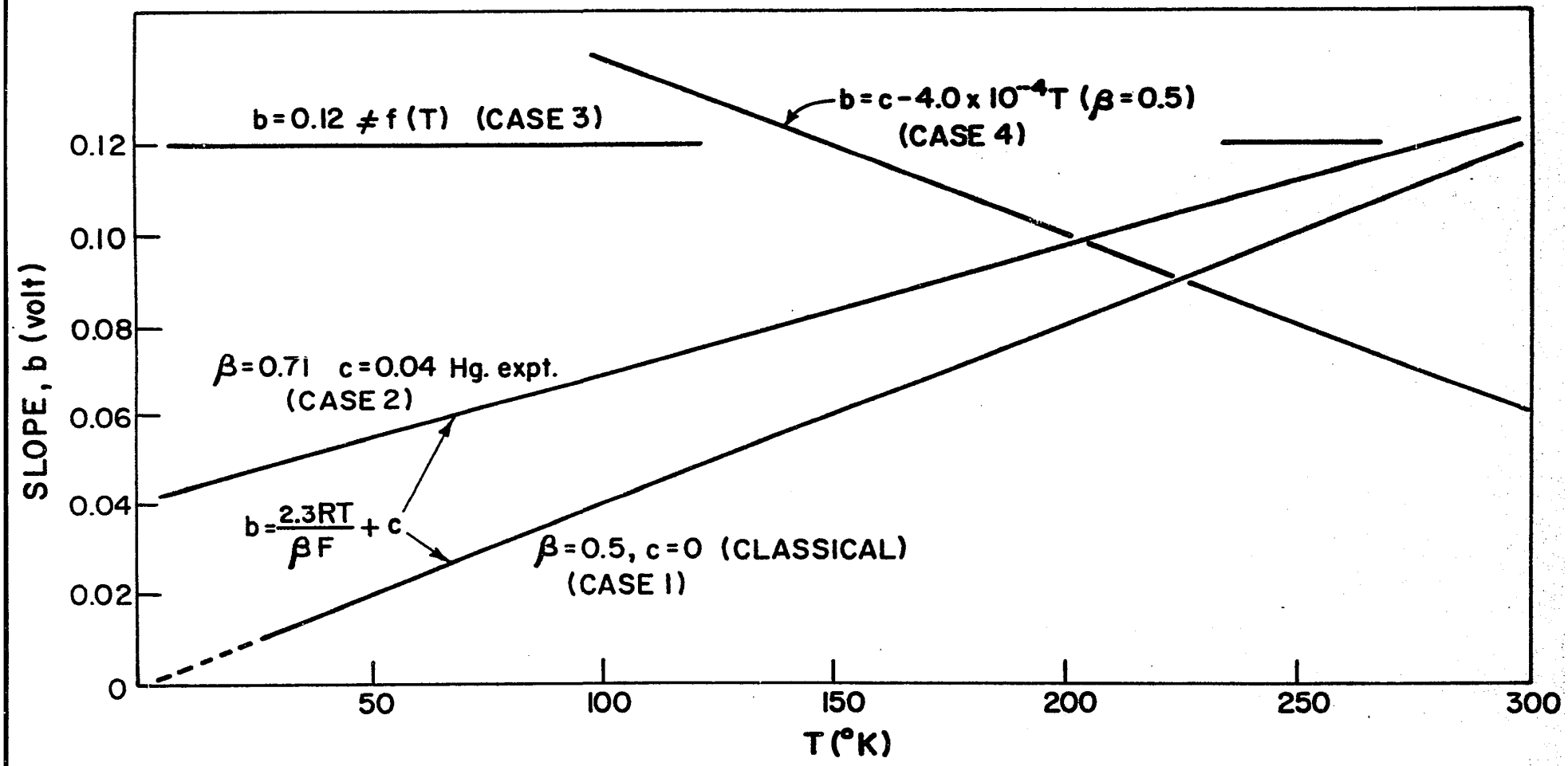
b = 0.12 ≠ f (T) (CASE 3)
b = c − 4.0 x 10⁻⁴T (β = 0.5)
(CASE 4)
β = 0.71 c = 0.04 Hg. expt.
(CASE 2)
b = 2.3RT/βF + c
β = 0.5, c = 0 (CLASSICAL)
(CASE 1)
SLOPE, b (volt)
0.12
0.10
0.08
0.06
0.04
0.02
0
50
100
150
200
250
300
T (°K)

(iii) Analytical Treatment

The above treatment based on numerical calculations leads to a number of interesting conclusions regarding the variation of $\Delta H_R^{o\ddagger}$ with η and T, so that further analytical exploration of this matter seems justified in order to examine the relation between the true and apparent heats of activation for cases where $b \neq RT/\beta F$.

Assuming the general relation

$$\ln i = \ln i_o + \eta / b \quad \text{(cf. equation [49])} \qquad [84]$$

and taking first the conventional Case 1, namely when $b = RT/\beta F$ and $\beta \neq f(T)$, which has previously been assumed to be generally applicable, the well known results (62, 68) given below are obtained:

$$(1) \quad \frac{d \ln i_o}{d\, 1/T} = -\frac{1}{R}[\Delta W^{o\ddagger} - \beta \Delta H^o] = -\Delta H_R^{o\ddagger}/R \quad \text{(cf. equation [48])} \qquad [85]$$

where ΔH^o is the experimentally undeterminable enthalpy change in the H_2/H^+ half-cell reaction and $\Delta W^{o\ddagger}$ is the true (but also experimentally inaccessible) heat of activation at zero metal-solution potential, i.e., $\phi = 0$.

$$(2) \quad \left[\frac{\partial \eta}{\partial T}\right]_i = -\frac{1}{\beta F T}[\Delta H_\eta^{o\ddagger}] = -\frac{1}{\beta F T}[\Delta H_R^{o\ddagger} - \beta \eta F] \text{ (cf. [58])} \qquad [86]$$

and

$$(3) \quad -\Delta H_R^{o\ddagger} = \beta F \left[\frac{\partial \eta}{\partial T}\right]_i - \beta \eta F \qquad [87]$$

For a number of the experimentally investigated cases, it has been shown that $b = \frac{RT}{\beta F} + c$, so that

$$\ln i = \ln i_o + \eta / \left[\frac{RT}{\beta F} + c\right] \qquad [88]$$

which gives, upon differentiation,

$$\left[\frac{\partial \eta}{\partial T}\right]_i = \frac{RT}{\beta F} \ln \frac{i}{i_o} - \left[\frac{RT}{\beta F} + c\right]\left[\frac{d \ln i_o}{dT}\right] \qquad [89]$$

so that substituting for $\ln (i/i_o)$,

$$\left[\frac{\partial \eta}{\partial T}\right]_i = \left[\frac{R}{RT + \beta cF}\right]\eta - \left[\frac{RT}{\beta F} + c\right]\left[\frac{d \ln i_o}{dT}\right] \qquad [90]$$

Expressing $\ln i_o$ in terms of a combined constant k, the true heat of activation $\Delta W^{o\ddagger}$ at $\phi = 0$ and the metal-solution p. d. ϕ_r at the reversible potential,

$$\ln i_o = \ln k - \frac{\Delta W^{o\ddagger}}{RT} + \phi_r \Big/ \left[\frac{RT}{\beta F} + c\right] \qquad [91]$$

Then differentiating w. r. t. T and noting $\phi_r F = -\Delta G^o$ and $\frac{F d\phi_r}{dT} = \Delta S^o$ for the hydrogen half-cell reaction,

$$H^+ + e \rightarrow 1/2\, H_2 ,$$

$$\frac{d \ln i_o}{dT} = \frac{\Delta W^{o\ddagger}}{RT^2} + \frac{\beta R}{(RT + \beta cF)^2}[\Delta G^o] + \frac{\beta}{(RT + \beta cF)}[\Delta S^o] \qquad [92]$$

which upon rearrangement gives

$$\frac{d \ln i_o}{dT} = \frac{\Delta W^{o\ddagger}}{RT^2} + \frac{1}{[RT + \beta cF]^2}[\beta R \Delta H^o + \beta^2 cF \Delta S^o] \qquad [93]$$

or

$$\frac{d \ln i_o}{d\, 1/T} = \frac{\Delta W^{o\ddagger}}{R} - \frac{\beta T^2}{(RT + \beta cF)}\left[\frac{R \Delta G^o}{RT + \beta cF} + \Delta S^o\right] \qquad [94]$$

and enables equation [85] to be recovered in the conventional case where $\beta cF = 0$.

Returning to the evaluation of $[\partial\eta/\partial T]_i$, $d \ln i_o/dT$ can now be substituted in equation [90] giving, after elementary algebra,

$$\left[\frac{\partial\eta}{\partial T}\right]_i \doteq \left[\frac{R}{RT+\beta cF}\right]\eta - \left[\frac{RT+\beta cF}{\beta F}\right]\Delta W^{o\ddagger} - \frac{1}{\beta F[RT+\beta cF]}[\beta R\Delta H^o+\beta^2 cF\Delta S^o] \qquad [95]$$

It is clear that neither of the derivatives $d \ln i_o/dT$ nor $d \ln i_o/d(1/T)$ can give directly even an apparent heat of activation which is a simple sum of $\Delta W^{o\ddagger}$ and $\beta\Delta H^o$ as is the case (equation [85]) when b is simply $RT/\beta F$. Similarly, $(\partial\eta/\partial T)_i$ is a complex quantity not simply related to $\Delta H^{o\ddagger}_\eta$ by equation [86] through $\beta\eta F$ nor involving a sum of ΔG^o and $T\Delta S^o$ terms that can be expressed in terms of ΔH^o with $\Delta W^{o\ddagger}$. Thus when b is not simply given by the quantity $RT/\beta F$, as is evidently the case experimentally under most conditions (refs. 104-106 and the present work), it cannot be expected that $\Delta H^{o\ddagger}_R$ from equation [85] based on $d \ln i_o/d(1/T)$ will be identical with the quantity evaluated from $-\beta FT\left[\frac{\partial\eta}{\partial T}\right]_i$ by adding $\beta\eta F$ (equation [86]).

Bockris and Matthews (51) have again (cf. 135) referred to the question of incompatibility of activation energies of ca. 11 kcal. $mole^{-1}$ observed at mercury in alcoholic solutions with values of $\eta > 1$ V (since $\beta\eta F$ is then already ca. 11.5 kcal. $mole^{-1}$). However, this value of $\Delta H^{o\ddagger}_R$ seems well authenticated (70,135) and is also found from the results of Bockris and Parsons (69). This difficulty is only an apparent one, of course, and is connected as has been pointed out elsewhere in discussion (135) with the question of temperature dependence of α or β, or the form of b as f(T) discussed above; a general explanation was given previously (135).

From the above calculations which are applicable to the case of Hg since b is experimentally of the form $(RT/\beta F) + c$ (with $c = 0.04$), it becomes clear how conclusions about barrier height cannot under any circumstances be made simply on the basis of the experimental derivatives $(\partial\eta/\partial T)_i$ or $d \ln i_o/d(1/T)$, both of which evidently give complex quantities not simply related to either the apparent activation energy, $\Delta H_R^{o\ddagger}$ at $\eta = 0$ or the true activation energy $\Delta W^{o\ddagger}$ at zero metal-solution p.d., i.e., at $\phi = 0$.

While some of the experimental results involve a Tafel slope of the form $b = \frac{RT}{\beta F} + c$, the possibility that $b = RT/\beta F$ but with β varying with T must be recognized as discussed earlier. This approach leads (cf. 135) to the following result: the apparent activation energy is then simply (contrast equation [94])

$$\Delta H_R^{o\ddagger} + \beta F d\phi_r/d\,1/T + F\phi_r/T[d\beta/d\,1/T] \qquad [96]$$

which differs from the barrier height at $\eta = 0$ by

$$(\beta F/T)d\phi_r/d\,1/T + F\phi_r/T\,[d\beta/d\,1/T] \qquad [97]$$

(iv) Coverage Effects in $\Delta H_R^{o\ddagger}$

In addition to the fact that the measured value of $\Delta H_R^{o\ddagger}$ is an apparent value on account of the variation of the reference electrode potential and of b with temperature, a further complication (as mentioned earlier in Chapter II) arises with processes involving an adsorbed intermediate. In such cases, the coverage Θ, e.g. by H atoms, can vary with temperature and give a contribution to the apparent heat of activation. The significance of Θ in the kinetic expressions for the exchange current was discussed by Devanathan and Selvaratnam (94).

For the kinetics at the reversible potential,

$$i_o = k_1 C_{H^+} (1-\Theta_H) \exp[-\Delta G_1^{o\ddagger}/RT] \exp[-\phi_r/b] \qquad [98]$$

for the h. e. r. proceeding by a discharge step, $\Delta G_1^{o\ddagger}$ and ϕ_r are the free energy of activation (corresponding to $\Delta W^{o\ddagger}$) and the metal-solution p. d. at the reversible potential. Alternatively, for an electrochemical H atom desorption step,

$$i_o = k_2 \Theta_H C_{H^+} \exp[-\Delta G_2^{o\ddagger}/RT] \exp[-\phi_r/b] \qquad [99]$$

or for an atom recombination step

$$i_o = k_3 \Theta_H^2 \exp[-\Delta G_3^{o\ddagger}/RT] \qquad [100]$$

where "k" terms are combinations of constants but not including the free energies of activation. In any of these cases, it is clear that $d \ln i_o / d\frac{1}{T}$ will involve not only the $\Delta W^{o\ddagger}$ terms in $\Delta G^{o\ddagger}$ and $d \phi_r / d\frac{1}{T}$ but also, depending on the type of mechanism involved, $d \ln (1 - \Theta_H)/d\frac{1}{T}$ or $d \ln \Theta_H / d\frac{1}{T}$. For a discharge process occurring at low coverage by H, (i.e. $1 - \Theta_H \rightarrow 1$) no significant additional effect will arise. For the electrochemical desorption or recombination steps, however, (except at $\Theta_H \rightarrow 1$) Θ_H can obviously vary with temperature and in general Θ_H has the form

$$\frac{K_1 C_{H^+} \exp[-\phi_r F/RT]}{1 + K_1 C_{H^+} \exp[-\phi_r F/RT]} \qquad [101]$$

for quasi-equilibrium in the proton discharge step [1] at a "Langmuir" surface; here K_1 is the "chemical part" of the electrochemical equilibrium constant at the reversible potential ϕ_r and is related to the standard free energy of adsorption of H, ΔG_H^o, in the usual way. The apparent activation energy will now be a function of the variation

of Θ_H with T and of ϕ_r with T but in the kinetic term exp $-\phi_r/b$ and in the quasi-equilibrium expression for Θ_H. The "chemical part" of the variation of Θ_H with T obviously arises from the variation of K_1 with T, i.e., from the heat of adsorption of H. Limitingly, for low Θ_H, at the reversible potential ϕ_r

$$\Theta_H = K_1 C_{H^+} \exp[-\phi_r F/RT]$$

$$= C_H + \exp[-\Delta G^\circ_H/RT] \exp[-\phi_r F/RT] \qquad [102]$$

or

$$\ln \Theta_H = \ln C_{H^+} - \Delta H^\circ_H/RT + \Delta S^\circ_H/R - \phi_r F/RT \qquad [103]$$

Then

$$d \ln \Theta_H/d\frac{1}{T} = -\Delta H^\circ_H/R - \frac{F}{RT} d\phi_r/d\frac{1}{T} - \frac{F\phi_r}{R} \qquad [104]$$

The latter two terms are the ones that also arise in the evaluation of the true activation energy of any electrode process and, as in the case considered above, are together equal to 1/R times ΔH°, the heat change in the half-cell process corresponding to the overall reaction $H_3O^+ + e \rightarrow H_2O + \frac{1}{2} H_2$; the latter heat differs from ΔH°_H since that term refers to the electrochemical discharge and adsorption partial process:

$$H_3O^+ + M + e \rightarrow H_2O + MH_{ads}$$

Hence

$$d \ln \Theta_H/d\frac{1}{T} = -\Delta H^\circ_H/R + \bar{\Delta H}^\circ/R \qquad [105]$$

Now, in the absence of any variation of coverage terms with temperature

$$d \ln i_o / d\frac{1}{T} = -(\Delta W^{o\ddagger}/R - \beta \Delta H^o/R) = -\Delta H_R^{o\ddagger}$$

so that when the variation of Θ_H with temperature is allowed for in equation [98], for example,

$$d \ln i_o / d\frac{1}{T} = \frac{1}{R}[-\Delta W^{o\ddagger} + \beta \Delta H^o - \Delta H_H^o + \Delta H^o] \qquad [106]$$

$$= -\frac{1}{R}[\Delta W^{o\ddagger} + \Delta H_H^o - (1+\beta)\Delta H^o] \qquad [107]$$

It is evident that $\Delta H_H^o - \Delta H^o$ is simply the energy of adsorption ΔH_{ads}^o of H from half a mole of H_2 so that

$$d \ln i_o / d(1/T) = -\frac{1}{R}[\Delta W^{o\ddagger} + \Delta H_{ads}^o - \beta \Delta H^o]$$

$$= -\frac{1}{R}[\Delta H_R^{o\ddagger} + \Delta H_{ads}^o] \qquad [108]$$

Since ΔH_{ads}^o is usually a negative quantity, the overall apparent heat of activation could be negative when $\Delta H_R^{o\ddagger} + \Delta H_{ads}^o < 0$. Such a case has been observed for Pb in the present work (see Figure 40(a)).

(v) Forms of Electrochemical Arrhenius Plots for the H. E. R.

Plots of log k vs. 1/T for the rate constant of a reaction, particularly one involving proton transfer, can deviate from linearity on account of (a) changes of solvent structure and hydrogen bonding with temperature; (b) proton tunneling and (c) changes of mechanism. The first two factors generally tend to produce opposite directions of deviation from linearity in the Arrhenius plots. These variations of log k vs. 1/T, some of which have been observed in this work, are shown schematically in Figure 64. Here, an attempt is made to interpret qualitatively the form of the observed Arrhenius plots reported for Ni, Pt, Pb and Cd in Chapter IV of this thesis.

Figure 64

Schematic representation of various forms of Arrhenius plots.

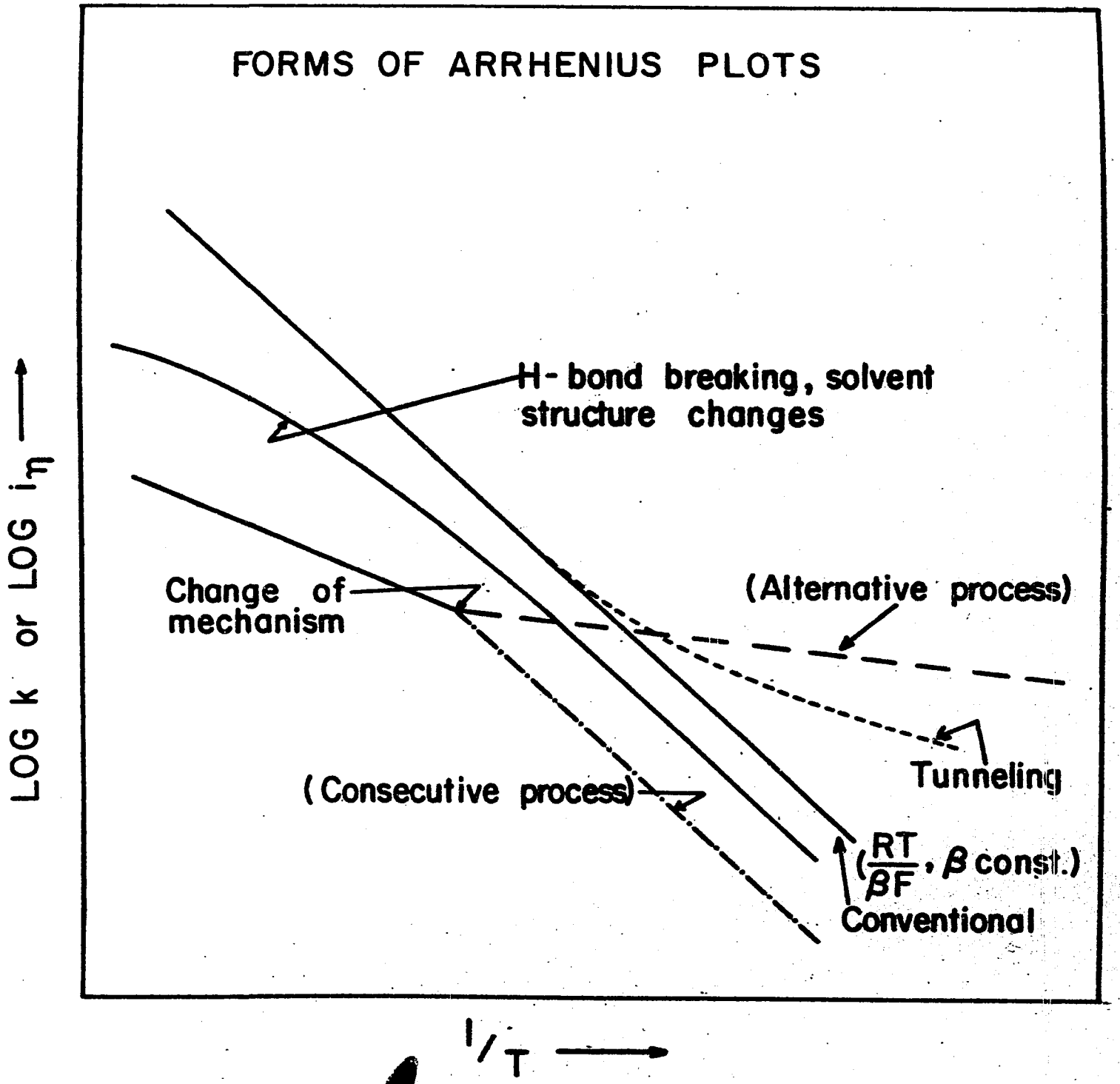
FORMS OF ARRHENIUS PLOTS
LOG k or LOG i_η ⟶
H-bond breaking, solvent structure changes
Change of mechanism
(Alternative process)
Tunneling
(Consecutive process)
$(\frac{RT}{\beta F}, \beta$ const.)
Conventional
$1/T$ ⟶

For the high c.d. region at Ni (Figures 38 and 46), $d \log i_o / d\, 1/T$ is progressively smaller at low temperatures than at high, i.e., the relation shows "concave" curvature at the low temperature end. Also the b values for this region, after falling initially with decreasing T, begin to increase again at the lowest temperatures ($< -75^{\circ}C$). Both these aspects of the low temperature behavior are characteristic of participation of proton tunneling in parallel with the classical transfer process. However, it has been mentioned earlier that the present work also shows that similar effects arise in the deuterium reaction at Ni (Figure 46) and furthermore the Tafel slopes for the d.e.r. are higher, rather than lower (cf. refs. 40, 47, 48, 49), than those of the h.e.r. Hence, the low temperature behavior in the $\log i_o$ vs. $1/T$ plots cannot be satisfactorily explained in terms of proton tunneling. It must therefore be supposed that the effect arises for reasons such as preferred orientation of solvent at the lower temperatures; solvent structure changes it seems, would lead to enthalpy effects opposite to those observed here at low temperatures, i.e., $\Delta H_R^{o\ddagger}$ would tend to be larger rather than smaller.

The effects of anion adsorption are obviously of importance here, as they are in determining the Tafel slopes (see Chapter V, Section b). Generally, at low temperatures, anion adsorption is found to be greater. For the upper lines at Ni, however, the role of anion adsorption effects must be presumed absent if the change of Tafel slope is attributed to desorption of anions at high η values (cf. the results for the $HClO_4$ solutions). It is to be noted also that as the temperature is lowered, the potential corresponding to the change in slope is increased; this is as expected if anion desorption is involved.

Under these circumstances, since tunneling has been discounted by the earlier argument, it may be suggested that the

anomalous Arrhenius plots of Figures 38 and 46 arise because of a temperature dependent activation entropy $\Delta S^{o\ddagger}$ (cf. Chapter V, Section d) or frequency factor term of the type discussed by Caldin and Harbron (66). For the discharge step, $\Delta S^{o\ddagger}$ will be expected to be positive for charge neutralization and release of solvent electrostriction (cf. the positive [corrected]* volume of activation (57,136)), so that with increasing solvent-structure in the interphase as temperature is lowered, $\Delta S^{o\ddagger}$ may be expected to become relatively more positive and the rate relatively less decreased. This would give the correct form of curvature for the plots of Figures 38 and 46.

A similar effect could also arise if at lower temperatures the methanol solvent becomes more strongly adsorbed resulting in weakening of H adsorption. In the step $H_3O^+ + MH_{ads} + e \rightarrow H_2$, this could lead to decreasing $\Delta H_R^{o\ddagger}$.

It may be anticipated that the behavior at Pt and Ni will be complicated by the temperature dependence of H coverage, Θ_H, discussed above (Chapter V, Section d) since it is well-known that the energy of adsorption of H (in equation [79]) can vary with Θ_H and also be dependent on anion adsorption (113). The combination of these effects could be complex and lead to the observed temperature dependence of d log i_o/d 1/T for Pt and the lower Tafel regions at Ni where Cl^- adsorption effects are apparently important (cf. Chapter V, Section c (ii)-2).

---

*It can be shown, as pointed out earlier by Conway (100), that the true volume of activation at the reversible potential is $(\partial \ln i_o/\partial p)_{\eta=0, C_{H^+}} = -1/RT\,(\Delta V^{\ddagger} - \beta \Delta V_R)$ where ΔV_R is the volume change in the single electrode process $2H_3O^+ + 2e \rightleftharpoons 2H_2O + H_2$ at equilibrium. Thus the true volume of activation, in analogy with the true electrochemical heat of activation (see Chapter II), is not experimentally accessible so that only an apparent value for the volume of activation is obtainable (cf. ref. 136).

The log i_o vs. 1/T plots for Pt and for the low c.d. region at Ni (Figures 39(a) and 38) exhibit curvature at the high temperature end, an effect which becomes more pronounced at the higher η values (see Figures 42 and 43(a)). This appears to be due to the progressive desorption (82, 83) of Cl^- which occurs at the higher temperatures and larger η values. Such an effect is consistent with the high values of Tafel slope b and the anomalous temperature dependence of the b values (as discussed earlier in Sections c and d of this Chapter). At Pt, for increasing temperatures in the cycle of measurements, irreversible adsorption of Cl^- ion indeed seems to be indicated (compare the two diagrams of Figure 39).

The Arrhenius plots for Pb and Cd (Figures 40(a) and 40(b) may also be interpreted in terms of specific adsorption of Cl^- ions and the apparent negative activation energy for Pb (Figure 40(a)) could receive an explanation in terms of temperature-dependent H coverage as mentioned earlier.

f) Some Problems with the Involvement of Solvated Electrons in the H.E.R.

(i) General

The hydrated electron is well known (137) as a transient intermediate in radiolysis of water and photolysis of certain aqueous solutions and the kinetics and mechanisms of its reactions have been extensively studied and reviewed (137). More recently, a number of suggestions have been made (55-58, 80, 100, 136, 139, 140) (and discussed in relation to various experiments (55-57, 140)) that hydrated electrons are the primary entities involved in cathodic hydrogen evolution and metal dissolution on open-circuit (corrosion processes). See Chapter I, Section h. From an electrochemical kinetic and

thermodynamic point of view, however, there are a number of serious difficulties which arise in these suggestions. It is the purpose of this Section of the thesis to give some careful consideration to these problems from an electrochemical point of view, since the mechanisms of cathodic hydrogen evolution involving the hydrated electron which have recently been proposed differ radically from all mechanisms considered previously (until about 1965) in at least one thousand papers published since the time of Tafel's original work in 1905. In some of these papers, particularly those published in recent years, is to be found certain critical evidence indicating involvement of protons directly discharged at the metal.

That hydrated electrons are the precursors of cathodically evolved hydrogen in electrochemical hydrogen production in aqueous solutions seems to have been first suggested by Walker (55, 56) as a general basis for cathodic hydrogen evolution and indicated experimentally by him (55, 56) under certain conditions (see below) by means of an ingenious multiple reflectance light absorption experiment, and by chemical experiments involving the use of scavengers (55, 56). (cf. Chapter I, p. 43). Photo-electrochemical emission of electrons at mercury electrodes was studied earlier by Barker (141) and in related work by Delahay (142) but under these conditions of photoexcitation the difficulties associated with the suggestions of refs. (55-58, 80, 100, 136, 139) are not involved. The deduction of a mechanism of e^-_{aq} formation from the kinetic studies of Hills and Kinnibrugh (57) on the hydrogen evolution reaction at high pressures are of interest but alternative explanations of the evaluated negative volume of activation which led to their mechanistic conclusions have already been offered (100).

(ii) Difficulties with e^-_{aq} Involvement in the H. E. R.

1. The first is a quasi-thermodynamic one: the standard potential for the hydrated electron e^-_{aq} on the hydrogen scale has been calculated from kinetic data to be ca. -2.67 V (143, 144) yet hydrogen is easily evolved on the more catalytic metals at appreciable rates already at 0.1 - 0.2 V cathodic to the reversible hydrogen potential. If the cathodic process were (cf. 55, 56)

$$M(e) + H_2O \rightarrow e^-_{aq} \qquad \text{I}$$

$$e^-_{aq} + H_2O \rightarrow H + OH^- \qquad \text{II}$$
$$\downarrow$$
$$H_2$$

or

$$e^-_{aq} + e^-_{aq} + 2H_2O \rightarrow H_2 + 2OH^- \qquad \text{III}$$

rather than direct discharge of a proton out of H_2O or H_3O^+, it would be necessary to suppose that the e^-_{aq} intermediate was produced in the boundary layer (58) near the electrode surface at a quasi-equilibrium concentration* C not exceeding values given by

$$\log_{10}C = (-2.67 - \eta)/0.059 \qquad [109]$$

where 0.059 is the factor $2.3\frac{RT}{F}$ at T = 300°K and η is the hydrogen overpotential (a negative quantity) at which the cathodic process is occurring. Obviously, for η = -0.2 V say, C is of the order of 10^{-40} g. electrons per litre. Since diffusion effects operate (55, 56), this will be an upper limit for the estimate of local concentration. It seems kinetically impossible to envisage

*The question of the extent of departure from equilibrium conditions, which necessarily arises on account of e^-_{aq} annihilation processes, is considered below.

hydrogen evolution occurring as it does at 10^{-5} - 10^{-3} A. cm.$^{-2}$ at the catalytic metals at η = -0.2 V, say, by such a mechanism involving, as is evidently indicated, ca. 10^{-20} actual electrons per cc. Even at dissolving amalgams, where η = -1.0 -1.2 V, it seems that the concentration C would be unrealistically small for the mechanism under discussion to occur significantly.

The essential point is that adsorbed H or molecular H_2 can be extensively produced without any difficulty at any cathodic overpotentials since such potentials are (by definition) negative with respect to the hydrogen reversible potential. Quite the opposite is the case with the supposed primary cathodic product e^-_{aq}; it must be produced at potentials very positive to the standard potential yet at a rate equal to twice the overall rate of hydrogen evolution (as H_2). In kinetic terms, this would imply an impossibly high exchange current for the process

$$M(e) \rightleftarrows e^-_{aq}$$

if it were occurring at its standard reversible potential, 2.67 V. Thus, it is easy to see that if H_2 can be evolved, as at Pt at e.g. 10^{-3} A. cm.$^{-2}$ at an overpotential of ca. -0.2 V, then with a normal Tafel slope of ca. 0.12 V, the exchange current for e^-_{aq} production would have to be $10^{2.47/0.12}$, i.e., $10^{+20.6}$ A. cm.$^{-2}$. This difficulty is not very much diminished if it is recognized, more realistically, that the relevant potential for this calculation should perhaps be 2.67 - 0.06 x 6, $\doteqdot$ 2.30 V, i.e., the potential corresponding to the presumed concentration limit for detection of e^-_{aq}, ca. 10^{-6} mole l^{-1}. by absorption spectrophotometry. For such conditions, the limiting exchange current would be lowered only to ca. $10^{+17.5}$ A. cm.$^{-2}$, still an impossibly high figure.

2. A problem of a different but related kind arises when the microscopic reversibility of an electrode process is considered. At the reversible potential (but not necessarily at other potentials where the electrochemical reaction is not at equilibrium, so that kinetic pathways may not be identical with those obtaining for the reversible process at equilibrium, i.e., when $\eta = 0$) the hydrogen evolution process may be regarded as proceeding either by

$$H^+ + e + M \rightarrow MH \qquad \text{IV}$$

with

$$2MH \rightarrow H_2 \qquad \text{V}$$

or with other desorption steps giving H_2. With the hydrated electron path, the reversible process would have to be written (cf. 80,143) for example, as

$$M(e) \rightleftarrows M + e^-_{aq} \qquad \text{VI}$$

$$e^-_{aq} + H^+ \rightleftarrows H \qquad \text{VII}$$

$$H \rightleftarrows \frac{1}{2}H_2 \qquad \text{V}$$

The back reaction pathway would therefore have to be envisaged as H giving e^-_{aq} spontaneously, with the latter entity being the one in charge-transfer equilibrium with the electrode. Similar processes should presumably occur in metal deposition if this type of mechanism were correct. Again it seems difficult to accept such a process of spontaneous e^-_{aq} formation (which would occur with very low concentrations of e^-_{aq}) as a basis for processes, including the h.e.r., which can occur with quite high, non-diffusion controlled exchange current densities of $10^{-3} - 10^{-1}$ A. cm^{-2} at certain metals.

3. In anodic electrolysis near the reversible potential of a metal, i. e., in the back reaction of metal deposition, electrons must pass along the metal electrode and conducting wires. It seems intuitively unlikely that they should first be produced anodically in solution and then return to the metal, e. g.

$$M \rightleftarrows M^{+} + e^{-}_{aq} \qquad \text{VIII}$$

$$e^{-}_{aq} + M \rightleftarrows M(e) \qquad \text{IX}$$

for a metal dissolution reaction proceeding very near the reversible potential and hence being subject to the requirements of microscopic reversibility. In the final process IX, the electron in the metal M(e) then passes, as it must, down the external circuit.

Similar difficulties would seem to arise in the interesting but unconventional suggestion of Dainton (80) that the absolute potential of the calomel half-cell reaction, written (80) as

$$2Hg + 2Cl^{-} \rightleftarrows Hg_2Cl_2 + 2e^{-}_{aq} \qquad \text{X}$$

can be calculated if the hydration energy of e^{-}_{aq} is known. If estimates of the calomel half-cell absolute potential are to be made (but cf. refs. 145,146 for other difficulties involved), it seems necessary, however, to consider the electron in a state at the Fermi level of the metal Hg rather than in a solvated condition in the aqueous solution, so that the work function of the metal, rather than the solvation energy of e^{-}, is involved in determining the half-cell potential. Thus if the calomel electrode were to be anodically polarized to a small extent, near equilibrium in process X, the anodic current in the connections to the Hg would have to pass by transfer of e^{-}_{aq} back to the metal in a separate process, presumably diffusion controlled. This appears kinetically unlikely since it has been shown theoretically (e. g. 8) that direct electron transfer

between anions or cations and metal surfaces can occur with quite low (5 - 7 kcal. mole^{-1}) activation energies, as observed experimentally (20, 76, 104). Moreover, processes involving formation or reduction of surface phases such as Hg_2Cl_2 or AgCl are Faradaically quantitative so that formation of e^-_{aq}, which could lead to secondary H_2 evolution, is not indicated.

The apparent direct spectroscopic observation by Walker (56) of the hydrated electron in the cathodic cycle of a.c. electrolysis at Ag in an important and interesting result that requires further consideration. Here the magnitude of the cathodic potential swing might have been sufficient (maximum potentials referred to a reference electrode were, however, apparently not measured) for e^-_{aq} to be generated, though at Ag it is known (147) that H_2 will be cathodically evolved at extremely high rates (see below) at any potentials sufficiently close to $E^o_{e^-_{aq}}$ (ca. -2.67 V) for it to be expected that a detectable concentration (say 10^{-6} mole l^{-1}) of e^-_{aq} would be generated in the "steady-state". In fact, for such a concentration to be achieved near the electrode, the hydrogen overpotential would have to be ca. 2.3 V at which potential hydrogen would normally be evolved at ca. 10^{16} A. cm^{-2} ! ($i_{o,Ag} = 10^{-8}$ A. cm^{-2}, b = 0.09 V for the h.e.r. at Ag (147).

Further, the argument (55) that e^-_{aq} is liberated at dissolving metals because N_2O is reduced to N_2 as it is (148, 149, 150, 151) under homogeneous conditions of e^-_{aq} production requires further examination since adsorbed, electro-catalytically active H at the metal surface may cause reductions not commonly encountered in homogeneous processes involving atomic H.

4. A further argument that makes it difficult to accept, in general, the hydrated electron view of metal dissolution is that the kinetic characteristics of corrosion processes at metals (the

steady-state corrosion current and the mixed potential) can be very well accounted for by means of polarization diagrams involving the individual cathodic and anodic partial reactions proceeding under appreciable polarizations at non-negligible currents; under such circumstances the arguments in (1) and (3) above apply, so that a mechanism of corrosion based on a primary process of e^-_{aq} production ($M \rightarrow M^{z+} + ze^-_{aq}$) with the associated cathodic process $H^+ + e^-_{aq} \rightarrow \frac{1}{2} H_2$ raises obvious difficulties.

5. Finally, at the noble metals Pt, Rh, Ir, electrochemically adsorbed H can be quantitatively and reproducibly determined (152,153) by electrochemical procedures and the potential dependence of its coverage follows relations that can be derived for an electrochemical quasi-equilibrium process of the type $H_3O^+ + M(e) \rightleftarrows MH_{ads} + H_2O$ and a corresponding process for alkaline solutions. Such behavior can indeed be studied sufficiently exactly that co-adsorption of other chemisorbed blocking species can be determined quantitatively. It seem unlikely that the observed behavior (152,153) could arise if the processes of formation and removal of adsorbed H were

$$M(e) + H_2O \rightarrow e^-_{aq} \qquad \text{I}$$

$$e^-_{aq} + H_3O^+ \rightarrow H + H_2O \text{ in solution} \qquad \text{XI}$$

with adventitious re-adsorption of H from the solution by the process

$$H_{(\text{from solution})} + M \rightarrow MH_{ads} \qquad \text{XII}$$

together with the corresponding back reactions, since the process of electrochemical adsorption of H (prior to H_2 evolution at slightly more cathodic potentials) is highly reversible (153), so all the steps

indicated above would have to be regarded as (a) reversible and (b) capable of proceeding at appreciable rates if the e^-_{aq} pathway for H adsorption (and hence H_2 evolution) were accepted. This seems unlikely particularly as step XI is known (149) to be irreversible. Only in <u>alkaline</u> solutions, however, can the process analogous to -XI, viz. $H + OH^- \rightarrow e^-_{aq} + H_2O$, occur at appreciable rates. For electrochemisorption of H at Pt, there is, however, no radical difference between the kinetic behavior in acid and in alkaline solutions (113).

The potentiodynamic behavior for electrochemisorption of H indicates that the formation of adsorbed H is through a <u>direct</u> discharge process. Thus, the charge associated with adsorbed H production is almost independent (153) of potential sweep-rate, and the pseudo-capacitance charging currents at the peak maxima are proportional to sweep-rate so that only a direct discharge, and not a diffusion-controlled (154) process can be involved.

Closely related to the matter of electrochemisorption of H at platinum (and other metals) in cathodic hydrogen evolution is the interpretation of the fundamental kinetic coefficient $b(= \frac{dV}{d \ln i})$ in Tafel's equation characterizing the dependence of rate of the electrochemical reaction on potential V. For certain metals, e. g. Pd (155) and Pt (156), and some alloys (155), $b = \frac{RT}{1+\beta} F$ or RT/2F where β is the usual electrochemical Brønsted factor (157), approximately equal to 0. 5. Such values of b are well characterized over an appreciable range of potentials and can be explained (21) on the satisfactory and quantitative basis that the coverage Θ_H by atomic hydrogen is appreciable and potential-dependent according to a relation of the form (130,158)

$$\frac{\Theta_H}{1 - \Theta_H} = K \exp VF/RT \exp r\Theta \quad \text{(cf. [78])} \qquad [110]$$

for the quasi-equilibrium, potential-dependent reaction

$$H^+ + e + M \rightleftarrows MH_{ads}$$

with a rate-determining desorption process characterizing the kinetics, (and in particular b) in a following step such as

$$MH_{ads} + H^+ + e \rightarrow H_2 \qquad b = RT/(1 + \beta)F$$

or in the heterogeneous atom recombination step (156)

$$MH_{ads} + MH_{ads} \rightarrow H_2 \qquad b = RT/2F$$

It is difficult to see how an electrochemical process involving electrons produced at various distances into the solution and reacting homogeneously to give hydrogen could possible lead to such values of b, less than $RT/\beta F$, as are observed in the kinetics of the h. e. r. at a number of metals including platinum studied by Walker (55) in regard to N_2O reduction. If an appreciable pathway of hydrated electron formation were involved, it would be expected that only a slope $b = RT/\beta F$ would be observed, corresponding to the electron tunneling process of Gurney (1). Similarly, the kinetics of the h. e. r. are highly specific to the cathode material, an effect which has been attributed to the role of chemisorbed H. Electron emission into solution with homogeneous hydrogen production could not give the observed specificities with regard to values of i_o and b.

From the above remarks, it will be seen that there are substantial difficulties of a basic electrochemical kind in the suggestions that cathodic reactions, and inter alia the kinetics at the reversible potential, proceed via the primary production of e^-_{aq}. If the cathodic potentials relative to the hydrogen electrode are sufficiently high, say 1.9 - 2.0 V it would be kinetically feasible to envisage the e^-_{aq} path operating at such potentials and this may be

the explanation (but see also below) of Walker's observation which cannot, however, be expected to be a general basis for cathodic processes as he has implied. Similarly, under illumination, photo-electrochemical generation of e^-_{aq} becomes feasible for, in effect, the reversible potential for e^-_{aq} production is then lowered by 300 $h\nu/e$ volts where ν is the excitation frequency and e the electronic charge. In this connection, it is interesting to speculate that the reason why Walker was able apparently to detect e^-_{aq} spectrophotometrically was because of his laser illumination of the silver electrode surface at 6330 Å. This supplies already an energy equivalent to ca. 1.96 V for excitation of electrons in the surface of the metal above the Fermi level, so that only a small extra potential is required to reach the reversible potential and liberate electrons to an appreciable extent. Expressed in another way, an applied potential V raises the Fermi level by an energy VF. The photo-electric threshold potential $h\nu_c$ corresponding to a critical frequency ν_c is then lowered by VF. In effect, then, it seems that Walker's result could arise because of electrochemical assistance to the photo-electric effect (141, 142) at the metal-solution interface, so that e^-_{aq} can be formed by assistance from absorption of quanta at 6330 Å below the normal threshold potential determined by the work function of silver. Effects of this kind have indeed been described by Heyrovsky (159). The result of Walker, interesting as it is, does not therefore seem to be an entirely adequate proof of production and involvement of solvated electrons in cathodic electrode processes in general, and the technique used would seem to render complicated any direct interpretation of the results in terms of involvement of solvated electrons in cathodic hydrogen evolution in the absence of irradiation. In fact, the effects observed seem best explained in terms related to photo-effects studied by Barker and Gardner (141) and by Delahay and Srinivasan (142).

If the local intensity in the narrow laser beam were sufficiently high, this explanation may form a basis for rationalization of the effects observed in the light of the difficulties which have been pointed out in (1) and (5) above.

The result of Yurkov (140), in which supposedly copper was deposited between two electrodes (an anode and a cathode) was also attributed (140) to neutralization of copper ions at a distance from the cathode by electrons in solution. This result seems more likely to have arisen by homogeneous reduction of anodically dissolved copper ions by atomic H diffusing from the cathode, an effect which has recently been demonstrated by Uhlig (160) in the dissolution of Mg and in the cathodic hydrogen evolution process at Ni, Pt or Sn in aqueous NaCl. The decay rate of reducing behavior produced under these conditions was found (160) to be independent of pH so that the reducing properties could not therefore (see various papers in ref. 137) to be attributed to the presence of e^-_{aq} entities.

Most of the above conclusions based on electrochemical arguments depend on the value of the standard redox potential (143, 144) being approximately correct. It is of course a calculated value based on rate constants but the revised value (144) quoted cannot, it seems, be excessively in error. For e^-_{aq} involvement to be appreciable in cathodic hydrogen evolution processes occurring up to say -0.5 V volt E_H, it seems that the E^o value would have to be in error by at least 2 V. It appears unlikely that the standard redox potential for e^-_{aq} could be so grossly in error*, since such an error would require revision of one of the rate constants by many powers of ten.

---

*In this connection, it is of interest to note that the polarographically determined value of the standard potential for electrons in liquid NH_3 is -1.95 ± 0.1 V. E_H (calculated for 25°C) (144) and for this case the uncertainties are small.

A final matter concerns electrochemical reductions of organic compounds at the mercury cathode which are stereoselective, e.g., in the electrolysis of diphenylcyclopropyl bromides (167), dimethyl maleic and fumaric acids (168) and 2-chloro, 2-phenyl-propionic acid (169). The stereoselectivity can only arise by direct electron transfer from the cathode to an adsorbed molecule, preferentially oriented in one direction at the electrode interface. If such reductions occurred homogeneously by an "SN2" type of mechanism through solvated electrons (cf. the reaction of chloroacetic acid with e^-_{aq} (170)) it is difficult to see how the observed stereoselectivity could arise.

The general conclusions made above for most electrode reactions proceeding at low potentials are, it is believed, not invalidated by the interesting positive identification by Bennet et al. (166) of the hydrated electron produced from Na or K atoms at 77°K on ice. Here a sufficiently small flux of Na or K atoms was condensed on a rotating layer of ice that, as the authors state, atoms adjacent to one another were rare. Under these conditions, the Na or K will be appreciably more reactive and "base" to an extent determined approximately by the free energy of sublimation. Taking this quantity as approximately 26 kcal. $mole^{-1}$, it is seen that Na or K atoms will be, from a thermodynamic point of view, appreciably more reactive than bulk metallic sodium and would have hypothetically an electrode potential some 1.1 volts more negative than that of sodium in its normal state. Under these conditions, e^-_{aq} production in the ice is easy to understand.

(iii) Standard Potential for e^-_{aq} and the Non-equilibrium Situation

It is clear that the thermodynamic objections (but not, however, the kinetic ones based on observed Tafel slopes and electrochemisorption behavior of H) may be diminished if the calculated reversible potential were substantially in error (but see above) and/or if the "equilibrium" potential were inapplicable. That the latter situation should receive further consideration* is indicated by the conditions imposed by the short life-time of the electron in acid media. Electrons may be ejected under suitable conditions of potential and/or irradiation but may not exist long enough for the reversible equilibrium I to be kinetically established. Under these conditions, this is equivalent to requiring that in the following equality of rates

$$\vec{v}_I = k_I \exp - \beta VF/RT = \overleftarrow{v}_I = k_{-1} C_{e^-_{aq}} \exp(1-\beta)VF/RT \qquad [111]$$

written for equilibrium conditions, the $\overleftarrow{v}_I$ term is actually appreciably less than the first term. In fact, a steady-state condition for production and annihilation of e^-_{aq} at a given potential V should be written and an approximate form of such a relation is shown below:

$$\frac{d\bar{C}_{e^-_{aq}}}{dt} = k_1 \exp(-\beta VF/RT) - k_{-I}\bar{C}e^-_{aq} \exp(1-\beta)VF/RT - k_{II}\bar{C}_{e^-_{aq}} = 0 \qquad [112]$$

*The Author is indebted to Dr. D. C. Walker for discussions, in correspondence, on this latter matter as a possible way out of the "thermodynamic" difficulties arising from the published E^o value for e^-_{aq}. It is shown here, however, that some other difficulties of an energetic nature still remain.

where $\bar{C}_{e^-_{aq}}$, for the approximation, expresses a mean concentration of solvated electrons near the surface and the rate constants refer to the reactions designated by I and II earlier. The difference between the first two terms in equation [110] is the net cathodic current. Then

$$\bar{C}_{e^-_{aq}} = \frac{k_I \exp[-VF/2RT]}{k_{-I} \exp[VF/2RT] + k_{II}} \qquad \text{for } \beta = 0.5 \qquad [113]$$

If e^-_{aq} were produced under true equilibrium conditions, the same concentration $\bar{C}_{e^-_{aq}}$ would be achieved when the potential was equal to the reversible, but not the standard, value V^* given by

$$\bar{C}_{e^-_{aq}} = k_I \exp[-V^*F/RT] \qquad [114]$$

The potential V required for reaching any given concentration in the steady-state and that V^* for attainment of the same concentration under quasi-equilibrium conditions therefore differ according to the relation

$$\exp[-(V-V^*)F/RT] = 1 + k_I \cdot \frac{k_{II}}{k_I} \exp[-VF/2RT] \qquad [115]$$

Since the r.h.s. is always > 1, $V-V^*$ is negative and since we have been considering throughout negative potentials for the cathodic process, V is a more cathodic potential than V^*. This is as expected on general kinetic principles for an irreversible electrode process such as the sequence I, II.

Alternatively, it is useful to enquire whether the concentration $\bar{C}_{e^-_{aq}}{}^*$ produced under equilibrium conditions will be greater or less than the concentration $\bar{C}_{e^-_{aq}}$ for steady-state conditions for any given potential V. The two concentrations are given by equations [113] and [112] respectively, now taking the same V in

each expression. The expressions for electron concentration are then

$$C^{*}_{e^-_{aq}} = k_I \exp[-VF/RT] \text{ and } C_{e^-_{aq}} = \frac{k_1 \exp[-VF/RT]}{1 + \frac{k_{II}}{k_{-1}} \exp[-VF/2RT]} \quad [116]$$

where equation [112] has been rearranged appropriately to have the same numerator as the r.h.s. of the expression for $C^{*}_{e^-_{aq}}$. Then, since under all conditions $1 + \frac{k_{II}}{k_I} \exp[-VF/2RT] > 1$, $C_{e^-_{aq}} < C^{*}_{e^-_{aq}}$, a result which is consistent with the foregoing analysis in terms of V and V^{*}. The conclusion from this calculation is that the estimates of limiting concentration of e^-_{aq} made in terms of equation [109] will be an upper rather than a lower limit so that the conclusions made in Section (ii)-1 are not invalidated by the fact that non-equilibrium conditions generally obtain.

It is useful to examine this question further in energetic terms related to the probability of electron tunneling in reaction I. Radiationless electron transfer to form the hydrated electron must obey Gurney's condition (1) that the so-called "neutralization energy" U is greater than or equal to ϕ - eV where ϕ is the work function of the cathode. For reaction I, no ionization potential or electron affinity is involved as in the case with cations or anions and only the solvation energy S_{e^-} of e^- determines U. That is, the condition for formation of e^{o}_{aq} by tunneling to solvation sites is simply

$$\phi - eV < |S_{e^-}| \quad [117]$$

S_{e^-} is ca. 1.74 e.v. (143), so that e^-_{aq} will tend to be formed only when ϕ - eV < 1.74 e.v. ϕ for Ag is ca. 4.5 and for Pt. ca. 5.2 e.v., so that the absolute p.d. at the electrode interface must be at least ca. -2.76 V for Ag and ca. -3.46 V for Pt for any electron emission

to occur forming e^-_{aq}. Conversion of such absolute p.d.'s to figures relative to a practical scale of measurement, e.g. with respect to the reversible hydrogen electrode, raises the usual and old problem of the absolute p.d. at the interface of an hydrogen electrode at, e.g. Pt or Ag (since the absolute single p.d. will depend on the metal) and in particular the influence of the χ potential.

Recent estimates (118) of the latter quantity indicate that it may be much smaller than hitherto assumed (146,161) so that together with the recent reliable estimate (64,162) of the hydration energy of the proton, viz. -261 ± 2.5 kcal. mole^{-1} and the known ionization potential of H and the dissociation energy of $\frac{1}{2}H_2$, the single p.d. at e.g. the standard H_2/Pt electrode can hardly be numerically in excess of -0.7 ± 0.3 V. Thus the condition in [117] is only realized for Pt when the potential V is at least $-3.46 - (-0.9)$ V, i.e. ca. -2.5 V referred to the reversible hydrogen scale. This result seems at least not inconsistent with the thermodynamic argument based on the supposed standard potential of the electron of -2.67 V.

It is of interest to note that the corresponding "neutralization energies" (1) for Na^+ and K^+ would be -10.8 and -15.8 kcal. mole^{-1} based on the ionization potentials and free energies of solvation (163). These figures are substantially smaller than the "neutralization energy" of +40 kcal. mole^{-1} for e^-_{aq} formation. The difference arises of course mainly because in the case of e^-_{aq} formation there is no gain of any energy corresponding to the negative of the ionization energy or the electron affinity in the case of anions. It is evident that these considerations, based on Gurney's conditions for tunneling, lead to the conclusion that formation of e^-_{aq} will be substantially more difficult than neutralization of hydrated Na^+ or K^+ ions.

(iv) Standard Potential and the Suggested (143) Absolute e^-_{aq} Scale

A final matter related to the question of electrode potentials arises from the earlier suggestion of Baxendale (143) (also recently discussed by Walker (164)) that an absolute scale of oxidation-reduction potentials could usefully be set up for so-called "real reactions" of the type

$$M^{z+} + e^-_{aq} \rightarrow M^{(z-1)+}$$

instead of arbitrarily assuming zero standard potential for the hydrogen electrode process corresponding to IV and V. There seems to be no advantage in this suggestion since it has been argued above that there are difficulties in supposing that most electrode processes in aqueous solution proceed by the e^-_{aq} mechanism and secondly, in any practical measurement of e.m.f. of cells, the electrons in the half-cell processes must surely be associated with the metal otherwise e.m.f. measurements "by definition" would be neither feasible nor indeed unambiguous and reliable thermodynamically. In any practical measurement in electrochemical thermodynamics there is of course never any question of the absolute state of the electrons involved: the half-reactions for the cell must be so written as to add up to an overall chemical reaction with no net electrons left over, e.g. $Fe^{+++}_{aq} + e_{Pt} \rightleftarrows Fe^{++}_{aq}$ coupled with $H^+_{aq} + e_{Pt} \rightleftarrows 1/2\ H_2$ is equivalent to $Fe^{+++}_{aq} + 1/2\ H_2 \overset{Pt}{\rightleftarrows} Fe^{++}_{aq} + H^+_{aq}$. Also it is important to note that it is not the potential for the isolated half-cell reaction $H^+_{aq} + e_{Pt} \rightleftarrows 1/2\ H_2$ that is assumed conventionally to be zero but rather the potential associated with that reaction at a metal M (not necessarily Pt) in combination in a measuring circuit with possibly, but not necessarily, another metal M' at which some other electrode process

is occurring reversibly. Such circuits always involve the contact potential between M and M' in addition to the metal/solution interfacial p. d. 's at the two electrode metals and it is the algebraic sum of such p. d. 's that is the measured e. m. f. In order to avoid this practical complication, it may, however, be useful to suggest that what can be assumed to be zero on the conventional hydrogen electrode scale is the p. d. at the interface of a metal M at which the reversible hydrogen electrode process is occurring, when that metal M is chosen to be the same as that which the other electrode process in the cell is taking place. Contact p. d. 's are thus avoided in the discussion of the e. m. f. and in principle (but not always in practice) any metal can be used for establishing the reversible hydrogen electron reaction (the only practical limiting factor is, of course, whether the reaction has a sufficiently high exchange current to be useful as a reversible electrode and whether side reactions, e. g. metal dissolution, that may be potential-determining, are insignificant or not). It has also been claimed (143) that a primary difficulty with the scale of potentials associated with the usual half-cell reaction of hydrogen involving electrons in the metal is the question of the value to be assigned to the work function of the metal. This again is not, in fact, a practical difficulty since in both of the cases considered above (i. e. where M and M' are different, or where hypothetically M consitutes also the metal at which the hydrogen electrode reaction is established reversibly) the work functions cancel out: in one case, because the metal at each of the two interfaces is the same; in the second case (metal M and reference electrode process established at M') because the different work function terms involved at each metal/solution interface are cancelled by the difference of work functions (and hence the contact potential) at the M/M' interface in the external circuit.

g) Concluding Remarks

The behavior of the Tafel slopes for the h. e. r. in regard to their dependence on temperature at a series of metals has been found to be complicated and dependent on the properties of the metal and the composition of the solution. Factors such as (a) solvent structure effects, (b) the role of the dipole surface potential, χ, (c) potential effects on the entropy of activation and (d) surface coverage by atomic H, have hitherto received relatively little attention with regard to the kinetics of the h. e. r., have been examined and, under certain conditions, can provide some account of the observed behavior.

The effects associated with specific adsorption of anions are prominent in cases where b increases with decreasing temperature (cf. the results for Pt and the low c. d. region at Ni). Contributions to the rate of the h. e. r. from proton tunneling are found not to be experimentally indicated and this conclusion is consistent with that reached in previous work (86) from this laboratory.

The anomalous Tafel slope behavior observed in the present work has important consequences for the interpretation and significance of experimental electrochemical activation energies. Under such conditions, the various methods that have been used for evaluating the apparent heat of activation at the reversible potential, $\Delta H_R^{o\ddagger}$, (see Chapter II) do not yield the same results. Furthermore, conclusions regarding the barrier height cannot, under any circumstances, be made simply on the basis of the derivatives $(\partial \eta / \partial T)_i$ or $d \ln i_o / d\, 1/T$ both of which give complex quantities not simply related to either $\Delta H_R^{o\ddagger}$ or $\Delta W^{o\ddagger}$, the "true", experimentally inaccessible heat of activation.

Finally, difficulties are shown to arise in mechanisms of cathodic hydrogen evolution and metal dissolution which have

been supposed to involve the solvated electron (e^-_{aq}) as the initially formed species. Under certain circumstances, for example, in the dissolution of the basest metals in water, i.e., at sufficiently high negative potentials, or in photo-assisted processes, a small steady-state concentration of e^-_{aq} could be established. It seems unlikely, however, that this can be the general mechanism for the h.e.r., particularly for the more catalytic metals which chemisorb hydrogen.

CLAIMS TO ORIGINAL RESEARCH

1. Current-potential relations were obtained for the hydrogen evolution reaction (h. e. r.) at Ni, Cd, and Pb in alcoholic-HCl solutions over the temperature range $+60^{\circ}$ to -125°C in order to establish accurately the form of the temperature dependence of the Tafel slope b. At Ni, two distinct and reproducible Tafel regions are observed with different b values which depend in opposite ways on temperature. At Cd, the behavior of the Tafel slope, b, as a function of temperature is always the same irrespective of the direction in which the temperature is varied.

2. New current-potential relations were obtained for the h. e. r. at Pt in alcoholic-HCl solutions over the temperature range $+60^{\circ}$ to -125°C. The Tafel lines are free from the depolarization effects which characterized earlier measurements (86). The temperature behavior of the Tafel slope is dependent on the manner in which the temperature is varied for this metal (distinction from the case of Cd) thus indicating that irreversible adsorption of Cl^- ion is occurring.

3. The previous measurements at Hg in alcoholic-HCl solutions (86) were extended to ca. $+60^{\circ}$C. The behavior of the Tafel slope as a function of temperature is best represented by a relation of the form $b = \frac{RT}{\beta F} + c$. Such a relation, also observed for part of the high current density region at Ni in alcoholic-HCl and for Ni in 0.5 M $HClO_4$-MeOH solutions, is interpreted in terms of (a) changes of solvent structure with temperature, (b) the role of the dipole surface potential, χ, (c) the effect of potential on the entropy of activation and (d) temperature-dependent hydrogen coverage effects.

4. Effects associated with specific adsorption of the Cl^- anion are suggested as being significant in the b vs. T behavior observed at Pt and the low current-density region at Ni. In addition to these effects, the possible formation of "hydride films" on Pb and Cd is suggested as a possible explanation for the behavior observed at lead and cadmium.

5. The question of the role of proton tunneling in the h. e. r. at Ni, Pt and Cd is examined critically and it is shown that the experimental evidence indicates it to be negligible. This conclusion is based on: (a) the fact that the Tafel slopes for the deuterium evolution reaction (d. e. r.) are always larger, rather than smaller, than those for the h. e. r., and (b) the curvature in the Arrhenius plots for the d. e. r. occurs at a higher temperature than that for corresponding effects in the h. e. r. The observed H/D isotope effect is qualitatively interpreted in terms of effects associated with (a) the interaction of specifically adsorbed Cl^- ions with the transition states for H^+ and D^+ transfer and (b) isotopically different solvent structural effects in the MeOH and MeOD solutions.

6. Current-potential relations were obtained for the bromine evolution reaction at graphite in acetonitrile over the temperature range of $+60^\circ$ to $-45^\circ C$. The fact that the Tafel slope, b, is independent of the temperature indicates that such behavior, previously reported for the h. e. r. (69, 104, 105), is not specific to proton transfer.

7. A critical evaluation of the significance of electrochemical activation energies is presented in regard to (a) methods for determination of these quantities and (b) the significance and

interpretation of such quantities particularly when the Tafel slopes are not temperature-dependent according to the conventional form for $b(=RT/\beta F)$.

8. Several arguments against the proposal (56, 57, 58) that the solvated electron is the primary entity in the cathodic evolution of hydrogen are presented.

REFERENCES

1. R. W. Gurney, Proc. Roy. Soc. (London), A134, 137 (1931).
2. J. Horiuti and M. Polanyi, Acta Physicochim., 2, 505 (1935).
3. J. A. V. Butler, Proc. Roy. Soc. (London), A157, 432 (1936).
4. F. P. Bowden, Proc. Roy. Soc. (London), A125, 446 (1929); A126, 107 (1929).
5. T. Erdy-Gruz and M. Volmer, Z. Physik Chem., A150, 203 (1930).
6. A. N. Frumkin, Z. Physik Chem., A164, 121 (1933).
7. R. Parsons and J. O'M. Bockris, Trans. Faraday Soc., 47, 914 (1951).
8. B. E. Conway and J. O'M. Bockris, Electrochim. Acta, 3, 340 (1961).
9. A. R. Despič and J. O'M. Bockris, J. Chem. Phys., 32, 389 (1960).
10. N. S. Hush, Trans. Faraday Soc., 57, 557 (1961).
11. R. A. Marcus, J. Chem. Phys., 26, 867 (1957).
12. R. A. Marcus, Can. J. Chem., 37, 155 (1959).
13. R. A. Marcus, Disc. Faraday Soc., 29, 21, 250 (1960).
14. R. A. Marcus, Trans. Sym. on Electrode Processes, Philadelphia, (Ed. by E. Yeager) New York; John Wiley and Sons (1959).
15. R. A. Marcus, J. Chem. Phys., 38, 1858 (1963).
16. R. R. Dogonadze and Y. A. Chizmadzhev, Dokl. Akad. Nauk. S. S. S. R., 145, 849 (1962).
17. R. R. Dogonadze and Y. A. Chizmadzhev, Dokl. Akad. Nauk. S. S. S. R., 150, 333 (1963).
18. M. Salomon and B. E. Conway, Disc. Faraday Soc., 39, 223 (1965).

19. J. O'M. Bockris and D. B. Matthews, Proc. Roy. Soc. (London), A292, 479 (1966).

20. J. O'M. Bockris and E. C. Potter, J. Electrochem. Soc., 99, 169 (1952).

21. J. O'M. Bockris, Chapter 4, Modern Aspects of Electrochemistry, Ed. J. O'M. Bockris and B. E. Conway, Butterworths, London, 1, 180 (1954).

22. N. F. Mott and R. J. Watts-Tobin, Electrochim. Acta, 4, 79 (1961).

23. S. G. Christov, Ber. Bunsenges, physikal chemie, 67, 117 (1963).

24. D. B. Matthews, Ph.D. thesis, Pennsylvania (1965).

25. S. G. Christov, Z. Elektrochem., 62, 567 (1958).

26. N. S. Hush, J. Chem. Phys., 28, 962 (1958).

27. R. Parsons and E. Passeron, J. Electroanal. Chem., 12, 524 (1966).

28. J. N. Brønsted and K. J. Pedersen, Z. Physikal Chem., 108, 185 (1924).

29. R. P. Bell, Proc. Roy. Soc. (London), A154, 414 (1936).

30. R. P. Bell, Acid-Base Catalysis, Oxford Univ. Press, Anne House, London E.C. 4 (1949).

31. B. E. Conway and M. Salomon, J. Chem. Phys., 41, 3169 (1964).

32. E. Z. Wigner, Physik. Chem., B19, 203 (1933).

33. R. P. Bell, Proc. Roy. Soc. (London), A139, 466 (1933).

34. C. Eckart, Phys. Rev., 35, 1303 (1930).

35. R. P. Bell, Proc. Roy. Soc. (London), A148, 241 (1935).

36. H. Pelzer and E. Wigner, Z. Physik. Chem., B15, 445 (1932).

37. R. P. Bell, J. A. Fendley and J. R. Hulett, Proc. Roy. Soc. (London), A235, 453 (1950).

38. B. E. Conway, J. O'M. Bockris and H. J. Linton, J. Chem. Phys., 24, 834 (1956).

39. B. E. Conway and J. O'M. Bockris, J. Chem. Phys., 28, 354 (1958).

40. B. E. Conway, Can. J. Chem., 37, 178 (1959).

41. V. J. Shiner and M. L. Smith, J. Amer. Chem. Soc., 83, 593 (1961).

42. V. J. Shiner and B. Martin, Pure Appl. Chem., 8, 371 (1964).

43. L. Funderburk and E. S. Lewis, J. Amer. Chem. Soc., 86, 2531 (1964).

44. J. R. Jones, R. E. Marks and S. C. Subba Rao, Trans. Faraday Soc., 63, 993 (1967).

45. C. E. H. Bawn and G. Ogden, Trans. Faraday Soc., 30, 432 (1934).

46. M. P. Appelby and G. Ogden, J. Chem. Soc., 1936, 163.

47. S. G. Christov, Electrochim. Acta, 4, 194 (1961).

48. S. G. Christov, Electrochim. Acta, 4, 306 (1961).

49. S. G. Christov, Electrochim. Acta, 9, 575 (1964).

50. B. Post and C. F. Hiskey, J. Amer. Chem. Soc., 72, 4203 (1950); 73, 161 (1951).

51. J. O'M. Bockris and D. B. Matthews, J. Chem. Phys., 44, 298 (1966).

52. G. Belanger, B. Sc. thesis, Ottawa (1965).

53. J. J. Weiss, J. Chem. Phys., 44, 1120 (1964).

54. M. Eigen, Disc. Faraday Soc., 39, 7 (1965).

55. D. C. Walker, Can. J. Chem., 44, 2226 (1966).

56. D. C. Walker, Can. J. Chem., 45, 807 (1967).

57. G. J. Hills and D. R. Kinnibrugh, J. Electrochem. Soc., 113, 1111 (1966).

58. T. Pyle and C. Roberts, J. Electrochem. Soc., 115, 247 (1968).

59. B. E. Conway, Trans. Roy. Soc. Can., Sect. III, 54, 19 (1960).

60. B. E. Conway, Electrochemical Data, Elsvier Publishing Co., Amsterdam (1952).

61. J. Eastman, J. Amer. Chem. Soc., 50, 283, 292 (1928).

62. M. I. Temkin, Z. Fiz. Khim., 22, 1081 (1948).

63. B. E. Conway, Theory and Principles of Electrode Processes, The Ronald Press Co., New York (1965).

64. H. F. Halliwell and S. C. Nyburg, Trans. Faraday Soc., 59, 1126 (1963); C. Herring and M. H. Nichols, Rev. Mod. Phys., 21, 185 (1949).

65. S. Glasstone, K. J. Laidler and H. Eyring, Theory of Rate Processes, McGraw-Hill Book Co. Inc., New York (1940).

66. E. F. Caldin and E. Harbron, J. Chem. Soc., 1962, 3454.

67. J. R. Jones, Trans. Faraday Soc., 61, 2456 (1965).

68. J. N. Agar, Disc. Faraday Soc., 1, 81 (1947); see also F. P. Bowden and J. N. Agar, Ann. Reports, Chem. Soc. (London), 35, 90 (1938).

69. J. O'M. Bockris and R. Parsons, Trans. Faraday Soc., 45, 916 (1949).

70. S. Minc and J. Sobkowski, Bull. Acad. Polon. Sci., 8, 29 (1959).

71. R. P. Bell, The Proton in Chemistry, Cornell University Press, Ithaca, New York (1959).

72. B. E. Conway, Disc. Faraday Soc., 39, 270 (1965).

73. K. J. Laidler, Can. J. Chem., 37, 138 (1959).

74. E. Sacher and K. J. Laidler, Chapter I, Modern Aspects of Electrochemistry, Ed. J. O'M. Bockris and B. E. Conway, 3, 1 (1964).

75. J. E. B. Randles, Trans. Faraday Soc., 48, 828 (1952).

76. J. E. B. Randles and K. W. Somerton, Trans. Faraday Soc., 48, 951 (1952).

77. J. A. V. Butler, Electrical Phenomenon at Interfaces, Methuen, London (1951), p. 23.

78. J. N. Brønsted and N. L. Ross Kane, J. Amer. Chem. Soc., 53, 3624 (1931).

79. J. R. Hulett, Quart. Rev., 18, 227 (1964).

80. F. S. Dainton, Endeavour, 26, 115 (1967).

81. A. M. Azzam, J. O'M. Bockris, B. E. Conway and H. Rosenberg, Trans. Faraday Soc., 46, 918 (1950).

82. Z. A. Jofa and V. Stepanova, Zh. fiz. Khim., 19, 125 (1945).

83. J. O'M. Bockris and D. B. Matthews, Electrochimica Acta, 11, 143 (1966).

84. A. Murray and D. C. Williams, Organic Synthesis with Isotopes, Part II, Interscience (1958), p.1336.

85. Handbook of Preparative Inorganic Chemistry, Vol. I, 2nd Ed., Ed. by George Brauer, Academic Press, New York (1963), p.129.

86. M. Salomon, Ph.D. thesis, Ottawa (1964).

87. J. O'M. Bockris, B. E. Conway and W. Mehl, J. Sci. Inst., 33, 400 (1956).

88. J. O'M. Bockris, Disc. Faraday Soc., 1, 229 (1947).

89. D. J. G. Ives and G. J. Janz, Reference ElectrodesTheory and Practice, Academic Press, New York and London (1961).

90. M. W. Breiter and S. Gilman, J. Electrochem. Soc., 109, 622 (1962).

91. S. S. Beskozovaiuaya, Y. B. Vasilev and V. S. Bagotskii, Electrochim. Acta, 12, 1323 (1967).

92. S. B. Brummer, J. Electrochem. Soc., 113, 1041 (1966).

93. J. O'M. Bockris and S. Srinivasan, Electrochimica Acta, 9, 31 (1964); also B. Kabanov and I. Filipov, J. Phys. Chem. (Russ.), 13, 341 (1939).

94. M. A. V. Devanathan and M. Selvaratnam, Trans. Faraday Soc., 56, 1820 (1960).

95. D. C. Grahame, Chem. Rev., 41, 441 (1947).

96. A. N. Frumkin, Chapter 2, Advances in Electrochem. and Electrochem. Eng., Ed. P. Delahay and C. W. Tobias, 1, 65 (1961).

97. K. J. Vetter, Electrochemical Kinetics, Theoretical and Experimental Aspects, Translated by Scripta Technica Inc., Academic Press, N. Y., 1967, p. 115.

98. H. H. Bauer, J. Electroanal. Chem., 16, 419 (1968).

99. B. E. Conway, R. E. Verrall and J. E. Desnoyers, Trans. Faraday Soc., 62, 2738 (1966).

100. B. E. Conway in Chemical Physics of Ionic Solutions, p. 577, Ed. B. E. Conway and R. G. Barradas, John Wiley and Sons, N. Y. (1966).

101. R. Parsons, Chapter 3, Modern Aspects of Electrochemistry, Eds. J. O'M. Bockris and B. E. Conway, Butterworths, 1, 103 (1954).

102. R. Parsons, Chapter 1, Advances in Electrochem. and Electrochem. Eng., Ed. P. Delahay and C. W. Tobias, 1, 1 (1961).

103. J. O'M. Bockris, R. Parsons and H. Rosenberg, Trans. Faraday Soc., 47, 766 (1951).

104. J. O'M. Bockris and E. C. Potter, J. Chem. Phys., 20, 614 (1952).

105. J. N. Butler, J. Electrochem. Soc., 112, 226 (1965).

106. H. P. Stout, Trans. Faraday Soc., 41, 64 (1945).

107. A. N. Frumkin, Adv. Electrochem. and Electrochem. Eng., Ed. P. Delahay and C. W. Tobias, 3, 287 (1963).

108. R. Parsons and M. A. V. Devanathan, Trans. Faraday Soc., 49, 673 (1953).

109. J. Jofa and A. N. Frumkin, Acta Physicochim., U. R. S. S., 4731, 10, (1939).

110. R. Parsons, Trans. Symposium Electrode Processes, Philadelphia, Ed. E. Yeager, John Wiley and Sons. Inc., N. Y. (1961), pp. 14-15.

111. R. Parsons, J. Electroanal. Chem., 21, 35 (1969).

112. Y. M. Kolotyrkin, Trans. Faraday Soc., 55, 455 (1959).

113. M. W. Breiter, Ann. N. Y. Acad. Sci., 101, 709 (1963).

114. D. J. G. Ives and F. R. Smith, Trans. Faraday Soc., 63, 217 (1967).

115. A. Hickling and F. W. Salt, Trans. Faraday Soc., 38, 474 (1942).

116. H. W. Salzberg, J. Electrochem. Soc., 100, 146 (1953); see also L. W. Gastivirt and H. W. Salzberg, ibid., 104, 701 (1957).

117. B. E. Conway and L. Laliberté, J. Phys. Chem., 72, 4317 (1968).

118. J. O'M. Bockris, M. A. V. Devanathan and K. Muller, Proc. Roy. Soc., (London), A274, 55 (1963).

119. D. B. Matthews, S. Srinivasan and J. O'M. Bockris, Disc. Faraday Soc., 39, 239 (1965).

120. B. E. Conway, Disc. Faraday Soc., 39, 266 (1965).

121. H. Nürnberg, Fortschitte chem. Forsch., 8, 241 (1967); see also idem, Zeit. Tech. Chem., 12, 713 (1967).

122. E.g. see L. I. Kristalik, Electrochimiya, 2, 624 (1966).

123. K. Muller, J. Res. Inst. Catalysis, Hokkaido Univ., 14, 224 (1967).

124. B. E. Conway and L. G. M. Gordon, J. Phys. Chem., (1969), in press.

125. R. A. Marcus, Ann. Rev. Phys. Chem., 15, 155 (1964).

126. G. J. Hills and R. Payne, Trans. Faraday Soc., 61, 326 (1965).

127. E. Wicke, M. Eigen and Th. Ackermann, Z. Phys. Chem., NF 1, 340 (1954).

128. R. Parsons, Trans. Faraday Soc., 54, 1053 (1958).

129. A. N. Frumkin, P. Dolin and B. V. Ershler, Acta Physicochim., U.R.S.S., 13, 779 (1940).

130. B. E. Conway and E. Gileadi, Trans. Faraday Soc., 58, 2493 (1962).

131. E. Gileadi and B. E. Conway, J. Chem. Phys., 19, 3420 (1963).

132. B. E. Conway, N. Marincic, D. Gilroy and E. J. Rudd, J. Electrochem. Soc., 113, 1144 (1966).

133. B. E. Conway, E. J. Rudd and L. G. M. Gordon, Disc. Faraday Soc., 45, 87 (1968); see also T. Biegler and R. Woods, J. Electroanal. Chem., 20, 347 (1969), where further development of this treatment is given.

134. B. E. Conway and M. Salomon, Ber. Bunsenges, 68, 331 (1964).

135. B. E. Conway and M. Salomon, Disc. Faraday Soc., 39, 270 (1965).

136. L. I. Kristalik, J. Electrochem. Soc., 113, 1117 (1966).

137. Various papers in "Solvated Electrons", Adv. in Chemistry, 50 (1965), American Chemical Society, Washington, D.C.; (see also E. G. Hart, Science, 146, 19 (1964), M. Anbar, Quarterly Rev. Chem. Soc., London, 22, 579 (1968) and U. Schindewolf, Angew. Chem. Int. Edn., 7, 190 (1968)).

138. D. C. Walker, Chem. Soc. Special Publ., No. 22, 277 (1967).

139. R. Parsons, J. Electrochem. Soc., 113, 1118 (1966); see also B. E. Conway, ibid., 113, 1120 (1966).

140. V. A. Yurkov, "Soviet Electrochemistry", Symposium 1959, II, 85 (1961), Consultants Bureau Trans., New York.

141. G. C. Barker and A. W. Gardner, Proc. C.I.T.C.E. Meeting, Moscow, 1963; see also P. J. Hillson and E. K. Rideal, Proc. Roy. Soc. (London), A199, 295 (1949).

142. P. Delahay and V. S. Srinivasan, J. Phys. Chem., 70, 420 (1966).

143. J. H. Baxendale, Rad. Res., 28, Suppl. 4, 139 (1964).

144. M. S. Matheson, p. 45 in ref. 137; for the value of E_e^o- for NH_3; see H. A. Laitenen and C. J. Nyman, J. Amer. Chem. Soc., 70, 2241 (1948).

145. W. M. Latimer, K. S. Pitzer and C. M. Slansky, J. Chem. Phys., 1, 108 (1939).

146. A. N. Frumkin, J. Chem. Phys., 1, 552 (1939).

147. J. O'M. Bockris and B. E. Conway, Trans. Faraday Soc., 48, 724 (1952).

148. F. S. Dainton and D. B. Peterson, Proc. Roy. Soc., (London), A267, 443 (1962).

149. J. Rabani, p. 242 in ref. 137.

150. S. Gordon, E. J. Hart, M. S. Matheson, J. Rabani and J. K. Thomas, Disc. Faraday Soc., 36, 193 (1963).

151. J. P. Keene, Rad. Res., 22, 1 (1964).

152. A. N. Frumkin and A. Slygin, Acta Physicochim., U. R. S. S., 3, 719 (1935); 4, 991 (1936); 5, 819 (1936).

153. F. Will and C. A. Knorr, Zeit. Elektrochem., 64, 258 (1960); D. Gilroy and B. E. Conway, Can. J. Chem., 46, 875 (1968).

154. P. Delahay and G. Perkins, J. Phys. Coll. Chem., 55, 586, 1146 (1951).

155. J. P. Hoare and S. Schuldiner, J. Electrochem. Soc., 104, 564 (1957); S. Schuldiner and J. P. Hoare, J. Phys. Chem., 61, 705 (1957); 62, 229 (1958).

156. J. O'M. Bockris and A. M. Azzam, Trans. Faraday Soc., 48, 145 (1952).

157. A. N. Frumkin, Zeit. Phys. Chem., 160, 116 (1932); cf. B. E. Conway, Disc. Faraday Soc., 39, 47 (1965); and Chapter 4 in "Progress in Reaction Kinetics", Ed. G. Porter, Pergamon Press, London (1967).

158. A. Euchen and B. Weblus, Zeit. Elektrochem., 55, 114 (1951).

159. M. Heyrovský, Nature, 206, 1356 (1965); M. Heyrovský, Proc. Roy. Soc., (London), A301, 411 (1967).

160. R. C. Krutenat and H. H. Uhlig, Electrochim. Acta, 11, 469 (1966); cf. N. Kobosew and N. Nekrassow, Zeit. Elektrochem., 36, 529 (1930).

161. A. N. Frumkin, Electrochim. Acta, 2, 351 (1960).

162. B. E. Conway and M. Salomon, Chapter 24, Chem. Phys. Ionic Solutions, Ed. B. E. Conway and R. G. Barradas, John Wiley and Sons, Inc., New York (1966).

163. D. D. Eley and M. G. Evans, Trans. Faraday Soc., 34, 1093 (1938).

164. D. C. Walker, Adv. in Chemistry Series, Radiation Chemistry I, 3, 49, American Chemical Society (1968).

165. B. E. Conway, Proc. Roy. Soc., (London), A256, 128 (1960).

166. J. E. Bennet, B. Milne and A. Thomas, J. Chem. Soc., 1967, 1393; see also idem, Nature, 201, 919 (1961).

167. R. Annino, J. Erickson, J. Michaelovich and B. MacKay, J. Amer. Chem. Soc., 88, 4424 (1966).

168. I. Rosenthal, J. R. Hayes, A. J. Martin and P. J. Elving, J. Amer. Chem. Soc., 80, 3050 (1958).

169. Z. R. Grabowski, B. Czochralska, A. Vincenz-Chodkowska and M. Balasiewicz, Disc. Faraday Soc., 45, 145 (1968).

170. E. Hayon and A. O. Allen, J. Phys. Chem., 65, 2181 (1961).

171. K. J. Laidler and R. L. Martin, Int. Journal Chemical Kinetics, 1, 113 (1969).

172. R. P. Bell, Trans. Faraday Soc., 55, 1 (1959).